Oestrogen receptor dynamics and cell signalling

Carol FitzGerald

BSc. (Hons), University College Cork

Medical Research Council
Human Reproductive Sciences Unit
Queens Medical Research Institute
47 Little France Crescent
Edinburgh, EH16 4TJ

Thesis submitted to the University of Edinburgh for the degree of Doctor of Philosophy

February 2010

For Lylie Hayes

Declaration

The research described in this thesis is the sole work of the author, except where acknowledgement is made and is not submitted in support of another degree or qualification at the University of Edinburgh or any other educational institute.

Carol FitzGerald

February 2010

Acknowledgements

There are a number of people to whom I am indebted for encouraging and supporting me through this journey over the past three (and a bit) years. First and foremost, I would like to thank my supervisor Professor Philippa Saunders for her continuous support and invaluable guidance throughout the entire course of my PhD. I would also like to express my gratitude to my co-supervisor Professor Hilary Critchley.

A special thanks to my lab manager, Frances McGarry who is the best lab mentor I could possibly have wished for. To all other members of the Saunders lab group, past and present; Karen, Audrey, Vincent, Catriona, Gillian, Rob, Elaine, Jacqui and Doug – best of luck with everything in the future. I extend my thanks to Carol Adam and all in the male lab who were a wonderful support network and fantastic group of people to work with.

The bulk of this thesis involves confocal microscopy – thank you so much to all members of the histology team; Mike, Sheila and Arantza for your enduring patience in answering my many many questions and queries. I am equally grateful to Dr. Pam Brown and her team in the biomolecular core group; Stuart and Yong for their help and providing me with the fluorescently labelled adenoviral constructs. To everyone in IT support, Steve, Keith and Adrian for being unduly patient in dealing with the ultimate technophobe.

This rollercoaster in my life would not have been as fun without my fellow Student's; in particular Alison, to Margaret and my office-mates; Matt, Naomi and Rowan – probably the greatest 'crew' in the world! It has been so much fun and an honour to share these past years with you guys – I will miss it.

A huge thank you to my mom and dad and my wee sister, Ciara – for putting up with my complaints and frustrations, your unrelentless support and belief in me at all times got me through. Finally, to all my family and friends in Ireland, many thanks for your support – *Go raibh míle maith agaibh go léir*.

Abstract

Oestrogen receptors (ER) have classically been described as ligand-inducible nuclear transcription factors. The pleiotrophic effects of ER function have a predominant role in the direct regulation of the growth, differentiation and development of tissues of the human reproductive system. There are two ER subtypes, ERα and ERβ which differ in their specificity for ligand and the consequent actions they orchestrate. Moreover, the latter exists in multiple splice variants of which ERβ is the only fully functional homologue. Research into the underlying differences in subtype responses to ligand has involved examination of the intranuclear dynamics of individual receptor subtypes. Studies into the mobility of ER in response to ligand have exclusively focused on studies of full length ERα and ERβ independently in transfected cell lines. The studies described in this thesis have investigated the kinetics of ER using Fluorescence Recovery After Photobleaching (FRAP) in infected cell lines which lends itself to more precise expression of the subtype of interest. The morphological impact of natural oestrogenic and synthetic ligands on ERs was examined and the influence on the intranuclear dynamics assessed. Further to this, the effect of co-expression of different ER subtype combinations was examined.

Studies on the intranuclear mobility of ER have confirmed and extended the findings of others. Previous work on the development of ER agonists and antagonists has been to target specific overexpressing ER subtypes in a physiological setting. In this study, we demonstrated for the first time an overwhelming ERβ-selective effect in slowing the rate of mobility within the nucleus, suggesting the study of intranuclear dynamics is an important parameter for the examination of efficacy of a compound. Differential responses to ligand based on co-infected partnerships indicate that heterodimerisation has a profound effect in augmenting ligand-dependent regulation and activity.

Several studies have claimed a dominant functional role for splicing variants of the full length ERs. In the current study we have focused on ERβ5, a truncated variant of ERβ with impaired ligand-binding capacity. Based on the widespread expression of ERβ5 that was determined in the normal endometrium, cell-based assays were implemented to explore the mode of activation and function of the ERβ5. To date, there have been no published reports on the intranuclear response of ERβ5 to ligand. In the current study, the mobility of ERβ5 tagged to yellow fluorescent protein (YFP) (ERβ5-YFP) was not influenced by incubation of cells with ligand (17β oestradiol-E2) independently but co-infection with unlabelled ERα resulted in a decrease in the mobility pattern of the ERβ5-YFP protein. Further to this, the co-expression of ERβ5 and ERα in cells incubated with E2 resulted in enhanced transcriptional activity. The induction of an oestrogen response element (ERE)-luciferase reporter resulted in an increase in expression of luciferase beyond that in cells infected with ERα alone. Taken together, these results suggest a role for ERβ5 as an active dimer partner in influencing E2-dependent gene expression in the human endometrium.

While the canonical mode of nuclear receptor activation is ligand-mediated, a role for growth factor (GF)-driven tyrosine signalling cascades in the phosphorylation of ER has been described as a ligand-independent mechanism of activation. In the current study, a direct role for epidermal growth factor (EGF) in mediating phosphorylation of ERα was shown. Activation of the extracellular signal-regulated kinase (ERK)1/2 mitogen-activated protein kinase (MAPK) pathway was also demonstrated in response to EGF treatment, suggesting a likely mechanism through which EGF can act to phosphorylate ER. To determine the mechanics of the responses to GF within the cell, FRAP analyses revealed an impact of EGF in slowing down the mobility of ERα, ERβ, ERβ2 and ERβ5 in a temporal manner. The latter results could therefore hold promise for studies into alternative modes of activation of truncated splice variants lacking a function ligand-binding domain.

In conclusion, this study has demonstrated important differences in intranuclear dynamics and transactivation of ER subtypes and splice variants when independently

or co-expressed in response to natural and synthetic compounds. The influence of EGF on splice variants with impaired ligand binding function has raised questions about an alternative mode of activation of these isoforms and thus, reaffirming a functional role for these ERs in human physiology.

Presentations relating to this thesis

Fertility 2009 (Jan 2009, Edinburgh) Short Paper Session: Establishing a role for the oestrogen receptor beta 5 (ERβ5) splice variant in human endometrium: potential impact on oestrogen signalling.

Simpson Symposium 2008 (Aug 2008, Edinburgh) Poster Session: Expression of the oestrogen receptor beta 5 (ERβ5) splice variant in human endometrium.

Society for Reproduction and Fertility (June 2008, Edinburgh) Student Oral Communication Prize Session: Expression of the oestrogen receptor beta 5 (ERβ5) splice variant in human endometrium: potential impact on oestrogen signalling.

British Endocrinology Society (Apr 2008, Harrogate, England) Oral Communication: Dynamic responses of oestrogen receptors revealed by fluorescent recovery after photobleaching (FRAP).

Abbreviations

4HT	4'-hydroxy-tamoxifen
AIB-1	Amplified in breast cancer-1
AD1	Activation domain 1
AD2	Activation domain 2
AF-1	Activation function 1
AF-2	Activation function 2
AR	Androgen receptor
cAMP	Cyclic adenosine monophosphate
CBP	CREB binding protein
CDK	Cyclin dependent kinase
COX-2	Cyclooxygenase-2
CREB	cAMP response element-binding
DBD	DNA binding domain
DNA	Deoxyribonucleic acid
DPN™	Diarylpropionitrile
E1	Oestrone
E2	17β oestradiol
EGF	Epidermal growth factor
EGFR	Epidermal growth factor receptor
eNOS	Endothelial nitric oxide synthase
ER	Oestrogen receptor
ERE	Oestrogen response element
ERK	Extracellular signal-regulated kinase
ERKO	Oestrogen receptor knockout
ERα	Oestrogen receptor alpha
ERβ	Oestrogen receptor beta
FRAP	Fluorescence recovery after photobleaching
GRIP	Glucocorticoid receptor interacting protein 1
GTP	Guanosine-5'-triphosphate

HAT	Histone acetyltransferase
HDAC	Histone deacetylase
HER	Human epidermal growth factor receptor
HRT	Hormone replacement therapy
hsp	Heat shock protein
IGF	Insulin-like growth factor
IGFR	Insulin-like growth factor receptor
LBD	Ligand binding domain
MAPK	Mitogen activated protein kinase
mRNA	Messenger ribonucleic acid
NCoR	Nuclear corepressor
NR	Nuclear receptor
PDGF	Platelet derived growth factor
PPT™	Propyl pyrazole triol
PR	Progesterone receptor
RAR	Retinoic acid receptor
RNA	Ribonucleic acid
SERM	Selective oestrogen receptor modulator
SHR	Steroid hormone receptor
SMRT	Silencing mediator for retinoid and thyroid hormone receptors
SRC	Steroid receptor coactivator
TR	Thyroid receptor
TRAP	Thyroid hormone receptor activating protein
UPP	Ubiquitin proteasome pathway

Table of Contents

List of figures

List of tables

Chapter 1

Literature Review

1 Literature Review

1.1 Oestrogens in reproductive health and disease

Oestrogens are sex steroids that play an essential role in regulating formation and function of the reproductive system and also have an impact on the cardiovascular system, the immune system, the skeleton, the breast and the brain (reviewed in Deroo and Korach, 2006). Oestrogens have been implicated in development of reproductive disorders including endometriosis and cancer (Fig. 1.1). Sex steroids are lipophilic ligands that readily cross cell membranes and alter gene expression by binding to receptors that function as ligand-activated transcription factors. Two oestrogen receptors (ERs), ERα and ERβ have been identified (section 1.5 and 1.6). Oestrogens play key roles in development of the mammary gland and endometrium (Klinge, 2000) and in the stimulation of bone growth and its maintenance (Manolagas and Kousteni, 2001). A deficiency in circulatory levels of oestrogen is associated with an increased risk of osteoporosis in postmenopausal and ageing populations worldwide (Riggs and Melton, 1995) arising from increased osteoclast-mediated resorption of the bone (Albright *et al.*, 1941, Riggs *et al.*, 1998). The use of oestrogen in hormone replacement therapy (HRT) in postmenopausal women has been linked to a reduced risk in the development of coronary heart disease (Campos *et al.*, 1993). Oestrogens act as cardioprotectants by increasing clearance of low-density lipoprotein cholesterol while increasing formation of high density lipoproteins and triglycerides (Guetta and Cannon, 1996, Campos *et al.*, 1997). They have also been implicated in the up-regulation of the atheroprotective prostacyclin PGI_2 through the activation of cyclooxygenase 2 (COX-2) in mice (Egan *et al.*, 2004).

Conversely oestrogen exposure has also been implicated in the development of some cancers. For example, the use of oestrogen-only HRT increases the risk of developing endometrial cancer (Shapiro *et al.*, 1985, Beral *et al.*, 2005). The menopausal transition (climacteric), a time when oestrogens may be elevated has been proposed as a possible ‘window of risk’ for the development of the disease later in life (Hale *et al.*, 2002).

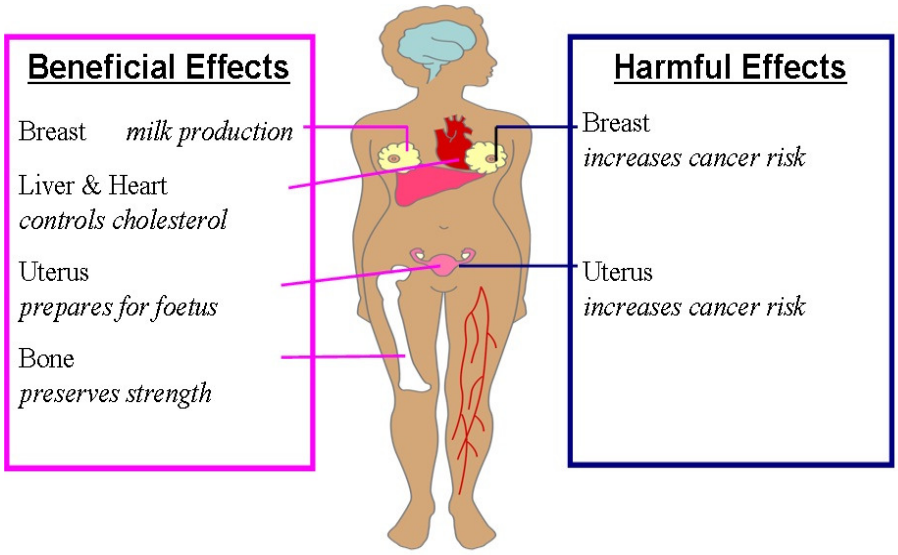

Figure 1.1 Overview of biological function of oestrogens.

The physiological relevance of oestrogenic function is exemplified in the bone, breast and reproductive tissues.

1.2 Biosynthesis of oestrogens

In pre-menopausal, non-pregnant women, the ovaries are the primary source of circulating oestrogen (Simpson *et al.*, 1999) (section 1.10). Oestrogen is the end-product of step-wise biosynthesis from cholesterol that is regulated by a series of cytochrome P450s (Mitrunen and Hirvonen, 2003) and hydroxysteroid dehydrogenases (3β and 17β) (summarised in Fig. 1.2). Cleavage of the cholesterol side-chain yields the C_{21} steroid pregnenolone that in turn is reduced to progesterone or androstenedione (Omura and Morohashi, 1995). The critical step in oestrogen biosynthesis (aromatisation) is accomplished by the action of the aromatase complex, an essential component of which is the aromatase cytochrome P450 enzyme (P450arom) (Simpson and Davis, 2001), either directly to produce oestrone (E1) or indirectly via the aromatisation of testosterone. Clinical studies implicate a role for the aromatase enzyme in the development of the reproductive organs and regulation of gonadotrophins (Fisher *et al.*, 1998) and overexpression of aromatase has been implicated in the pathogenesis of breast cancers (reviewed in Kristensen and Borresen-Dale, 2000).

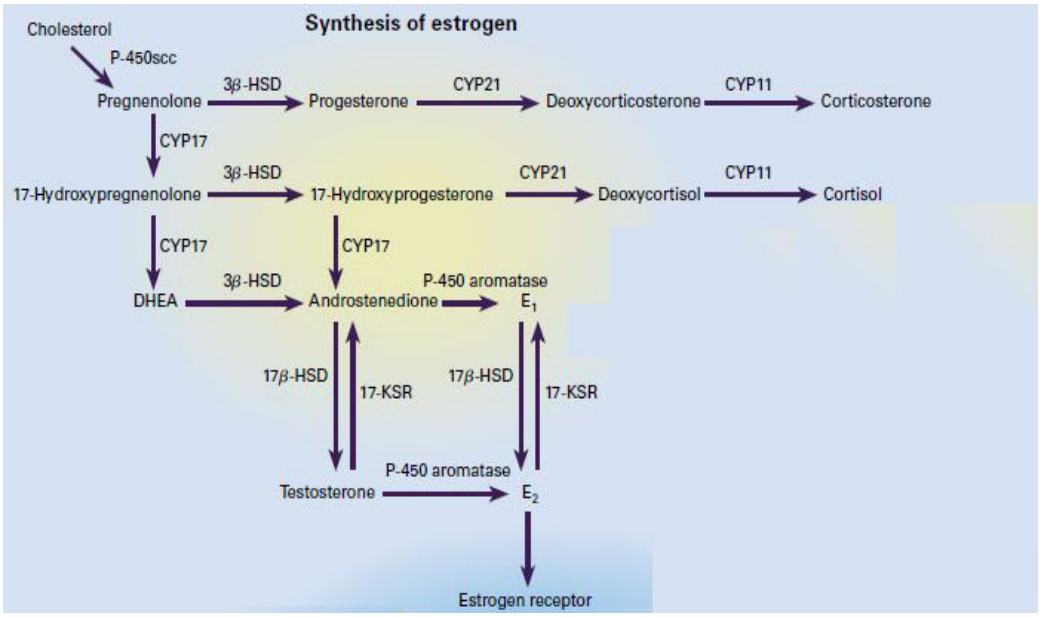

Figure 1.2 Oestrogen biosynthesis.

The sequential production of the C_{18} oestrogenic steroids (oestrone and oestradiol) from the C_{19} androgen precursors (androstenedione and testosterone) is catalysed by a series of aromatase and hydroxysteroid dehydrogenases. 3β-HSD denotes 3β-hydroxysteroid dehydrogenase, 17β-HSD 17β-hydroxysteroid dehydrogenase, 17-KSR 17-ketosteroid reductase, DHEA dehydroepiandrosterone, P-450 cytochrome P-450, SCC side-chain–cleavage enzyme, CYP17 17β-hydroxylase, CYP21 21-hydroxylase, CYP11 11β-hydroxylase, E_1 oestrone and E_2 oestradiol. Adapted from Clemons and Goss, 2001.

1.3 Oestrogen receptors

Critical evidence that ERs existed in oestrogen target tissues such as the uterus originated from the demonstration of high affinity binding sites for 17-tritiated oestradiol in the rat uterus (Jenson and Jacobson 1962). The first ER gene was cloned in 1986 (Green *et al.*, 1986b, Greene *et al.*, 1986) and together with the androgen, glucocorticoid and mineralocorticoid receptors was one of the founder members of a superfamily of ligand activated transcription factors that channel the actions of steroid hormone as well as retinoids and thyroid hormones (Katzenellenbogen and Katzenellenbogen, 1996, Escriva *et al.*, 2000). The nuclear receptor superfamily is regarded as one of the most significant groups of transcriptional regulators in eukaryotes playing a key role regulating the expression of hormone-responsive genes (Tsai and O'Malley, 1994a, Robinson-Rechavi *et al.*, 2003). Based on phylogenetic analysis of vertebrates it has been proposed that this family evolved from a common

ancestral gene that most closely resembles the sequence of an ER (Thornton, 2001). The pioneering studies that isolated the sex steroid receptors led to subsequent isolation of a large number of related proteins to the extent that the superfamily now also includes a number of proteins currently classified as 'orphan' receptors because they have no known ligand (Mangelsdorf *et al.*, 1995, Giguere, 1999). Grouping of steroid hormone receptors (SHRs) into four subtypes (I-IV) was proposed based on the nature of the binding of family members to deoxyribonucleic acid (DNA) (Mangelsdorf *et al.*, 1995). This is illustrated in Fig. 1.3. The binding of oestrogen receptors to direct palindromic repeat sequences known as EREs is covered in detail in section 1.4.2.

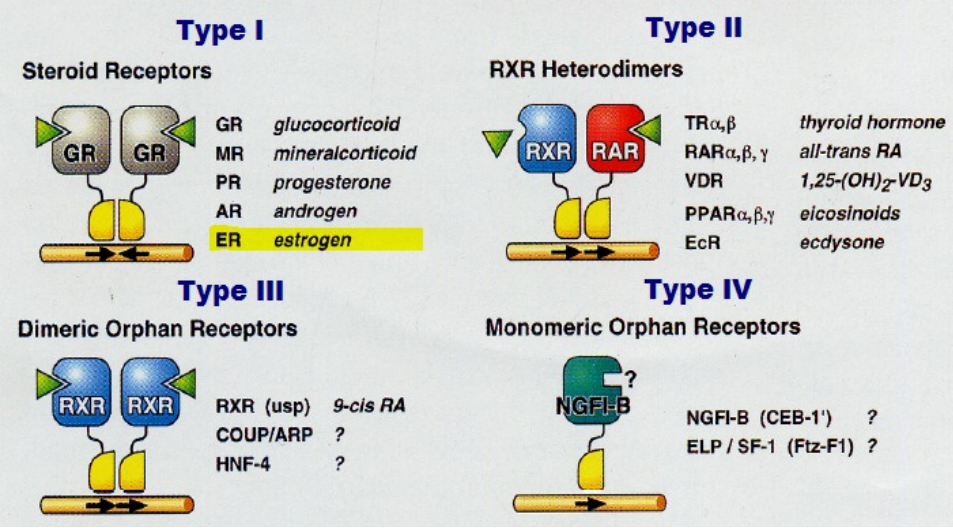

Figure 1.3 Nuclear receptor classification system.
Type I receptors are ligand-inducible receptors that bind palindromic DNA half-sites. Type II receptors constitutively bind DNA at direct repeat sequences. Type III receptors have undefined ligands ('orphan receptors') and bind as homodimers at direct repeats. Type IV orphan receptors bind DNA as monomers (adapted from Mangelsdorf et al., 1995).

More recently, cluster analysis based on patterns of expression of SHRs in mouse tissues and information relating to their impact on gene expression has been used to classify the receptors into five functional groups. Notably in this scheme ERs are assigned to group IB together with the receptors for androgens (androgen receptor,

AR) and progestins (progesterone receptor, PR) that each play a key role in formation and function of reproductive tissues (Bookout *et al.*, 2006) (Fig. 1.4).

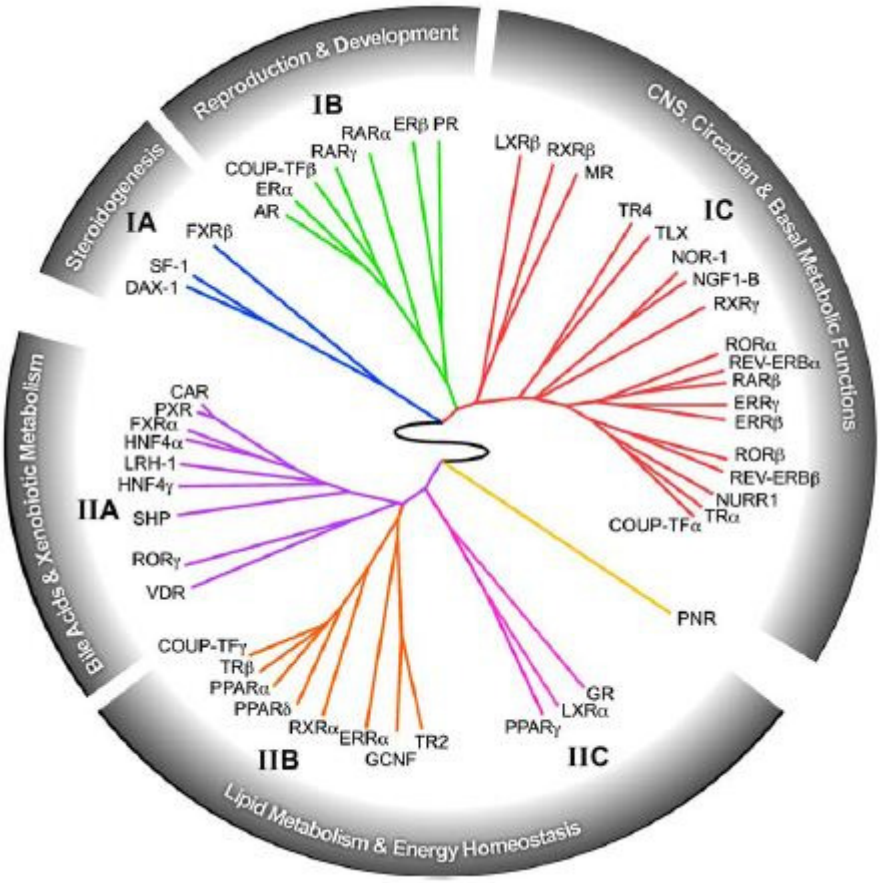

Figure 1.4 Nuclear receptor classification according to expression pattern and function.

This analysis revealed a higher-order network linking nuclear receptor function to reproduction, development, central, and basal metabolic functions, dietary-lipid metabolism, and energy homeostasis. Taken from Bookout et al., 2006.

1.4 Structural organisation of oestrogen receptors

In common with other members of the SHR superfamily, oestrogen receptors are composed of five distinct structure/function domains (Fig. 1.5). These are: an N-terminal A/B domain, a DNA-binding (C) domain (DBD), an interacting hinge (D) region and a ligand-binding (E/F) domain (LBD) (Griekspoor *et al.*, 2007).

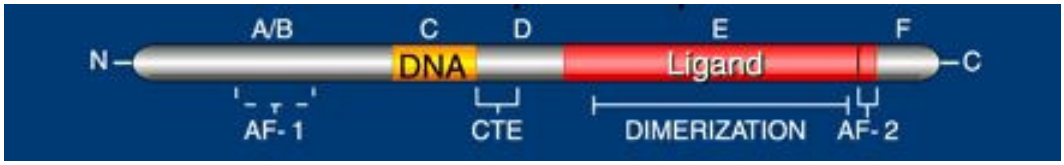

Figure 1.5 Structural organisation of the nuclear receptor superfamily.

The N-terminal A/B domain comprises the first of two activation function domains (AF-1), the C domain is responsible for receptor tethering to the DNA, the D domain is a hinge region that has been shown to encompass a carboxyl terminal extension (CTE) for optimal DNA binding of the androgen receptor, the E domain facilitates binding of ligand and is the location of the constitutive AF-2 sequence, the functionality of the C-terminal F domain is largely unknown. Adapted from Olefsky, 2001.

The functional activity of the different domains of the oestrogen receptors has been deciphered by studies *in vitro*, receptor modelling and domain swapping (Klinge, 2001, Metzger *et al.*, 1995, Tanenbaum *et al.*, 1998) and are covered in more detail in the subsequent subsections (1.4.1 to 1.4.4 inclusively).

ERα and ERβ are transcribed from two genes, *ESR1* and *ESR2*, found on different autosomes, and both receptor proteins are encoded by 8 exons. The relationship between the exons and the domains they each encode is summarised below (Fig. 1.6A). Although ERα and ERβ share a common structural architecture and both are able to bind oestrogenic ligands, the two ER proteins differ in their patterns of expression (Saunders *et al.*, 1997, Saunders *et al.*, 2000, Saunders *et al.*, 2001, Saunders and Critchley, 2002) and function (Enmark *et al.*, 1997).

Human ERα and ERβ share a high degree of homology at the DBD (96%) (Mosselman *et al.*, 1996) and consequently have been shown to similarly bind *cis*-acting ERE sites (Pettersson and Gustafsson, 2001a). Differences in their sequence homology at the LBD (~59% homology) (Fig. 1.6B), the smaller (20%) ligand-binding cavity of ERβ (Brzozowski *et al.*, 1997, Pike *et al.*, 1999) and the individual characteristic repertoires of coregulators (Warnmark *et al.*, 2001, An *et al.*, 2001) account for the differential response of the two ERs to certain ligands (including

xenoestrogens and phytoestrogens) and the LBD is the target domain for pharmacological exploitation in the development of novel ER selective therapeutics (Barkhem *et al.*, 1998, Sun *et al.*, 1999, Routledge *et al.*, 2000, Hall and Korach, 2002).

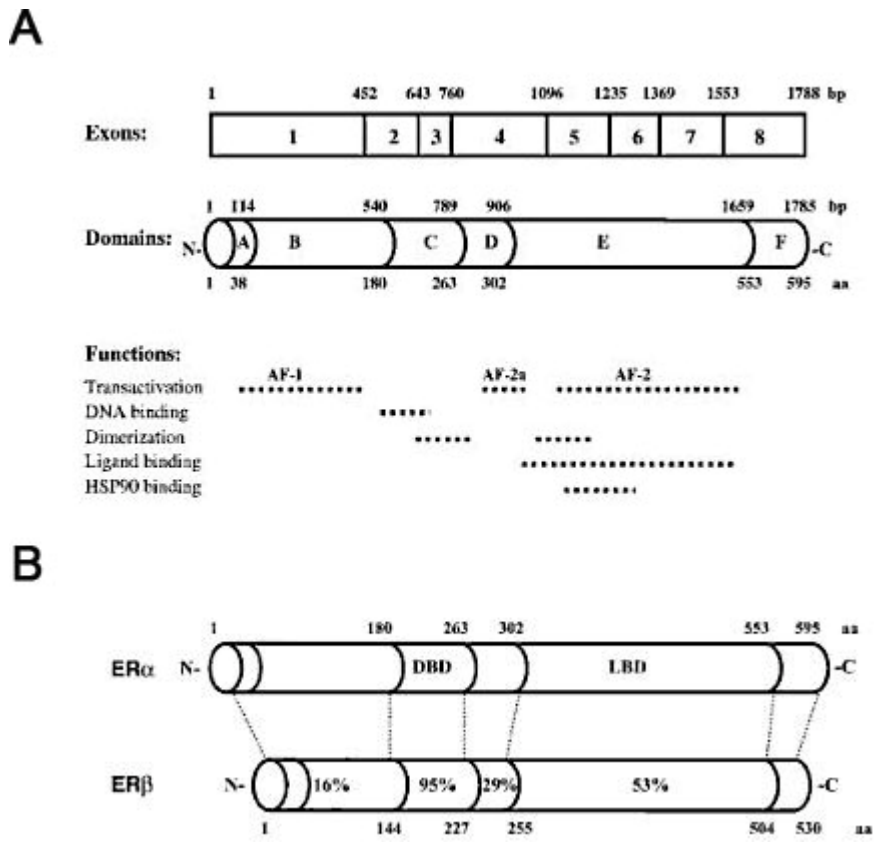

Figure 1.6 Schematic overview of ERα and ERβ structural architecture.
A. The top exon structure is aligned to the functional domains encoded by each exon. The function of each domain is outlined below the structural outline; B. Comparative analysis of ERα and ERβ functional domain homology (Adapted from Schiff, 2002).

Alternative splicing of the pre-messenger ribonucleic acid (mRNA) wild type ERs has rendered numerous additional isoform variants that have broadened the diversity of the proteome and may also have an impact on the activities of their full-length counterparts. The human ERα isoforms are largely lacking the full complement of coding exons (Poola *et al.*, 2000) (section 1.5.1) while many of the defined human ERβ variants arise from differing sequences at the C terminus (exon 8) (Moore *et al.*, 1998, Poola *et al.*, 2002) (section 1.6.1).

1.4.1 The A/B domain

The N-terminus of the oestrogen receptors is the least conserved between the steroid receptor family members. For example the amino acid sequences of human ERα and ERβ only have ~16% identity (Schiff, 2002). This region contains the first of two acidic transactivational function domains called the activation-function 1 (AF-1). Ligand-dependent phosphorylation of ERα by mitogen activated protein kinase signalling pathways at serine residues 104, 106 and 118 has been shown to potentiate AF-1 activity (Ali *et al.*, 1993, Le Goff *et al.*, 1994a) (section 1.7.4 and 1.10.1). The AF-1 of ERα has been demonstrated to be receptive to coactivator recruitment of steroid receptor coactivator 1 (SRC-1) (Onate *et al.*, 1998) and glucocorticoid receptor-interacting protein-1 (GRIP1), members of the p160 family of coactivators (Webb *et al.*, 1998) (section 1.9.1). Studies examining the function of ERα AF-1 in chinese hamster ovary cells suggest that AF-1 synergises with AF-2 at the C-terminal of the protein under the influence of SRC-1 to enhance agonist-mediated activity (McInerney and Katzenellenbogen, 1996). Domain swapping experiments involving alteration of the A/B domains between ERα and ERβ determined an improved transcriptional activity profile of ERβ chimera when fused to the A/B domain of ERα in human endometrial cancer (HEC-1) and human breast cancer (MDA-231) cells. Furthermore the ERβ chimeric cells demonstrated an anti-oestrogen agonist response with 4-hydroxy-tamoxifen that is not observed with ERβ alone, implicating the A/B domain of ERα for these specific responses (McInerney *et al.*, 1998). Subsequently, a study investigating the co-expression of ERα and ERβ in MDA-MB-231 cells established the dominant negative effects of ERβ in a heterodimer with ERα in response to anti-oestrogen stimulation are AF-1 dependent (Gougelet *et al.*, 2007).

1.4.2 The DNA-binding (C) domain

The DBD of SHRs is highly conserved and shares ~97% homology between human ERα and ERβ (Enmark *et al.*, 1997). The DBD is composed of two cysteine-rich zinc finger domains, two α-helices, a number of sequence elements designated P, D, T and A boxes and a COOH tail involved in sequence recognition and dimerisation (Umesono and Evans, 1989, Klinge, 2001, Pike *et al.*, 1999). The zinc finger

sequences, EGCKAF in finger one and CPATNQC of the second finger are specifically involved in promoter sequence recognition at the ERE and dimerisation of the ERs respectively (Forman and Samuels, 1990, Pettersson and Gustafsson, 2001b) (section 1.8). Molecular modelling of DBDs from type I nuclear receptors bound to DNA has revealed specific binding at a palindromic sequences comprising two consensus half sites (Luisi *et al.*, 1991, Schwabe *et al.*, 1993) that is regulated by P box activity (Germain *et al.*, 2006) in contrast to type II NRs that constitutively bind at direct repeats of their specific promoter sites (Tsai and O'Malley, 1994b).

1.4.3 The D (hinge) domain

Domain D is a flexible hinge region that harbours a nuclear localisation signal in SHRs and precludes steric hindrance by activated DBD and LBD conformational changes. This region is poorly conserved amongst SHR family members (Robinson-Rechavi *et al.*, 2003).

1.4.4 The ligand-binding (E/F) domain

In addition to determining ligand binding and specificity, the LBD has roles in nuclear localisation, dimerisation, chaperone binding and coregulator recruitment through the second of the activation function domains AF-2 (Griekspoor *et al.*, 2007). Crystallography studies have determined the secondary structure of the carboxyl-terminal LBD as an α-helical 'sandwich' that encompasses twelve α-helices (Helix 1-12) with a short β-turn (s1-s2) (Bourguet *et al.*, 1995, Tanenbaum *et al.*, 1998). Helix 12 behaves as a 'molecular switch' that can form multiple response conformations that can dictate the type(s) of co-regulatory proteins recruited to the receptor-ligand complex (Fig. 1.7). For example, following binding of an agonist, the helix 12 adopts a stable structure in which it locks the ligand into a cavity, exposes specific sequences on the protein in the AF-2 domain and enables binding of coactivators (Fig 1.7A and B). Conversely, x-ray crystallography structural studies have revealed antagonist binding to the ERα and ERβ results in an 'inhibitory' orientation of helix 12 that prohibits AF-2 activity and hinders the recruitment of coregulators (Fig. 1.7C) (reviewed in Pike, 2006). The AF-2 is composed of residues from helices 3, 4, 5 and 12 that form a shallow hydrophobic cleft (Henttu *et al.*,

1997, Wurtz *et al.*, 1996) that recognises and accommodates the LxxLL motif (NR box; L = leucine, x = any amino acid) of co-regulator proteins such as members of the p160 family of proteins (Heery *et al.*, 1997, Kalkhoven *et al.*, 1998). The sequence homology between the LBD of ERα and ERβ is ~53% which is accountable for the selectivity of different natural oestrogens and selective oestrogen receptor modulators (SERMS) for these subtypes (Enmark *et al.*, 1997) (section 1.10.3). The F domain is highly variable among NRs and the function remains unknown (Robinson-Rechavi *et al.*, 2003).

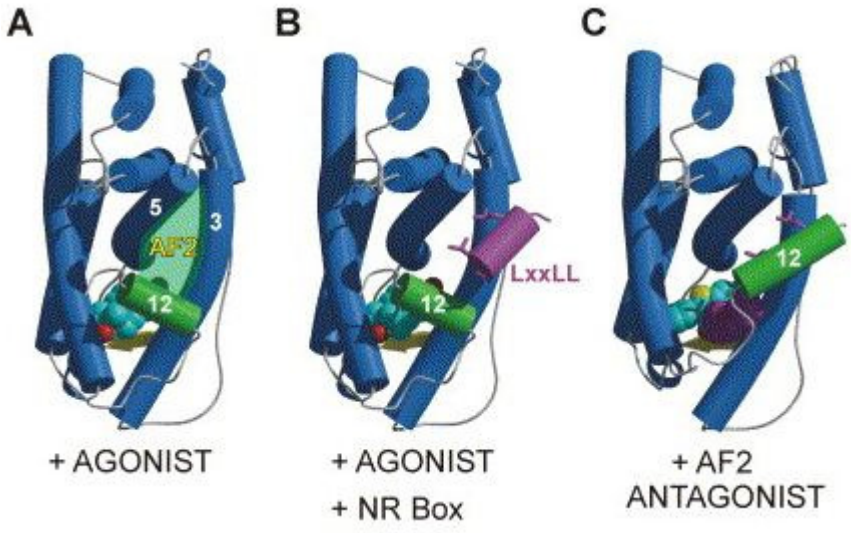

Figure 1.7 Schematic models illustrating the unique conformations adopted by the ER ligand-binding domain (LBD) in response to ligand.
A. The binding of an agonist (e.g. E2) facilitates the 'on' conformation of helix 12 (green cylinder) and active state of AF-2; B. Adoption of the agonist-mediated conformation enables coactivator interaction of the LxxLL sequence motif (purple cylinder) at the hydrophobic AF-2 groove; C. Antagonist (e.g. raloxifene) binding at the LBD displaces helix 12 and occludes the coactivator binding groove. Taken from Pike, 2006.

1.5 Oestrogen receptor alpha (ERα)

ERα was originally cloned and characterised from the MCF-7 breast cancer cell line (Walter *et al.*, 1985, Green *et al.*, 1986a). The gene was identified as a 14-kb DNA sequence comprising eight exons localised to human chromosome 6q25.1 (Ponglikitmongkol *et al.*, 1988, Reid *et al.*, 2002). This gene (*ESR1*) encodes a protein of ~66kDa with 595 amino acids with a high binding affinity for oestradiol

(K_D ~ 0.4nM) (Green *et al.*, 1986b). ERα protein conforms to the signature modular structure of the NR superfamily (section 1.4) and is transcribed from at least three different promoter sites (Green *et al.*, 1986b, Keaveney *et al.*, 1991, Grandien, 1996). ERα is widely expressed, notably within in female reproductive tissues and the breast, the growth of which is regulated by oestradiol. ERα protein has been immunolocalised to the uterine vascular smooth muscle cells (tunica media) (Perrot-Applanat *et al.*, 1988), the granulosa cells of mature antral follicles and the surface epithelium of the ovary (Saunders *et al.*, 2000), the stromal and epithelial compartments of the mammary gland (Pelletier and El-Alfy, 2000) and to stromal and epithelial compartments of the endometrium with decreasing levels of mRNA and protein detected in the functional endometrial layer coincident with advancement of the menstrual cycle (Critchley, 2000, Saunders and Critchley, 2002).

1.5.1 ERα splice variants

Two splicing variants of the full-length human ERα protein have been described (Fig. 1.8). ERα-46 is a protein with a molecular weight of 46kDa and is transcribed from an mRNA splice variant of the ERα gene that lacks sequences encoded by exon 1. As a result the protein lacks the first 173 amino acids of the A/B domain (Flouriot *et al.*, 2000). Expression of ERα-46 *in vitro* suggested a role for the protein as a dominant inhibitor of the ERα-66 splice variant. ERα-46 has been shown to actively and preferentially heterodimerise with its full length homologue and has been detected in osteoblasts and vascular endothelial cells (Denger *et al.*, 2001b, Russell *et al.*, 2000). It has been proposed that the ERα-46 isoform is subject to post-translational modification by palmitoylation after which it becomes membrane-associated, activates endothelial nitric oxide synthase (eNOS) production and channels E2-mediated signals to the endothelium (Li *et al.*, 2003).

A second splicing variant of ERα generated by a promoter sequence in the first intron of the full-length receptor is ERα-36. This isoform was cloned from HEK293 cells and is devoid of both transactivation functions; AF-1 and AF-2 but has retained DNA-binding function and dimerisation capability (Wang *et al.*, 2005). Like ERα-46

it has been suggested that the ERα-36 variant can mediate membrane-initiated oestrogen signalling (Li *et al.*, 2003, Wang *et al.*, 2005).

Figure 1.8 Structure of ERα isoforms.
The primary functional domains; AF-1, DBD and LBD (AF-2 within) are outlined. The short length splice variants ERα-46 and ERα-36 are devoid of the N-terminal A/B structural domain. (Adapted from Heldring et al., 2007).

1.6 Oestrogen receptor beta (ERβ)

The cloning of a second oestrogen receptor, usually known as ERβ, from the rat prostate in 1996 (Kuiper *et al.*, 1996) and its localisation to the granulosa cells of the rat ovary was followed by the identification of a homologous protein in human (Mosselman *et al.*, 1996). The human gene (*ESR2*) was subsequently localised to 14q23.2 (Enmark *et al.*, 1997). The full length human ERβ protein is 58kDa in size but a second 'short type' receptor that lacks the first 54 amino acids of its full length counterpart and is 53kDa arising from internal ribosomal entry has been described (Denger *et al.*, 2001a). Expression of ERβ protein in female reproductive tissues has been localised to the granulosa cells of the follicles within the ovary (Saunders *et al.*, 2000), stromal and epithelial compartments of breast tissue (Pelletier and El-Alfy, 2000) and the stroma, epithelium and exclusively the endothelial cells of the endometrium (Critchley *et al.*, 2001). In addition, ERβ protein expression has been determined in a wide range of human tissues including the lungs, kidney, heart and most regions of the brain (except hippocampus that exclusively expresses ERα) (Taylor and Al-Azzawi, 2000) as well as in cancers such as breast cancer tissue (Saunders *et al.*, 2002) suggesting a potential role for this isoform in the mediation of oestrogenic transcriptional activity both in reproductive and non-reproductive tissues.

1.6.1 ERβ splice variants

Multiple C-terminal truncated protein isoforms of human ERβ (ERβ2-5) that diverge at amino acid 469 of the wild type receptor have been determined that result from the alternative splicing of the last exons (exon 8 and 9) (Fig 1.9A) (reviewed in Scobie *et al.*, 2002, Leung *et al.*, 2006, Zhao *et al.*, 2008).

ERβ2/ERβcx encodes a protein composed of 495 amino acids including a signature 26 amino acid sequence in place of the last 61 amino acids of ERβ at its carboxyl terminal domain (Moore *et al.*, 1998). Similarly to ERβ, the use of alternative ATG sites within the ERβ2 coding sequence results in long and short forms of the splice variant with protein weights of 55kDa and 51kDa respectively (Ogawa *et al.*, 1998c). Crystallography studies have revealed that this protein has an incomplete AF-2 domain and disoriented Helix 12 that is consistent with studies that suggest this variant does not activate reporter genes in response to incubation with oestrogenic ligands (Leung *et al.*, 2006, Ogawa *et al.*, 1998c). However, ERβ2 is reportedly capable of forming heterodimers (preferentially with ERα) (Ogawa *et al.*, 1998c, Zhao *et al.*, 2007). Unlike ERβ2, the molecular models demonstrate that ERβ4 and ERβ5 are completely devoid of Helix 12 (Leung *et al.*, 2006) (Fig. 1. 9B) and *in vitro* studies have reported formation of mixed dimers with full length ERs (Poola *et al.*, 2005a). ERβ4 has a unique sequence encoded by an exon between the ERβ and SYNE2 genes and the signature 3' sequence of ERβ5 is the product of a retained sequence betweens exons 7 and 8 (Poola *et al.*, 2005a).

Expression of ERβ2 has been detected in endothelial cells within the placenta, granulosa cells of the ovary and stromal and epithelial cells in the normal endometrium throughout all phases of the cycle of the human female reproductive tract (Scobie *et al.*, 2002, Critchley *et al.*, 2002). ERβ3 mRNA expression has only been described in the testis (Moore *et al.*, 1998). There are several studies addressing the expression and putative role of the ERβ truncated isoforms in the aetiology of tumourigenesis and as novel biomarkers in cancer tissues. Shaaban *et al.* have demonstrated the importance of identifying ER localisation with a correlation

between ERβ2 cytoplasmic expression and reduced overall survival but conversely better outcome for patients with nuclear ERβ2 expression (Shaaban *et al.*, 2008). Furthermore, ERβ2 expression is associated with a favourable outcome in endometrial cancer where downregulation was associated with endometrioid cancer progression (Chakravarty *et al.*, 2007). Increased ERβ5 mRNA transcript levels were determined in breast (Park *et al.*, 2006) and endometrial carcinoma when compared with normal endometrial specimens (Skrzypczak *et al.*, 2004) and in breast cancer cell lines when compared with ERβ levels (Leygue *et al.*, 1999b).

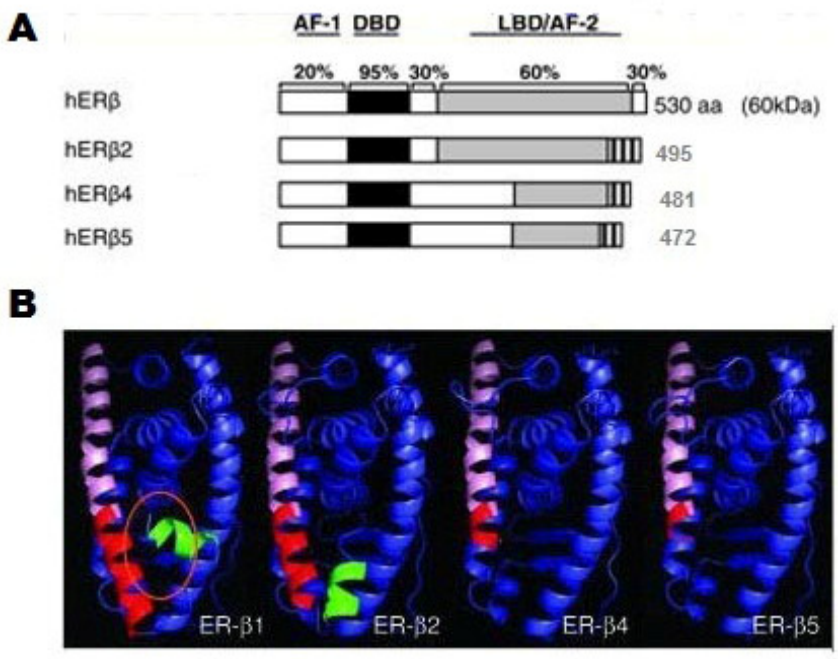

Figure 1.9 Structure of ERβ isoforms.
Comparison of the structural domains of ERβ splice variants reveals divergence at the carboxy (C)-terminus LBD (A). Molecular modelling reveals disruption at the C-terminus translates to disruption of helix 12 (green) optimal positioning (ERβ2) and complete ablation of helix 12 from ERβ4 and ERβ5 (B). Adapted from Heldring et al., 2007 and Leung et al., 2006.

1.7 Mechanisms of oestrogen receptor dependent gene activation

Four molecular pathways mediated by oestrogen receptors have been identified, three of which are dependent upon binding of receptor(s) to oestrogenic ligands (Fig. 1.10). These modes of activation can be summarised as 1) direct binding to DNA at oestrogen response elements (ERE-dependent), 2) ERE-independent activity involving indirect binding to DNA at AP-1 or Sp1 sites, 3) non-genomic activity and 4) steroid ligand-independent activation resulting from phosphorylation downstream of growth factor-dependent cascades (reviewed in Hall *et al.*, 2001, Nilsson *et al.*, 2001, Heldring *et al.*, 2007).

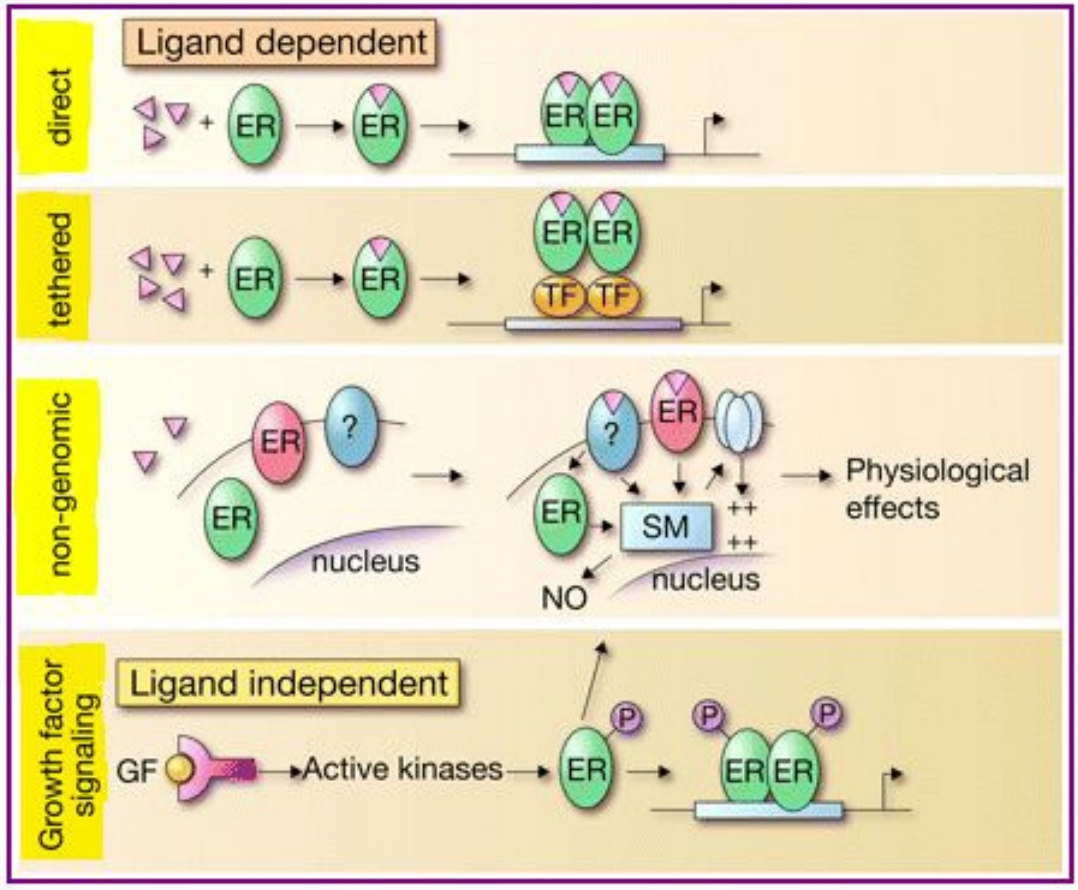

Figure 1.10 Overview of the distinct regulatory pathways of ER actions
1. Canonical ligand-dependent ER activation enables binding at the ERE. 2. ERE-independent genomic action makes use of transcription factors such as c-fos and c-jun and bind at alternative promoter sites (e.g. AP-1 sites). 3. Non-genomic membrane-ER signalling via protein-kinase cascades. 4. Ligand-independent genomic actions potentiated by growth factor mediated signalling (Adapted from Heldring et al., 2007).

1.7.1 Ligand-dependent gene activation

The characteristic activation paradigm of the Type I NRs (including both ER subtypes) involves disruption of the association of receptor binding to heat shock proteins (hsp56, hsp70 and hsp 90) and corepressors (Onate *et al.*, 1998). Ligand-binding induces dissociation from this multiprotein inhibitory complex and a conformational change of the receptor such that it can dimerise (McKenna *et al.*, 1999), and the newly-exposed DBD can bind DNA. ER DNA-binding at the core *cis*-acting consensus 13bp ERE sequence 5'-GGTCAnnnTGACC-3' was first identified in the *Xenopus* vitellogenin A2 gene promoter (Klein-Hitpass *et al.*, 1988). Additional non-consensus EREs have also been identified (Berry *et al.*, 1989) and it has been reported that the ER-ERE binding affinity can be modulated by flanking regulatory factors such as hsp70 (Driscoll *et al.*, 1998). The subsequent interaction with coregulatory proteins (through the transactivation function domains AF-1 and AF-2) and other transcription factors stabilises the DNA-bound ERs and facilitates binding of ribonucleic acid (RNA) polymerase II and initiation of transcription (reviewed in Zawel and Reinberg, 1995). More recently however, there is data to suggest that the ER interaction with ERE motifs is insufficient for receptor-chromatin association and the search for additional binding sites by chromosome-wide mapping has revealed additional sites in close proximity to the ERE consensus sequences such as the Forkhead factor sites (Carroll *et al.*, 2005). Chromatin immunoprecipitation (CHIP)-microarray mining has revealed that binding of the Forkhead factor FoxA1 to these numerous specific sites is involved in directing and tethering ERα to the chromatin while ERβ-bound regions tend to cluster at GC-rich sites and consequently drive oestrogen-mediated transcription (Carroll and Brown, 2006).

1.7.2 ERE-independent gene activation

The non-classical ERα-dependent activation of genes has been demonstrated through ER interaction with the Fos/Jun transcription factors (Jakacka *et al.*, 2001). Insulin-like growth factor-1 (IGF-1) and collagenase expression is mediated through the ER-Fos/Jun complex action at activator protein-1 (AP-1)/12-*O*-tetradecanoyl-phorbol-

13-acetate-responsive promoter sites *in vitro* (Philips *et al.*, 1993, Umayahara *et al.*, 1994, Webb *et al.*, 1995b). Differential ERα- and ERβ-mediated responses to E2 and the anti-oestrogen ICI 164, 384 have been demonstrated at the AP-1 site whereby ICI 164, 384 behaves as an agonist of ERβ (Webb *et al.*, 1995a, Paech *et al.*, 1997). ERα-AP-1 activation is mediated by the concerted effects of AF-1 and AF-2 that enable coactivator recruitment (Webb *et al.*, 1999) while the action of ERβ at AP-1 in response to the binding of SERMs has been shown to be AF-independent (Kushner *et al.*, 2000). Specific recruitment of histone deacetylases and corepressors from AP-1 to the SERM-ERβ complex underpins the AF-independent paradigm such that the AP-1 site is rendered free to transcribe incoming activation signals (Jackson *et al.*, 1997, Lavinsky *et al.*, 1998). Specificity protein 1 (Sp1) is another example of a ubiquitous transcription factor that channels ER-mediated signalling and binds DNA at specific consensus sequences 5'-GGCGGG-3' (GC boxes) in the presence and absence of ligand (Porter *et al.*, 1997). Co-operative action of ER and Sp1 has been exemplified in the regulation of cathepsin D, RARα and Hsp27 *in vitro* (Krishnan *et al.*, 1995, Rishi *et al.*, 1995, Porter *et al.*, 1996). Differences in E2-driven gene expression between ERα and ERβ is understood to partly stem from differential DNA binding patterns where ERα has been found to preferentially localise at TA-rich sites that include forkhead binding sites (section 1.7.1) while ERβ predominantly interacts with the chromatins at GC-rich motifs (Liu *et al.*, 2008).

1.7.3 Non-genomic gene activation

An alternative mode of ER-dependent gene activation is non-genomic signalling and involves extranuclear ER that induces post-translational modifications and indirect activation of gene expression within the nucleus (Watson and Gametchu, 1999, Mendelsohn, 2000). Investigations into the non-genomic actions of E2 have employed oestrogen-dendrimer conjugates that exist outside of the nuclear membrane and revealed a mechanistically distinct mode of ER activation via protein kinase signalling that can be abrogated by kinase inhibitors and anti-oestrogen compounds (Madak-Erdogan *et al.*, 2008). This study also determined a pool of genes that were preferentially expressed via extranuclear non-genomic signalling in MCF-7 cells (Madak-Erdogan *et al.*, 2008).

Plasma membrane ERα and ERβ comprises 5-10% of total cellular ER (Levin, 2009) and it has been reported that the membrane and nuclear forms of ER arise from the same gene transcript, share similar affinities for oestradiol (E2) (Razandi *et al.*, 2000) but differ in their response to the pure anti-oestrogen ICI 182, 780 (Gu *et al.*, 1999). Membrane ER and other E2-binding proteins such as the orphan G protein-coupled receptor, GPR30 have been implicated in the rapid E2-dependent signalling to downstream kinase cascades (Levin, 2009, Prossnitz *et al.*, 2008, Revankar *et al.*, 2005). For example, the vascular protective function (vasodilation) of E2 is mediated via the activation of eNOS by the interaction of membrane-ER with tyrosine kinases. Specifically, E2-bound membrane ER has been shown to bind the p85α subunit of the phosphatidylinositol-3-OH kinase at the caveolae (plasma membrane microstructures) that in turn leads to eNOS production (Simoncini *et al.*, 2000). Further non-genotropic functions of ER activity include maintenance of bone density via activation of an Src/Shc/ERK-dependent pathway (Kousteni *et al.*, 2001) and anti-apoptotic effects *in vitro* (Razandi *et al.*, 2000).

1.7.4 Ligand-independent gene activation

Extracellular signals can also activate the ERs as a consequence of phosphorylation in the absence of oestrogenic ligands (Cenni and Picard, 1999). Seminal studies in the 1980's demonstrating a role of analogues of cyclic adenosine monophosphate (cAMP) in replacing progesterone-mediated reproductive activity in ovariectomised rats were the first to identify the potential for ligand-independent activation of NRs in regulating gene expression (Beyer *et al.*, 1981). Subsequently ERα-dependent induction of progesterone receptor expression in response to incubation with insulin-like growth factor was demonstrated in MCF-7 cells (Katzenellenbogen and Norman, 1990). Phosphorylation of ERα and ERβ at specific serine and threonine residues potentiates transcriptional function in the presence of oestrogenic hormones as well as peptide growth factors through mitogen-activated protein signalling cascades *in vitro* (Kato *et al.*, 1995d) (section 1.11.1) and expression of the regulatory subunits of cyclin-dependent kinases (CDKs); cyclin D1 (Zwijsen *et al.*, 1998) and cyclin A (Trowbridge *et al.*, 1997). The activity of growth factor–mediated signalling cascades and cyclin D1 on ERs has been implicated in cancer development and

progression and been associated with the development of resistance to endocrine therapy during treatment of breast cancers (Picard *et al.*, 1997, Neuman *et al.*, 1997) (sections 1.11 to 1.11.3 inclusive).

1.8 ER dimerisation

Binding of oestrogenic ligands to the LBD of both ERα and ERβ induces a change in receptor conformation (see above) and favours formation of homo or hetero-dimers depending upon whether one or more subtype is expressed in the cell (Fig. 1.11). In a particular cell context, the formation of hetero-dimers in response to binding of oestrogenic ligands *in vivo* in mice adds to the complexity of ER regulatory and signalling patterns (Pettersson *et al.*, 1997). It has been reported that the ERα-ERβ conformation is a more favourable arrangement compared with ERβ homo-dimers for binding at the ERE (Cowley *et al.*, 1997). In common with homodimers, the ERα-ERβ hetero-dimer actively recruits members of the p160 family of coactivators (Cowley *et al.*, 1997). Moreover, mutation studies have revealed that only the DBD of ERα is a pre-requisite for formation of a ERα-ERβ hetero-dimeric complex (Pace *et al.*, 1997) and as such, this is competent when only one receptor within the dimer can actively bind ligand (Tremblay G.B. *et al.*, 1999) (section 1.4.2). Studies using hetero-dimeric complexes have elucidated that the dominant effects of one partner that can determine the efficacy of the activity of the complex, specifically the ERβ-selective responses of an ERα-ERβ heterodimer to 4-hydroxytamoxifen (4HT) and basal levels of E2 (Hall and McDonnell, 1999). Differential activation of reporter gene expression by ERα and ERβ homo-dimers also occurs at the AP-1 binding site where ERβ opposes signalling in response to E2 and behaves as a transcriptional inhibitor in response to incubation with 4HT and the anti-oestrogen ICI 164, 384 (Paech *et al.*, 1997).

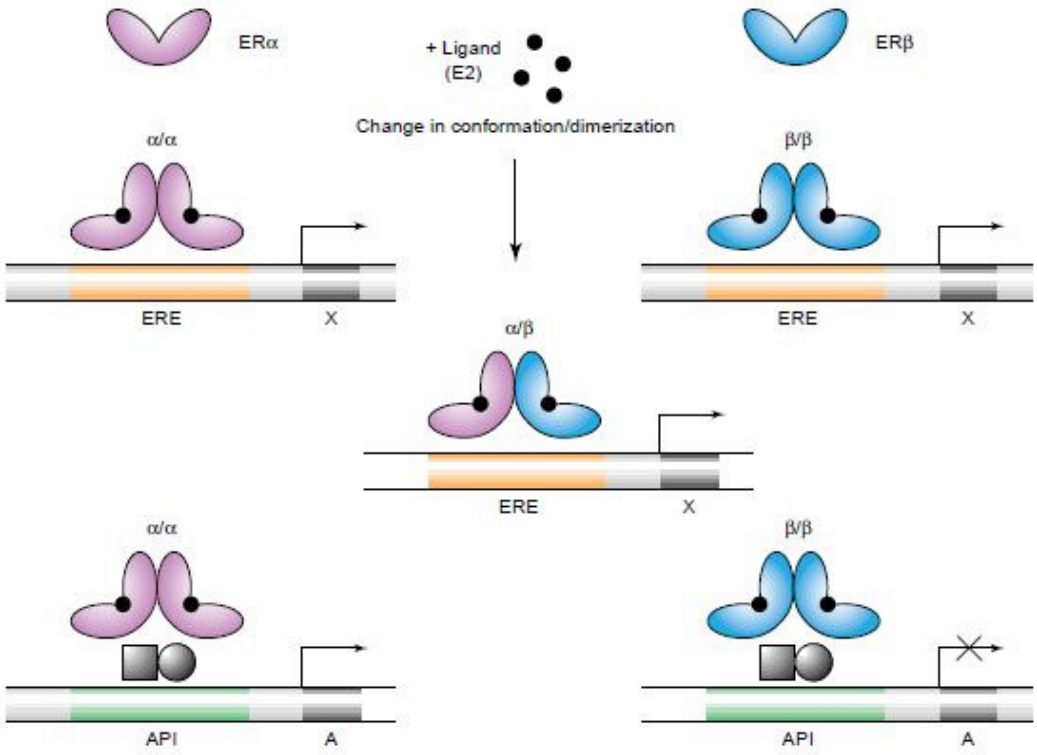

Figure 1.11 Schematic overview of ERα/ERβ homo- and hetero-dimerisation patterns.

Taken from Saunders, 1998.

1.9 ER transcriptional coregulators

Evidence for additional modulatory factors impacting on the function of NRs stemmed from preliminary studies that revealed the phenomenon of 'squelching' between competing receptors on promoter sequences (Gill and Ptashne, 1988, Meyer *et al.*, 1989). ER coregulators play a critical role as mediators of transcriptional regulation through direct interaction at the pre-initiation complex and covalent modifications at the DNA double-helix. The ER coregulators also serve as points of convergence for integrating ligand-dependent and independent signalling pathways (Robyr *et al.*, 2000). Coactivators are transactivation factors that function to enhance transactivation by acetyltransferase activity and conversely the corepressor interaction with ERs reduces transcription through histone deacetyltransferase activity (Fig. 1.12) (reviewed in O'Malley *et al.*, 2008).

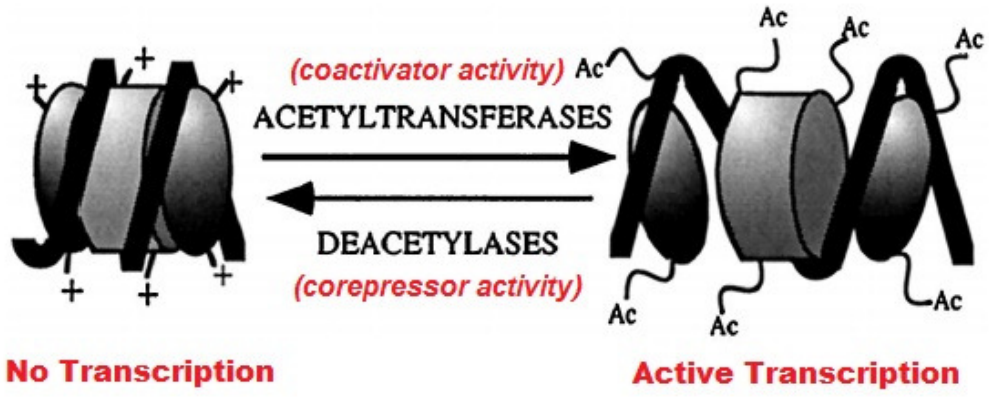

Figure 1.12 Opposing actions of co-regulator activity.

Coactivators behave as histone acetyltranferases (HATs) that disrupt the nucleosomal structure and facilitate ease of access by the transcriptional machinery. Corepressors exhibit histone deacetylase (HDAC) activity that controls the loss of acetyl groups from individual nucleosomes causing condensation of the chromatin and blocking access by the transcriptional activation complex. (Adapted from McKenna et al., 1999).

1.9.1 ER coactivators

The initial characterisation of the SRC-1/NCoA-1 protein (Onate *et al.*, 1995) led to the subsequent unveiling of a complete myriad of structurally and functionally related modular factors termed the p160 family of coactivators that bind at the AF-2 domain of ER LBDs through LxxLL motifs (Heery *et al.*, 1997). This family of coactivators also includes SRC-2/human homolog of glucocorticoid receptor-interacting protein 1, the transcriptional intermediary factor 2 (TIF2) and SRC-3/amplified in breast cancer-1 (AIB-1) (McDonnell and Norris, 2002). These SRC coactivators contain multiple LxxLL motifs that facilitate binding to NRs following their conformational changes in response to ligand-binding (Heery *et al.*, 2001). In addition, the coactivators are composed of two conserved activation domains (AD1 and AD2) that are involved in the recruitment of secondary coactivators, an amino-terminal basic helix-loop-helix/Per-Arnt-Sim (bLHL-PAS) region and a protein dimerisation domain (Belandia *et al.*, 2002).

A number of other coactivators that also behave as histone acetylases to remodel the chromatin structure and enable better accessibility of the basal transcription machinery are targeted to the AF-2 domain of ERs. These include the cointegrator

cAMP response element-binding (CREB)-binding protein (CBP)/p300, thyroid hormone receptor activating protein (TRAP)/DRIP (Heery *et al.*, 2001) and the activating signal co-integrators 1 and 2. CBP/p300 has intrinsic histone acetyltransferase activity and acetylation of the specific sequences K266 and K268 of the hinge region (D) of ERα enhances receptor DNA binding (Subramanian *et al.*, 2008).

Recruitment of coactivators to the AF-1 domain of ERα and ERβ by steroid receptor RNA activator (SRA) and exclusively to ERβ by the p68 RNA helicase has also been described (Lanz *et al.*, 1999, Endoh *et al.*, 1999). Adding to the complexity of the ER transcriptional apparatus is a further layer of secondary coactivators that indirectly act on the ERs through the aforementioned p160 coactivators which in turn act as bridging molecules. These include the arginine-specific protein methyltransferases; PRMT1 and coactivator associated arginine methyltransferase 1 that bind at the C-terminal AD2 of the p160 proteins (Stallcup *et al.*, 2000) and coiled-coil coactivator that binds at the bHLHs/PAS domain of the p160 coactivators (Kim *et al.*, 2003). An overview of ER coactivators is presented in Table 1.1 below.

Table 1.1 ER coactivator listing of coregulators that enhance functional activity. *(Adapted from Hall and McDonnell, 2005).*

	CoFactor	Full Name	Other Names	Function	Interaction with ER
AF-2 Coactivators	SRC-1 (p160)	Steroid receptor coactivator-1	NCoA-1	HAT (Histone acetlytran-serase)	Binds ERs AF-2 through LXXLL motifs
	SRC-2 (p160)	Steroid receptor coactivator-2	GRIP1, TIF-2, NCoA-2	HAT	Binds ERs AF-2 through LXXLL motifs
	SRC-3 (p 160)	Steroid receptor coactivator-3	AIB1, ACTR, p/CIP, RAC3, TRAM-1, NCoA-3	HAT	Binds ERs AF-2 through LXXLL motifs
	CBP/p300	CREB-binding protein		HAT	Binds ERs AF-2 through LXXLL motifs
	TRAP220, TRAP/DRIP	Thyroid hormone receptor activating protein of 220 kDa	mediator; PBP		Binds ERs AF-2 through LXXLL motifs
	ASC-1 ASC-2	Activating signal cointegrator-1 Activating signal cointegrator-2	RAP250, TRBP, AIB3	Bind HATs and NRs	Binds ERs AF-2 through LXXLL motifs
AF-1 Coactivators	SRA	Steroid receptor activator		Splicing	Binds ERα AF-1
	p68	p68 RNA helicase		RNA helicase	Binds ERα AF-1
Secondary Coactivators	CARM1	Protein methyltransferase 1		Arginine histone methyltransferase	Binds ERs AF-2 indirectly through association with p160s
	PRMT1	Protein methyltransferase 1		Arginine histone methyltransferase	Binds ERs AF-2 indirectly through association with p160s
	CoCoA	Coiled-coil coactivator			Binds ERs AF-2 indirectly through association with p160s

1.9.2 ER corepressors

ER corepressors function to blunt ER activity and prevent hyperstimulation of ER signalling pathways. Corepressors act by occlusion of coactivator binding and histone deacetyltransferase activity (Table 1.2, Fig. 1.12). At unbound ERs, the nuclear corepressor (NCoR) and silencing mediator for retinoid and thyroid hormone receptors (SMRT) maintain the receptors in an inactive state that is disrupted following ligand binding (Chen and Evans, 1995, Horlein *et al.*, 1995). Like the LxxLL motif of the AF-2 coactivators, these corepressors contain two corepressors NR-interacting (CoRNR) boxes (Hu and Lazar, 1999). These proteins have also been shown to function indirectly through secondary cofactors such as mSin3, a histone deacetyltransferase linker molecule to mediate their inhibitory effect (Hu and Lazar, 2000).

Table 1.2 ER corepressors that decrease oestrogen stimulatory function.
(Adapted from Hall and McDonnell, 2005).

Compressor	Full Name	Function/Activity	Repression of ER	Interaction with ER
NCoR	Nuclear receptor corepressor	HDAC (Histone deacetylase)	Pharmacological	Binds ERs AF-2 through CoRNR box motifs
SMRT	Silencing mediator for retinoid and thyroid receptors	HDAC	Pharmacological	Binds ERs AF-2 through CoRNR box motifs
RIP140 (NRIP)	Receptor interacting protein of 140 kDa	Competes for AF-2 coactivator binding; associates with HDACs	Physiological and Pharmacological	Binds ERs AF-2 through LXXLL motifs
REA	Repressor of estrogen receptor activity	Interferes with SRC-1 access to the ERs	Physiological	Indirect
RTA	Repressor of tamoxifen transcriptional activity	Interferes with SRC-1 access to the ERs RNA binding; represses tamoxifen agonist activity through ERα	Pharmacological	Binds ER AF-1
mSiah2	Mammalian homolog of *Drosophila* Seven in absentia (sina)	Mediates cell-specific repression of NRs by targeting NCoR for proteasomal degradation	Pharmacological	Associates with ER indirectly through binding NCoR

1.10 ER Ligands

The most abundant oestrogen in human serum is 17β-oestradiol (E2) although two other oestrogens, oestrone and oestriol are also present and exhibit weaker agonist properties. E2 is a small hydrophobic lipophilic molecule structurally composed of four rings (A-D) that can bind both ERα and ERβ via the LBD (reviewed in Anstead *et al.*, 1997). E2 binding induces the conformational change and dimerisation of the occupied ER to facilitate recruitment of coregulators and binding at the DNA promoter sequence (section 1.7.1) (Fig. 1.13). The binding affinity of E2 for ER does not discriminate between the full-length receptor subtypes with IC_{50}s of 2.35nM and 1.98nMs determined for ERα and ERβ respectively (Harris *et al.*, 2002). Phytoestrogen is an umbrella term for plant oestrogens encompassing flavanoids, coumestans and lignans that occur naturally in the diet and demonstrate preferential binding affinity for the ERβ subtype (e.g. genistein) (Miller *et al.*, 2003). Epidemiological reports have advocated a role for these exogenous proteins as chemoprotectants (Messina *et al.*, 1994, Kurzer and Xu, 1997).

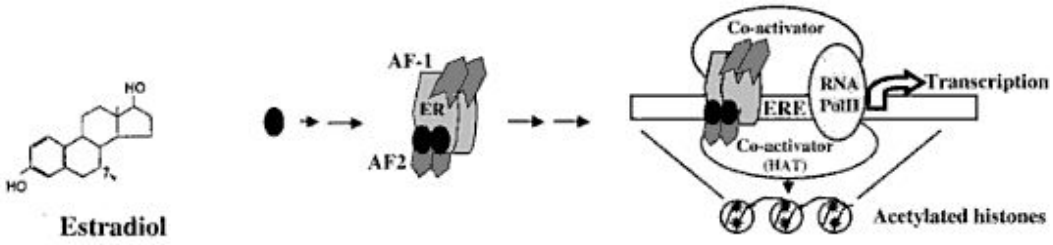

Figure 1.13 E2 binding enables activation at the ERE.
The chemical structure of oestradiol is outlined on the left hand side. E2 binding in the region of the AF-2 domain stimulates receptor conformational changes, dimerisation, recruitment of coregulators and the transcriptional machinery to form the pre-initiation complex at the ERE. Taken from Schiff, 2002.

The primary function of E2 is to mediate cellular differentiation and proliferation. Alterations in the regulation of this natural steroid and its metabolites is associated with tumourigenesis (reviewed in Yager, 2000). The current treatment modalities to combat excess E2 activity target 1) circulatory oestrogen levels directly with aromatase inhibitors or 2) the ER signalling path by antagonising ER function through endocrine therapy with SERMs and downregulating ER activity with the use of 'pure anti-oestrogens' (Fig 1.14).

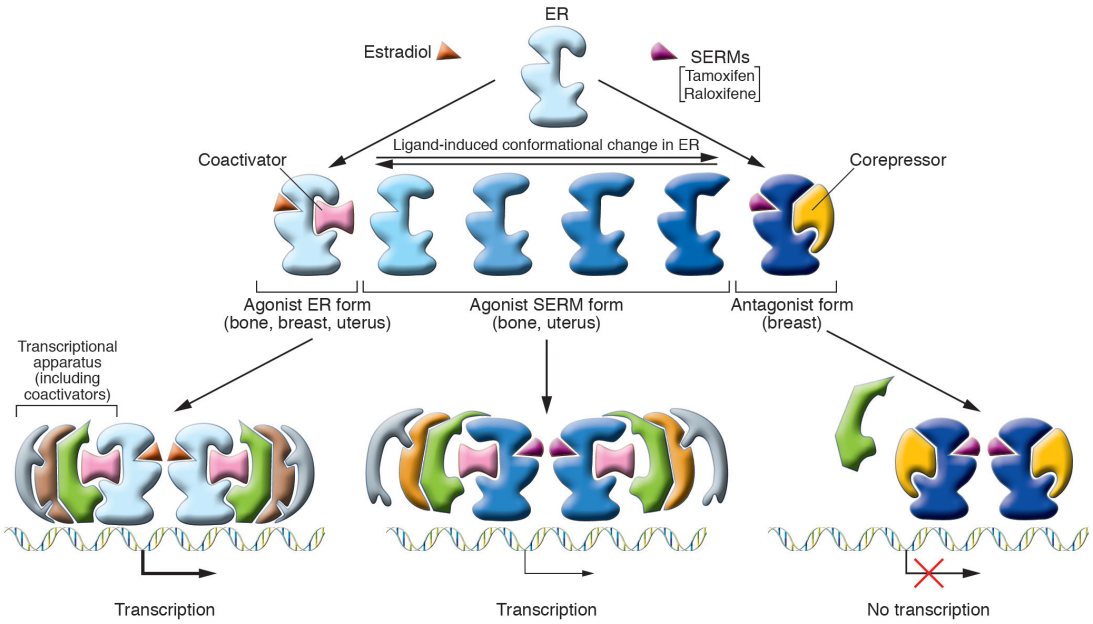

Figure 1.14 Schematic overview of ER agonist, antagonist and SERM activity.
Taken from Deroo and Korach, 2006.

1.10.1 ER Selective agonists

The differential expression profiles of the ER subtypes are suggestive of differences in their biological function at the tissue level. In parallel to the development of SERMs, synthetic ERα and ERβ-selective ligands have been developed that exploit differences in the two LBDs (~53% homology), in particular the existence of Met-421 and Leu-384 in ERα that correspond to Ile-373 and Met-336 in ERβ that distinguish the receptor subtypes (Katzenellenbogen *et al.*, 2003).

ER-selective agonists include modified oestrogen derivatives; oestradiol-16α-lactone and 8β-vinyl oestradiol that selectively bind ERα and ERβ respectively (Hillisch *et al.*, 2004). Furthermore, propyl pyrazole triol (PPT™) has a binding affinity for ERα that has been determined as 410 fold stronger than for ERβ and in addition this compound is reported to act as an agonist when bound to ERα while behaving as an antagonist in complex with ERβ (Stauffer *et al.*, 2000).

Diarylpropionitrile (DPN™) is a xenoestrogen that shows a 70 fold higher affinity for ERβ than ERα (Meyers *et al.*, 2001) owing to the preferential interaction of the nitrile group of DPN™ with the Met-336 residue of ERβ (Sun *et al.*, 2003). Genistein is an isoflavanoid that exhibits preferential binding for ERβ (Barkhem *et al.*, 1998). Other compounds that have demonstrated ERβ selectivity include WAY-358 (157 fold ERβ-selective) and the benzoxazole derivative ERβ-041 (≥200 fold ERβ-selective) (Manas *et al.*, 2004, Malamas *et al.*, 2004).

1.10.2 Anti-oestrogens

ICI 182,780 (ICI/Faslodex™) is a potent anti-oestrogen that is reported to block activity of both ERα and ERβ by disrupting nucleocytoplasmic shuttling (Dauvois *et al.*, 1993b), receptor dimerisation and by increasing receptor turnover (Parker, 1993) (Fig. 1.15A). ICI 182,780 has a greater affinity for the ERs than the ICI 164,384 compound owing to the fluorine atoms that increase its solubility (Wakeling *et al.*, 1991). X-ray crystallography studies determined that the bulky alkylamide side chain at the 7α position of ICI 182,780 displaces Helix 12 of ERβ and extends beyond the

ligand-binding pocket to the coactivator-binding groove (Pike *et al.*, 2001). The principle practical application of the pure anti-oestrogen is as a second-line therapy against tamoxifen-resistant breast tumours (Howell *et al.*, 1995).

1.10.3 Selective Oestrogen Receptor Modulators

A class of structurally distinct therapeutics dubbed the SERMs target oestrogen-regulated genes and exhibit partial agonist and antagonist behaviour based on promoter and tissue context (reviewed in Osborne *et al.*, 2000) (Fig. 1.15B). The canonical SERM introduced in 1977 for use in the management of metastatic breast cancer patients is 4HT (Osborne, 1998). Based upon the conformation adopted with helix 12 (Brzozowski *et al.*, 1997), 4HT is used as an adjuvant therapy to block oestrogen activity in the ERα-positive breast tissue but prolonged exposure has been linked with low grade endometrial cancers (Fisher *et al.*, 1994). Toremifene is another first generation SERM that has positive influence on bone mineral density but shares the uterotrophic effects of 4HT and as such is only prescribed as an adjuvant therapy in postmenopausal patients with metastatic breast cancer (Holli, 2002). The consequence of the dual activity of 4HT and toremifene spawned the search for alternative SERMs and led to the development of second generation SERM compounds such as raloxifene (reviewed in Burger, 2000 and Shang, 2006). Like 4HT, raloxifene has antiproliferative activity in the breast but does not exhibit agonism in the endometrium and as a result has a reduced chance of inducing endometrial cancer (Goldstein *et al.*, 2000).

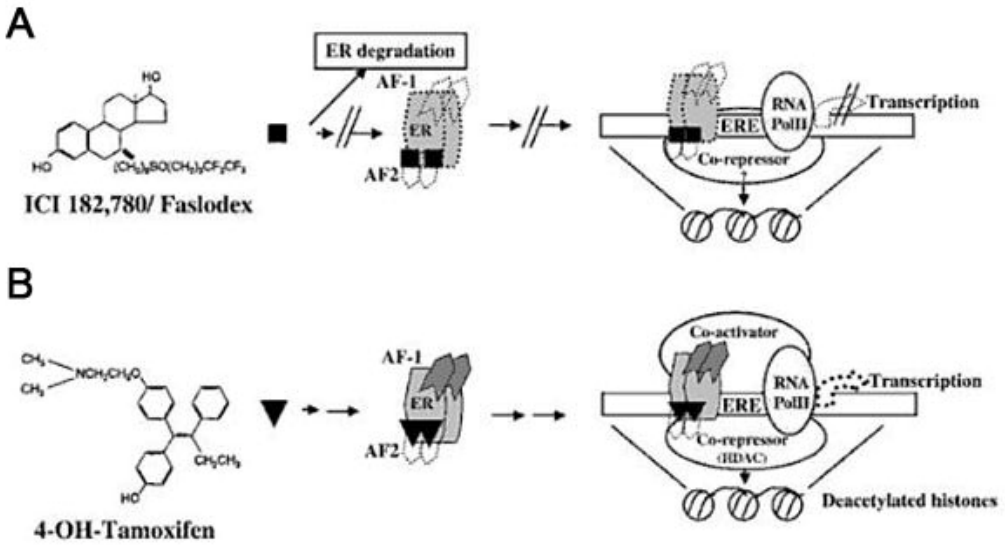

Figure 1.15 Comparison of anti-oestrogen and selective oestrogen receptor modulator activity.

A. ICI 182,780 chemical structure is on the left hand side. ICI 182, 780 binds ERα or ERβ with a similar affinity to E2, induces rapid degradation of the receptor and facilitates weak ER binding at the ERE. This conformation recruits corepressors and inhibits transcriptional activity. B. 4-hydroxy-tamoxifen binding exerts partial agonist and antagonist activity that is tissue-context dependent. Taken from Schiff, 2002.

1.11 Growth Factors

Growth factors have an important role in the cell development, differentiation and proliferation of their target tissues (Force and Bonventre, 1998). The peptide growth factors are defined by a consensus signature composed of six conserved cysteine residues bound by intramolecular disulphide bonds. The growth factor precursor ligands are transmembrane proteins that are released as mature growth factors through proteolytic activity at the cell surface (Harris *et al.*, 2003). Human EGF is a 53 amino acid protein product of the gene localised to 4q25-27 (Morton *et al.*, 1986). EGF channels its effects through binding of its cognate receptor, the epidermal growth factor receptor (EGFR) (reviewed in Harris *et al.*, 2003) that was the first receptor tyrosine kinase to be described (Carpenter *et al.*, 1978).

EGFR/HER1 is one of four members of the human epidermal growth factor receptor (HER1-4) family of transmembrane glycoproteins (Wells, 1999) originally labelled

due to their homology to the erythroblastoma gene – *v-erbB*. The HER/ErbB family of protein tyrosine kinase receptors are responsive to 13 polypeptide ligand factors (Prigent and Lemoine, 1992, Citri and Yarden, 2006). Each are comprised of 4 distinct domains: 1) the extracellular ligand binding domain that is made up of four subdomains responsible for change of state during ligand-binding; leucine-rich 1 and 2 (domains I and III) and cysteine-rich 1 and 2 (domains II and IV), 2) the transmembrane domain, 3) a small intracellular tyrosine kinase juxtamembrane domain and 4) the C-terminal tail that serves as a docking site for effector signalling molecules such as Grb2 (Fig. 1.16). Over the course of the evolution of the HER family, accumulated mutations have rendered HER2 and HER3 non-autonomous such that HER2 cannot bind ligand (Klapper *et al.*, 1999) and the intracellular kinase activity of HER3 is abrogated (Citri and Yarden, 2006). Despite this, both receptors actively form heterodimer partnerships and have been implicated in important roles in clinical pathologies (e.g. breast cancer) (Osborne *et al.*, 2003, Kirkegaard *et al.*, 2007). HER1, and the neuregulin-activated HER3 and HER4 (Plowman *et al.*, 1993) proteins can form both homo- and heterodimers. Gene mutation experiments modifying the function of EGFR have revealed key roles in the brain, kidney and skin (Harris *et al.*, 2003).

1.11.1 GF-mediated Phosphorylation of ER subtypes: The MAPK signalling cascade

As previously described (section 1.7), the functional output of ER does not solely stem from a linear ligand-mediated dogma but is attributable to a myriad of both divergent and integrated activating signals and pathways. The growth factor family of Type I glycosylated transmembrane proteins play a pivotal role in activation of ERs through kinase-dependant signalling pathways (reviewed in Levin, 2003). The concept of GF-interacting with the multifaceted activation of ER was borne out by early mouse studies elucidating an effect of the extracellular ligands on ER-dependent transcriptional responses (Nelson *et al.*, 1991, Ignar-Trowbridge *et al.*, 1992). Growth factor-mediated ER transcriptional activity is governed by the reversible phosphorylation of specific target serine and threonine residues that can occur in the presence or absence of oestrogenic ligands (Lannigan, 2003) and on ERα

they are largely concentrated within the 180 amino acid region of the AF-1 domain (Bunone *et al.*, 1996b)

Phosphorylation is a reversible process regulated by kinases and phosphatases. Activation of the MAPKs of which there are four, namely: extracellular signal-regulated kinase (ERK), big MAP kinase-1 BMK/ERK5), c-Jun-N-terminal kinase (JNK) and p38 kinase is orchestrated by GF mediated stimulation at the extracellular domain of cognate membrane-bound receptors (Smith, 1998). The tyrosine signalling cascades involve a three-tier system with sequential activation of MAPK kinase kinase (MAPK KK/MEKK) that phosphorylates a MAPK kinase (MEK) that in turn activates a specific MAPK (reviewed in Pearson *et al.*, 2001).

GF induction (e.g. EGF) of the ERK1/2 MAPK is well described and outlined in Fig. 1.16 (reviewed in Force and Bonventre, 1998). EGF binding induces EGFR dimerisation and intracellular autophosphorylation (Renshaw *et al.*, 1997). Linked by the src homology-2 (SH2) domain of GF receptor binding protein 2 (Grb2) at the specific phosphorylated tyrosine residues within the cytoplasmic domain of the EGFR, this docking site (Grb2) propagates the tyrosine kinase signal. Grb2 recruits the guanine nucleotide exchange factor, sons of sevenless (SOS) that in turn can activate Ras (Force and Bonventre, 1998). Guanosine-5'-triphosphate (GTP)-bound activated Ras activates the Raf family of proteins (Jelinek *et al.*, 1996) that are in complex with coregulators such as the molecular chaperone heat shock proteins (hsp50 and hsp 90) and the 14-3-3 proteins (Xiao *et al.*, 1995). Activated Raf induces the phosphorylation of MEK1 and 2 that in turn phosphorylates the tyrosine and threonine residues of ERK1 and 2. Activation of the MAPKs ERK1 and 2 can induce p90ribosomal S6 kinases (RSKs) and these in turn have been demonstrated to activate the ERα through phosphorylation at specific residues within the AF-1 domain (Joel *et al.*, 1998b).

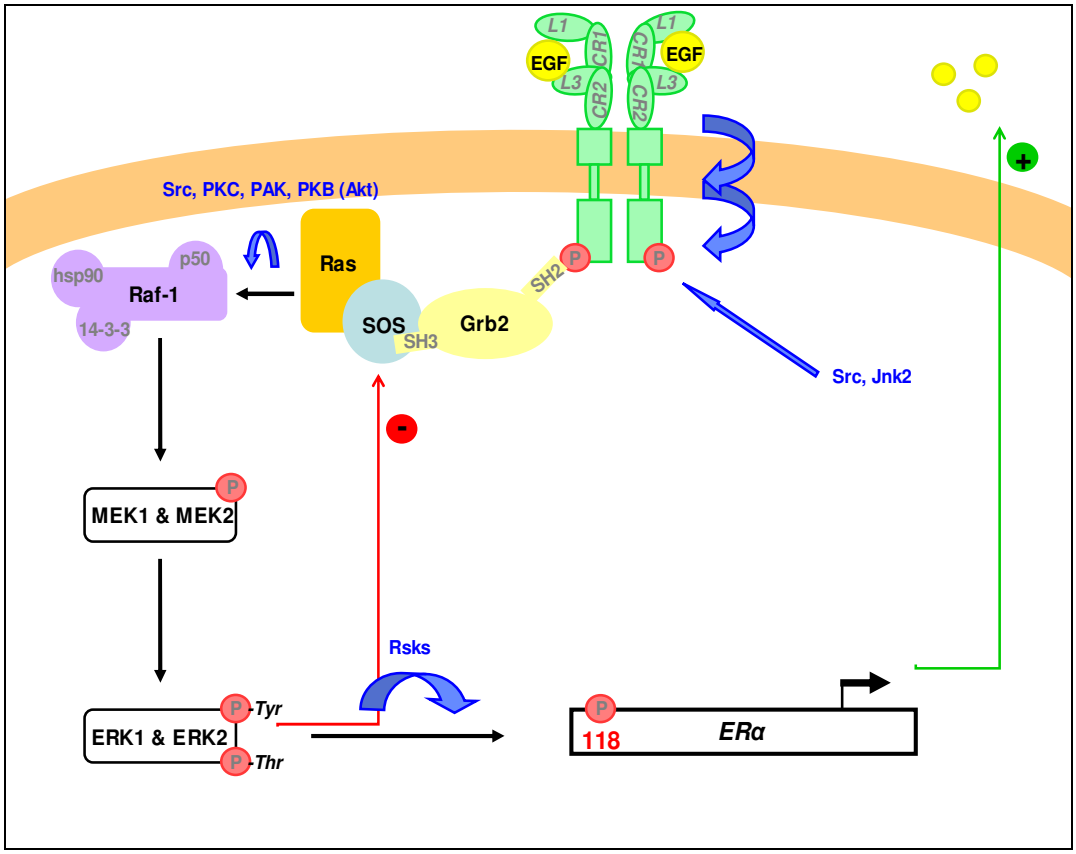

Figure 1.16 Schematic overview of the MAPK (ERK1/2) tyrosine signalling cascade and its regulation.

GF-induced phosphorylation of the ER is the result of a series of stepwise catalytic reactions involving MAPKs. The phosphorylated ER end-product fuels the positive feedback loop via the regulation of EGF protein.

1.11.2 GF-mediated Phosphorylation of ER subtypes: The target sites

There are eight target sites of protein kinase-directed phosphorylation on the ERα protein that have been identified *in vitro* at the serine 102 (Ser102)/Ser104 motif, Ser106 (Joel *et al.*, 1998c, Thomas *et al.*, 2008, Rogatsky *et al.*, 1999), Ser118 (Joel *et al.*, 1995, Bunone *et al.*, 1996b), Ser167 (Arnold *et al.*, 1994, Joel *et al.*, 1998b, Martin *et al.*, 2000a, Campbell *et al.*, 2001), Ser236 (Le Goff *et al.*, 1994b, Chen *et al.*, 1999) Ser 305 (Rayala *et al.*, 2006, Tharakan *et al.*, 2008) T311 (Lee and Bai, 2002) and Y537 (Weis *et al.*, 1996, Arnold *et al.*, 1997) (Fig. 1.17). Three phospho-

target residues at Ser16, Ser106 and Ser 124 have been mapped on the mouse ERβ subtype (Cheng and Hart, 2001, Tremblay A. *et al.*, 1999).

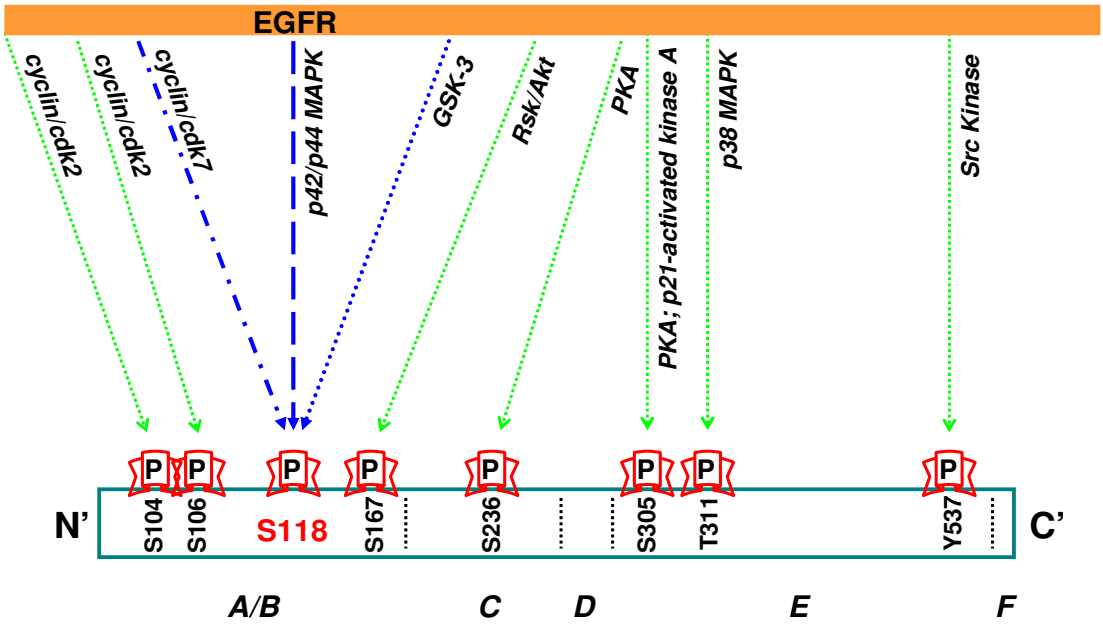

Figure 1.17 Overview of ERα residues that are targets for phosphorylation and the signalling pathways that control them.

Of the four documented target sites within the AF-1 of ERα (Ser104, Ser106, Ser118 and Ser 167), the phosphorylation of Ser118 is the best characterised. It has been deemed imperative in modulating the functional capacity of ERα (Kato *et al.*, 1995b) and roles for both direct and indirect EGF- and IGF-mediated signalling (in addition to the canonical E2-dependent mechanism) have been linked to this site (Bunone *et al.*, 1996b, Murphy *et al.*, 2004). Ser118 is phosphorylated by the complex of TFIIH and cyclin-dependent kinase-7 (cdk7) directly (Chen *et al.*, 2000) and also by ERK1/2 (p44/p42 MAPK) triggered by EGF activation of the EGFR (Kato *et al.*, 1995d) (Fig. 1.17). The phosphorylation status of ERα at Ser118 is inherently linked to the regulation of receptor activity in a positive and negative manner. Phospho-Ser118 ERα has been shown to govern the specific recruitment of the coactivator splicing factor (SF)-3ap120, a component of the spliceosome (Masuhiro *et al.*, 2005). Phospho-Ser118 ERα has also been shown to be negatively regulated by protein phosphatase 5 (PP5) activity (Ikeda *et al.*, 2004) and the stromelysin-1 platelet-derived growth factor (PDGF)-responsive element binding protein (SPBP)

corepressor (Gburcik *et al.*, 2005) resulting in the attenuation of the transcriptional capacities attributable to EGF-dependant and E2-dependant phosphorylation.

Additional sites identified as phosphorylation targets within the AF-1 (A/B) domain of ERα include Ser-102, -104, -106, -167 and -236. The phosphorylation of Ser104 and/or Ser106 works in concert with phospho-Ser118 as co-operative MAPK binding sites (Thomas *et al.*, 2008) and all three sites also carry the signature consensus sequence that confers activity by CDKs (Trowbridge *et al.*, 1997, Rogatsky *et al.*, 1999). Furthermore, there is evidence to suggest susceptibility of serine residues -102, -104, -106 and -118 to glycogen-synthase 3 kinase (GS3K), itself the product of GF or hormonal regulation (Medunjanin *et al.*, 2005). Phosphorylation of Ser167 has been demonstrated in response to ligand binding (Arnold *et al.*, 1994) and in response to MAPK signalling activity through the serine/threonine protein kinase; p90 ribosomal S6 kinase 1 ($pp90^{rsk1}$) (Joel *et al.*, 1998b) and AKT signalling (Martin *et al.*, 2000b, Campbell *et al.*, 2001).

The importance of the AF-2 functional domain in response to ERα phosphorylation has been revealed by phospho-target sequences (Ser236, Ser305, threonine311 (T311) and tyrosine537 (Y537)) detected at this region. In the absence of ligand, the AF-2 domain is in a conformation that prevents AF-1 activity. Molecular modelling has revealed that ligand binding facilitates exposure of the AF-1 for coregulator recruitment and activation via phosphorylation (Tharakan *et al.*, 2008). In studies using cancer cell lines, phospho-Ser305 was found to be under the regulation of two kinase dependent pathways directed by p21-activated kinase 1 (Wang *et al.*, 2002) and protein kinase A (PKA) (Michalides *et al.*, 2004). It was also reported that Ser305 imparted an effect with Ser118 on ERα activity in response to 4HT in treated HeLa cells (Rayala *et al.*, 2006). This effect may be in part due to the increased binding affinity of phospho-Ser305 ERα at target gene promoter sites (Tharakan *et al.*, 2008). Located within helix 1 of the LBD, T311 phosphorylation has been associated with increased coregulator recruitment and nuclear localisation (Lee and

Bai, 2002) while Y537, also in the LBD has been implicated as a modulator of ligand and DNA binding functions (Likhite *et al.*, 2006).

1.11.3 Evidence for an interplay between growth factor and oestrogen receptor signalling cascades

The bidirectional crosstalk between the GF-regulated kinase networks and ER-dependent signalling pathways are reported to be of clinical significance in patients with breast cancer that develop endocrine resistance (reviewed in Smith, 1998). For example, Osborne *et al.* have reported that breast tumour growth is regulated by the concerted activity of ER and GF dependent signalling and that the latter is responsible for HER2 amplification that may underlie resistance to 4HT (Osborne *et al.*, 2005). In addition to MAPK-mediated phosphorylation of the ER protein, ER coregulators are substrates for tyrosine kinase cascades (Arpino *et al.*, 2008) and act as points of convergence between the two signalling pathways. In particular, HER-mediated signalling has been reported to potentiate the activity of the coactivator, amplified in breast cancer-1 (AIB1)/SRC-3 (Font de Mora and Brown, 2000, Lopez *et al.*, 2001). Further to this, a number of studies attribute 4HT resistance and poor prognosis with the co-expression of AIB1, HER2 and HER3 and the interplay of their respective signalling functions (Schiff *et al.*, 2003, Osborne *et al.*, 2003, Kirkegaard *et al.*, 2007).

1.12 Functional analysis of ERs: gene knockout studies

Mouse 'knockout' (KO) models of ER subtypes have been engineered to decipher precise roles for the individual ER subtypes in transducing oestrogen-dependent and independent signalling pathways (Table 1.3) (reviewed in Couse and Korach, 1999, Hewitt and Korach, 2003). These studies have revealed an essential role for ERα and ERβ in female fertility. Early-onset infertility in the female α-ERKO mice is believed to stem from dysregulation at the pituitary resulting in increased production of luteinising hormone (LH) and its cognate receptor (LHR), that in turn results in the development of haemorrhagic cysts within the ovary and anovulation (Lubahn *et al.*, 1993, Schomberg *et al.*, 1999). The uterus of the α-ERKO mice is underdeveloped (hypoplastic) and non-responsive to oestradiol (Couse *et al.*, 1995). Studies

investigating the uterine response to IGF-1 using α-ERKO mice revealed the importance of the presence of ERα in uterine nuclear proliferation, although phosphorylation of MAPK was independent of ERα and this result strengthens the concept of crosstalk between the IGF receptor (IGFR) and ER signalling pathways (Klotz *et al.*, 2002).

β-ERKO female mice exhibited differential sub-fertility patterns with continuous matings that included decreased pregnancy rate or reduced number of pups per litter compared with wild type animals (Krege *et al.*, 1998, Dupont *et al.*, 2000) that did not influence animal behaviour (Ogawa *et al.*, 1999). Like α-ERKO mice, the αβ-ERKOs are infertile but are phenotypically distinct from the single gene knockouts and had abnormal follicles lacking an oocyte that increased in abundancy with age and no corpora lutea (Dupont *et al.*, 2000). The uteri of αβ-deficient mice were hypoplastic and resistant to oestrogenic activity (Couse and Korach, 1999).

Examination of non-reproductive function in the KO models has revealed exclusive roles for ERα in maintaining bone density and behaviour as a cardioprotectant while the β-ERKO female mice had increased bone mineral density and were non-responsive to crossing with apolipoprotein E, suggesting a receptor-mediated role for ERα in these processes (Hewitt and Korach, 2002, Hodgin *et al.*, 2001).

Table 1.3 Overview of ER knockout mice model phenotypes.
(Adapted from Walker and Korach, 2004).

	 α-ERKO	β-ERKO 	αβ-ERKO 
		Fertility	
	Both sexes are infertile	Males are fertile Subfertile females; infrequent pregnancies and reduced litter size	Both sexes are infertile
		Female Reproductive System	
Uterus	Hypoplastic uterus; insensitive to estradiol; no implantation	Normal response to estradiol; supports normal pregnancy	Resembles αERKO phenotype; insensitive to estradiol
Ovary	No ovulation; immature follicles; hemorrhagic cysts developing at puberty due to chronic elevated LH;[a] elevated levels of estrogen and testosterone	Normal appearance; reduced ovulation	Granulosa cells undergo transdifferentiation into Sertoli-like cells
Mammary Gland	Immature; only a ductal rudiment present	Normal structure; normal lactation	Immature; resembles αERKO phenotype
		Nonreproductive Phenotypes	
Bone	Both sexes are shorter than wild-type; females have decreased bone diameter; males have decreased density	Females have increased density; normal in males	Both sexes are shorter than wild-type
Cardiovascular	Estrogen protection retained in vascular injury study	Estrogen protection retained in vascular injury study	Estrogen protection lost in vascular injury study

[a]LH, luteinizing hormone.

1.13 Oestrogens, oestrogen receptors and human endometrial function

The human endometrium is a dynamic tissue regulated by the sequential exposure to oestrogen and progesterone over distinct phases termed the menstrual cycle (Fig. 1.18) (Simmen and Simmen, 2006). The endometrium consists of functional and basal layers. The functional layer responds to the rising concentrations of oestrogen during the proliferative phase by thickening and then differentiates in response to a surge in progesterone (Jabbour *et al.*, 2006). The follicular phase occurs after the functional layer has been shed at menstruation and is characterised by intense mitotic activity occurring in the endothelial, epithelial and stromal cellular components under the influence of oestrogen (Ferenczy, 1993) and angiogenesis controlled by EGF and vascular endothelial growth factor (Nelson *et al.*, 1991, Taylor *et al.*, 2001).

The secretory phase follows the luteinising hormone surge that signals ovulation and under the control of progesterone is synonymous with glycogen accumulation in the

cytoplasm of the epithelial cells and secretion into the tortuous glandular lumens (Ferenczy, 1993). In the absence of fertilisation and the decrease in circulating progesterone, the endometrium is shed from the functional layer and regenerated by the underlying basal layer during another round of the cycle (reviewed in Jabbour *et al.*, 2006).

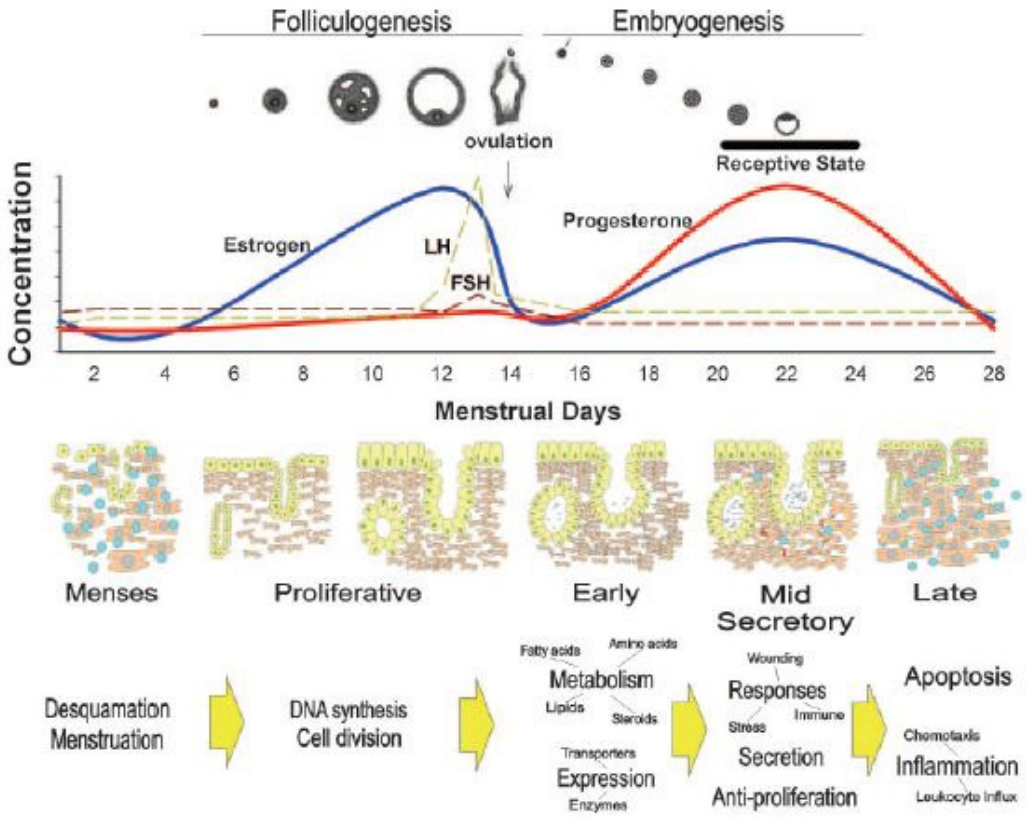

Figure 1.18 Schematic overview of the differentially regulated phases of the menstrual cycle.
Upon shedding of the functionalis layer of the endometrium during menstruation, oestrogen influences the thickening of the uterine lining once more during the follicular phase of the cycle. After ovulation and in response to progesterone levels produced from the corpus luteum, the endometrial columnar epithelium and stroma secrete glycogen in preparation for implantation. In the absence of implantation and decreasing levels of progesterone the tissue is broken down once more during menstruation. Taken from Simmen and Simmen, 2006.

1.13.1 Oestrogen expression in the human endometrium

In the human uterus expression of both ER proteins has been immunolocalised using staged, full thickness endometrial biopsies (including the functional and basal zones of the endometrium and adjacent myometrium). These results have revealed that the expression of ERα, ERβ1 and ERβ2 vary in intensity during the normal menstrual cycle (Critchley *et al.*, 2001, Critchley *et al.*, 2002, Saunders and Critchley, 2002, Henderson *et al.*, 2003). ERα and ERβ are both expressed in endometrial glands and stromal fibroblasts. In the functional layer the intensity of immunoexpression of ERα is highest at the proliferative phase (oestrogen dominated) but declines during the secretory phase (Snijders *et al.*, 1992, Critchley *et al.*, 2001). Like ERα, ERβ was expressed in both epithelial and stromal cells during the proliferative phase but whereas expression in the glandular epithelial cells declined, expression in the stromal fibroblasts and luminal surface epithelium was maintained (Taylor and Al-Azzawi, 2000, Critchley *et al.*, 2001). Notably expression of both ERα and ERβ remains unchanged in the basal compartment (Critchley *et al.*, 2001).

Although the functional significance of the expression of ERβ in the human endometrium is still to be determined, it is notable that ERβ is expressed in vascular endothelial cells and immune cells including a phenotypically distinct population of natural killer cells that are believed to play an essential role in placentation (Critchley *et al.*, 2001, Critchley *et al.*, 2002, Lecce *et al.*, 2001, Krikun *et al.*, 2005, Henderson *et al.*, 2003).

1.14 Aims of the thesis

The overall aim of this thesis was to examine the sub-nuclear kinetics of ERs and their transcriptional activity in response to ligands and to delineate differences in the response patterns between full-length receptors and splice variants. For this study, endometrial cell lines were used as an *in vitro* model.

The specific aims were:

- To establish and optimise methods for measuring the intranuclear mobility of both full length ERα and ERβ and splice variant isoforms of human ERβ (ERβ2 and ERβ5).
- To determine whether ERβ5 may play a role in oestrogen responsiveness in the normal human endometrium.
- To examine alternative ligand-independent modes of activation of ER with particular reference to the truncated ERβ5 splice variant.

Chapter 2

General materials and methods

2 General materials and methods

2.1 Cell Culture

2.1.1 MDA human caucasian breast adenocarcinoma cells

The MDA-MB-231 cell line was obtained from the European Collection of Cell Cultures (ECACC, Wiltshire, UK, Cat. No.92020424), a health protection agency culture collection. These epithelial cells were originally isolated from the pleural effusions of a 51 year old Caucasian breast cancer patient (Cailleau *et al.*, 1974). The cells were maintained in Dulbecco's modified Eagle's medium (DMEM) (Sigma, St. Louis, MO, USA, Cat. No.; D5546) that was supplemented with 10% heat-inactivated foetal calf serum (FCS) (Invitrogen, Paisley, UK, Cat. No. 10082-147), 1% Non-essential amino acids (Sigma, Cat. No. M7145), 0.5% Fungizone (Invitrogen, Cat. No. 15290-018), 1% L-Glutamine (Sigma, Cat. No. G-7513) and 1% Penicillin-Streptomycin (Sigma, Cat. No.; P-4333). The cells were incubated at 37°C under conditions of 5% CO_2 in air. These cells were transferred to phenol-red free DMEM containing 10% charcoal-stripped FCS and supplemented in the same way as the DMEM above for 48 hours prior to use in all experimental assays to eliminate endogenous growth factor and ligand presence.

2.1.2 Ishikawa endometrial adenocarcinoma cells

The Ishikawa cell line was purchased from ECACC (Cat. No.99040201). This well differentiated endometrial adenocarcinoma cell line was isolated from a 39-year old Asian patient and is positive for ERα (Nishida *et al.*, 1985). These epithelial cells were cultured in supplemented DMEM (as outlined above) and kept at 37°C under 5% CO_2 in air.

2.1.3 hTERT endometrial epithelial cells (hTERT)

The human TERT (hTERT)-endometrial epithelial cells are positive for endogenous ERα expression and were obtained from Dr. Thomas Klonisch, Dept. of Human Anatomy and Cell Science, University of Manitoba, Canada. This cell line was isolated from the proliferative phase (day 7) of a normal endometrium from a 37 year

old nulliparous patient following surgery on uterine myomatosis. Immortalisation of these primary cells was conducted by stable transfection of the catalytic human telomerase subunit (TERT) and further culturing of the cells (Hombach-Klonisch *et al.*, 2005). These cells were kept in Ham's F-10 media (Lonza Biologics plc, Slough, UK, Cat. No.; BE12-618) with 10% charcoal-stripped foetal calf serum, 1% Non-essential amino acids, 1% insulin, human transferrin and selenous acid (ITS) Premix (Becton Dickinson BioSciences, Oxfordshire, UK, Cat. No.; 354351), 1% L-Glutamine (Sigma, Cat. No. G-7513) and 1% Penicillin-Streptomycin (Sigma, Cat. No. P-4333) and maintained at 37°C in 5% CO_2.

2.2 Human Tissue

2.2.1 Human Endometrial Samples

Human endometrial biopsies from different stages of the menstrual cycle were obtained following hysterectomy, hysteroscopy or laparoscopic sterilisation performed at the Royal Infirmary, Edinburgh, UK. Histological staging analysis was performed by an expert histologist as previously reported (Critchley *et al.*, 2001) (Critchley *et al.*, 2002). Patients provided informed consent consistent with national guidelines (Polkinghorne, 1989) and ethical approval was bestowed from the Lothian Research Ethics Committee. All recruits from whom endometrial tissue was acquired were of reproductive age (30-48 years) and reported regular cycles.

2.2.2 Tissue processing

Endometrial tissue samples were fixed in 4% neutral buffered formalin overnight at 4°C and transferred into 70% ethanol prior to being embedded in paraffin wax according to standard methods by the histology team at the MRC Human Reproductive Sciences Unit, Edinburgh. Additional endometrial samples required for RNA and protein experimentation were immersed in RNA Later (Ambion, Warrington, UK) and stored at 4°C.

2.3 Ligands

2.3.1 Oestrogenic Ligands

2.3.1.1 Natural Oestrogenic Ligand

The E2 ($C_{18}H_{24}O_2$) was purchased from Sigma (Cat. No. E-8875) and the lyophilised product was reconstituted in dimethyl sulfoxide (DMSO). E2 was subsequently diluted in PBS giving a variety of serial dilutions (10^{-3}-10^{-8}M) stored at -20°C.

2.3.1.2 Synthetic Ligands

The synthetic agonist compounds 2,3-bis(4-Hydroxyphenyl)-propionitrile (DPN™) ($C_{15}H_{13}NO_2$) and 4,4',4''-(4-Propyl-[1H]-pyrazole-1,3,5-triyl)trisphenol (PPT™) ($C_{24}H_{22}N_2O_3$) were purchased from TOCRIS (Ellisville, MO, USA) (Cat. No.'s 1494 and 1426 respectively). Serial dilutions (10^{-3}-10^{-8}M) of both ligands were prepared by reconstitution and dilution in 100% DMSO and stored at -20°C. DPN™ is reported to exhibit 70X selective activity for ERβ (Meyers *et al.*, 2001) whilst PPT™ has been described as ERα selective (Stauffer *et al.*, 2000).

2.3.2 Growth Factors

The EGF was bought from PeproTech EC Ltd., London, UK (Cat. No. AF-100-15), reconstituted and diluted to form serial dilutions (10^{-5}-10^{-8}M) in distilled H_2O. Insulin-like growth factor-I was obtained from Sigma (Product No. I3769), was made up from its lyophilised state in sterile phosphate buffered saline (PBS) and subsequently diluted to give a range of serial dilutions (10^{-5}-10^{-8}M). All growth factors were kept in storage at -20°C.

2.3.3 Inhibitors

The pure ER antagonist 7a,17b-[9-[(4,4,5,5,5-Pentafluoropentyl)sulfinyl]nonyl] estra-1,3,5(10)-triene-3,17-diol (ICI 182,780) ($C_{32}H_{47}F_5O_3S$) was purchased from TOCRIS (Cat. No. 1047). A stock solution of 1mM of this compound was prepared in 100% ethanol. The proteosome inhibitor MG132 ($C_{26}H_{41}N_3O_5$) was bought from Sigma (Cat. No. C2211-5MG). A stock solution of 1mg/ml of MG132 was prepared using 100% ethanol. The selective inhibitor of p22/44 MAPK kinase 1, PD98059,

was purchased from Promega (Cat. No. V1191, Southampton, UK). The dried product was resuspended in DMSO to a stock concentration of 20mM. All inhibitors were stored at -20°C.

2.4 Immunohistochemistry

Immunohistochemical staining (IHC) is a method which enables visualisation of specific proteins of interest (antigens) in tissue sections through the binding of antibodies to small, unique regions (epitopes) of the antigen under investigation (Fig.2.1).

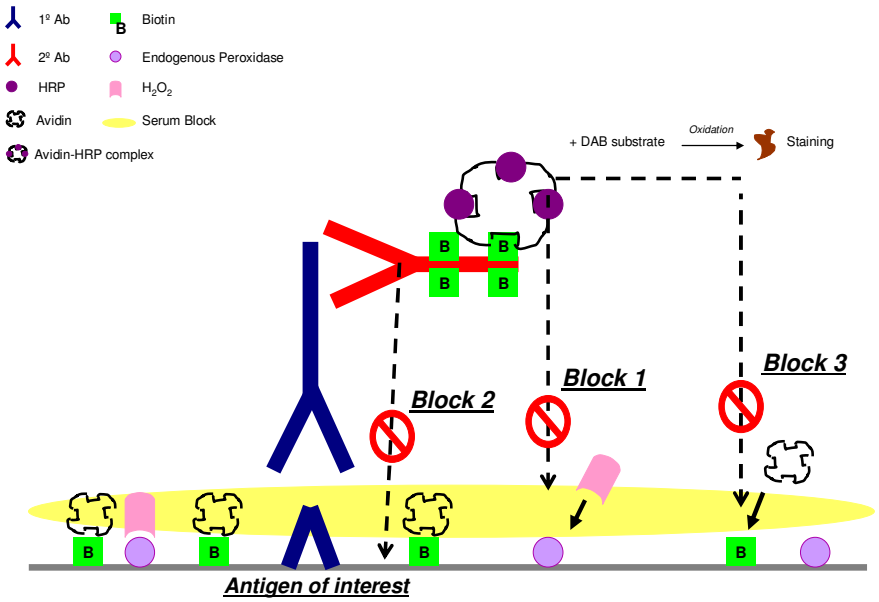

Figure 2.1 Schematic overview of immunohistochemistry process.

Figure includes demonstration of the three blocking steps imposed on all experiments: Block 1, methanol peroxide block (section 2.4.3.1); Block 2, serum block (section 2.4.3.2); Block 3, avidin-biotin block (section 2.4.3.3).

2.4.1 IHC of endometrial tissue sections

IHC was conducted on endometrial tissue in accordance with standard laboratory protocols to establish the presence and localisation of the proteins of interest.

2.4.1.1 Tissue processing (sectioning)

Wax-embedded tissue was pre-chilled on ice to ensure rigidity and enable ease of the sectioning process. Sections were cut at 5 microns in thickness using a microtome (model RM2135, Leica Microsystems, Wetzlar, Germany) and floated on H_20 at 45º ± 5ºC (model E/65, RA Lamb, Waltham, MA, USA). The sections were picked up on glass slides coated with positive charge used to attract the negatively charged proteins of the tissue (Cat. No., 406/0179/00; BDH, Lutterworth, UK). All slides were placed in an oven (model E28.5, Lamb RA) at 55ºC overnight to ensure complete adhesion of tissue section to the slide.

2.4.1.2 Dewaxing of tissue

To ensure optimal antibody penetration of the sectioned tissue, complete removal of the wax was carried out. The dewaxing process involved plunging slides into two consecutive xylene troughs. This was followed by rehydration of tissue in diminishing concentrations (100%, 95% and 70%) of alcohol before a final wash in tap H_20.

2.4.2 Antigen retrieval

During the formalin-fixed paraffin embedding (FFPE) process of tissue, changes in the orientation of epitopes (antigen recognition sites) of the proteins can arise due to formation of cross linkages between Ca^{++} and other divalent metal cations and proteins. These 'masked' changes can be disrupted by applying intense heat to the tissue and placing in a buffered solution to allow precipitation or chelation of the released metal ions (Cattoretti *et al.*, 1993). Antigen retrieval was conducted in a pressure cooker for 5 minutes at full pressure preceding a 20 minute standing time with slides submerged in either a citrate or an ethylenediamine tetra-acetic acid (EDTA) solution (Morgan *et al.*, 1994). EDTA was considered a more suitable buffer for particular antibodies tested on endometrial tissue as gave cleaner and stronger results.

2.4.3 Blocking to promote specific signal amplification

In a pre-emptive effort to control non-specific antibody binding, a number of blocking stages were employed and are detailed below.

2.4.3.1 Methanol Peroxidase Block

To prevent endogenous peroxidase responding to chromogens such as horseradish peroxidise (HRP), sections were immersed in a solution of 3% H_2O_2 in methanol and placed on a rocker for 30 minutes. After this time, slides were washed in Tris-Buffered Saline (TBS) solution on a rocker for 5 minutes.

2.4.3.2 Serum Block

The use of serum from the species in which the secondary antibody was raised was used to prevent non-specific binding of the secondary antibody. For most IHC experiments conducted in this project, a secondary antibody raised in goat was used and therefore slides were incubated in normal goat serum (NGS; Autogen Bioclear UK Ltd., Wiltshire, UK) that was diluted 1:4 in TBS solution mixed with 5% bovine serum albumin (BSA; Sigma, Poole, Dorset, UK) for 30 minutes at room temperature under humidified conditions. Excess buffer was removed from all sections after this blocking stage.

2.4.3.3 Avidin-Biotin Block

The use of biotinylated secondary antibodies in the IHC process is dependent on the strong affinity of avidin and streptavidin for the vitamin biotin. To prevent avidin-peroxidase complexes binding directly to the tissue where endogenous biotin is expressed, an avidin-biotin blocking stage was performed. Sections were incubated with avidin-D (Vector Laboratories, Peterborough, UK) for 15 minutes, underwent 2x5 minute TBS washes on a rocker, incubated with biotin (Vector Laboratories, Peterborough, UK) for 15 minutes before a final 2x5 minute washes in TBS solution.

2.4.4 Primary Antibodies

All primary antibodies were prepared by dilution in their appropriate blocking serum. Sections were incubated with the primary antibody to the target antigen in a

humidified chamber and stored overnight at 4ºC. Table 2.1 outlines the optimised conditions used for each antibody. Negative controls were conducted with each experiment where the primary antibody was replaced by blocking solution incubation alone.

2.4.5 Secondary Antibodies

Sections underwent 2x5 minute TBS washes after primary antibody incubations. Biotinylated secondary antibodies that had been diluted in their appropriate blocking serum were applied to the sections for 30 minutes at room temperature in a humidified environment.

2.4.6 Antigen detection, counterstaining and mounting

A streptavidin-horseradish peroxidise complex (DAKO, Cambridge, UK) diluted in TBS solution was applied to sections for 30 minutes at room temperature in a humidified chamber. Following 2x5minute TBS washes, the chromogenic substance 3, 3'-diaminobenzidine (DAB, K3468; DAKO) was diluted in its substrate and applied to the sections and given 2-3 minutes to allow for optimal development. Upon sufficient staining, slides were plunged in distilled H_2O. Sections were counterstained in Harris' haemotoxylin (cell nuclei turn blue), rehydrated and immersed in increasing concentrations of alcohol and finally xylene. The immunostained sections were mounted with coverslips using pertex glue (Cell Path, Hemel Hempstead, UK).

2.4.7 Immunofluorescence

Dual immunofluorescent staining facilitates the detection of co-localised target antigens. The principle requisites are that the primary antibodies are derived from unique species (although this can be overcome with the use of monovalent secondary antibodies with attached FAB fragments) and the dyes used have discernable spectral properties. An initial series of titrations were run to determine the most efficient dilution concentrations of antibody required to give optimal staining and the determined dilutions were employed for all subsequent experiments (Table 2.1). Experiments were conducted in the same manner as described for DAB with the use

of PBS in place of TBS washes and dilutions. Secondary antibodies used included biotinylated or peroxidise forms and these were incubated on sections for 30 minutes and 1 hour respectively (Table 2.2). The biotinylated antibodies were proceeded by incubation with streptavidin-conjugated alexa 488 or 546 diluted in PBS (1:200) for 1 hour. Peroxidase antibody treatment was followed by tyramide-Cy3 chromogen diluted (1:50) in tyramide buffer for 10 minutes. Sections were counterstained using 4', 6-diamidino-2-phenylindole (DAPI) nuclear stain (1:1000) and mounted using permafluor (Immunotech, Marseille, France) mounting medium.

Table 2.1 Summary of primary antibodies used for immunohistochemistry

Antigen	Host Species	Dilution	Retrieval	Source
ERα	Mouse	1:20	Citrate	Vector [1]
ERβ	Mouse	1:20	EDTA	AbD Serotec[2]
ERβ2	Mouse	1:200	EDTA	AbD Serotec[2]
ERβ5	Mouse	1:40	EDTA	In house
ErbB1 (HER1)	Sheep	1:100	Citrate	Upstate[3]
ErbB2 (HER2)	Mouse	1:75	Citrate	Abcam[4]
ErbB3 (HER3)	Mouse	1:75	Citrate	Abcam[4]
ErbB4 (HER4)	Mouse	1:40	Citrate	Abcam[4]

[1]Vector Laboratories Ltd., Peterborough, UK

[2]AbD Serotec, Kidlington, Oxford, UK

[3]Upstate Biotechnology Inc., New York, USA

[4]Abcam plc, Cambridge, UK

Table 2.2 Summary of secondary antibodies used for immunohistochemistry

Target	**Host Species**	**Dilution**	**Source**
anti-mouse biotinylated	Goat	1:500	Sigma[1]
anti-rabbit biotinylated	Goat	1:500	DAKO[2]
anti-sheep biotinylated	Rabbit	1:500	DAKO[2]
anti-mouse biotinylated Fab fragment	Goat	1:500	Abcam[3]
anti-mouse Fab peroxidase	Goat	1:200	DAKO[2]
Anti-rabbit Alexa Fluor 488	Goat	1:200	Molecular Probes[4]
Anti-rabbit Alexa Fluor 546	Goat	1:200	Molecular Probes[4]
Tyramide fluoroscein		1:50	Perkin Elmer Life Sciences[5]

[1]Sigma-Aldrich, St. Louis, MO, USA

[2]Dako UK Ltd., Cambridge, UK

[3]Abcam plc, Cambridge, UK

[4]Molecular Probes Europe BV, Leiden, The Netherlands

[5]PerkinElmer Life Sciences, MA, USA

2.4.8 Image Analysis

DAB positive images were captured using a PROVIS microscope (Olympus Optical, London, UK) with an attached Canon DS126131 camera. Dual fluorescent images were viewed using a LSM 510 Meta-Confocal (Carl Zeiss, Hertfordshire, UK).

2.5 Ribonucleic Acid (RNA) Analysis

2.5.1 RNA extraction from cell lines and human tissue

Total RNA was extracted using the RNAeasy® Mini extraction kit (Qiagen, Crawley, UK) and was carried out in accordance with the manufacturer's protocol. Cell samples were harvested following trypsinisation and collected in Buffer RLT (a potent denaturing buffer that inactivates RNase activity) supplemented with β-mercaptoethanol (10µl/ml). Cells were homogenised using a QIAshredder® spin column. Sample preparation from frozen endometrial tissue was conducted using a Qiagen Tissue Lyser. Defrosted tissue was weighed out (approximately 30mg) and homogenised in a solution of 600µl Buffer RNeasy® lysis buffer (RLT) (Qiagen, Crawley, UK) to which β-mercaptoethanol (10µl/ml) was added using a handheld tissue lyser (Z35,997-1, Sigma). A 1:1 volume of ethanol was added to the homogenates (cell and tissue) to provide optimal binding conditions. This solution was transferred to a RNeasy® spin column placed in a 2ml collection tube and briefly centrifuged (15 seconds) at 10,000 rpm. RNA binds to the silica membrane of the RNeasy® spin column and all contaminants were discarded in the flow-through following successive washing and subsequent spinning steps with Buffer RPE (Qiagen, Crawley, UK). Extracted RNA from all samples (cell and tissue) was subjected to on-column DNase digestion treatment involving a DNase I incubation mix of DNase I stock solution and Buffer RNeasy® DNase digestion (RDD, Qiagen, Crawley, UK) to prevent any genomic DNA contamination. Pure, concentrated RNA was eluted in a final volume of 50µl RNase-free H_2O.

2.5.2 RNA Quantification (Nanodrop®)

Extracted RNA was eluted in 50µl RNase-free H_20 and quantified using the Nanodrop® ND-1000 Spectrophotometer (Nanodrop Technologies, Wilmington, DE,

USA). Prepared RNA sample concentration was adjusted to 100ng/µl using RNase-free water to enable further accurate analysis between corrected samples and stored at -80°C.

2.5.3 Qualitative Polymerase Chain Reaction (PCR)

2.5.3.1 Reverse transcription of RNA using oligo dTs

Oligo dTs are specific to the poly-A tail of mRNAs and exclusively amplify mRNA. Oligo dTs (Applied Biosystems, Warrington, UK, Cat. No. N808-0128) were annealed to the RNA by incubation of 1µg RNA with 2.5µM oligo dTs (Applied Biosystems) made up to a final 12µl with RNase free H_2O and heating to 70°C for 5 minutes. The Bioscript Reverse Transcriptase (RT) reaction mastermix (Bioline, Germany) was then added and incubated with individual samples at 40°C for 60 minutes followed by 72°C for 10 minutes to produce cDNA.

	Final Concentration
RNase Inhibitor	0.5U/µl
5X Reaction Buffer	1X
dNTPs	200µM
Bioscript RT	2.5U/µl

The reaction mix for each individual reaction was made up to 9µl using RNase-free H_2O.

The subsequent PCR reaction was performed using GoTaq® (Promega) in 10µl under the following conditions;

95°C for 10 minutes

95°C for 1 minute

55-58°C for 1 minute

72°C for 10 minutes

for 30-35 cycles and a final 72°C for 10 minutes.

The housekeeping gene glyceraldehyde-3-phosphate-dehydrogenase (GAPDH) was used as a positive control for these reactions and is routinely used because it is constitutively and stably expressed to high levels in a wide range of cell and tissue types.

2.5.4 Quantitative-Real Time-PCR (Taqman® Method)

Figure 2.2 outlines an overview of the steps involved in a Taqman® quantitative real time PCR (qRT-PCR). This *in vitro* method for enzymatic amplification of defined RNA sequences can be subdivided into two main steps; a) the preparation of samples by reverse transcription of the RNA to complementary DNA (cDNA) sequences and subsequent mixing with the specific primer/probe mix from the Universal Probe Library™, and b) running the PCR process on the ABI 7900 instrumentation to sensitively acquire a measure of the transcription levels of specific genes of interest.

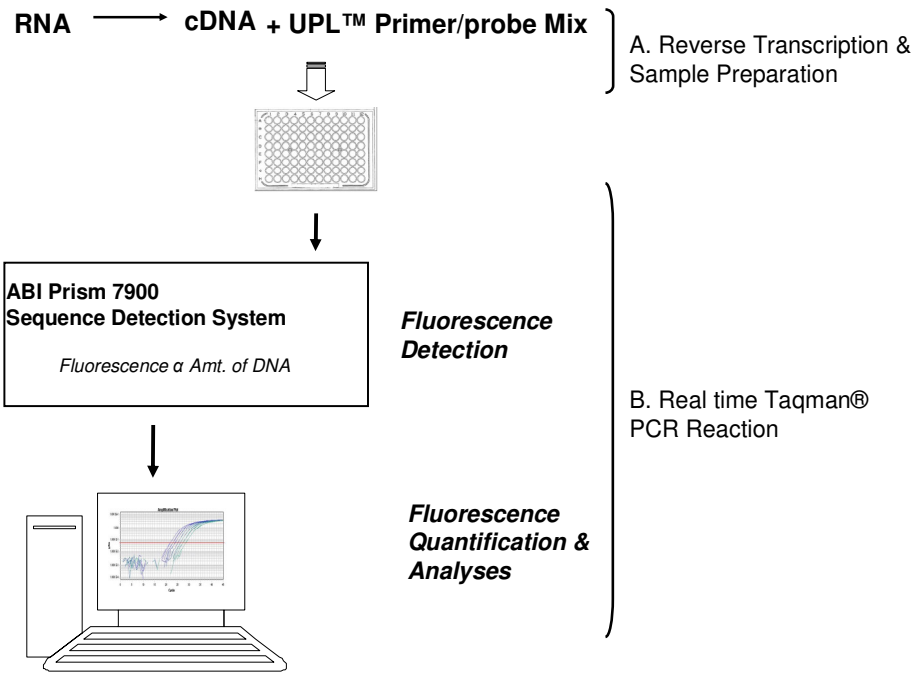

Figure 2.2 Overview of qRT-PCR experimental setup.

2.5.4.1 Reverse transcription of RNA using random hexamers

The use of random hexamers enables total RNA to be amplified including that of the 18S ribosomal RNA used for analysis as an internal control measure. The preparation of cDNA was carried out using a final concentration of 400ng of the total RNA extract (RNA Extraction; section 2.5.1) per 20µl reaction mix. A mastermix was prepared using reagents from the Applied Biosystems Taqman Reverse Transcription Kit at the following final concentrations; PCR buffer I (1x), $MgCl_2$ (5mM), dNTPs (1mM), RNase inhibitor (1µg/µl), Multiscribe reverse transcriptase (2.5µg/µl), random hexamers (2.5µM) and 5µl of H_2O per 20µl reaction mix. Individual reactions were mixed together in sterile PCR tubes and placed in a Biometra PCR machine set according to the following conditions;

25°C for 20 minutes

42°C for 60 minutes

95°C for 5 minutes.

2.5.4.2 Preparation of Taqman® reaction mix using the universal probe library™

The Universal Probe Library™ (UPL) (Roche, West Sussex, UK) is comprised of short (8-9 nucleotides in length) hydrolysis probes that are labelled with fluorescein (FAM) at the 5' end and a dark quencher dye at their 3'end. These short probes are based on locked nucleic acids (LNAs) as they have a 'locked' ribose ring where the 2'-O atom is connected to the 4'-C atom via a methylene bridge and have the ability to bind to their target sequences despite their short length. The resultant specificity of these short LNA-probes facilitates distinction between transcripts of various splice variants (e.g. ERβ isoforms) by using a probe that can only bind to one transcript or the other (Table 2.3).

Primers were designed by using the Roche online 'probe finder' assay design method at **https://www.roche-appliedscience.com/sis/rtpcr/upl/.**

Table 2.3 Primer and Probe Sequences (UPL) used in qRT-PCR

Gene	5' Sequence	3' Sequence	Probe No.
hERα	TTACTGACCAACC TGGCAGA	ATCATGGAGGGT CAAATCCA	69
hERβ	GCTCCTGTCCCAC GTCAG	TGGGCATTCAGC ATCTCC	62
hERβ2	TGGGTGATTGCCA AGAGC	GTTTGAGAGGCC TTTTTCTGC	52
hERβ5	GCTCCTGTCCCAC GTCAG	CACATAATCCCA TCCCAAGC	17

2.5.4.3 Quantitative real time Taqman® PCR

Quantitative Real Time Taqman® PCR is an automated, high throughput variation of conventional PCR. The Taqman® method employs the use of fluorogenic probes from the UPL (section 2.5.4.2) to enable quantification of DNA content based on a measure of fluorescence detection after each PCR cycle. Fluorescence emission occurs upon cleavage of the probe resulting from the activity of the Taq polymerase during each PCR cycle. Each reaction was prepared using the qPCR Supermix with Premixed ROX kit (11795-01K; Invitrogen), conducted in triplicate, plated in a 96-well MicroAmp Fast Optical reaction plate (Applied Biosystems) and run on the fast cycling programme of the ABI Prism 7900 Sequence Detection System (Applied Biosystems).

Reagent	Final Concentration	Vol. /15µl reaction (µl)
2X Express Supermix	1X	7.5
Forward Primer 20µM	200nM	0.15
Reverse Primer 20µM	200nM	0.15
Probe 10µM	100nM	0.15
18S	(10nM primer, 40nM probe)	0.1125
H_20		5.4375
cDNA		1.5

2.5.4.4 Analysis of computational output

An absolute quantification is processed and presented as an amplification plot on the ABI7900 sequence detection system. Levels of fluorescence are determined at each PCR cycle and are directly proportional to the amount of DNA product present at that point in the reaction. The FAM threshold cycle (Ct) value is the point on the exponential curve at which the level of fluorescence reached is considered statistically greater than background levels. The Ct value equates to the amount of PCR product formed and a change of one-fold Ct value represents a two-fold in the initial cDNA concentration.

Analysis was performed using the comparative Ct method where the fold change expressed is relative to a reference sample (e.g. untreated endogenous sample). First, the reporter signal was measured against that of an internal 18S ribosomal RNA control to correct for fluctuations between samples; ΔCt = FAM Ct – 18S VIC Ct. The average of the ΔCt triplicates was determined. ΔΔCt = ΔCt sample – ΔCt reference sample. The fold change in gene expression is calculated as $2^{-\Delta\Delta Ct}$ where the reference control was given a $2^{-\Delta\Delta Ct}$ of 1 and is based on the mathematical equation that describes the exponential amplification of a PCR: $Xn = X_0 \times (1+E_x)^n$ (Xn = number of target molecules at cycle n of the reaction, X_0 = number of target molecules, E_x = efficiency of target amplification, n is the number of cycles) (Livak and Schmittgen, 2001).

2.5.4.5 Primer/probe Validation

To validate use of the primer/probe mix, log ng cDNA values are plotted against the average of the ΔCt values. Serial dilutions of the prepared cDNA (neat, 1:10, 1:100, and 1:1000) were analysed and the resultant straight graph depicts efficiency of the primer/probe mix over a range of cDNA concentrations (Figure 2.3).

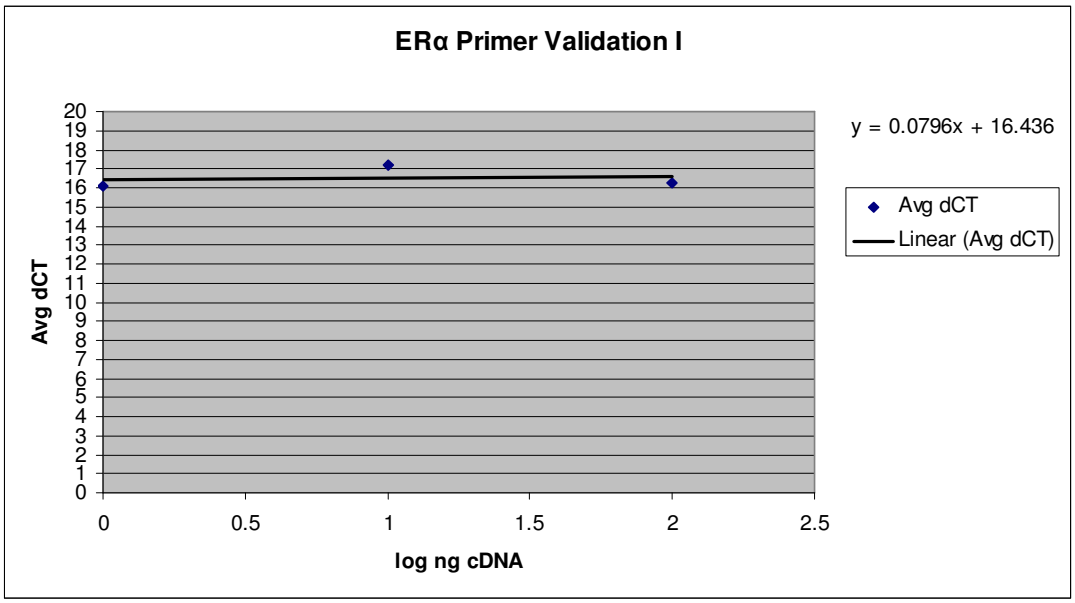

Figure 2.3 Validation of primer/probe mix used in Taqman® reactions.

A comparison of the efficiency of the primer/probe (e.g. ERα) to the 18S primer/probe is important to establish the efficacy of the sample primers relative to the endogenous 18S control (Figure 2.4).

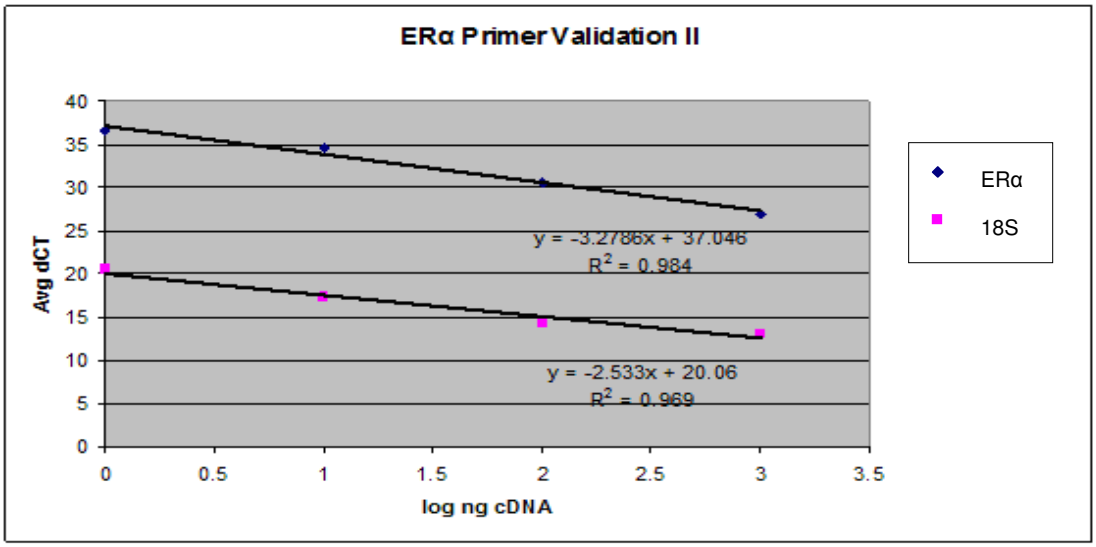

Figure 2.4 Validation of gene of interest primer/probe usage relative to 18S primer/probe control mix.

2.6 Protein Extraction and Quantification

2.6.1 Total protein extraction from cell lines and human tissue

During the process of protein extraction, all materials were kept on ice to prevent protein degradation. Total protein was extracted directly by disruption of PBS-washed cells using 1X RIPA buffer (section 2.10). For endometrial protein extraction, approximately 30mg of tissue was placed in 1ml of complete 1X RIPA buffer and homogenised with a rotostator homogeniser set at 20Hz for 2 minutes. The homogenates (both cell and tissue) were spun at 2,500 rpm for 10 minutes at 4°C and resulting supernatants (total protein content) were transferred to pre-chilled tubes for storage at -80°C. In some cases where the RIPA extraction method was too harsh to preserve phosphorylation status, NP-40 lysis buffer was used. The 0.1% SDS detergent content of this recipe promotes disruption of non-covalent bonds and adding negative charge to proteins to facilitate ease of separation during electrophoresis.

2.6.2 Nuclear protein extraction from cell lines

Nuclear protein isolation was conducted using reagents from the Active Motif Nuclear Extraction Kit (Cat. No. 40010, Active Motif Inc., Carlsbad, California, USA) and in accordance with manufacturer's instructions. This assay involved the preparation of a PBS/phosphatase inhibitor solution in H_2O and using this mix to wash the cells. This step precludes further protein modifications such as dephosphorylation and proteolysis from occurring. In this solution cells were centrifuged at 4°C for 5 minutes at 500rpm; the supernatant was discarded and the residual pellet was resuspended in a 1X hypotonic buffer solution (used to swell the cytoplasmic membrane) and detergent (which enables leakage of the cytoplasmic proteins into the supernatant). Following a brief 30 second spin at 4°C, this solution was separated into the cytoplasmic supernatant fraction and the pelleted nuclear fraction. Pellets were resuspended in lysis buffer AM1 (Active Motif Inc., Carlsbad, California, USA) (causing lysis of nuclear pellets) to which 10mM of the reducing agent dithiothreitol (DTT) and protease inhibitor cocktail were added. Following incubation for 30 minutes in slushy ice on a rocking plate the suspensions were vortexed briefly followed by a final centrifugation of 10 minutes at 14,000g at 4°C. The resultant nuclear supernatants were transferred to pre-chilled tubes for storage at -80°C.

2.6.3 Protein Quantification (Lowry method)

The quantification of protein samples was carried out in a 96-well flat bottomed plate using the Biorad DC Protein Assay Kit (Hemel Hempstead, Herts, UK) that is based on the Lowry method of protein quantification. The underlying principle of this method is a reaction between copper and the protein sample in an alkaline medium followed by a reduction of folin reagent by this copper treated protein sample. This reduction reaction yields a reduced species that gives rise to the characteristic blue colour observed. Detected protein values were compared to a standard curve formed by the use of a series of controls prepared with a known concentration of bovine serum albumin (BSA) (0.125-1.5 mg/ml) diluted in the same lysis buffer as that used for the collection of the protein extract being quantified. In accordance with the

guidelines provided by the manufacturer, 5µl of each sample being tested were used. To each sample 25µl of reagent mix 'A/S' was added (25µl of reagent S/ml reagent A) and followed by 200µl of reagent B. Thereafter the sample/reagent mixtures were left to incubate in the dark for 15 minutes at room temperature before being read on a plate reader (Labsystems Miltiskan Ex, VWR) at 690nm. Final concentrations of sample proteins were derived by comparison with the standard curve generated from the BSA standard series.

2.7 Western Blotting

Western blotting was conducted using NuPAGE® (Invitrogen, Paisley, UK) reagents, gels and buffers.

2.7.1 Sample preparation

Protein samples (~25µg) were prepared by suspending in 4X NuPAGE LDS Sample Buffer and 10X NuPAGE Reducing Agent and heating the final solutions at 70°C for 10 minutes. Following the denaturation process, samples were loaded on precast 4-12% Bis-Tris NuPAGE polyacrylamide gels alongside 10µl of 1X SeeBlue Plus2® Prestained marker dye (Invitrogen).

2.7.2 NuPage® Polyacrylamide Gel Electrophoresis

Loaded gels plunged in an electrophoresis tank filled with 1X NuPAGE® MOPS SDS Running Buffer (supplemented with NuPAGE® antioxidant) (Invitrogen) were run at 200V for approximately 50 minutes or until the bromophenol blue dye got to the bottom of the gel.

2.7.3 Protein transfer

Following protein separation, the gels were set up for transfer on to polvinylidene fluoride (PVDF) membranes (Millipore, Bedforf, UK). Each gel and its matching membrane (pre-soaked in methanol) were carefully placed in a cassette sandwiched between Whatmann paper and porous fibre pads (pre-soaked in transfer buffer to prevent dehydration of the gel during cassette assembly) in a transfer unit with 1X NuPAGE® Transfer Buffer (Invitrogen) with the gel at the negative electrode side for

4 hours at 40V. This assembly facilitates the movement of separated (negatively charged) proteins of the gel from the cathode towards the membrane at the anode. After transfer, membranes were blocked in a solution of 40% Odyssey Blocking Buffer (LI-COR™), 40% PBS, 20% pure goat serum for 1 hour at room temperature to prevent non-specific binding before 2x5 minute washes in PBS 0.1% Tween-20 (Sigma). Blocked membranes were incubated in the appropriate dilution of primary antibody (Table 2.4) at 4°C overnight. As a loading control measure, a β-tubulin antibody was included.

2.7.4 Antibodies (and peptides)

Following overnight incubation with the primary antibody to the protein of interest, the membrane was washed in PBS 0.1% Tween-20 (Sigma) for 4x5 minute washes to ensure the removal of residual primary antibody. Fluorescently labelled secondary antibodies (Table 2.5) that had been diluted 1:10,000 in Odyssey Blocking Buffer (LI-COR™) were applied to membrane for 1 hour at room temperature followed by 4x5min washes in PBS 0.1% Tween-20. The membrane was then transferred to a PBS only solution before being scanned for visualisation using the LI-COR™ machine.

Table 2.4 Primary antibodies used for Western blotting

Antigen	Host Species	Dilution	Source
ERα	Mouse	1:200	Vector[1]
ERβ (H-150)	Rabbit	1:200	Santa Cruz[2]
ERβ2	Mouse	1:200	Serotec[3]
ERβ5	Mouse	1:100	In-house[4]
ErbB1 (HER1)	Rabbit	1:200	Santa Cruz[2]
ErbB2 (HER2)	Mouse	1:40	Abcam[5]
ErbB3 (HER3)	Mouse	1:1000	Abcam[5]
ErbB4 (HER4)	Rabbit	1:4000	Abcam[5]
IGF-IRα (N-20)	Rabbit	1:200	Santa Cruz[2]
IGF-IRβ (C-20)	Rabbit	1:200	Santa Cruz[2]
β-tubulin	Mouse	1:600	Sigma[6]
β-tubulin	Rabbit	1:600	Santa Cruz[2]

[1]Vector Laboratories Ltd., Peterborough, UK

[2]Santa Cruz Biotechnology, CA, USA

[3]AbD Serotec, Kidlington, Oxford, UK

[4]In collaboration with Prof. N. Groome, Oxford Brookes University, Oxford, UK

[5]Abcam plc, Cambridge, UK

[6]Sigma-Aldrich, St. Louis, MO, USA

Table 2.5 Secondary antibodies used for Western blotting

Target	Dilution	Excitation Wavelength (nm)/ (colour emitted)	Source
Goat anti rabbit	1:10000	800(green)	Rockland[1]
Goat anti mouse	1:10000	680 (red)	Molecular Probes[2]

[1]Rockland Immunochemicals Inc., PA, USA

[2] Molecular Probes Europe BV, Leiden, The Netherlands

2.7.5 Protein expression assessment (LI-COR™ Instruments)

Protein determination was visualised using the LI-COR™ fluorescence detection system that enables simultaneous detection of two proteins distinguishable by use of different coloured fluorescent markers of the secondary antibodies. The use of direct infrared detection on membranes equate to the high sensitivity of this assay. Correction for sample variation in the amounts of proteins recognised by the primary antibody can be determined by quantitating the fluorescence levels (by drawing a rectangular marker around the band in question) of each protein under investigation and expressing it relative to the amount of protein detected using the control antibody (β-tubulin) for that same sample.

2.8 Fluorescent Recovery After Photobleaching (FRAP)

2.8.1 Background

FRAP is an in vivo microscopy technique that enables the study of intra-cellular protein dynamics and functionality. Originally described with associated mathematical quantitations in the mid-1970s (Poo and Cone, 1973, Axelrod *et al.*, 1976), FRAP is a useful and robust method to infer information regarding patterns of mobility of biological proteins. The mid-1990s saw a resurgence in popularity of the use of FRAP owing to the advances in confocal laser scanning microscopes coupled with the advent of green fluorescent protein (GFP)-derived fluorophores

(Cole *et al.*, 1996, Lippincott-Schwartz and Smith, 1997). The experiments in this study used yellow fluorescent protein (YFP)-appended ER proteins (section 2.8.4). The process itself exploits the phenomenon of photobleaching of fluorescent molecules of a defined region (strip) of the nucleus and monitoring recovery as a function of time as this region becomes repopulated with unbleached fluorescent molecules from outside of the bleached region (Fig. 2.5).

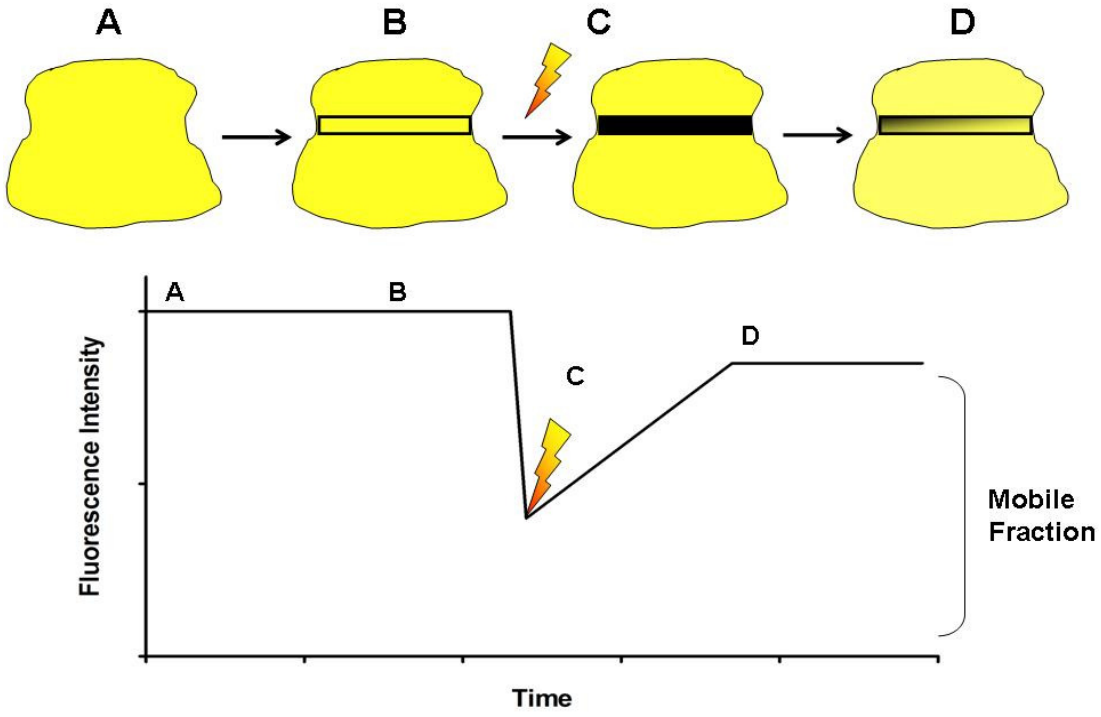

Figure 2.5 Overview of the concept of a FRAP experiment.

A cell is selected based on relatively uniform distribution of fluorescence (A), a region within the cell is selected for bleaching (termed Region of Interest I, B), the process of photobleaching abolishes fluorescence within this zone (C) and the redistribution of fluorescence back into the zone is recorded over time (D).

2.8.2 Live Cell Maintenance

Cells were cultured on 35mm glass bottom microwell dishes (Plastik® Cultureware, MatTek Corp., Ashland, MA, USA) at a density of 1 x 10^5cells/ml. For live cell image acquisition, infected/transfected cells were maintained in a 2.5% HEPES (Sigma, Cat. No. H-0887)/PBS solution (50µl/2ml) and in a heated chamber at 37°C.

2.8.3 Transient Transfection (Controls)

After plating for twenty-four hours, cells were transfected with the CY24 Plasmid (YFP tag) as a positive control (gratefully received from Dr. Rory Duncan, University of Edinburgh) using the JetPEI (Autogen Bioclear, Nottingham, UK, Cat. No.; 205-10) transfection reagent. The CY24 plasmid contained a cDNA construct encoding YFP (27kDa donor fluorophore) and CFP (27kDa acceptor fluorophore) separated by a flexible 25 amino acid linker. CY24 plasmid DNA (2µg/confocal dish) was added to 200µl 150mM NaCl and this mixture in turn was added to a solution made up of a 2:1 ratio of µg of plasmid DNA to JetPEI in 200µl 150mM NaCl. Following 30 minute incubation at room temperature, this mixture was added to the cells following removal of the existing media and the wells were topped up with DMEM only (no additions). Transfection efficiency was determined by monitoring the fluorescence levels emitted from cells by observation under a Plan-Apochromat 20X on an Axiovert 200M inverted microscope (Zeiss, Germany) twenty-four hours later.

2.8.4 Cell Infection

The cells were infected with adenoviral constructs expressing the ER of interest tagged with the 27kDa YFP at the N terminus of the protein (Table 2.6). YFP was selected for use on the basis of being a readily bleachable fluorophore that is insensitive to oxygen scavengers and other radical quenchers due to protection of the chromophore element of the molecule by a bulk solvent. The constructs were produced by insertion of full length cDNA clones to the ER of interest between the Eco RI and Bam HI restriction sites of a YFP shuttle vector (pEYFP-C1, Clontech, Mountain View, CA, USA). The shuttle vector was then co-transfected with the

adenoviral genome (pBHG1oxΔE1, 3Cre, Microbix, Ontario, Canada) for recombination in HEK293 cells and the resultant plaques were purified for the viral particles. These viral particles were then amplified in the HEK293 cell line and concentrated with the use of a commercial kit system (Vivascience, Littleton, MA, USA) by the Biomolecular Core Facility within the MRC Human Reproductive Sciences Unit, Edinburgh.

Table 2.6 Concentrations of Adenoviral Constructs used

Adenoviral Construct	**Plaque forming unit no./ml**
ERα-YFP	2.49×10^{11}
ERβ-YFP	7.08×10^{10}
ERβ2-YFP	2×10^{10}
ERβ5-YFP	8.9×10^{10}

2.8.5 The Process

In setting up a FRAP experiment, three Regions of Interest (ROI) are selected, each with the same dimensions (width and height) within the field of view. ROI I and ROI II were defined strips within the nucleus and ROI III is a region outside of the actual cell being investigated. ROI I was the region to be bleached while ROI II served as the reference region within the same nucleus. The use of strip-FRAP permitted change in the orientation of the strips and therefore allowed us to identify anisotropic diffusion patterns within the nucleus. ROI I was subjected to focused photobleaching whereby irreversible quenching of the fluorophores occur. Photobleaching involves the use of focused rapid pulses (iterations) of a high intensity laser to extinguish fluorescence and arises due to the covalent modifications involved in converting the molecule from an excited singlet to an excited triplet state and the photon-induced damage to the excited molecule. The photobleaching period was kept to a minimum as diffusion of molecules was still taking place during this time and the exchange of

bleached molecules outside of the ROI I would have an impact on the fluorescence levels outside of the ROI I. Fluorescence recovery back into the ROI I was measured as a function of time and occurs as quickly as possible after the bleach period to capture the most accurate data for the recovery curves (Fig. 2.5). This recovery was assessed under conditions of minimal laser power. The fluorescence intensity values are the output of the experiments and were used to quantify the parameters of activity and mobility (http://www.embl.de/eamnet/downloads/courses/FRAP2004/lsm510_inlivecellimaging.pdf).

2.8.6 Instrumentation Setup

FRAP was conducted using a Zeiss LSM 510 confocal inverted light scanning microscope equipped with acousto-optical tunable filters (AOTFs). AOTFs function to enable rapid switching between high and low intensity powers during and after the photobleaching process (Meyvis *et al.*, 1999). Images were captured in a 256 X x 100 Y frame through 63X objective lens before and after ligand treatment at 3 sec intervals for (~30sec) time periods after bleaching. Bleaching was carried out on a single z-section of the chosen cell (ROI I) with excitation of the Argon 12 laser (488 and 514nm) and emission via the 530-600 band pass yellow filter. The pinhole was kept open to the maximum and the number of iterations kept at 100.

2.8.7 Quantitative Interpretation

Raw data in the form of total of averaged pixel values acquired was the output from the Zeiss LSM 510 microscope. These values were transferred to Microsoft Excel software and the data was corrected for and normalised as outlined below.

Data from ROI I and ROI II were first corrected for background noise levels of fluorescence by subtraction of the fluorescence intensity values of ROI III. The corrected ROI I value was expressed as a percentage figure of corrected ROI II to normalise against decay in overall fluorescence levels throughout the nucleus due to

acquisition bleaching. Acquisition bleaching could arise from the exchange of bleached molecules outside of ROI I during the bleaching period (Eq. 2.1).

$$\frac{\left(fl_{ROI\ I} - fl_{ROI\ III}\right)}{\left(fl_{ROI\ II} - fl_{ROI\ III}\right)} \times 100 \Rightarrow fl_{Norm.\ 1} \tag{2.1}$$

where

$fl_{ROI\ I}$ = fluorescence intensity value of ROI I

$fl_{ROI\ II}$ = fluorescence intensity value of ROI II

$fl_{ROI\ III}$ = fluorescence intensity value of ROI III

$fl_{Norm,\ 1}$ = fluorescence intensity following normalisation step 1

The percentages of recovery were deducted by expressing the normalised percentages over the average of percentage values for scans taken prior to the bleaching process (Eq. 2.2). This reveals the fraction of molecules actually bleached and the recovery percentages over time arising from the flux of fluorescent molecules back into ROI I.

$$\frac{fl_{Norm.\ 1}}{\left(prebleach_{Avg.}\right)} \Rightarrow fl_{Norm.bleached\ pop.} \tag{2.2}$$

where

$fl_{Norm,\ 1}$ = fluorescence intensity following normalisation step 1

$prebleach_{Avg.}$ = average of two prebleach intensity values

$fl_{Norm,\ bleached\ pop.}$ = fluorescence intensity value of bleached molecule following normalisation

Finally, the data was normalised by setting the time of the first scan taken post bleach at 0 (Eq. 2.3) and subtracting the original value at this timepoint from all subsequent scan times.

$$T_0 = fl_{\,Norm.\,postbleach\ 1} \tag{2.3}$$

where

T_0 = time at which first postbleach value is plotted, sec

$fl_{\,Norm.\,postbleach\ 1}$ = normalised fluorescence intensity value of first scan postbleach

This first percentage recovery value at T_0 was also set to 0 and all successive percentage values were normalised to this first value (Fig. 2.6, red dotted line) (van Royen *et al.*, 2009).

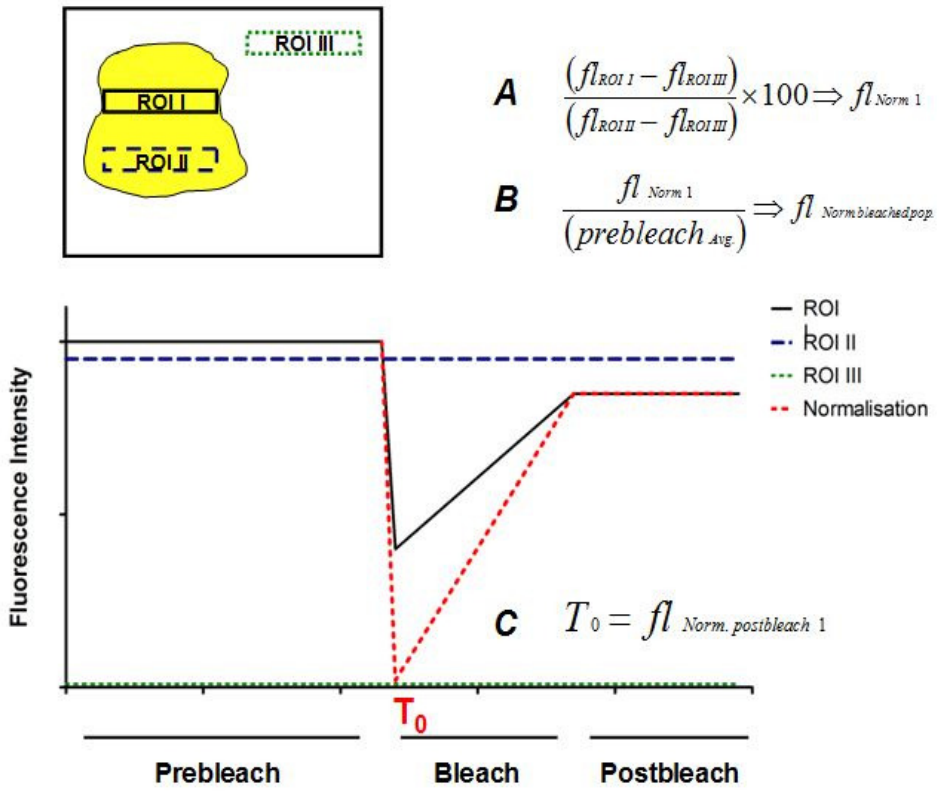

Figure 2.6 FRAP normalisation methodology.

Statistical evaluation of the normalised data values was conducted using GraphPad Prism version 5.02 for Windows (GraphPad Software, SanDiego California, USA, www.graphpad.com). In this context, a one-phase association non-linear regression analysis was applied (Eq. 2.4).

$$Y=Y_0 + (Plateau-Y_0)*(1-exp(-K*x)) \quad (2.4)$$

where

Y_0 = Y value when X (time) is zero, sec

Plateau (Y_{MAX}) = Y value at infinite times; the asymptote of the ROI I fluorescence recovery curve, % recovery

K = rate constant, sec^{-1}

Half-time = ln(2)/K, time taken for curve to reach 50% of plateau fluorescence intensity level, sec

Goodness of fit was determined by a $R^2 \geq 0.9$ and any set of values which did not achieve this value were designated outliers and dismissed from further analysis at this stage. The non-linear regression output values of Y_{MAX}, K and half-time were assessed for normality using the D'agostino-Pearson normality test (the less sensitive Shapiro-Wilk and Kolmogorov-Smirnov normality tests were also performed at this stage to reaffirm normality of the values). Assuming Gaussian distribution following tests for normality, an unpaired t-test was performed between untreated and treated datasets to discern statistical power.

2.9 Luciferase Gene Reporter Assay

2.9.1 Bright-Glo™ Luciferase Assay System (Promega)

Reporter Assays were performed using the Bright-Glo™ Luciferase System Protocol (Promega). Cells were seeded at ~1 x 10^5 cells/ml in charcoal-stripped foetal calf serum DMEM on 24-well plates 24 hours prior to infection. Cells were infected at a multiplicity of infection (MOI) of 50 for each of the adenoviral constructs ERα-YFP, ERβ-YFP, ERβ2-YFP and ERβ5-YFP independently or at a MOI of 25 when co-infecting the cells. The 3x ERE-tk-luciferase required to enable quantification of ER action at the ERE is an adenoviral vector containing three copies of the vitellogenin consensus ERE fused to the firefly luciferase cDNA clone and was a gift provided by Prof. DP McDonnell (Nagel *et al.*, 2001) (Duke University Medical Centre, North Carolina, USA). Infection with the 3x Ad-ERE-tk-luciferase was kept at a constant MOI of 50. After infection, cells were incubated for 4 hours in 200µl phenol-free DMEM to enable uptake of the constructs. Thereafter, wells were topped up to 500µl media. After 24 hours, cells were treated with DMSO alone or ligands diluted in DMSO for a further 24 hours. Cells were washed in cold-PBS, lysed in Glo lysis buffer (Promega) and harvested. Luciferase activity was assessed as per the Bright-Glo™ Luciferase Assay System (Promega) protocol. This system works on the premise of the luciferase enzyme catalysing a reaction that involves the mono-oxygenation of firefly luciferin to oxyluciferin that generates a luminescent signal. Luminescence was measured using the FLUOstar OPTIMA luminometer (BMG

Labtech, Offenburg, Germany). The relative light unit values were normalised to total protein values of the samples from the same experiment (section 2.6.3).

2.10 Commonly used Buffer Solutions

Phosphate Buffered Saline (PBS) (1X Stock)

NaCl	8.00g
KCl	0.20g
Na_2HPO_4	2.29g
KH_2PO_2	0.20g

Stock solution was made up to 1L with distilled water.

Tris Buffered Saline (TBS) (10X Stock)

Tris (Sigma)	60.5g
NaCl	87.6g
HCl	300ml

pH was adjusted to 7.4.

Stock solution was made up to 10L, 1X solution was prepared for use by diluting with distilled water.

RIPA Protein Extraction Lysis Buffer

	Final Concentration
HEPES-NaOH (pH7.5)	15mM
EDTA	10mM
Sodium orthovanadate	1mM
NaCl	0.15mM
Triton X-100	1.0%
Sodium deoxycholate	1.0%
Sodium dodecyl sulphate (SDS)	0.1%
Protease inhibitor cocktail (Roche)	10X

NP-40 Protein Extraction Lysis Buffer

	Final Concentration
NaCl	150mM
Tris Cl (pH 7.4)	50mM
EDTA	10mM
EGTA	10mM
NP-40 (Igepal)	0.6%
Glycerol	10.0%

Chapter 3

Agonist and antagonist influences on the dynamics of ER subtypes

3 Agonist and antagonist influences on the dynamics of ER subtypes

3.1 Introduction

ERα and ERβ are the products of different genes that appear to promote different functions (reviewed in Griekspoor *et al.*, 2007). X-ray crystallography studies have resolved the protein structures of the ligand binding domains of both proteins (Brzozowski *et al.*, 1997). Sequence comparisons have revealed almost 100% conservation in the DNA-binding domains, ~53% sequence homology in the LBD and limited homology at the N-terminus (Cowley and Parker, 1999). Ligands that exhibit selective binding to ERα and ERβ have been developed (reviewed in Katzenellenbogen *et al.*, 2000). Gene targeting experiments in mice have revealed a role for ERβ in having an influence on the function of ERα through reversing and inhibiting its effects (Damdimopoulos *et al.*, 2008). Expression of ERβ has been negatively associated with tumour grade and changes in the mRNA expression of cognate splice variants (i.e. ERβ2) have been related to tumourigenesis in breast cancer tissue (Leygue *et al.*, 1999a).

The canonical mode of ER activation is through ligand binding. Differential responses to ligand arise from the binding of ligand to receptor with associated changes in conformation and binding to cofactors and other transcription factors. The differences in the sequences of the ER N termini and the LBD are likely to underpin the differential responses observed between ligand treatments. It is believed that the AF-1 region plays a significant role in eliciting the differential responses to ligand observed between receptor subtypes (Pettersson and Gustafsson, 2001a, Picard *et al.*, 2008). The impact of the pure anti-oestrogen ICI 182,780 (Fulvestrant™) on receptor function arises from its capacity to physically disrupt the active conformation adopted between Helix 12 and the LBD during agonist binding which in turn prevents binding of coactivators such as SRC-1 that are required to necessitate functional responses (Pike *et al.*, 2001, Stenoien *et al.*, 2001a).

FRAP is a technique that is commonly employed to address the influence of compounds on intracellular mobility that has been made possible by advances in fluorescence labelling of proteins and the technology associated with advanced confocal microscopy (van Royen *et al.*, 2009). This method reveals the changes in mobility owing to changes in the nuclear distribution and allows one to probe the importance of associations with the nuclear architecture (Misteli, 2001). A number of studies have reported details of FRAP studies investigating ERα intranuclear dynamics in transfected cell lines (Stenoien *et al.*, 2001b, Reid *et al.*, 2003, Sharp *et al.*, 2006). However, there is limited data relating to the intranuclear kinetics of ERβ with only recently published reports on mouse ERβ mobility (Picard *et al.*, 2008) and a single report using human constructs (Damdimopoulos *et al.*, 2008).

The discovery of ERβ in the rat (Kuiper *et al.*, 1996) and human (Mosselman *et al.*, 1996) and the identification of ERβ splice variants isoforms of the human gene (Moore *et al.*, 1998, Ogawa *et al.*, 1998b) has increased the range of possible combinations for heterodimeric partnerships. Previous studies have demonstrated preferential binding of ERβ to ERα in a heterodimeric state (Cowley *et al.*, 1997) and the ability of the truncated ERβ2 isoform to form heterodimers with ERα (Leygue *et al.*, 1999a, Leung *et al.*, 2006). The formation of heterodimers between full length ER subtypes as well as the splice variants may facilitate cross talk between different signalling pathways and as such, may expand the regulatory potential of ERs.

3.1.1 Aims of this chapter

The primary objective of the studies in this chapter was to analyse the subnuclear dynamics of ERα, ERβ and ERβ2. In order to achieve this objective, studies were undertaken to establish and optimise the FRAP methodology for studies on YFP-tagged ERs. The impact of ligands on subnuclear distribution and mobility of receptors (homodimers) was examined in addition to the effect of co-expression of receptors (formation of heterodimers) on receptor dynamics. Furthermore, an assessment of correlations between receptor dynamics and transcriptional activity using a 3X-ERE-tk-luciferase reporter gene was addressed.

3.2 Materials and Methods

3.2.1 Cells

MDA, Ishikawa and hTERT cells were used for this study and maintained as described in section 2.1.

3.2.2 Taqman® qRT-PCR

RNA was extracted from lysed cells using a Qiashredder™ spin column for cell homogenisation (section 2.5.1) and quantified using the Nanodrop® ND 1000 (Labtech International, East Crawley, UK). Complimentary DNA (cDNA) was prepared using random hexamers (section 2.5.4.1) and was used for the Taqman reaction protocol outlined in section 2.5.4.3. Taqman analysis was conducted in triplicate and run on the ABI Prism 7900 using the Roche Universal Probe Library™ for ERα, ERβ and ERβ2. Data output from the detection system was quantified in accordance with the $2^{-\Delta\Delta Ct}$ algorithm (section 2.5.4.4). Results are expressed as means and standard errors and statistical analysis was conducted using a Student's t-test.

3.2.3 Adenoviral Infection

MDA cells were seeded at a density of 1 x 10^5 cells/ml on a 24 well plate and infected with the adenoviral constructs of ERα, ERβ, and ERβ2 that all included an N-terminal 'tag' consisting of a YFP independently or in combination (Chapter 2, section 2.8.4). Adenoviral uptake is through the Coxsakie-Adenovirus Receptor (CAR) on the cell surface and enables greater efficiency of uptake of receptor constructs than comparable methods employing transient transfection. The adenoviral constructs were infected over a wide range of MOI values (10, 25, 50 and 100). MOI values reflect the number of adenoviral particles infected per cell and are derived by calculation with using the titre of the virus involved. Adenoviral titre is determined by the number of plaques formed in response to viral inoculation into the growth media of cells and is expressed as plaque forming units/ml (pfu/ml). To define the amount of virus to use in a given assay, the total number of viral particles required (i.e. MOI value x no. of cells present) is divided by the viral titre. Infected cells were imaged using a Plan-Apochromat 20X on an Axiovert 200M inverted microscope (Zeiss).

3.2.4 Western Immunoblotting

Western blotting was performed on total protein extracts from MDA cells that had been infected with viral particles containing YFP-tagged or untagged cDNA constructs of ERα, ERβ and ERβ2. The infected cells were lysed with high-salt RIPA buffer (section 2.6.1) and quantified in accordance with the Biorad DC Protein Assay (section 2.6.3). The protein extracts were separated on polyacrylamide gels by electrophoresis (section 2.7.2) and electro-transferred to PVDF membranes (section 2.7.3). Membranes were incubated with antibodies specific for ERα or ERβ (specific to the N-terminal domain that is common to all ERβ splice variants) for verification of infected protein size. After incubation with appropriate secondary antibody (Table 2.4) they were scanned using the LI-COR™ infrared detection system (2.7.5).

3.2.5 Cell Treatments

To establish the impact of different ligands on ER receptor activity, cells were incubated with E2 or the selective agonists PPT™ and DPN™ all at final concentrations of 10^{-8}M or the ER antagonist ICI 182,780. Control treatments using a DMSO vehicle at 10^{-8}M were run in parallel. Ligands were added 1 hour prior to live-cell FRAP analyses and 24 hours in advance of cell harvesting for luciferase assays (see section 3.2.7 below).

3.2.6 Fluorescence Recovery After Photobleaching

FRAP analysis was carried out on a LSM 510 confocal inverted light scanning microscope (section 2.8.6). In brief, live cells were maintained in PBS buffered with 10mM HEPES in an enclosed chamber heated to 37°C (section 2.8.2). Cells expressing YFP were selected for bleaching on the basis of uniform distribution of levels of fluorescence. Three ROIs of equal dimension were chosen (section 2.8.5). Two prebleach images were captured at 3 second intervals followed by photobleaching resulting from a series of focused pulsed iterations using the Argon 12 laser (488 and 514nm) at maximal power. Eight subsequent images were taken to establish recovery patterns using an attenuated laser (514nm set between 1-5% power) (section 2.8.6). Data collation and quantitation was conducted and subject to correction, normalisation and statistical evaluation as outlined in section 2.8.7.

3.2.7 Luciferase Gene Reporter Assay

Ligand activation was assessed using a luciferase reporter assay carried out as described in section 2.9.1. Luciferase activity expressed as 'relative light units' detected on the FLUOstar OPTIMA luminometer (BMG Labtech) was normalised against total protein content from samples of the same experiment and conditions using data obtained with the Biorad DC Protein Assay (section 2.6.3).

3.3 Results

3.3.1 Characterisation of Cell lines

3.3.1.1 Expression of mRNAs in cell lines

Expression of ERα, ERβ and ERβ2 mRNA was measured by Taqman™ qRT-PCR for each of the three cell lines (MDA, Ishikawa and hTERT) and compared to a human RNA control (Fig. 3.1). Expression of ER mRNAs was barely detectable in MDA cells and this line was used for FRAP in order to optimise the imaging techniques for the study of the impacts of treatments on ERs in a background of low basal endogenous receptor. In line with published results (Nishida *et al.*, 1985), the Ishikawa cell line was ERα positive but expressed low ERβ and no ERβ2 mRNAs. hTERT cells were ERα+ve/ERβ+ve/ERβ2+ve (Fig. 3.1). After optimising the conditions required for optimal imaging and FRAP assays, the Ishikawa cells were employed to study the role of ligands in an endometrial adenocarcinoma background and subsequently the hTERT studies were conducted to decipher the role of ligand-dependent ER activity in untransformed endometrial epithelial cells.

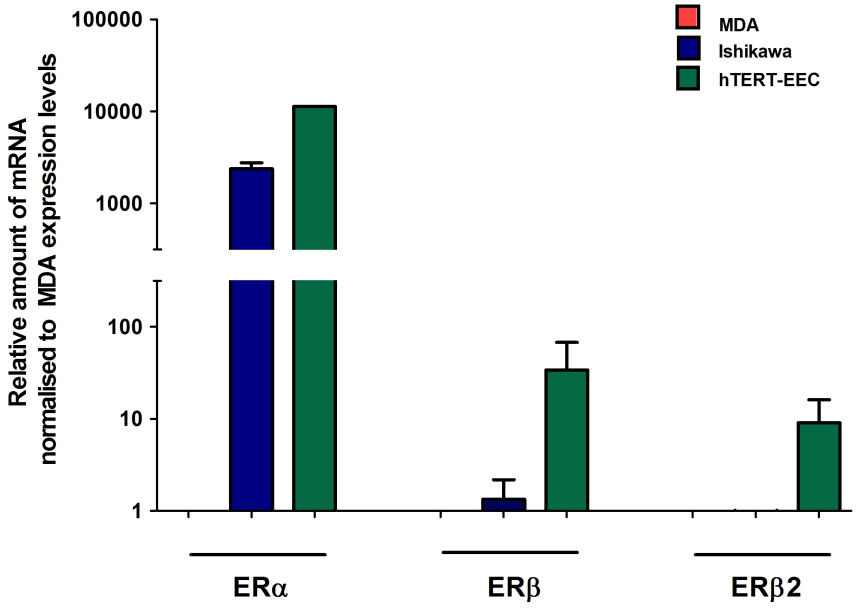

Figure 3.1 Comparison of mRNA expression of endogenous ERα, ERβ and ERβ2 in Ishikawa and hTERT cell lines relative to the MDA cell line.

Ishikawa and hTERT cells are ERα-positive and hTERT cells are ERβ and ERβ2 positive; the MDA cell line lacked endogenous ER expression.

3.3.1.2 Multiplicity of Infection determination; single infections

The effect of adenoviral-mediated ER expression on cell viability was examined. Titration assays were carried out in the MDA cells to define the optimum number of adenoviral particles required, i.e. MOI value, to infect a given number of cells (1 x 10^5). Cells were infected with increasing amounts (MOI) of virus expressing ERα, ERβ and ERβ2 for 24 hours with the resultant images presented in Fig. 3.2. The merged phase contrast and fluorescent images presented highlight the ratio of relative infectivity levels to the actual number of cells present. All YFP-tagged ERs were detected in the nuclear compartment of the cells consistent with the pattern of expression of endogenous ERs. The optimal level of infectivity was determined as a compromise between fluorescence expression and cell viability. At MOIs of 10, 25 and 50 the ratio of infected cells to the overall cell population was low. At an MOI of 100, infectivity was deemed significant with ~55-60% of cells expressing fluorescent ER and was selected as the optimal MOI to be used for all constructs in future

experiments. At an MOI of greater than 100, significant cell death occurred (data not shown).

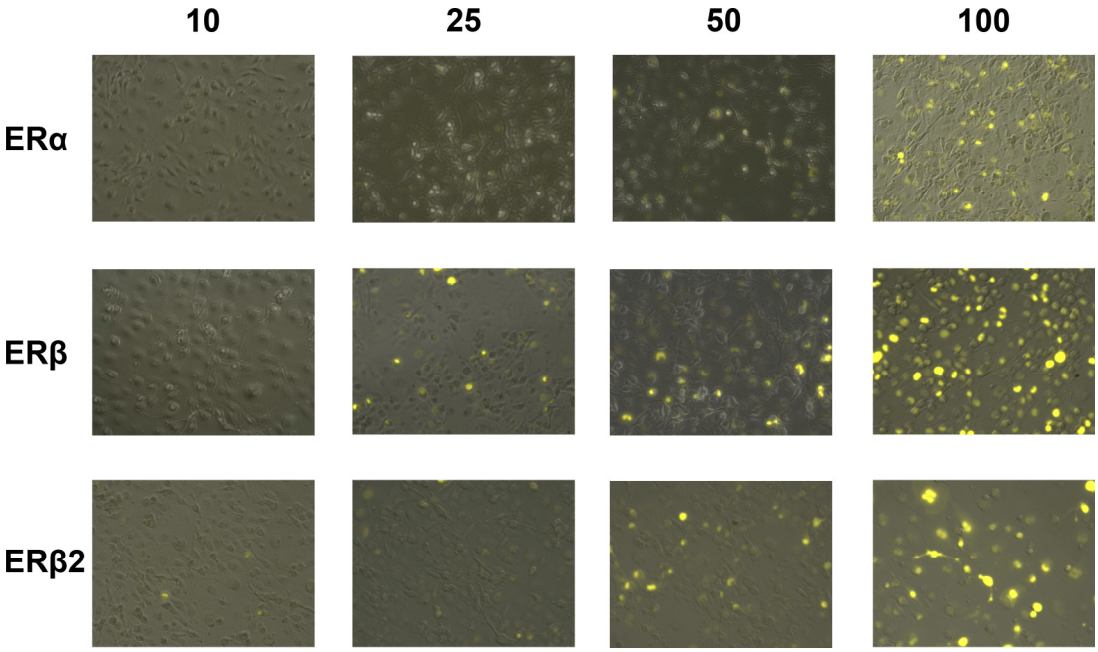

Figure 3.2 Observational evaluation of MDA cells infected with yellow fluorescent labelled adenoviral ER constructs.

Cells were infected over a range of MOI values (namely 10, 25, 50 and 100) with either of the constructs ERα, ERβ or ERβ2 to establish optimum viral levels required for infection and localisation at the nucleus. A final MOI value of 100 was chosen for infection of cells with a single ER construct. Images presented are merged representations of phase contrast and fluorescent cells to establish infection rates relative to the actual number of cells present. Images were captured at 20X using a Zeiss Axiovert 200M microscope.

3.3.1.3 Optimal MOI determination; multiple infection

The morphological appearance of MDA cells infected simultaneously with two fluorescent-labelled ER constructs is depicted in Fig. 3.3. At low MOI values of 10 and 25 for each construct, there were insufficient levels of fluorescence to warrant further experimentation. An MOI of 50 for each of the fluorescent constructs was selected thereby giving a final total MOI of 100 per 1 x 10^5 cells. An MOI of 100 for each infected construct yielded cytotoxic effects on cells where a significant reduction in cell viability was associated with floating and rounded up cells.

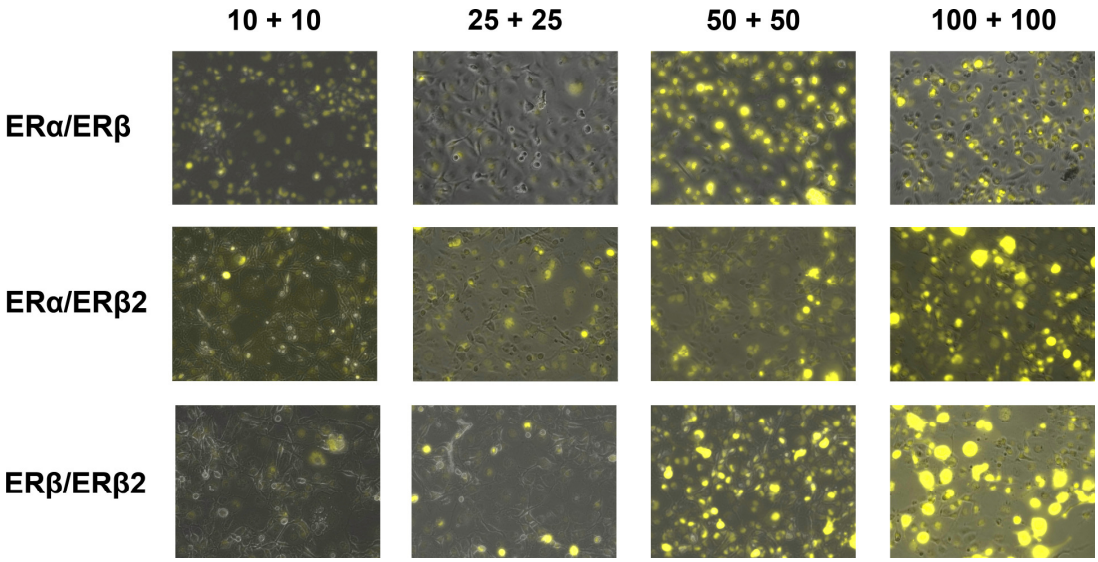

Figure 3.3 Observational evaluation of MDA cells infected with two YFP-tagged ER constructs.

Cells were infected over a range of MOI values (namely 10, 25, 50 and 100) to establish optimum viral levels required for infection and localisation at the nucleus. A final MOI value of 50 for each construct was considered optimum for infection of cells. Images presented are merged representations of phase contrast and fluorescent cells taken at 20X using a Zeiss Axiovert 200M microscope.

3.3.1.4 Expression of mRNAs in cells infected with viral constructs

Further to the observation that infection of the ER constructs was optimal at an MOI of 100 (section 3.3.1.2), ER mRNA expression in cells infected with MOI values of 50 and 100 was evaluated by qRT-PCR. The data presented have been normalised in accordance with the comparative CT method outlined in Section 2.5.4.4. Compared with endogenous ERα levels in MDA cells, infected cells with a MOI of 50 and 100 ERα-YFP showed ~10,000 and 30,000 fold increase in mRNA concentrations respectively (Fig 3.4; A). The expression of ERβ and ERβ2 mRNA was also significantly increased following infection with ERβ-YFP (~7000 and ~28000 fold induction respectively) and ERβ2-YFP (~15000 and ~35000 fold induction respectively) at MOI values of 50 and 100 (Fig 3.4; B and C). Table 3.1 illustrates the raw threshold cycle (Ct) values acquired from the Taqman™ run. The high Ct values determined from endogenous ERα, ERβ and ERβ2 samples reaffirm the low basal expression of ERs in the MDA cell line.

Endogenous ERα mRNA expression was readily detectable in Ishikawa cells by quantitative Taqman™ PCR. Compared with endogenous ERα levels in Ishikawa cells, infected cells at MOI values of 50 and 100 ERα-YFP demonstrated a negligible effect on mRNA levels (~1.5 and 3 fold increase respectively) (Fig 3.5; A). The expression of ERβ and ERβ2 mRNA was significantly increased following infection with ERβ-YFP (~15000 and ~85000 fold induction respectively) and ERβ2-YFP (~70000 and ~100000 fold induction respectively) at MOIs of 50 and 100 (Fig 3.5; B and C). Table 3.1 illustrates the raw threshold cycle (Ct) values acquired from the Taqman™ run. A relatively low Ct value of 24.5 was obtained for endogenous ERα levels in Ishikawa cells and infection of more ERα-YFP into these cells did not significantly impact on the doubling rates of the original cDNA content (Table 3.1). Significant changes to Ct values were determined with infection of ERβ and ERβ2 with respect to their cognate endogenous high Ct values. This data establishes the Ishikawa cells as an ERα positive cell line with comparably low ERβ basal levels of expression.

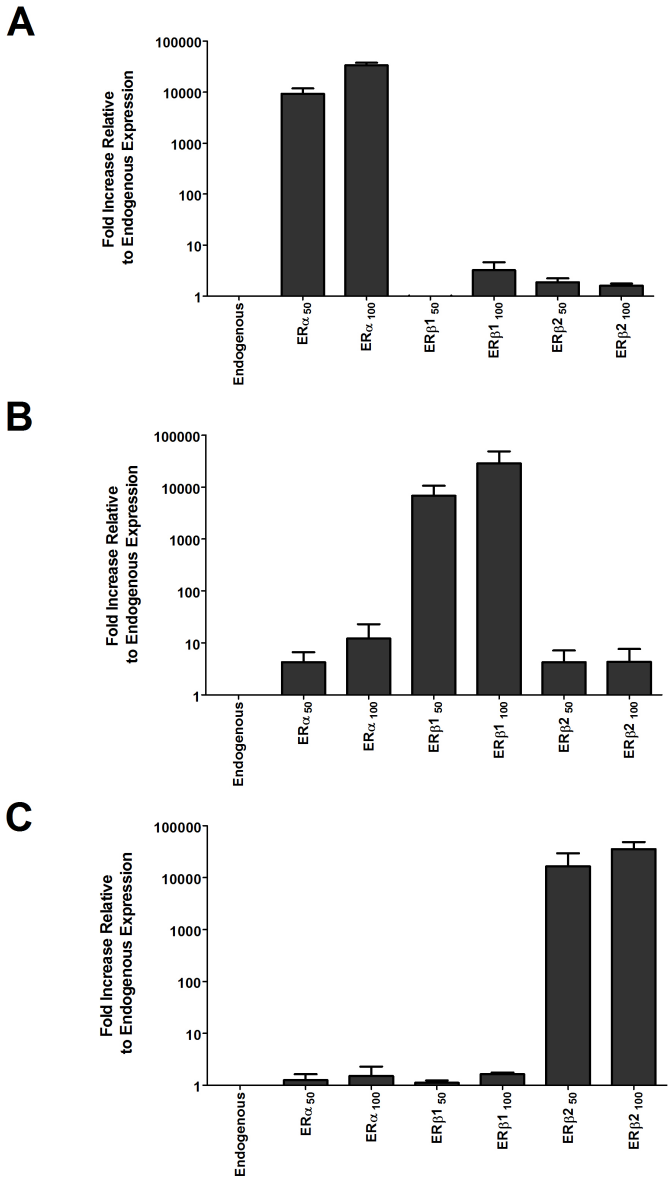

Figure 3.4 ER mRNA expression in MDA cells.

Cells were infected with constructs of ERα (A), ERβ (B) and ERβ$_2$ (C) at multiplicity of infection values of 50 and 100 respectively via adenoviral delivery. Messenger RNA levels are presented relative to endogenous oestrogen receptor expression levels in MDA cells and are representative of N=3±SEM.

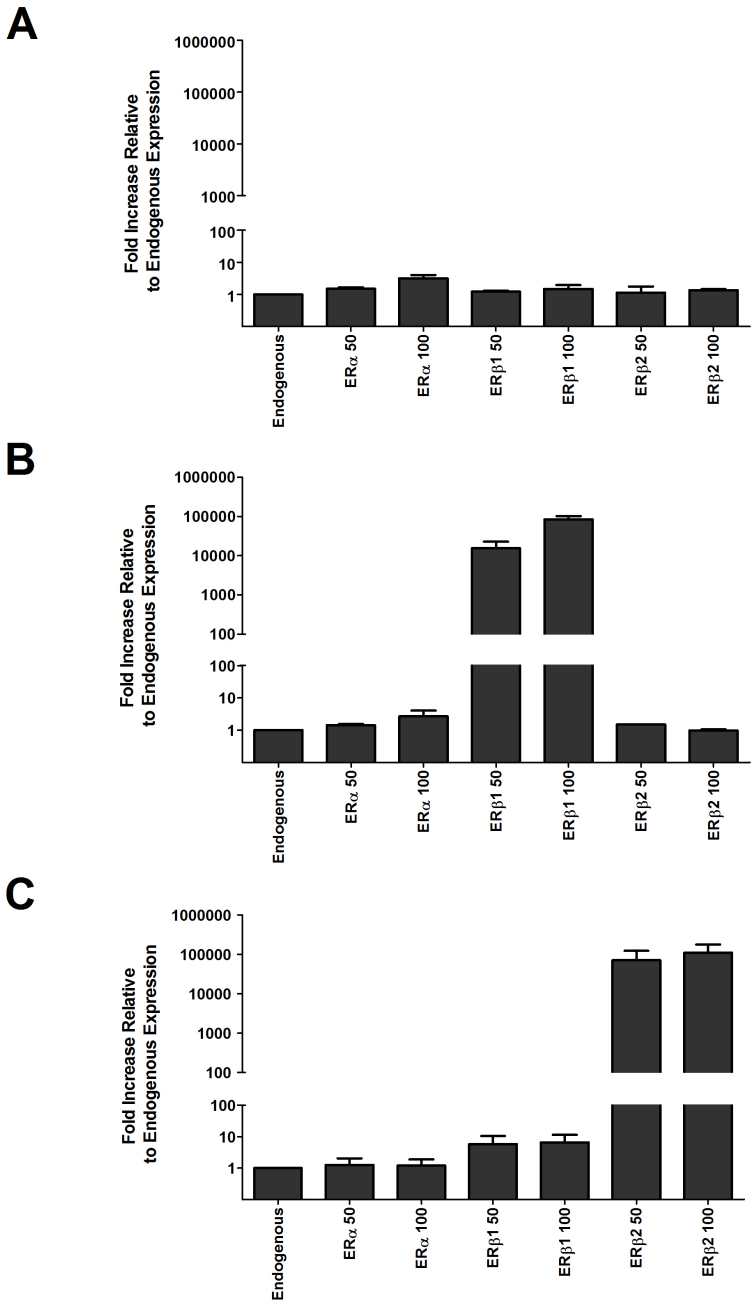

Figure 3.5 ER mRNA expression in Ishikawa cells.

Cells were infected with constructs of ERα (A), ERβ (B) and ERβ$_2$ (C) at multiplicity of infection values of 50 and 100 respectively via adenoviral delivery. Messenger RNA levels are presented relative to endogenous oestrogen receptor expression levels in Ishikawa cells and are representative of N=3±SEM.

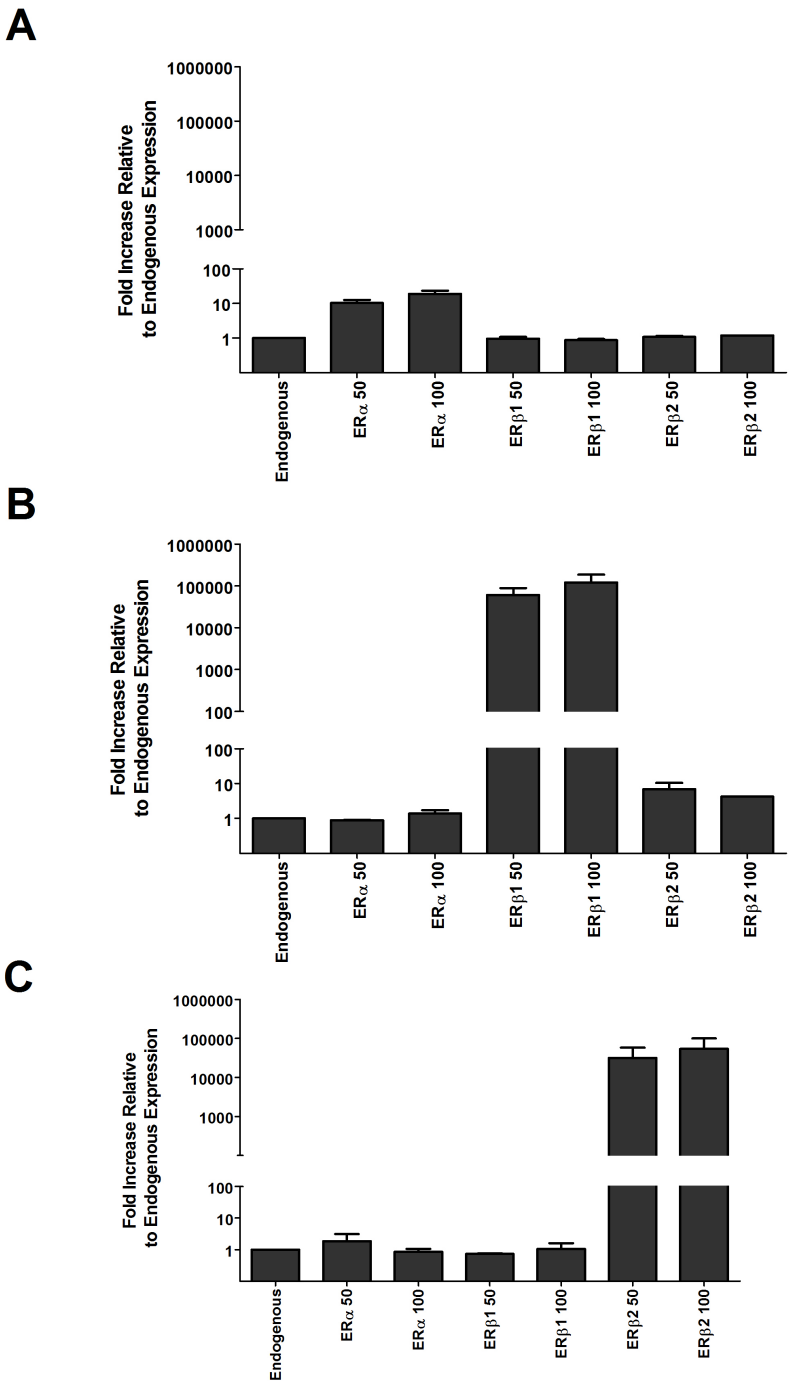

Figure 3.6 ER mRNA expression in hTERT cells.

Cells were infected with constructs of ERα (A), ERβ (B) and ERβ$_2$ (C) at multiplicity of infection values of 50 and 100 respectively via adenoviral delivery. Messenger RNA levels are presented relative to endogenous oestrogen receptor expression levels in hTERT cells and are representative of N=3±SEM.

ERα mRNA expression was readily detectable in hTERT cells by quantitative Taqman™ PCR. Compared with endogenous ERα levels in hTERT cells, infected cells at MOI values of 50 and 100 ERα-YFP exhibited a minor effect on mRNA levels (~10 and 20 fold increase respectively) (Fig 3.6; A). The expression of ERβ and ERβ2 mRNA was significantly increased following infection with ERβ-YFP (~60000 and ~125000 fold induction respectively) and ERβ2-YFP (~30000 and ~60000 fold induction respectively) at MOI values of 50 and 100 (Fig 3.6; B and C). The raw threshold cycle (Ct) values acquired from the Taqman™ run revealed early detection of endogenous ERα in comparison to endogenous ERβ and ERβ2. Significant changes to these Ct values were produced following infection of the YFP-tagged ERs at MOI values of 50 and 100.

Table 3.1 Average threshold cycle (Ct) values determined by the ABI 7900 sequence detection system (Applied Biosystems).

Specific primer and probe sequences from the Universal Probe Library™ to ERα, ERβ and ERβ2 were used to compare the doubling rates of DNA in samples infected with MOIs of 50 and 100 of individual ERs in comparison to the endogenous amount of ER present in MDA, Ishikawa and hTERT cell lines (prior to normalisation with the 18S ribosomal RNA control).

	ERα	**ERβ**	**ERβ2**
MDA			
Endogenous	37.0	37.0	35.0
MOI 50	24.0	23.0	21.0
MOI 100	22.0	21.0	20.0
Ishikawa			
Endogenous	24.5	35.0	34.0
MOI 50	24.0	23.0	19.0
MOI 100	23.0	21.0	18.0
hTERT			
Endogenous	22.0	33.0	33.0
MOI 50	19.0	18.0	19.0
MOI 100	18.5	17.0	18.0

3.3.1.5 Protein expression

MDA cells did not contain detectable amounts of ERα or ERβ proteins (Control Lane 1: Fig. 3.7 and 3.8) as was predicted from the low basal levels of mRNA as determined by qRT-PCR (Fig. 3.1). On this basis, this cell line was selected and utilised for further experimentation to assess the impact of natural and synthetic compounds on individual ERs both independently and in combination. To validate the use of the ER constructs, total protein was extracted from cells that had been transfected with a control plasmid encoding a YFP protein linked to a cyan fluorescent protein (CFP) (Lane 2) and cells that had been infected with both the tagged and untagged constructs (MOI of 50 each) of either the ERα (Lane 3), ERβ1 (Lane 4) or

ERβ2 (Lane 5). Western blot analysis confirmed ERα untagged protein (red band) at ~66kDa and the addition of a YFP tag (27kDa) generating a product size of ~93kDa (Fig.3.7). The antibody specific to the YFP detected the YFP/CFP plasmid (Lane 2) at ~54kDa and the YFP label of the cells infected with tagged ERβ1 and ERβ2 (green bands) (Lanes 4 and 5).

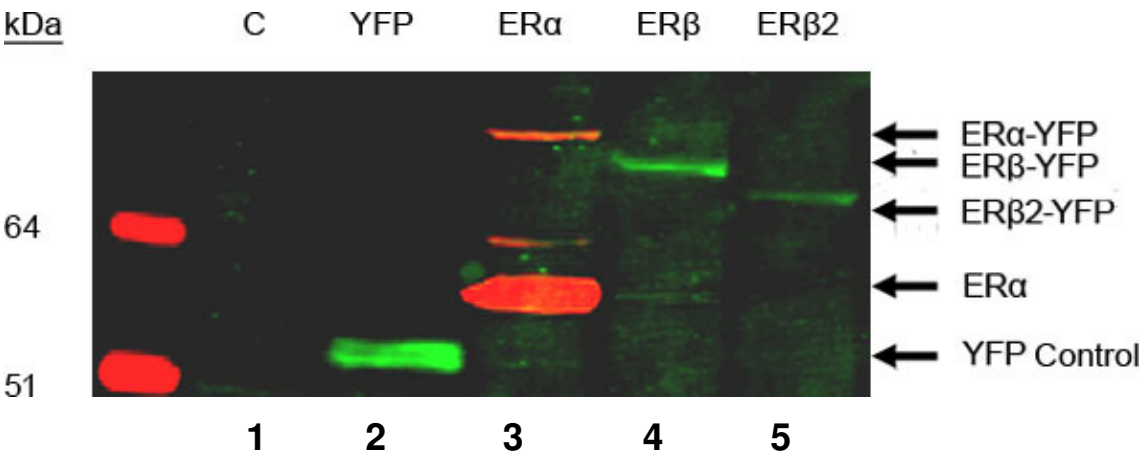

Figure 3.7 Western blot analysis of ERα and YFP-labelled protein expression in MDA cells.

Protein extracted from: Lane 1, Uninfected cells (C); Lane 2, cells transfected with a control plasmid expressing YFP and CFP separated by a 25 amino acid linker sequence (total size ~55kDa); Lane 3, cells co-infected with untagged and YFP-tagged ERα constructs; Lane 4, cells infected with untagged and YFP-tagged ERβ constructs; Lane 5, cells infected with untagged and YFP-tagged ERβ2 constructs. Membrane was incubated with anti-ERα (red) and anti-YFP (green).

The same samples were used to generate a membrane that was probed with an anti-ERβ antibody that was specific to the N-terminus of the receptor (Fig. 3.8). This antibody should detect all ERβ splice variants (which only differ at the C terminal domain). No ERβ was detected in the control lane, but both untagged (green) and YFP-labelled ERβ (red) were detected at the correct sizes in lanes 4 and 5. A very weak YFP band was detected in the ERα-YFP infected sample but it is thought that this sample did not run properly and may have been contaminated with salt.

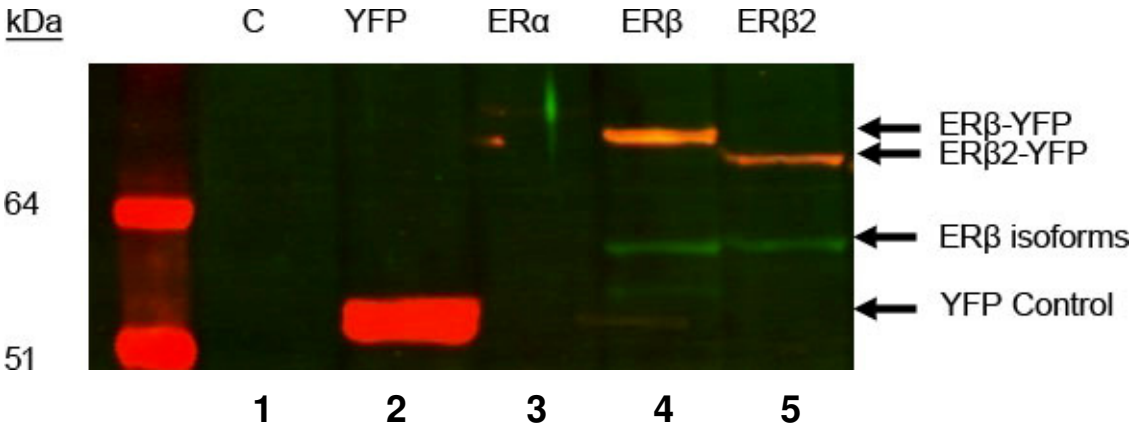

Figure 3.8 Western analysis of ERβ protein expression in MDA cells.

Protein extracted from: Lane 1, Uninfected cells (C); Lane 2, cells transfected with a control plasmid expressing YFP and CFP separated by a 25 amino acid linker sequence (total size ~55kDa); Lane 3, cells co-infected with untagged and YFP-tagged ERα constructs; Lane 4, cells infected with untagged and YFP-tagged ERβ constructs; Lane 5, cells infected with untagged and YFP-tagged ERβ2 constructs. Membrane was incubated with a generic anti-ERβ (green) antibody directed against the N-terminus of ERβ and anti-YFP (red).

3.3.2 Intranuclear dynamics of ER homodimers

The spatiotemporal response of ER subtypes to ligand activation was examined. For each treatment, an observational assessment of ER sub-nuclear distribution was made. Secondly, the temporal effect of treatments on intranuclear mobility was further investigated using FRAP quantitation methods.

3.3.2.1 Agonist Response

A panel of ligands was used to investigate the influence of natural (E2) and synthetic (PPT™ and DPN™) agonist compounds on the intranuclear dynamics of ERα, ERβ and ERβ2 in different cell contexts. Following infection with an individual ER subtype, experiments were conducted using a DMSO vehicle control. The results obtained after agonist stimulation were compared to this vehicle control response

3.3.2.1.1 MDA cells

ERα

Infection of ERα-YFP into MDA cells yielded homogenous nuclear distribution of fluorescence (Fig 3.9). The application of a DMSO vehicle control for 1 hour had no impact on this observation. Treatment of cells with E2 for 1 hour induced the redistribution of the receptor with the accumulation of 'speckles' throughout the nucleoplasm giving a punctate appearance to the nucleus. This punctate appearance was observed albeit to a lesser extent with 1 hour PPT™ and DPN™ incubations (Fig 3.9).

Under conditions of FRAP, the region enclosed within the red box represents the area to undergo photobleaching (ROI I). Fig 3.9 depicts a snapshot of the images captured following photobleaching of cells incubated with DMSO (control), E2, PPT™ or DPN™. Re-equilibrium of ERα-YFP after DMSO treatment was achieved at 18 seconds following bleaching (left hand panel). There was no significant apparent recovery of fluorescent molecules into the red zone (ROI I) following E2 incubation up to and including 18 seconds after photobleaching. It was noted that there is some recovery of fluorescent ERα-YFP molecules back into the ROI I of nuclei treated with PPT™ and DPN™.

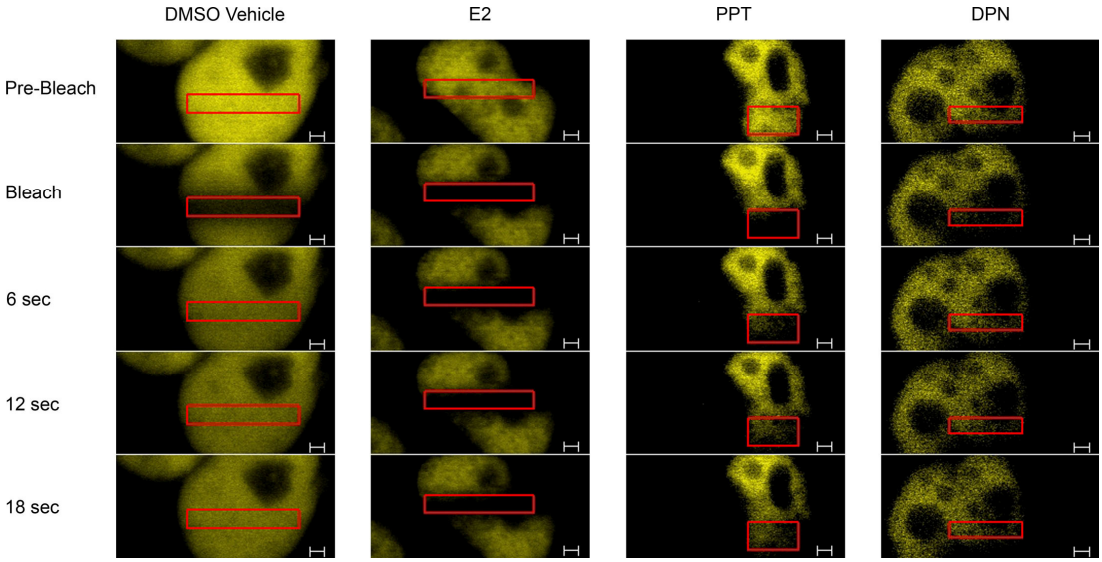

Figure 3.9 Qualitative FRAP assessment.

Live MDA cells were infected with ERα-YFP and subjected to treatment with either a DMSO vehicle control, E2 10^{-8}M, PPT™ 10^{-8}M or DPN™ 10^{-8}M for 60 minutes. The fluorescent molecules of a designated region (red box) were annihilated during the bleaching process and recovery back into this zone was monitored up to 18 seconds. This time period was chosen on the basis of full recovery observed in the control nuclei.

A number of parameters were quantified to substantiate the observational findings from the ligand treatments on ERα in MDA cells. Measurements were normalised and corrected for background fluorescence as well as varying fluorescent levels between nuclei. In cells incubated with DMSO (control), total recovery into the bleached ROI I was averaged at ~60% of the initial fluorescence in this zone after 25 seconds (Fig. 3.10; A, B, C: black line). All ligand treatments were compared against this result. In all cells recovery into the bleached zone was maximal at ~25 seconds. This value is designated as the Y_{MAX} value (i.e. the point following a number of successive equal values where the response has reached a plateau level in all subsequent result sections). Fig 3.10A shows data obtained with ERα which confirmed the impact of E2 on ERα mobility within the nuclear domain with an obvious and significant effect on the percentage of recovery into ROI I. The Y_{MAX} was used as a parameter for direct comparison between vehicle-treated and ligand-treated ERs. In the DMSO treated

control cells the percentage recovery for ERα was ~60%. Notably, treatment of ERα with the agonists PPT™ and DPN™ also resulted in a significant impact on the recovery rates of ERα molecules back into the bleached zone (Fig. 3.10B and C respectively) although the changes in Y_{MAX} were less pronounced that that with E2 treatment.

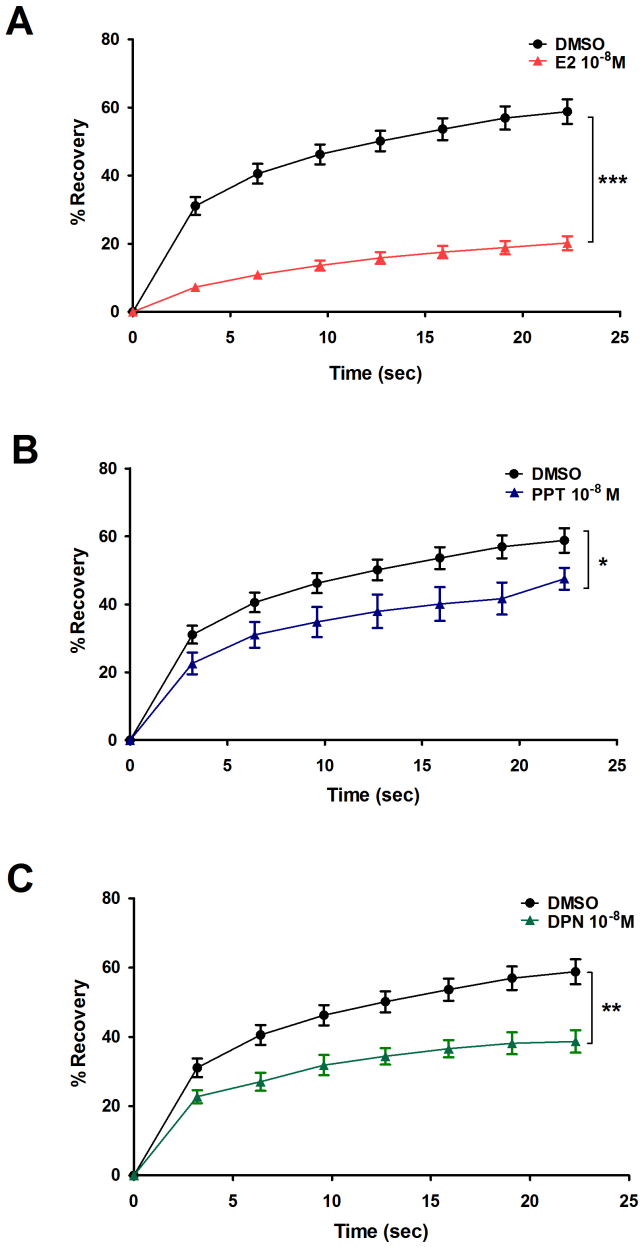

Figure 3.10 Quantitative analysis of intra-nuclear kinetics of ERα-infected MDA cells.

*Graphical depiction of impact of ligand treatment on the recovery rates of ERα fluorophores over time back into the bleached zone. This recovery is denoted by the point at which the Y_{MAX} is achieved and a plateau is reached on the graph. Recovery rates of ERα-infected MDA cells are presented in response to E2 (A), PPT™ (B) and DPN™ (C) stimulation at a concentration of 10^{-8}M. *** (P<0.001), ** (P<0.01) and *(P<0.05) denotes significance in variation of ligand treatments compared with the vehicle control (black column) as derived from the Student's t-test (N≥8).*

ERβ

The distribution of ERβ-YFP in the nuclei of MDA cells was not uniform and the ERβ-YFP appeared to localise to certain regions within the nuclear architecture in its endogenous unliganded state. The DMSO vehicle control had no impact on this distribution (Fig 3.11 left hand panel). Treatment with E2 augmented the accumulation of speckles throughout the nucleoplasm giving a punctate appearance to the nucleus and limited recovery into ROI I was observed. This punctate appearance and reduced mobility (recovery) was also observed after incubation with DPN™. The distribution of ERβ-YFP following PPT™ treatment mirrored the pattern of the control nuclei and rapid recovery after bleaching resembled that in the DMSO cells (Fig 3.11). In DMSO treated cells the Y_{MAX} recovery of ERβ after ~25 seconds was ~40%. The impact of E2 on ERβ-YFP recovery within the nucleus was readily apparent on the Y_{MAX} curves (Fig. 3.12A) with E2 treatment having a significant effect on slowing the recovery rate of fluorescing molecules back into ROI I. The treatment of cells expressing ERβ with the synthetic compound PPT™ had no impact on ERβ-YFP dynamics with regard to Y_{MAX} (Fig 3.12B). Treatment with DPN™ had a significant impact on Y_{MAX} in line with expectations (Fig. 3.12C).

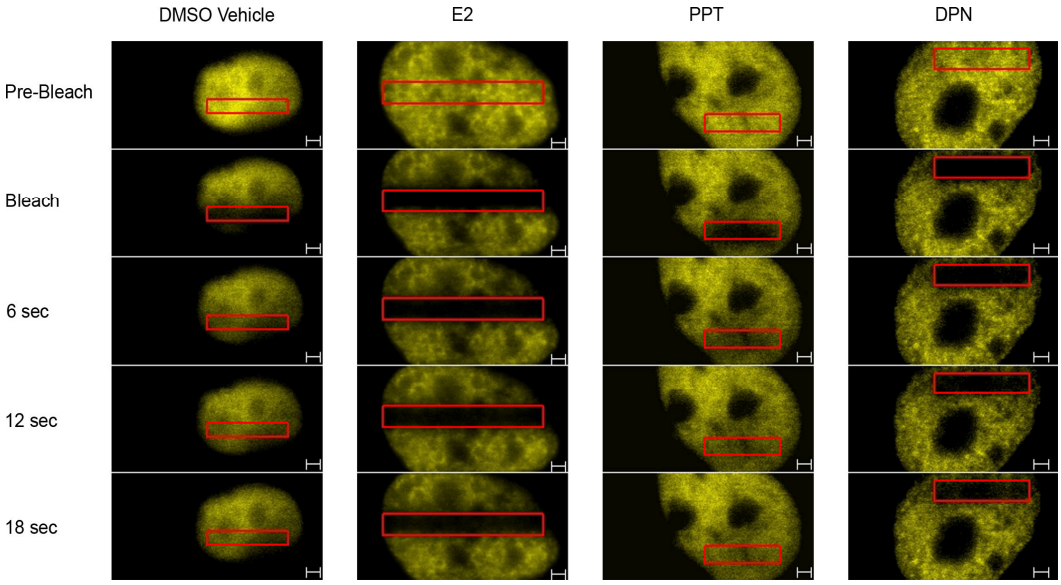

Figure 3.11 Qualitative FRAP assessment of ERβ infected MDA cells.

Cells were treated with a DMSO vehicle control, E2 10^{-8}M, PPT™ 10^{-8}M or DPN™ 10^{-8}M for 60 minutes.

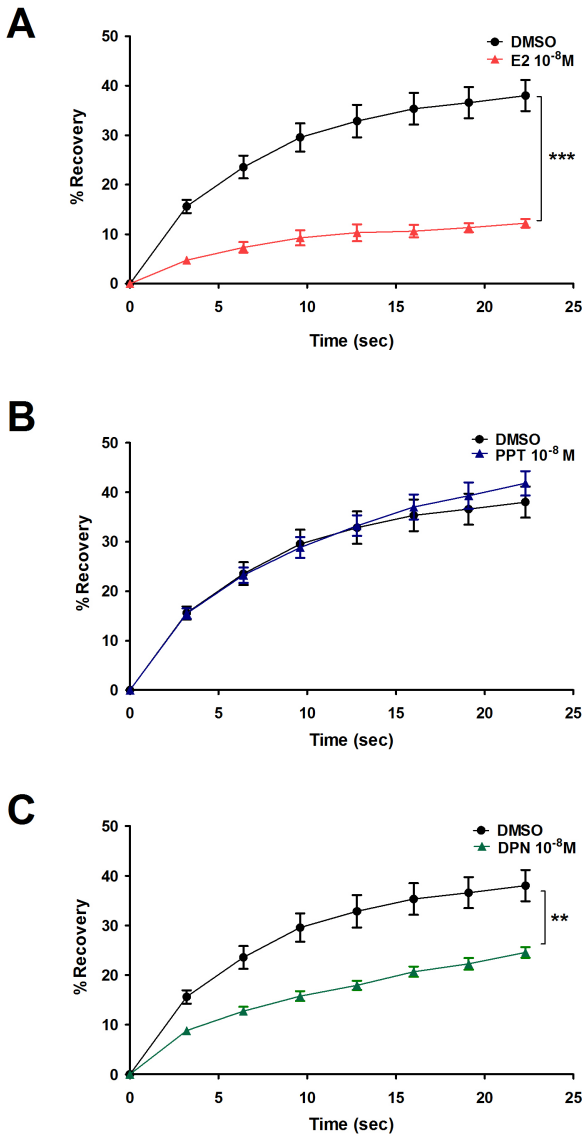

Figure 3.12 Quantitative analysis of intra-nuclear kinetics of ERβ-infected MDA cells.

*Graphical depiction of impact of ligand treatment on the recovery rates of ERβ fluorophores over time back into the bleached zone. This recovery is denoted by the point at which the Y_{MAX} is achieved and a plateau is reached on the graph. Recovery rates of ERβ-infected MDA cells are presented in response to E2 (A), PPT™ (B) and DPN™ (C) stimulation at a concentration of 10-8M. *** (P<0.001) and ** (P<0.01) denotes significance in variation of ligand treatments compared with the vehicle control as derived from the Student's t-test (N≥8).*

ERβ2

Uniform nuclear distribution of fluorescence was observed following infection of MDA cells with YFP-labelled ERβ2 adenoviral constructs. This appearance was retained following all treatments including DMSO, E2, PPT™ and DPN™. Regardless of the presence or absence of ligand, a rapid (~6 second) recovery to the primary state of fluorescence was also observed following each treatment upon bleaching (Fig. 3.13). In the control (DMSO-treated) cells maximum recovery was ~40%. There were no significant ligand-mediated influences by any treatment (E2, PPT™ and DPN™) when Y_{MAX} was calculated (Fig. 3.14A-C).

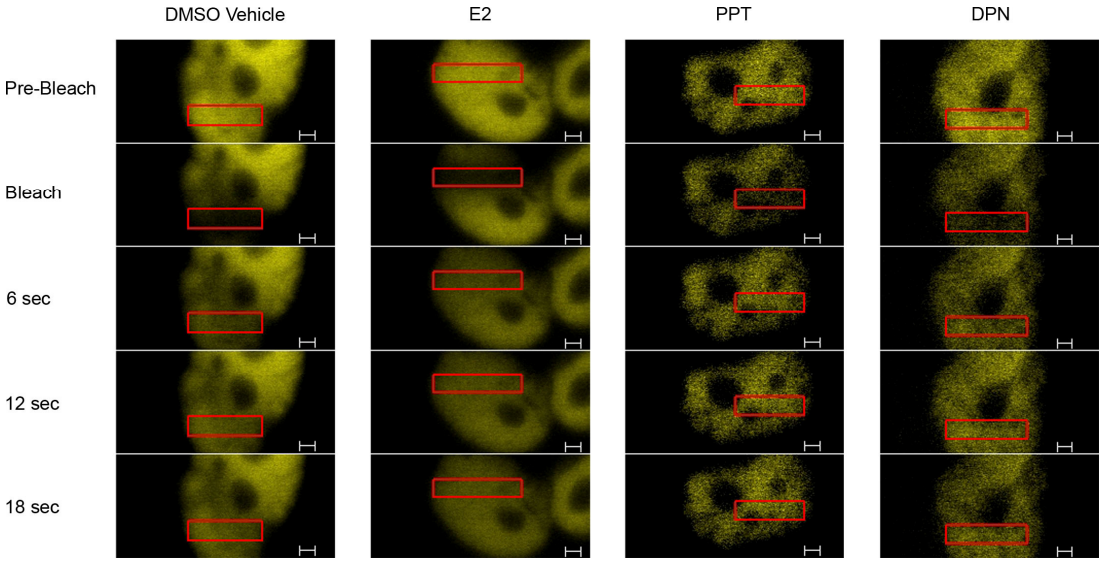

Figure 3.13 Qualitative FRAP assessment of ERβ2 infected MDA cells.

Cells were treated with a DMSO vehicle control, E2 10^{-8}M, PPT™ 10^{-8}M or DPN™ 10^{-8}M for 60 minutes.

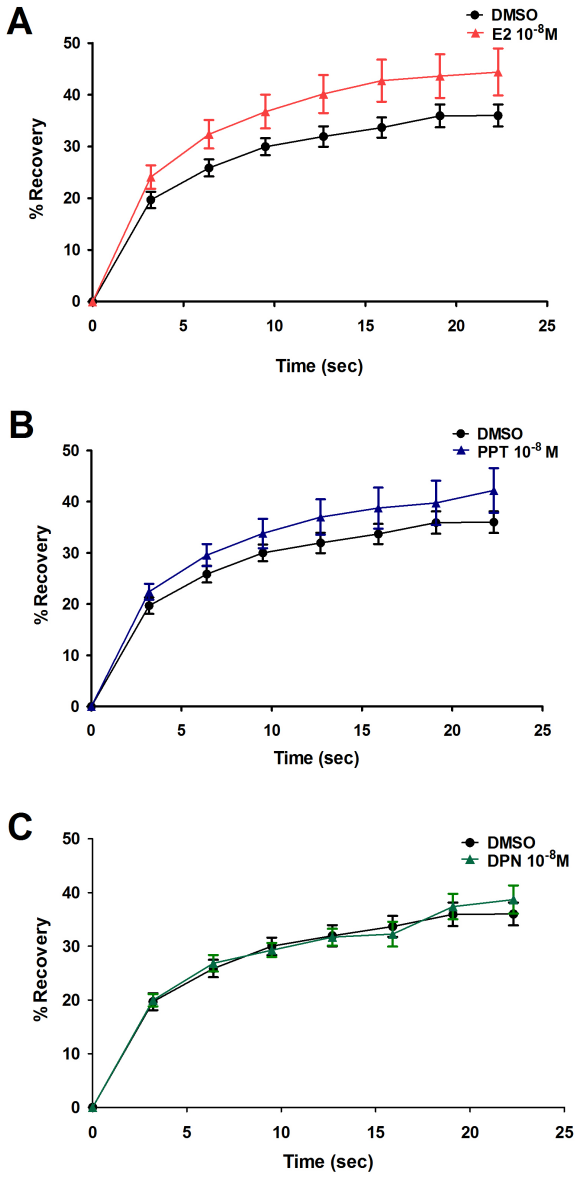

Figure 3.14 Quantitative analysis of intra-nuclear kinetics of ERβ2-infected MDA cells.

Graphical depiction of impact of ligand treatment on the recovery rates of ERβ2 fluorophores over time back into the bleached zone. This recovery is denoted by the point at which the Y_{MAX} is achieved and a plateau is reached on the graph. Recovery rates of ERβ2-infected MDA cells are presented in response to E2 (A), PPT™ (B) and DPN™ (C) stimulation at a concentration of 10^{-8}M. Ligand treatments were compared with the vehicle control as derived from the Student's t-test (N≥8).

3.3.2.1.2 Ishikawa cells

Ishikawa cells express endogenous ERα (section 3.3.1.1). When cells were transfected with the CY24 plasmid comprising the YFP tag linked to the CFP tag, maximal recovery following photobleaching was instantaneous (Y_{MAX} levels reached at first scan post-bleach) (Fig. 3.15A) and treatment with E2 had no marked effect on this response model (Fig. 3.15B). This confirms that the YFP protein did not interact with endogenous ERα and therefore any changes in mobility of YFP-tagged ERs is due to the ER itself and not the tag.

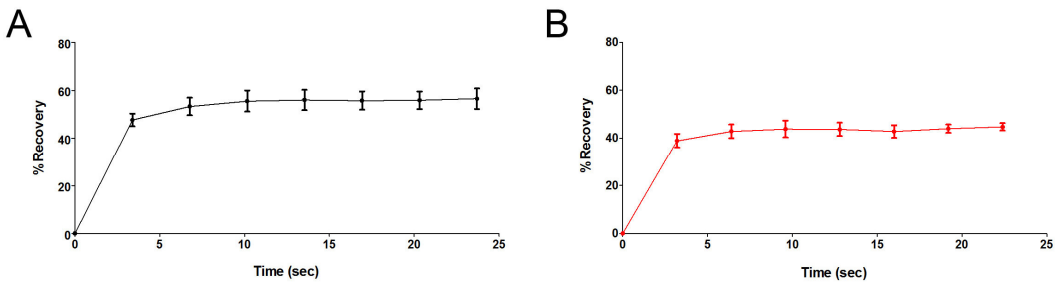

Figure 3.15 Control FRAP experiments in Ishikawa cells.

Cells were transfected with the CY24 plasmid consisting of a YFP tag conjugated to a CFP tag by a 25 amino acid sequence linker. Transfected cells were treated with a DMSO vehicle control (A) or E2 10^{-8}M (B).

ERα

Infection of ERα-YFP into Ishikawa cells generated a homogenous nuclear dissemination of fluorescence, addition of the DMSO vehicle control for 1 hour had no impact on subnuclear distribution patterns. Treatment with E2 for 1 hour induced relocation of receptor resulting in a punctate appearance of fluorescence in the nucleus and low levels of recovery back into the bleached zone. This distinctive reorganisation of receptor distribution was also seen after 1 hour incubation with PPT™ incubation but not with DPN™ (Fig 3.16).

In DMSO treated cells, the percentage recovery was ~60%. Fig 3.17 shows analysis of cells such as those shown in Fig. 3.16. Incubation with E2 (Fig. 3.17A) and PPT™

(Fig. 3.17B) on ERα had a significant impact on Y_{MAX} values whereas the impact of DPN™ was minimal (Fig. 3.17C).

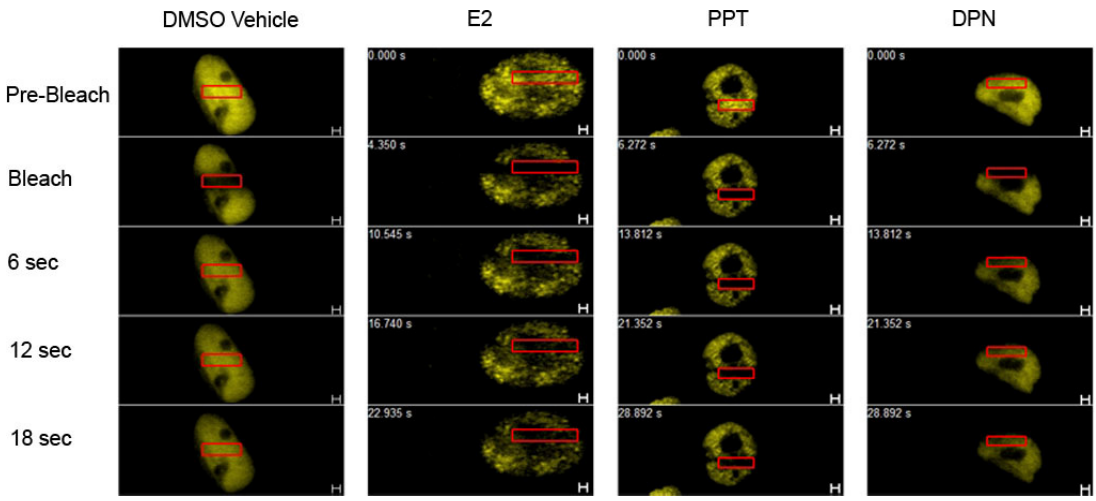

Figure 3.16 Qualitative FRAP assessment of ERα infected Ishikawa cells.

Cells were treated with a DMSO vehicle control, E2 10^{-8}M, PPT™ 10^{-8}M or DPN™ 10^{-8}M for 60 minutes.

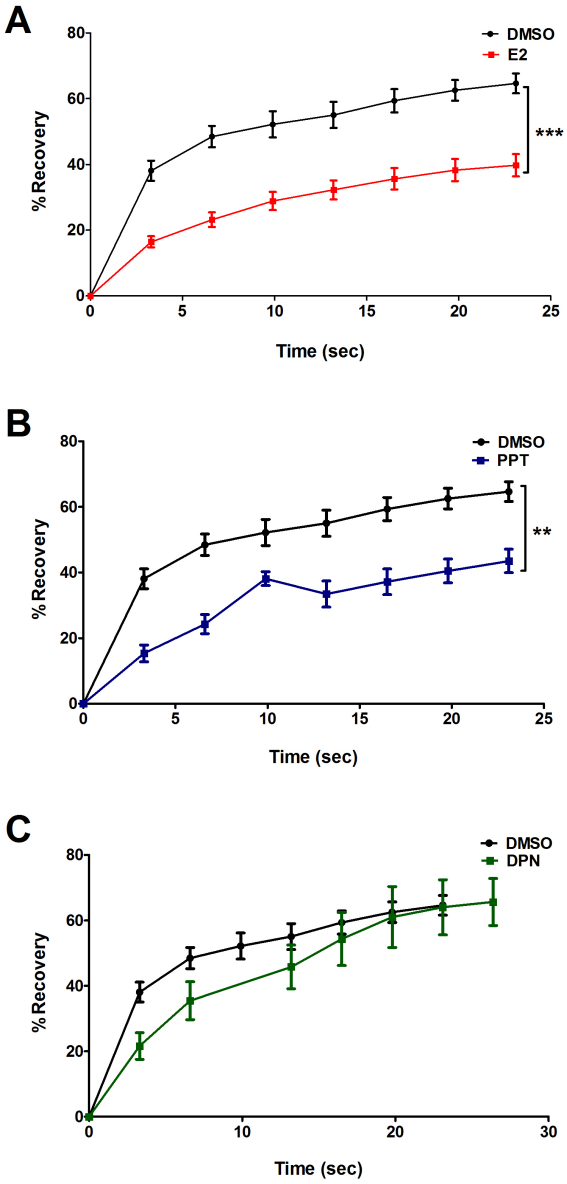

Figure 3.17 Quantitative analysis of intra-nuclear kinetics of ERα-infected Ishikawa cells.

*Graphical depiction of impact of ligand treatment on the recovery rates of ERα fluorophores over time back into the bleached zone. This recovery is denoted by the point at which the Y_{MAX} is achieved and a plateau is reached on the graph. Recovery rates of ERα-infected Ishikawa cells are presented in response to E2 (A), PPT™ (B) and DPN™ (C) stimulation at a concentration of 10^{-8}M. *** (P<0.001) and ** (P<0.01) denotes significance in variation of ligand treatments compared with the vehicle control as derived from the Student's t-test (N≥8).*

ERβ

Distribution of ERβ-YFP in the nuclei of Ishikawa cells was not as uniform as that observed following infection with ERα-YFP in the same cell line. ERβ-YFP appeared to be localised to certain regions within the nuclear architecture and the application of a DMSO vehicle control for 1 hour had no impact on this distribution. Incubation with E2 resulted in a more pronounced accumulation of 'speckles' throughout the nucleoplasm. Poor levels of recovery following bleaching of E2-treated ERβ-YFP molecules were also noted consistent with reduced mobility. This punctate appearance and reduced mobility was also observed after incubation with DPN™. Treatment with PPT™ did not alter the mobility of ERβ (Fig 3.18).

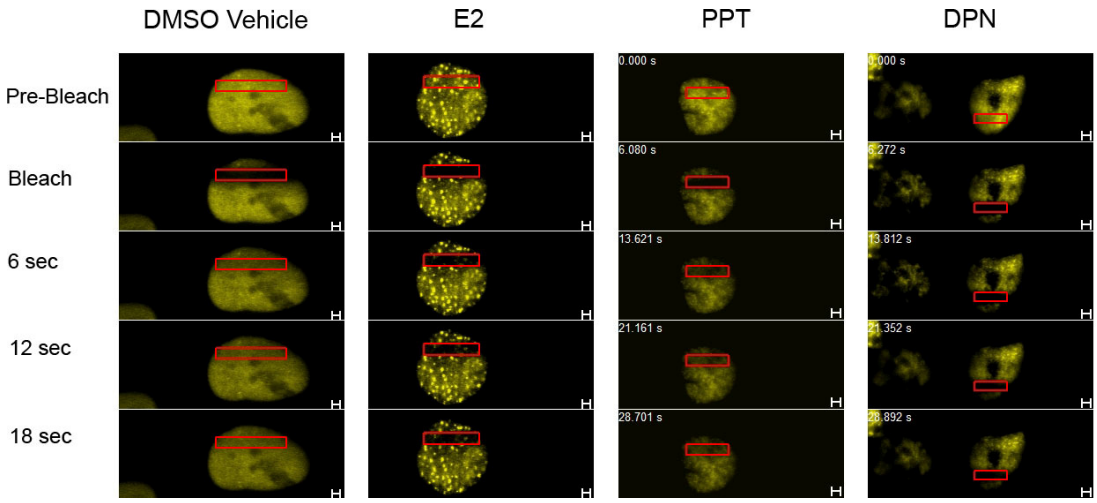

Figure 3.18 Qualitative FRAP assessment of ERβ infected Ishikawa cells.

Cells were treated with a DMSO vehicle control, E2 10-8M, PPT™ 10-8M or DPN™ 10-8M for 60 minutes.

The impact of E2 on ERβ-YFP recovery within the nucleus was also studied over a longer time course (~80 seconds) but little change in the Y_{MAX} levels was recorded after 25 seconds and they remained significantly reduced compared with control cells (Fig. 3.19A). E2 treatment had a significant effect in slowing the recovery rate of fluorescing molecules back into the bleached zone. Incubation of cells expressing ERβ with PPT™ had no impact on ERβ-YFP dynamics with regard to Y_{MAX}

analysis. Treatment with DPN™ had a striking and significant impact on percentage recovery which remained less than ~10% after 30 seconds (Fig. 3.19C).

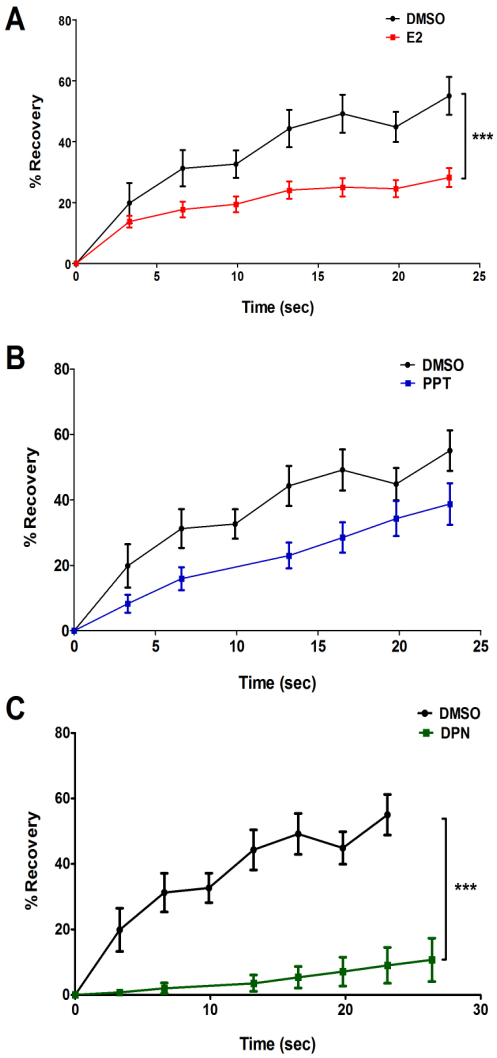

Figure 3.19 Quantitative analysis of intra-nuclear kinetics of ERβ-infected Ishikawa cells.

*Impact of ligand treatment on the recovery rates of ERβ fluorophores over time into the bleached zone. Recovery is denoted by the point at which the Y_{MAX} is achieved and a plateau is reached on the graph. Recovery rates of ERβ-infected Ishikawa cells are in response to E2 (A), PPT™ (B) and DPN™ (C) at a concentration of 10^{-8}M. *** (P<0.001) denotes significance in variation of ligand treatments compared with the vehicle control as derived from the Student's t-test (N≥8).*

ERβ2

Uniform nuclear distribution of fluorescence was achieved following infection of Ishikawa cells with YFP-labelled ERβ2 adenoviral constructs (Fig. 3.20). This appearance was retained following all treatments including DMSO, E2, PPT™ and DPN™. Rapid recovery in fluorescence (~6 seconds) was observed after photobleaching with each of the treatments (Fig. 3.20). No significant influences by either treatment E2, PPT™ or DPN™ were found from analysis of the statistical parameter of Y_{MAX} (Fig. 3.21).

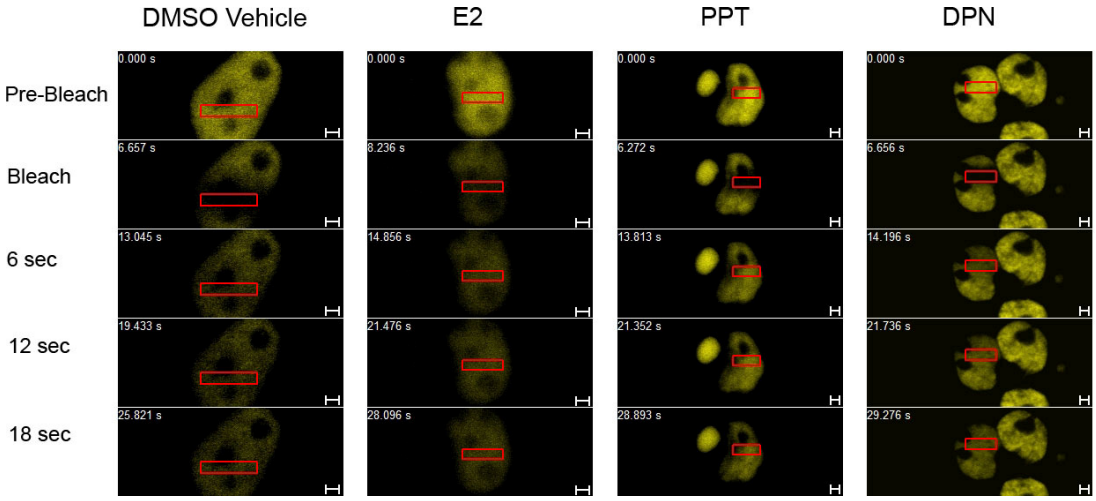

Figure 3.20 Qualitative FRAP assessment of ERβ2 infected Ishikawa cells.

Cells were treated with a DMSO vehicle control, E2 10^{-8}M, PPT™ 10^{-8}M or DPN™ 10^{-8}M for 60 minutes.

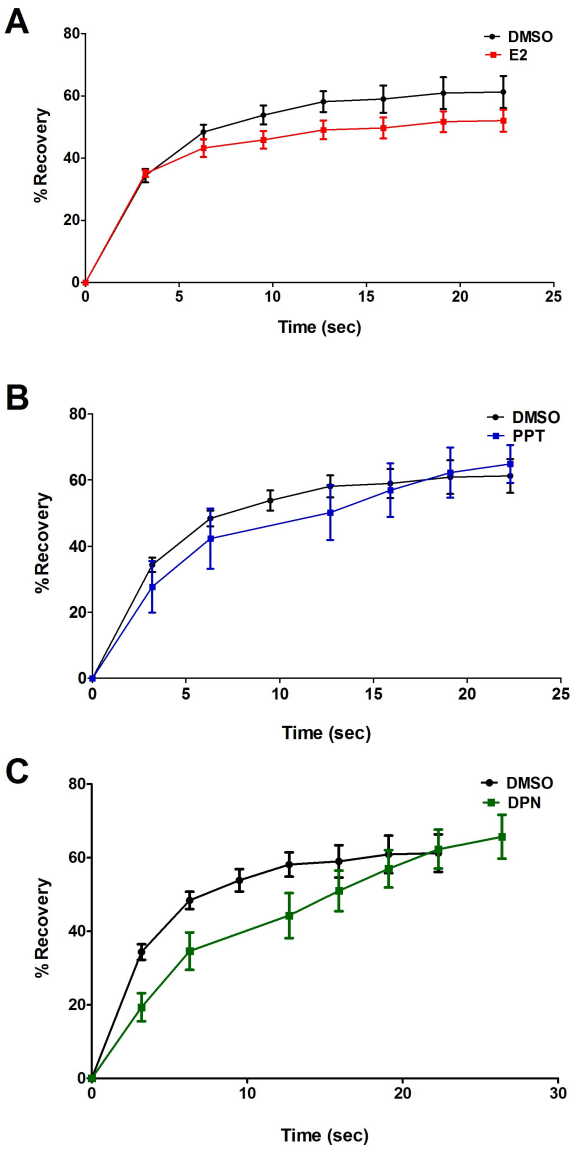

Figure 3.21 Quantitative analysis of intra-nuclear kinetics of ERβ2-infected Ishikawa cells.

Graphical depiction of impact of ligand treatment on the recovery rates of ERβ2 fluorophores over time back into the bleached zone. This recovery is denoted by the point at which the Y_{MAX} is achieved and a plateau is reached on the graph. Recovery rates of ERβ2-infected Ishikawa cells are presented in response to E2 (A), PPT™ (B) and DPN™ (C) stimulation at a concentration of 10^{-8}M. Significance in variation of ligand treatments compared with the vehicle control was assessed by the Student's t-test (N≥8).

3.3.2.1.3 hTERT cells

hTERT cells transfected with the CY24 plasmid comprising the YFP tag linked to the CFP tag only were studied following treatment with and without E2. Following photobleaching, maximal recovery was almost instantaneous (Y_{MAX} levels reached at first scan post-bleach) (Fig. 3.22A) and treatment with E2 did not effect this response (Fig. 3.22B) suggesting that the fluorescent proteins on their own did not associate with DNA, ligand or ERs.

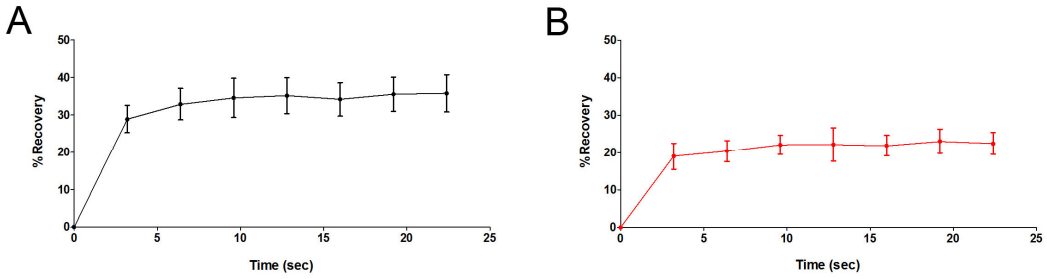

Figure 3.22 Control FRAP experiments in hTERT cells.

Cells were transfected with the CY24 plasmid consisting of a YFP tag conjugated to a CFP tag by a 25 amino acid sequence linker. Transfected cells were treated with a DMSO vehicle control (A) or E2 10^{-8}M (B).

ERα

The infection of ERα-YFP for into hTERT cells resulted in uniform levels of fluorescence throughout the nucleus when cells were examined after 24 hours. Treatment with the DMSO vehicle control for 1 hour did not have any impact on nuclear distribution of ERα-YFP. However incubation with E2 for 1 hour resulted in redistribution of receptor that adopted a punctate appearance in the nucleus associated with very low levels of recovery back into the bleached zone. This distinctive appearance was also seen after 1 hour incubation with PPT™ but not following DPN™ treatment (Fig. 3.23).

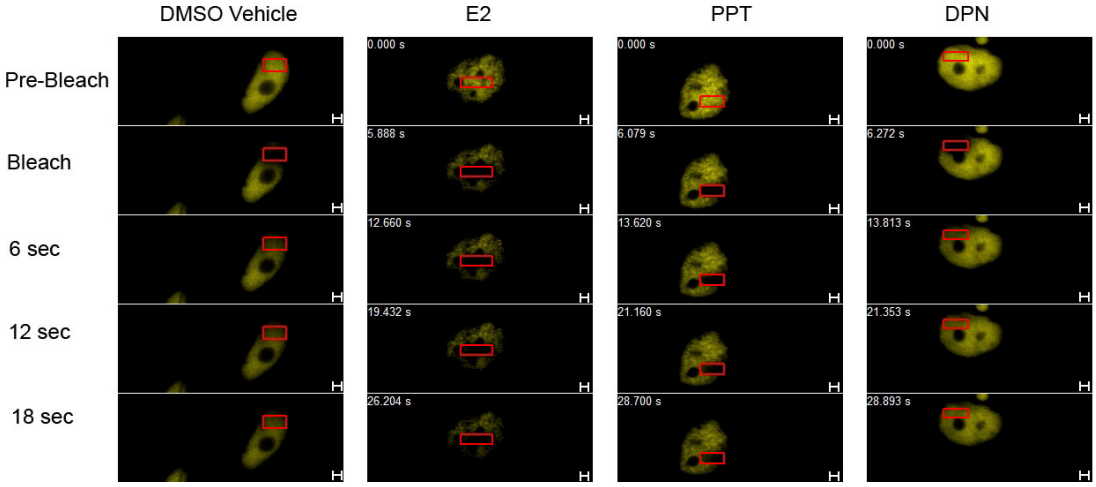

Figure 3.23 Qualitative FRAP assessment of ERα infected into hTERT cells.

Cells were treated with a DMSO vehicle control, E2 10-8M, PPT™ 10-8M or DPN™ 10-8M for 60 minutes.

Fig 3.24A illustrates the significant impact of E2 on ERα-YFP mobility within the nuclear domain. E2 treatment has a significant effect in slowing the percentage of recovery into ROI I resulting in a reduction of Y_{MAX} from ~60% to less than ~40% after 25 seconds. Treatment of ERα-YFP molecules with the agonist PPT™ resulted in an effect on recovery rates of fluorescent ERα molecules with a significant reduction in Y_{MAX} (Fig. 3.10B). DPN™ had no impact on ERα-YFP molecules in the hTERT cell environment (Fig. 3.10C).

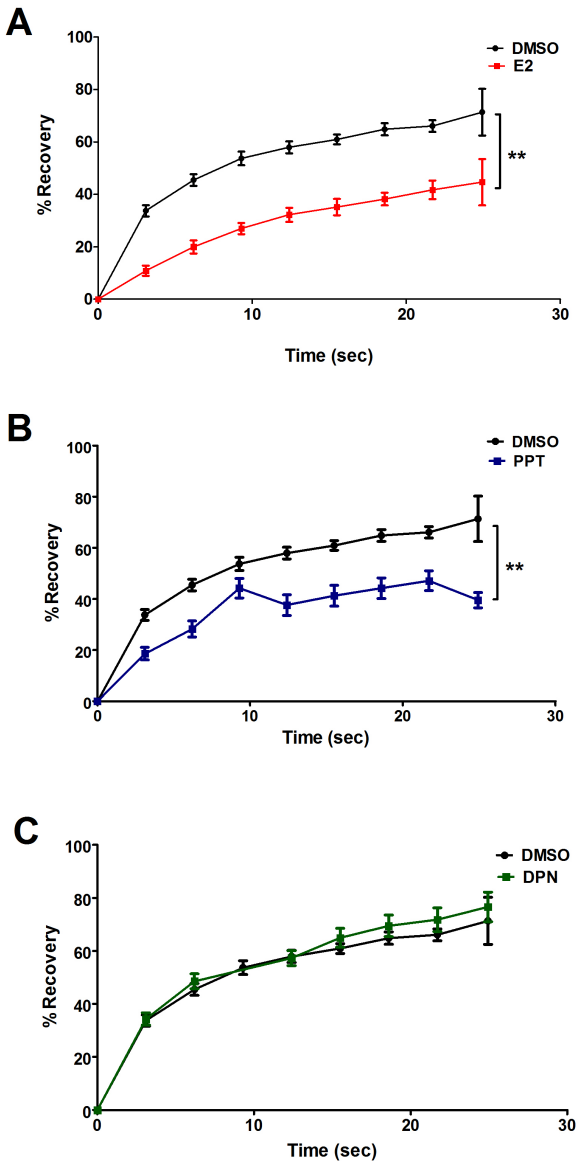

Figure 3.24 Quantitative analysis of intra-nuclear kinetics of ERα-infected hTERT cells.

*Graphical depiction of impact of ligand treatment on the recovery rates of ERα fluorophores over time back into the bleached zone. This recovery is denoted by the point at which the Y_{MAX} is achieved and a plateau is reached on the graph. Recovery rates of ERα-infected hTERT cells are presented in response to E2 (A), PPT™ (B) and DPN™ (C) stimulation at a concentration of 10^{-8}M. ** (P<0.01) denotes significance in variation of ligand treatments compared with the vehicle control as derived from the Student's t-test (N≥8).*

ERβ

Expression of ERβ-YFP in the hTERT cell line is not as uniform as that observed following infection of ERα-YFP in the same cells. The application of a DMSO vehicle control for 1 hour had no impact on ERβ-YFP distribution but incubation with E2 resulted in redistribution of ERβ and a pronounced accumulation of 'speckles' throughout the nucleoplasm (Fig 3.25). Reduced rates of recovery following bleaching of E2-treated ERβ-YFP molecules were also noted. Y_{MAX} reduced to ~30% compared with ~40% in control untreated cells (Fig 3.26). This punctate appearance and reduced Y_{MAX} was also observed with a 1 hour DPN™ incubation. Uniform distribution of ERβ-YFP induced fluorescence was observed in nuclei following PPT™ treatment (1 hour) both before and after bleaching (Fig 3.25) and there was no impact on Y_{MAX} (Fig 3.26C).

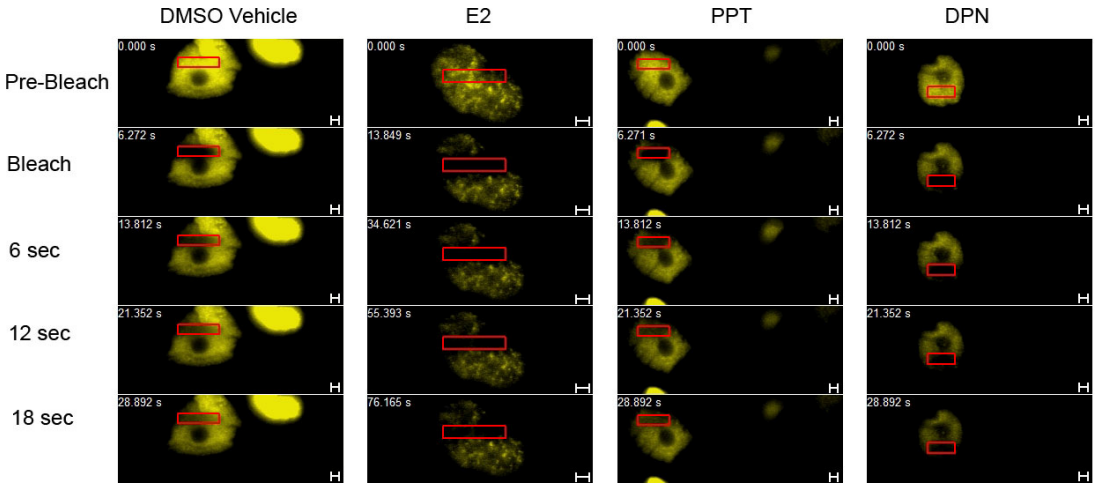

Figure 3.25 Qualitative FRAP assessment of ERβ infected hTERT cells.

Cells were treated with a DMSO vehicle control, E2 10-8M, PPT™ 10-8M or DPN™ 10-8M for 60 minutes.

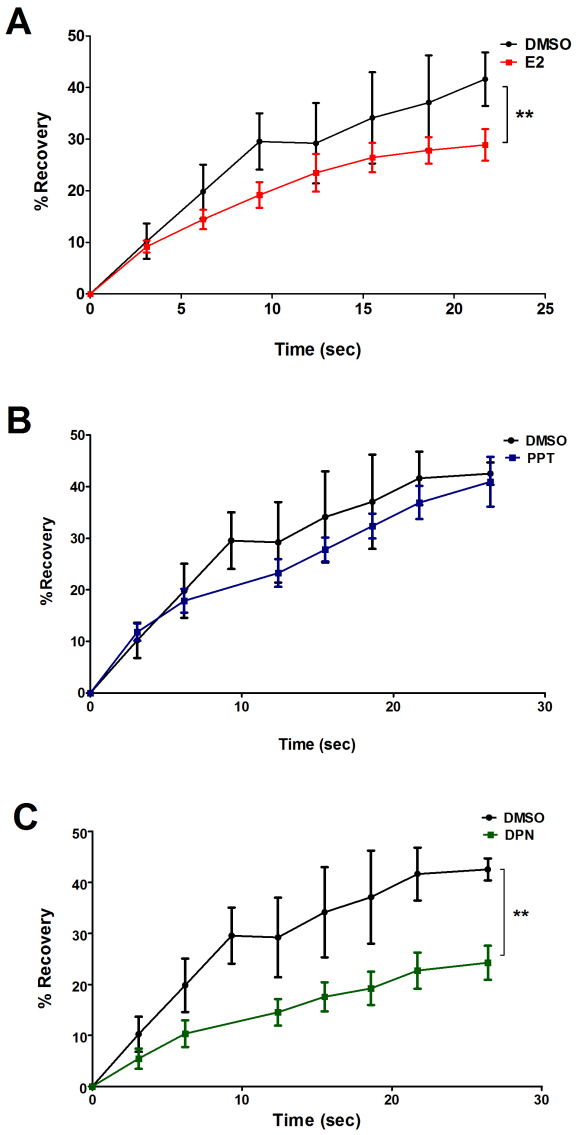

Figure 3.26 Quantitative analysis of intra-nuclear kinetics of ERβ-infected hTERT cells.

*Graphical depiction of impact of ligand treatment on the recovery rates of ERβ fluorophores over time back into the bleached zone. This recovery is denoted by the point at which the Y_{MAX} is achieved and a plateau is reached on the graph. Recovery rates of ERβ-infected hTERT cells are presented in response to E2 (A), PPT™ (B) and DPN™ (C) stimulation at a concentration of 10^{-8}M. ** (P<0.01) denotes significance in variation of ligand treatments compared with the vehicle control as derived from the Student's t-test (N≥8).*

ERβ2

Homogenous nuclear distribution of fluorescence was achieved following infection of hTERT cells with YFP-labelled ERβ2 adenoviral constructs. This appearance was retained following all treatments including DMSO, E2, PPT™ and DPN™. A rapid (~6 second) recovery to the primary state of fluorescence was also observed following each treatment upon bleaching (Fig. 3.27). A slight but significant effect on Y_{MAX} was observed on ERβ2-YFP molecules following E2 stimulation with reduction by ~5% compared with controls (Fig. 3.28A). Treatment with PPT™ or DPN™ had no impact on Y_{MAX} (Fig. 3.28B and C).

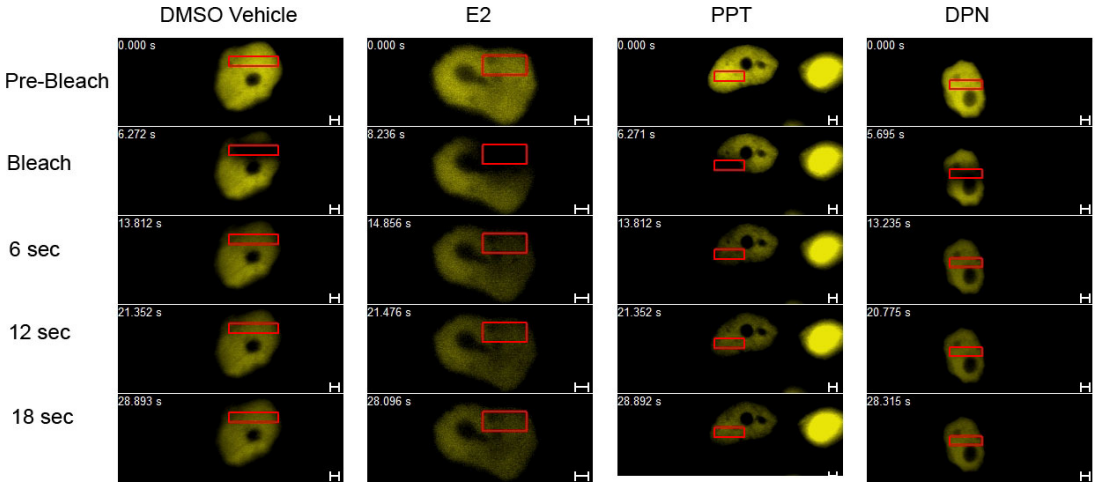

Figure 3.27 Qualitative FRAP assessment of ERβ2 infected hTERT cells.

Cells were treated with a DMSO vehicle control, E2 10-8M, PPT™ 10-8M or DPN™ 10-8M for 60 minutes.

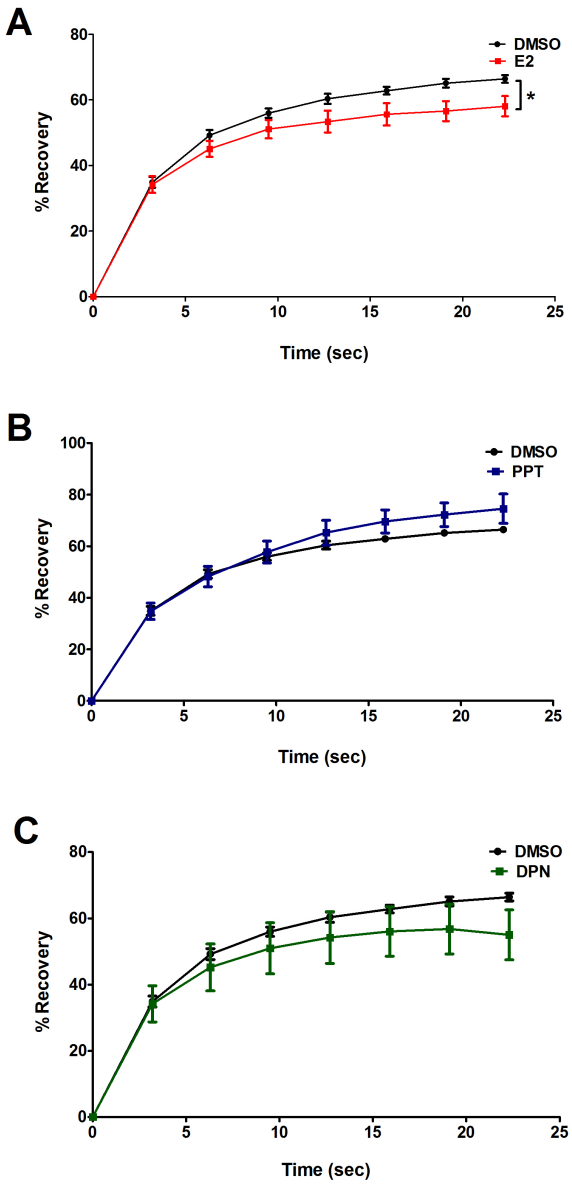

Figure 3.28 Quantitative analysis of intra-nuclear kinetics of ERβ2-infected hTERT cells.

Depiction of impact of ligand treatment on the recovery rates of ERβ2-YFP over time back into the bleached zone. This recovery is denoted by the point at which the Y_{MAX} is achieved and a plateau is reached on the graph. Recovery rates of ERβ2-infected hTERT cells are presented in response to E2 (A), PPT™ (B) and DPN™ (C) stimulation at a concentration of 10^{-8}M. Significance in variation of ligand treatments compared with the vehicle control was assessed by the Student's t-test (N≥8).

3.3.2.2 Impact of anti-oestrogen on receptor dynamics

Following the study of E2 and the selective ER agonists on the intranuclear dynamics of ERs, the impact of the pure anti-oestrogen ICI 182.780 (Fulvestrant™) was examined. Analysis of treatment outcome was conducted after incubation of cells for 1 hour with ICI 182,780.

3.3.2.2.1 Ishikawa cells

The impact of ICI 182,780 was identical in both the cell lines tested (Ishikawa and hTERT cells) and only the data from the Ishikawa cell line is presented here.

ERα

The interaction of the ICI 182,780 molecule with ERα-YFP in the Ishikawa nuclei resulted in a punctate appearance similar to that observed following E2 treatment. In comparison to the weak recovery of E2 treated ER molecules back into the bleached zone, no recovery was observed in the cells treated with ICI 182,780 for 1 hour followed by E2 for 1 hour (Fig 3.29).

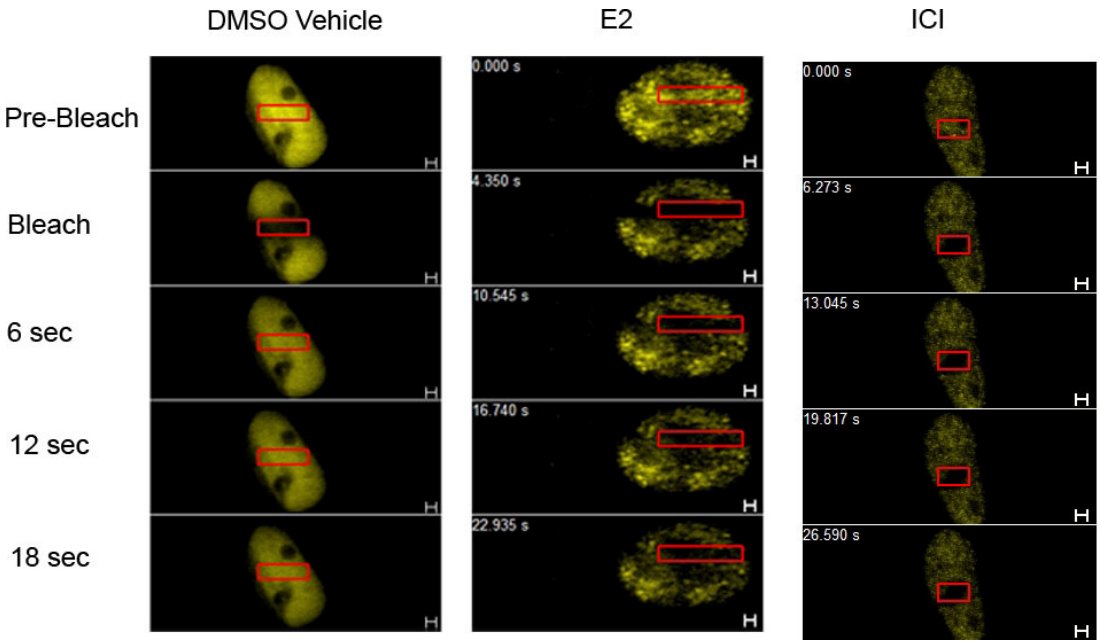

Figure 3.29 Qualitative FRAP assessment of ERα infected Ishikawa cells.
Cells were treated with a DMSO vehicle control, E2 10^{-8}M and ICI 182,780 10^{-8}M.

The percentage of recovery observed in ICI 182,780/E2-treated cells was extremely low (<10%) (Fig. 3.30) and did not climb above this value over extended time periods (data not shown).

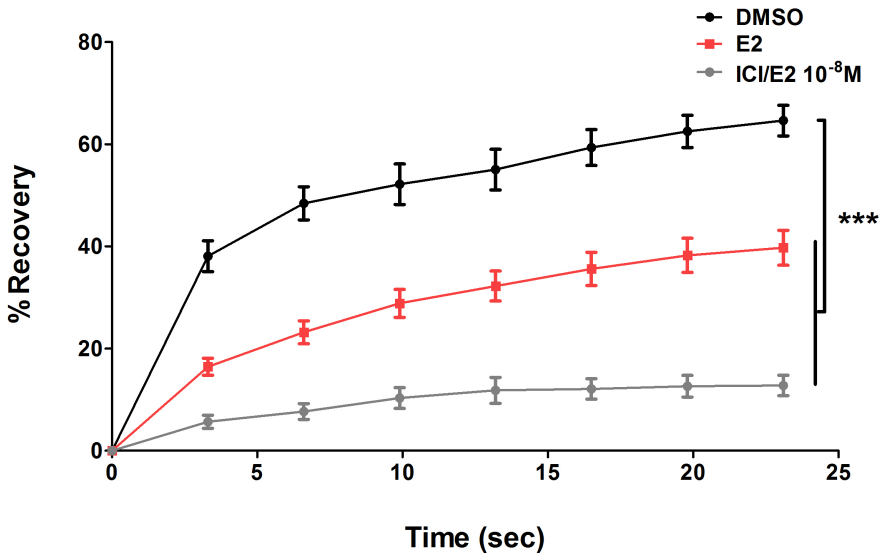

Figure 3.30 Quantitative analysis of intra-nuclear kinetics of ERα-infected Ishikawa cells.

*Graphical depiction of impact of ligand treatment on the recovery rates of ERα fluorophores over time back into the bleached zone. This recovery is denoted by the point at which the Y_{MAX} is achieved and a plateau is reached on the graph. Recovery rates of ERα-infected Ishikawa cells are presented in response to E2 (red) and ICI 182,780 with E2 (grey) stimulation at a concentration of 10^{-8}M. *** (P<0.001) *(P<0.05) denotes significance in variation of ligand treatments compared with the vehicle control as derived from the Student's t-test (N≥8).*

ERβ

Incubation of ERβ-infected Ishikawa cells with ICI 182,780 resulted in receptor redistribution and the development of a punctate appearance in the nucleoplasm not dissimilar to that displayed by E2-treated cells (Fig. 3.31). The incubation of ICI 182,780 for 1 hour followed by E2 for 1 hour with ERβ-YFP molecules in Ishikawa nuclei resulted in a significant impact on the Y_{MAX} (Fig. 3.32).

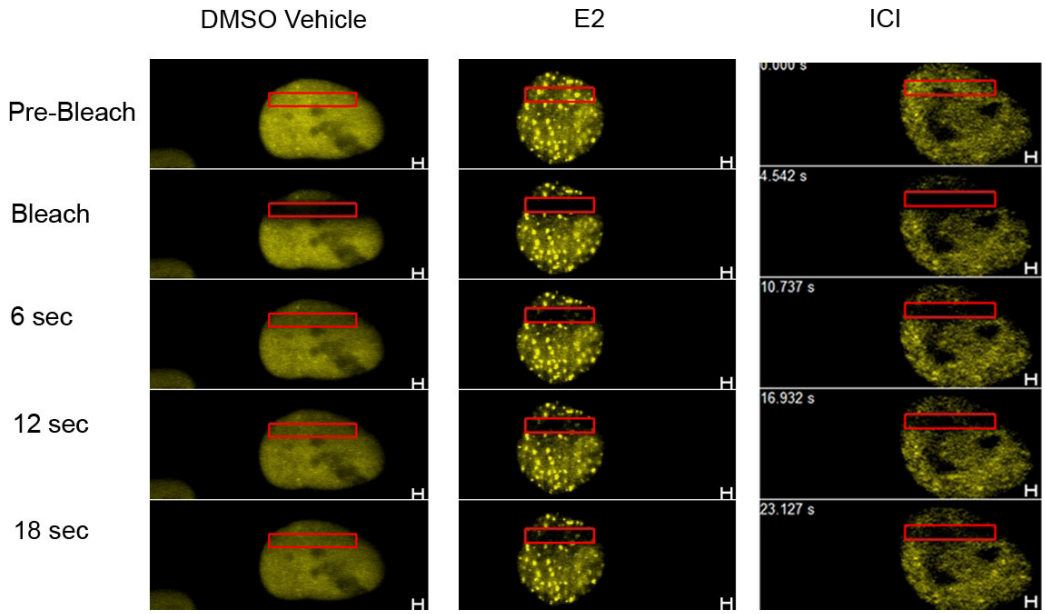

Figure 3.31 Qualitative FRAP assessment of ERβ infected Ishikawa cells.

Cells were treated with a DMSO vehicle control, E2 10^{-8}M and ICI 182,780 10^{-8}M.

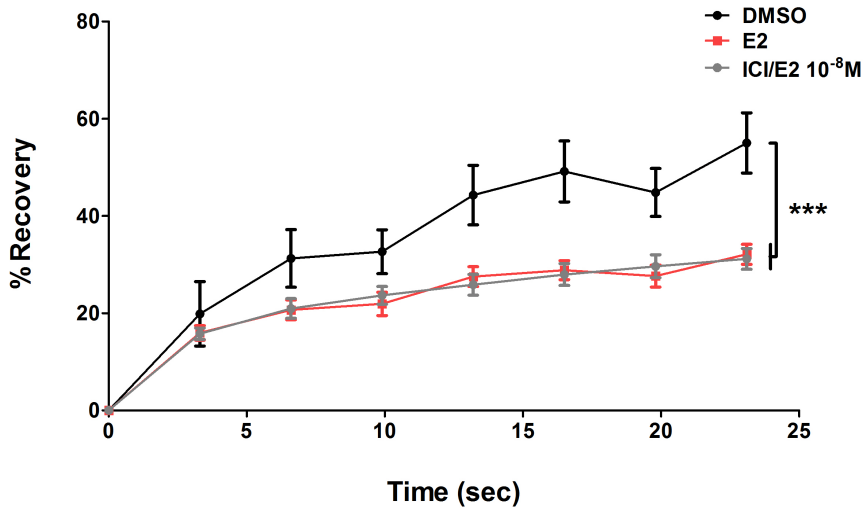

Figure 3.32 Quantitative analysis of intra-nuclear kinetics of ERβ-infected Ishikawa cells.

*Impact of ligand treatment on the recovery rates of ERβ fluorophores over time back into the bleached zone. This recovery is denoted by the point at which the Y_{MAX} is achieved and a plateau is reached on the graph. Recovery rates of ERβ-infected Ishikawa cells are presented in response to E2 (red) and ICI 182,780 followed by E2 (grey) at a concentration of 10-8M. *** (P<0.001) denotes significance of*

treatments compared with the vehicle control as derived from the Student's t-test (N≥8).

ERβ2

In comparison to the null effect of E2 stimulation on ERβ2-YFP dynamics within the Ishikawa nucleus, the treatment with ICI 182,780 did have a significant effect a phenotypic appearance of the receptor with the appearance of strong fluorescent foci clearly visible after treatment (Fig. 3.33). While the effect of ICI 182,780 treatment with E2 did not yield significant results on the dynamic mobility when this was assessed quantitatively (Fig. 3.34), a trend similar to that observed with the full length ERα (Fig. 3.30) and ERβ (Fig. 3.32) subtypes was observed.

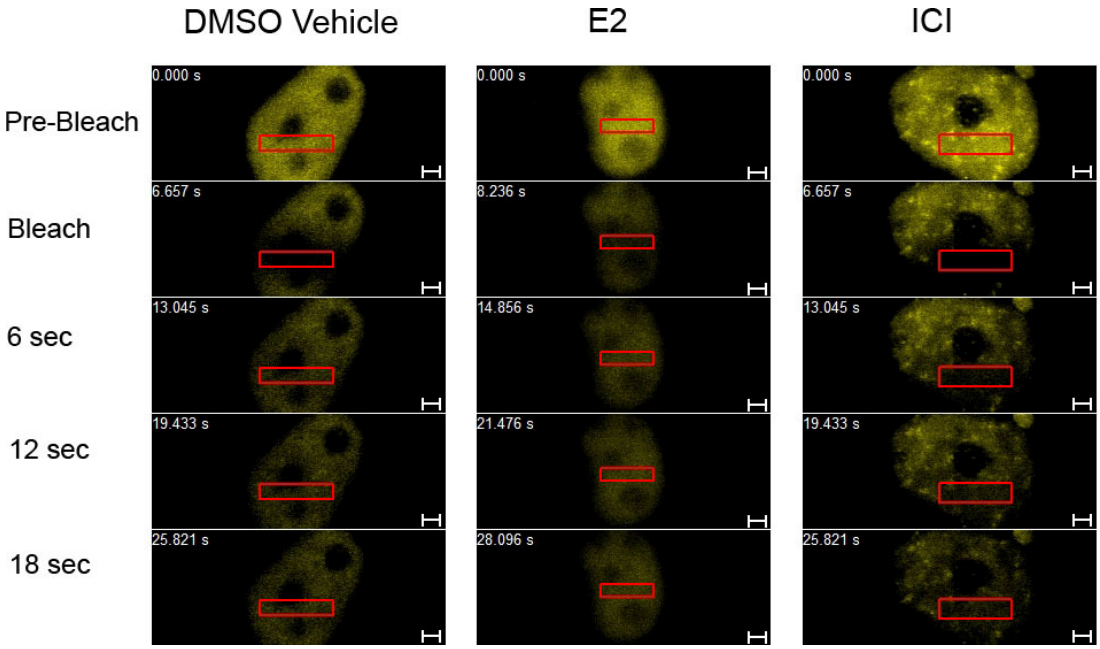

Figure 3.33 Qualitative FRAP assessment of ERβ2 infected Ishikawa cells.

Cells were treated with a DMSO vehicle control, E2 10^{-8}M and ICI 182,780 10^{-8}M.

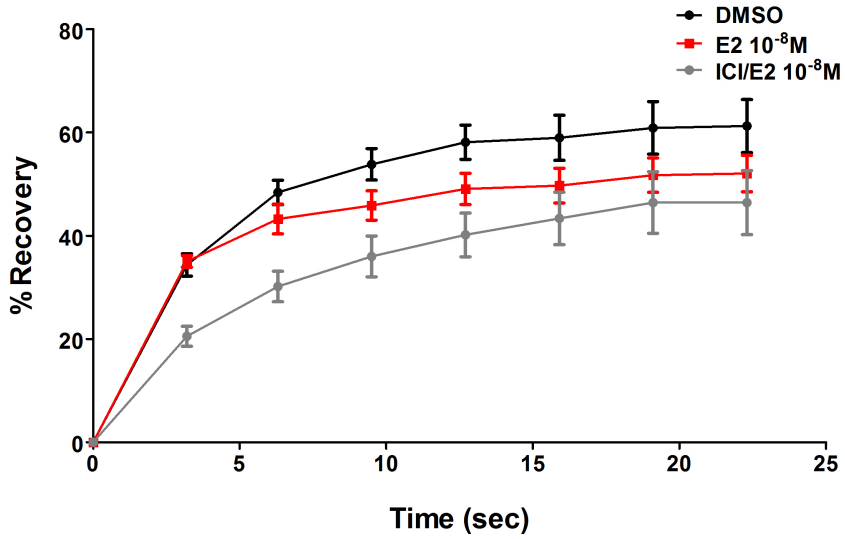

Figure 3.34 Quantitative analysis of intra-nuclear kinetics of ERβ2-infected Ishikawa cells.

Graphical depiction of impact of ligand treatment on the recovery rates of ERβ2 fluorophores over time back into the bleached zone. This recovery is denoted by the point at which the Y_{MAX} is achieved and a plateau is reached on the graph. Recovery rates of ERβ2-infected Ishikawa cells are presented in response to E2 (red) and ICI 182,780 in combination with E2 (grey) stimulation at a concentration of 10^{-8}M. Significance in variation of ligand treatments was compared with the vehicle control using the Student's t-test (N≥8).

3.3.3 Intranuclear dynamics of ER heterodimers

After examination of the ER responses to a panel of ligands as individual entities, the impact of ligand treatment on cells that were co-expressed with two ER subtypes was investigated. This study was conducted in MDA cells to prevent interference from background levels of ER expression. Fluorescence resonance energy transfer (FRET) studies performed within the lab derived results suggestive of effective dimerisation arising from co-expression of the combinations of ER subtypes presented below.

3.3.3.1 Agonist Response

The impact of E2 and the synthetic compounds PPT™ and DPN™ on intranuclear mobility was retested following co-expression of two ER subtypes in the MDA cell line.

ERα and ERβ-YFP

Unlabelled ERα and ERβ-YFP were co-infected into MDA cells so as to assess the impact of ERα on ERβ-YFP intra-nuclear mobility when they had the potential to form heterodimers. Incubation with E2 resulted in a pronounced impact on the dual infected nuclei with reduced recovery observed into the bleached region. In comparison, rapid recovery of fluorescence levels was observed in the bleached region in PPT™ treated cells but repopulation of the bleached zone was reduced in DPN™ treated cells (Fig. 3.35).

In line with the observational study, quantitative analysis confirmed that E2 treatment had a significant impact on ERβ-YFP mobility and Y_{MAX} in MDA cells co-infected with ERα (Fig. 3.36A). Surprisingly incubation of cells with PPT™ generated a recovery curve matching that of the DMSO vehicle control (Fig. 3.36B). In contrast incubation with DPN™ for 1 hour had a significant impact with striking reduction in the value of Y_{MAX} (Fig. 3.36C).

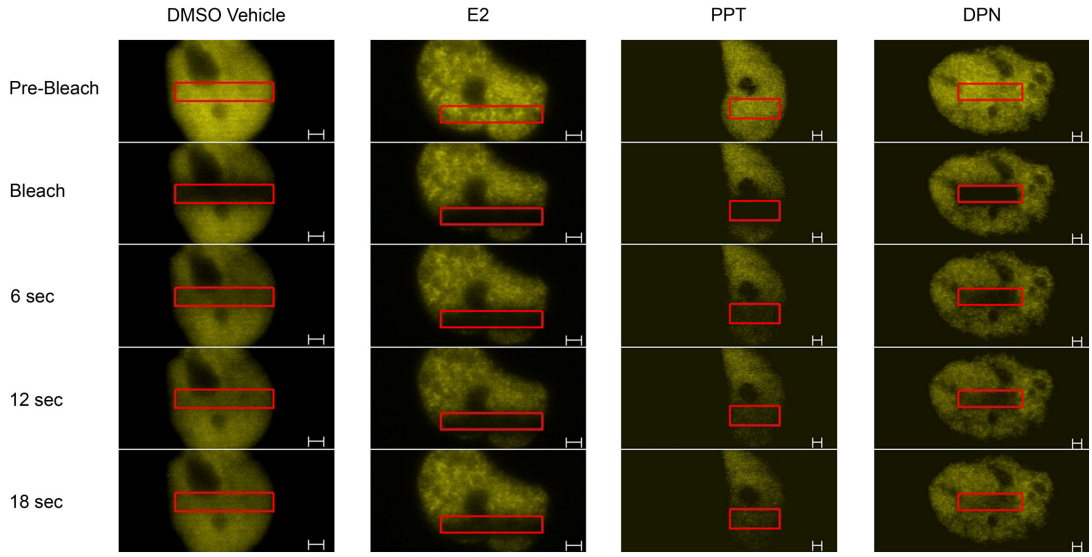

Figure 3.35 Qualitative FRAP assessment of dual infected MDA cells.

Cells were infected with unlabelled ERα and ERβ-YFP to assess the effect of ligand on heterodimers. Heterodimeric status is assumed based on relative proximity calculations verified by FRET studies conducted in the lab (data not presented). Cells were subjected to treatment with either a DMSO vehicle control, E2 10^{-8}M, PPT™ 10^{-8}M or DPN™ 10^{-8}M for 60 minutes. The fluorescent molecules of a designated region (red box) were annihilated during the bleaching process and recovery back into this zone was monitored over time. This time period was chosen on the basis of full recovery observed in the control nuclei.

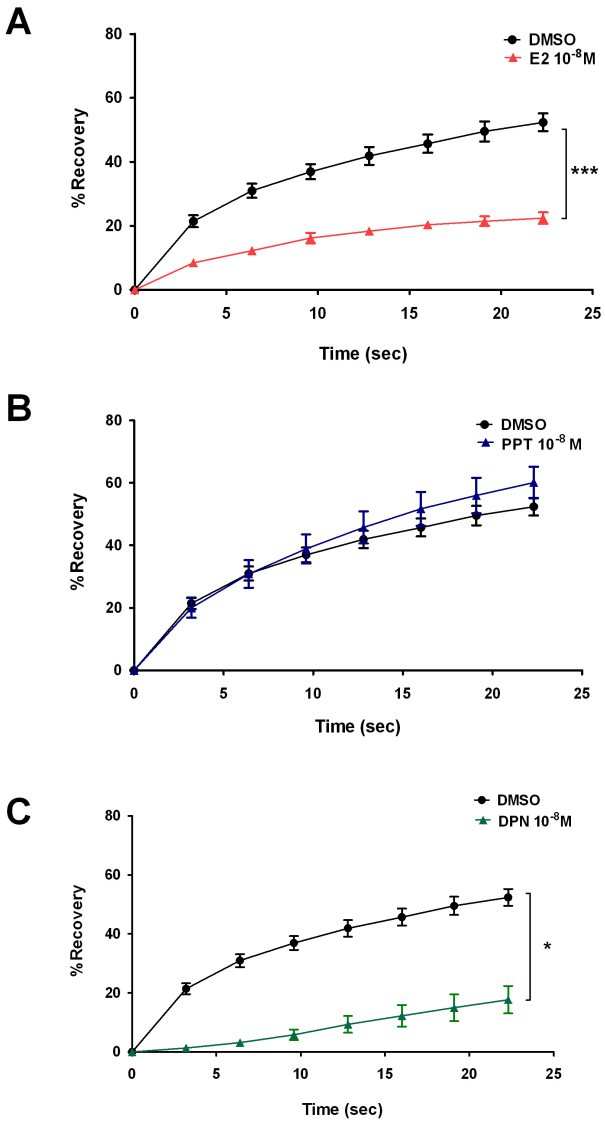

Figure 3.36 Quantitative analysis of intra-nuclear kinetics of dual infected MDA cells.

*Graphical depiction of impact of ligand treatment on the recovery rates of ERβ-YFP over time in a background of untagged ERα constructs back into the bleached zone. This recovery is denoted by the point at which the Y_{MAX} is achieved and a plateau is reached on the graph. Recovery rates of ERβ-YFP infected MDA cells are presented in response to E2 (A), PPT™ (B) and DPN™ (C) stimulation at a concentration of 10^{-8}M. *** (P<0.001), and *(P<0.05) denotes significance in variation of ligand treatments compared with the vehicle control as derived from the Student's t-test (N≥8).*

ERα and ERβ2-YFP

E2 treatment of MDA cells co-expressing unlabelled ERα and ERβ2-YFP resulted in reduced mobility of ERβ2-YFP compared with that seen in cells exposed to DMSO (control). Exposure of cells to PPT™ and DPN™ did not have an obvious impact on mobility (Fig. 3.37). Quantitative analysis of cells incubated with ERβ2-YFP and ERα confirmed that treatment with E2 resulted in a significant decrease in the percentage recovery of fluorescent molecules (Y_{MAX}) in comparison with those cells treated with DMSO alone (Fig. 3.38A). Treatment of cells with PPT™ or DPN™ had no significant impact on the dynamics of ERβ2-YFP compared to DMSO controls (Fig. 3.37B, C).

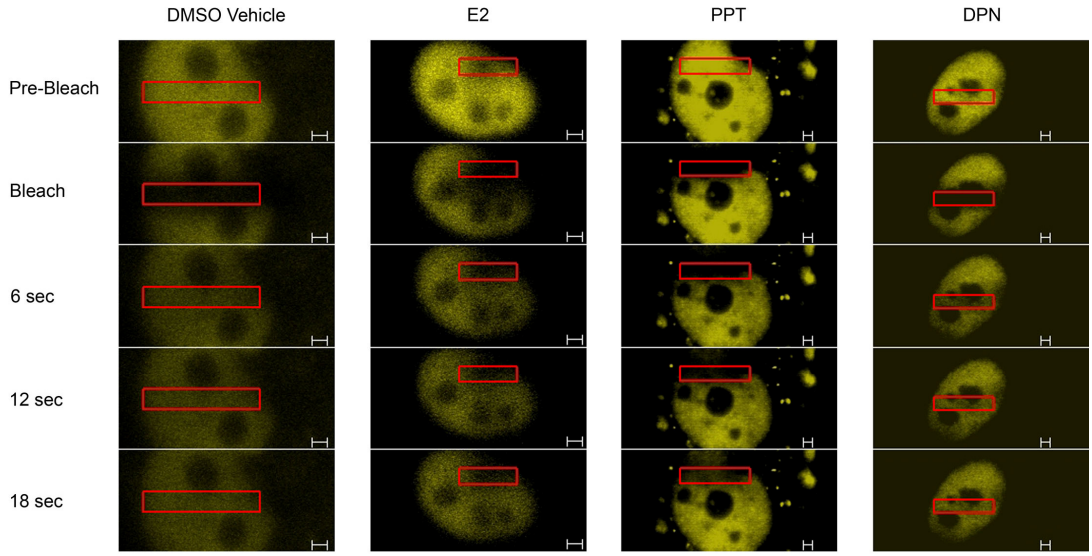

Figure 3.37 Qualitative FRAP assessment of dual infected MDA cells.

MDA cells were infected with ERβ2-YFP and unlabelled ERα to assess the effect of ligand on heterodimers. Heterodimeric status is assumed based on relative proximity calculations verified by FRET studies conducted in the lab (data not presented). Cells were subjected to treatment with either a DMSO vehicle control, E2 10^{-8}M, PPT™ 10^{-8}M or DPN™ 10^{-8}M for 60 minutes. The fluorescent molecules of a designated region (red box) were annihilated during the bleaching process and recovery back into this zone was monitored over time. This time period was chosen on the basis of full recovery observed in the control nuclei.

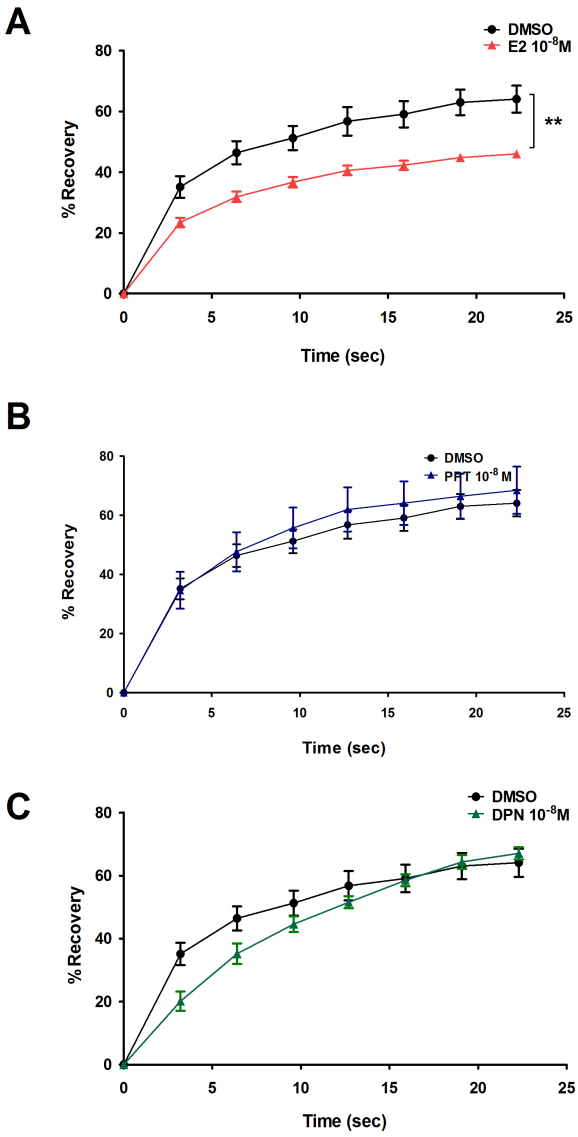

Figure 3.38 Quantitative analysis of intra-nuclear kinetics of dual infected MDA cells.

*Graphical depiction of impact of ligand treatment on the recovery rates of ERβ2 fluorophores over time in a background of untagged ERα constructs back into the bleached zone. This recovery is denoted by the point at which the Y_{MAX} is achieved and a plateau is reached on the graph. Recovery rates of ERβ2-YFP infected MDA cells are presented in response to E2 (A), PPT™ (B) and DPN™ (C) stimulation at a concentration of 10-8M. ** ($P<0.01$) denotes significance in variation of ligand treatments compared with the vehicle control as derived from the Student's t-test ($N\geq8$).*

ERβ (+/-YFP) and ERβ2 (+/-YFP)

MDA cells were co-infected with a combination of ERβ and ERβ2 and for each co-infection one subtype was fluorescently labelled with a YFP tag while the other subtype was untagged. When the mobility of ERβ2-YFP was assessed following treatment of cells for 1 hour with E2 the recovery of fluorescence following photobleaching was identical to that of the DMSO vehicle control. In the study with the alternative combination (ERβ-YFP and ERβ2 untagged), the ERβ-YFP molecule remained largely mobile in the presence of PPT™ but incubation with DPN™ resulted in an apparent reduction in mobility (Fig. 3.39). Statistical analysis of the impact of E2 treatment on co-infected ERβ2-YFP and ERβ MDA cells demonstrated no effect of E2 on ERβ2-YFP (Fig. 3.40A). In cells co-expressing ERβ-YFP and ERβ2, PPT™ treatment did not alter the mobility pattern of ERβ-YFP (Fig.3.40 B) while DPN™ induced a significant reduction in the mobility of ERβ-YFP molecules under the same experimental conditions (Fig. 3.40 C).

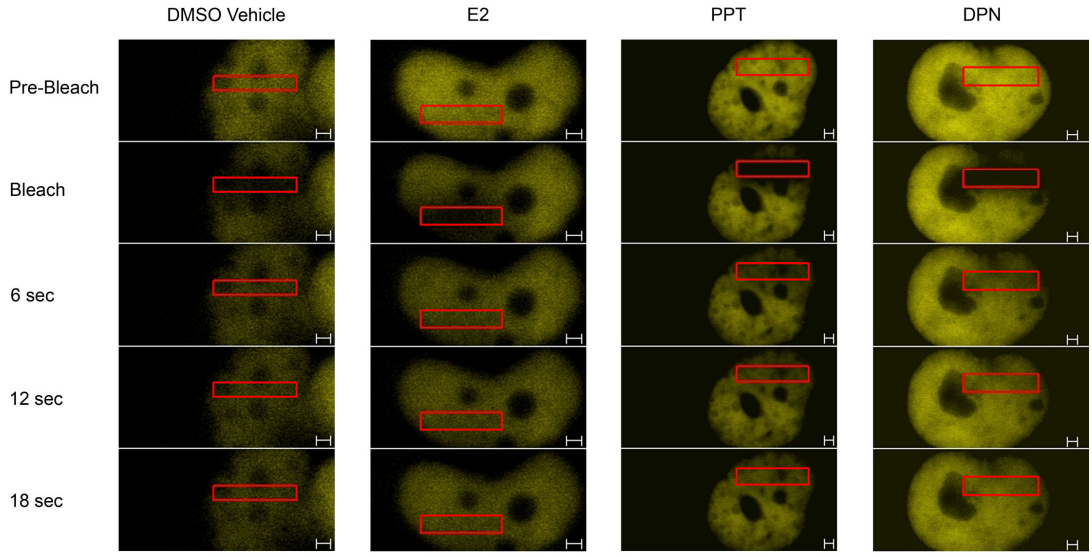

Figure 3.39 Qualitative FRAP assessment of dual infected MDA cells.

MDA cells were infected with ERβ (-YFP) and ERβ2 (-YFP) to assess the effect of ligands on heterodimers. Cells infected with ERβ2-YFP and ERβ were subjected to treatment with either a DMSO vehicle control or E2 10^{-8}M. MDA cells infected with ERβ-YFP and ERβ2 were incubated with PPT™ 10^{-8}M or DPN™ 10^{-8}M.

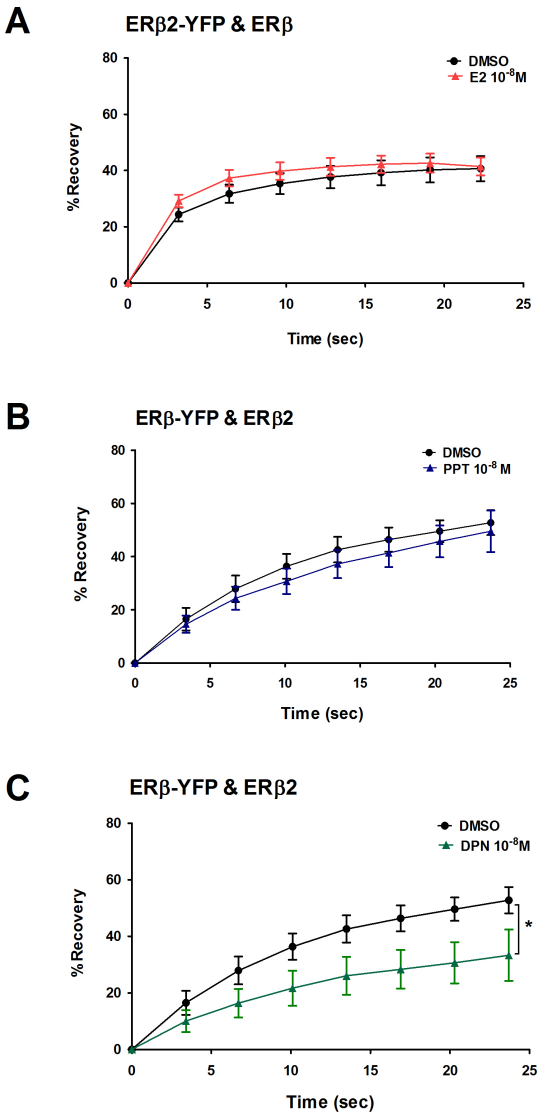

Figure 3.40 Quantitative analysis of intra-nuclear kinetics of dual infected MDA cells.

*Impact of E2 treatment on the recovery rates of ERβ2-YFP over time in a background of untagged ERβ constructs back into the bleached zone (A). Recovery is denoted by the point at which the Y_{MAX} is achieved and a plateau is reached. Recovery rates of ERβ-YFP and untagged ERβ2 co-infected MDA cells are presented in response to PPT™ (B) and DPN™ (C) stimulation at a concentration of 10^{-8}M. *(P<0.05) denotes significance in variation of ligand treatments compared with the vehicle control as derived from the Student's t-test (N≥8).*

3.3.4 Analysis of reporter gene activation in response to ER activity

As an extension of the investigations into the impact of natural and synthetic ER agonists on receptor mobility, their impact on transcriptional efficiency of the same ER subtypes in various combinations was examined after a 24 hour treatment period. This study involved an examination of the amount of luciferase activity generated as a result of activation of a 3X-ERE-tk-luc construct co-infected with the ER subtypes in MDA cells. Parallel control studies run using MDA cells that were not infected with ER constructs and infected with or without the 3X-ERE-tk-luc construct did not respond to E2 stimulation (data not presented).

3.3.4.1 Homodimeric Response

As expected incubation of E2 of cells infected with ERα alone resulted in a significant increase in the amount of luciferase activity that equated to ~17X greater activity than that recorded in DMSO-treated cells. A similar, significant, increase was induced by PPT™ treatment while incubation with DPN™ did not result in an increase in luciferase (Fig. 3.41A). The figure inset shows the results of the same experiment conducted with ERα-YFP infected cells and shows that tagged receptor had identical activity to that of ERα-YFP at the ERE (Fig. 3.41A).

Incubation of ERβ infected MDA cells also resulted in a significant increase in luciferase activity (~12 fold) although this was slightly less than that in the ERα-infected cells. Incubation with PPT™ had no impact on luciferase levels compared with control but incubation with DPN™ had a significant effect on the transcriptional activation of ERβ that emulated the response to E2 (Fig. 3.41B). The same panel of ligand treatments were ineffective in generating a transcriptional response and increase in luciferase activity in cells that had been infected with ERβ2 (Fig. 3.41C).

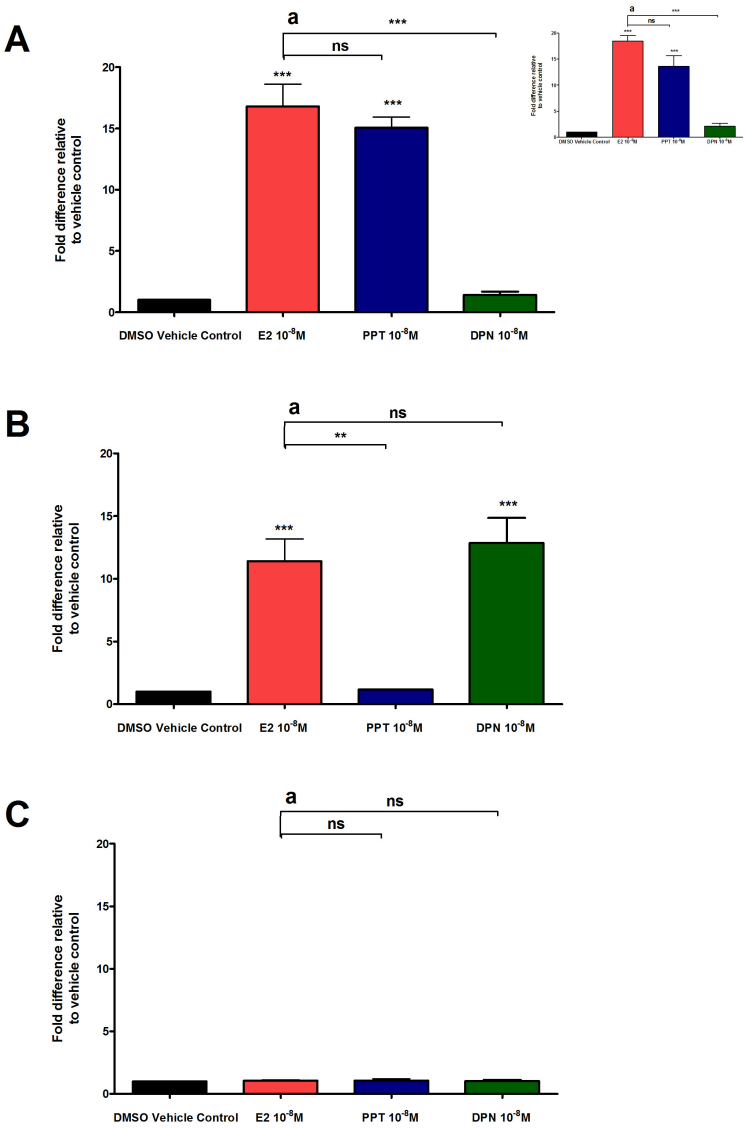

Figure 3.41 Impact of natural and synthetic agonists with ERs on luciferase reporter activity in MDA cells.

*Cells were infected with ERα-YFP (A), ERβ-YFP (B) or ERβ2-YFP (C) and each with the 3xERE-Luc reporter. The YFP tag on the constructs had no discernable effect on the assay results. The results of cells infected with an untagged ERα (inset) were use to assess this. Treatment was with a DMSO vehicle control (black column), E2 10^{-8}M (red column), PPT™ 10^{-8}M (blue column) or DPN™ 10^{-8}M (green column) for 24hours prior to luciferase production reading. Fold difference is expressed relative to the vehicle-treated cell, each bar represents N=3±SEM, is comparison of PPT™ and DPN™ treatments to the response observed with E2 treatment. *** (P<0.001) denotes significance in variation of ligand treatments compared with the vehicle control as derived from the Student's t-test (N≥8).*

3.3.4.2 Heterodimeric Response

Further to the FRAP study of ligand impact on the intranuclear dynamics of cells expressing two ER subtypes, a series of luciferase assays were performed using cells that had been co-infected with two untagged ERs.

In cells infected with ERα and ERβ in equal ratios, following treatment with either E2 or DPN™ an approximate 12 fold increase in luciferase activity was noted when compared to cells treated with the DMSO vehicle control. Interestingly, no increase in luciferase activity occurred in response to PPT™ treatment (Fig. 3.42A).

MDA cells co-expressing equal levels of ERα and ERβ2 appeared to respond equally well to both E2 and PPT™ (~15X increase in luciferase activity observed) with no significant discrepancy between the luciferase activity in the two treatments. In contrast, there was no increase in luciferase activity following incubation with DPN™ (Fig. 3.42B). Fig. 3.42C illustrates the luciferase responses recorded following co-infection of MDA cells with ERβ and ERβ2. While lower fold differences (~7 fold) were determined in comparison to the other co-infection experimental studies, significant increases in luciferase activity of approximately equal measure were observed following E2 and DPN™ treatment. There was no significant response as a result of PPT™ treatment.

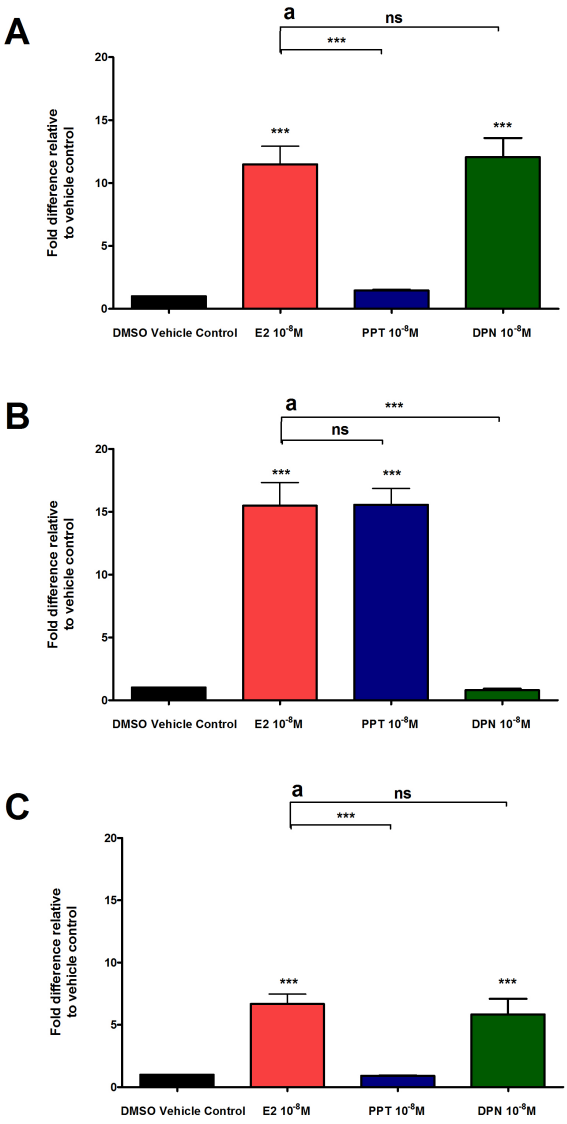

Figure 3.42 Impact of natural and synthetic agonists with two ERs on luciferase reporter activity in MDA cells.

*Cells were infected with combinations of ERα and ERβ (A), ERα and ERβ2 (B) ERβ and ERβ2 (C) and each with the 3x ERE-Luc reporter. Treatment was with a DMSO vehicle control (black column), E2 10^{-8}M (red column), PPT™ 10^{-8}M (blue column) or DPN™ 10^{-8}M (green column) for 24hours prior to luciferase production reading. Fold difference is expressed relative to the vehicle-treated cell, each bar represents N=3±SEM, a is comparison of PPT™ and DPN™ treatments to the response observed with E2 treatment. *** (P<0.001) denotes significance in variation of ligand treatments compared with the vehicle control as derived from the Student's t-test (N≥8).*

3.4 Discussion

The studies described in this chapter have compared and contrasted the impact of ligand on the intranuclear mobility of ERα, ERβ and ERβ2 and their ability to activate an ERE-dependent reporter gene. Previous studies in our own laboratory using transient transfections enjoyed mixed success when we attempted to examine dynamic properties, therefore in the current studies it was decided to infect the cells using an adenoviral delivery system. This method avoids issues such as auto-squelching due to overexpression of the protein of interest which may mask true behaviour and results. After trial experiments, an optimal final MOI value of 100 per 1 x 10^5 cells was deemed appropriate as it resulted in relatively uniform fluorescent distribution in ~60-70% of the cell population.

Immunohistochemical studies have revealed cell-specific patterns of expression of ERs in reproductive tissue but these do not provide information regarding the dynamic nature of the ER response to different ligands (Saunders *et al.*, 2001, Saunders *et al.*, 2002, Saunders and Critchley, 2002, Critchley *et al.*, 2002, Saunders *et al.*, 2003, Collins *et al.*, 2009). A thorough interrogation of the impact of ligand binding on the function of ERs requires investigation of real-time activities to address the numerous interactions that take place between the ER and a contingent of cofactors and other transcription factors prior to binding at the DNA helix. FRAP analysis facilitates the spatio- and temporal probing of responses to ligand stimulation through the marriage of time-lapse microscopy combined with photobleaching (Axelrod *et al.*, 1976). The photobleaching process is irreversible resulting from the transition of the excited molecule from a singlet to an excited triplet state. Nuclear dimming and incomplete recovery curves are a direct result of photobleaching of the ROI I whereby the fluorescence of this sub-population (ROI I) of fluorophores has been irreversibly destroyed or immobilised at the site of bleaching (Houtsmuller and Vermeulen, 2001). In the current study all data output was normalised to take account of any overall dimming as outlined in section 2.8.7.

3.4.1 Differential ER subtype nuclear distribution and expression patterns

The MDA breast adenocarcinoma cell was selected to conduct initial FRAP experiments on the basis of low levels of basal endogenous ER expression. This milieu afforded the analysis of YFP-tagged ER proteins individually and without the influence of endogenous ER. Strip-FRAP was used for all cell contexts and treatments. Interchanging strip orientation was used to assess for anisotropic effects of ligand treatment. There were no discrepancies in the results acquired between horizontal and vertical strips which confirms the stochastic model of unliganded ER in the nucleus as described by Reid *et al.* (Reid *et al.*, 2003).

Infection of the MDA cell line with ERα-YFP recapitulated the endogenous expression of nuclear ER with homogenous fluorescent expression throughout the nucleus. In contrast, infection of the MDA cells with ERβ-YFP did not result in uniform distribution of fluorescence within the nucleus and 'regions/pockets' of more intense fluorescence were observed. This expression pattern concurs with recent observations of the distribution of ERβ in transfected MCF-7 cells (Damdimopoulos *et al.*, 2008). Following infection of cells with the ERβ2 splice variant, the intranuclear pattern was consistently even and uniform. To date, there have only been limited studies published that have examined the effect of ligand incubation on mouse ERβ (Picard *et al.*, 2008) and human ERβ (Damdimopoulos *et al.*, 2008) in transfected HEK293 and MCF-7 cells respectively with no reported studies conducted on the subnuclear mobility of ERβ splice variants.

3.4.2 Changes in intranuclear dynamics are cell context dependent

In order to give a comprehensive insight into the behaviour of ERα, ERβ and ERβ variants in different cell environments, parallel studies were conducted using two different cell lines of endometrial origin (Table 3.2) in addition to the MDA cells (section 3.4.1). These Ishikawa cells and hTERT cells were used to examine the impact of the cellular environment of an adenocarcinoma endometrial cell line compared with that of an epithelial cell line derived from cells recovered from a

healthy endometrium. In contrast to the MDA breast cancer cells both of these cell lines express endogenous ERα and basal levels of ERβ and ERβ2 (Fig. 3.1).

Regardless of the cell line used, ERα-YFP responded in a similar fashion to incubation with E2 10^{-8}M. The response was characterised by a striking reduction in receptor recovery into the bleached zone during FRAP and was associated with rapid adoption of a 'punctate' appearance. This redistribution of receptor in response to E2 treatment may be reflective of the association of ERα homodimers with specific nuclear components (Press *et al.*, 1989) such as lysine/arginine rich motifs in nuclear lysosomes (Ylikomi *et al.*, 1992, Dauvois *et al.*, 1993).

Reduced mobility (i.e. decreased Y_{MAX}) also occurred in response to the ERα selective agonist PPT™ and this was more significant in Ishikawa and hTERT cells in comparison to MDA cells. It is tempting to speculate that this may be due to a more complete repertoire of cofactors and the other transcription factors required for formation of the preinitiation complex being present in the endometrial cells. DPN™ is reported to have 70-fold higher affinity for ERβ than ERα (Meyers *et al.*, 2001). Therefore it was surprising that incubation of MDA cells with DPN™ had a significant impact on mobility of ERα-YFP molecules. This effect was not observed when using Ishikawa and hTERT cell lines, where no significant impact on the Y_{MAX} levels of ERα was detected.

The ERβ response to E2 also displayed a trend towards a decrease in the mobility and stochastic dynamics of this receptor, albeit to slightly less significance in the hTERT cell line. Like ERα, cell nuclei expressing ERβ-YFP also adopted a speckled punctate appearance after exposure to E2. Incubation of ERβ-YFP with PPT™ had no impact on receptor mobility in all three cell lines. PPT™ has previously been described as ERα-selective arising from a selective interaction between the C(4)-propyl group and pyrazole core of the compound with a confined region of the ERα that is smaller than in ERβ (Stauffer *et al.*, 2000) and the data in the current study are consistent with this. Exposure to DPN™ resulted in a decrease in mobility of ERβ-

YFP in all three cell lines, with the most striking impact observed in the Ishikawa cell line. While a dominant effect of DPN™ on ERβ activity by the selective binding affinity and relative potency in comparison to ERα (70X and 170X greater respectively) dictated by its nitrile functionality has been described (Meyers *et al.*, 2001), DPN™ is not entirely ERβ selective as determined from the results of the ERα-YFP study in MDA cells. It is believed that the current study is the first to examine the impact of synthetic ligands on the intranuclear dynamics of human ERβ.

ERβ2 is a splice variant isoform of human ERβ, also known as ERβcx (Ogawa *et al.*, 1998c) that lacks amino acids encoded by the gene for exon 8. Molecular modelling of the protein suggests that it lacks an intact binding pocket (Leung *et al.*, 2006). In agreement with this, incubation of ERβ2 with a panel of natural and synthetic agonists had minimal impact on ERβ2 mobility in all the cell lines. A weak but significant response to E2 was detected in the hTERT cells, suggestive of heterodimeric associations with endogenous ERs within the hTERT nucleoplasm. A summary of the FRAP findings and differences across cell lines is presented in Table 3.2.

3.4.3 Incubation with anti-oestrogenic ligand influences ER sub-nuclear mobility

ICI 182,780 (Fulvestrant™) is a commercially available pure anti-oestrogenic drug used in the treatment of tamoxifen-resistant advanced breast cancers (Howell *et al.*, 2002). ICI 182,780 is reported to act by inducing increased turnover of receptors (Dauvois *et al.*, 1993b). In the current study the impact of ICI 182,780 on the mobility of all three ER subtypes within the Ishikawa nucleus was examined. Following 1 hour incubation with ICI 182,780 reduced levels of fluorescence were observed in comparison with DMSO treated control cells. The reduction in fluorescence intensity and the formation of well defined speckled accumulations within the nuclei may reflect ER turnover due to processing via the ubiquitin proteosomal pathway (UPP) (Reid *et al.*, 2003). Comparison of ERα and ERβ mobility revealed a more pronounced impact on ERα than ERβ. Although ICI

182,780 treatment caused a significant decrease in ERβ mobility, ERβ molecules were still dynamic while the impact on ERα resulted in complete immobilisation. This effect is in line with a recent report using transfected MCF-7 and HEK293 cells (Damdimopoulos *et al.*, 2008). In our study the ERα response was not rescued following a 1 hour additional incubation with E2 (data not presented), suggesting a dominant effect of ICI 182,780 over oestrogenic compounds. There are two plausible explanations for this observation; firstly that since only one ligand can bind at any one time to a receptor, ICI 182,780 may be imparting a dominant effect and altering the Helix 12/LBD region such that E2 is unable to physically interact with the receptor after ICI 182,780 binding or secondly the impact of ICI 182,780 binding may alter ER to the extent that it ablates the functional capacity of the receptor and no E2-mediated effects can occur.

In addition to differential responses between subtypes, cell specific differences in the response of ERβ2 to ICI 182,780 treatment was demonstrated with a clear reduction in mobility observed in the hTERT cells (data not shown) and no impact on mobility in the Ishikawa cells. It is possible that this is merely the effect of formation of heterodimers within these cells as it is known that only one partner of a heterodimer is required to be bound to ligand to initiate a response (Tremblay G.B. *et al.*, 1999). Conversely, it has also been reported that ICI 182,780 causes disruption of the dimerisation process of ERs thus facilitating turnover (Dauvois *et al.*, 1993). The ICI 182,780-induced change in ERβ2-YFP mobility observed in the hTERT cells is surprising as it has been documented that this splice variant lacks an intact ligand binding pocket (Leung *et al.*, 2006). The conformation adopted from binding of the 7α-alkylamide bulky side chain of the ICI 182,780 anti-oestrogenic compound appears to transcend the inability of agonist ligands to mediate an effect at ERβ2. Previous studies have resolved the conformation formed by the interaction of ICI 182,780 with ERα by X-ray crystallography analyses and have described an interaction that is distinct from that observed following agonist binding where ICI 182,780 disrupts association between Helix 12 and the rest of the ligand binding domain (Pike *et al.*, 2001). The results observed with ERβ2 could negate the

controversial observation that Helix 12 is essential for ICI 182,780 efficacy as described by Stenoien *et al.* (Stenoien *et al.*, 2001b) that was questioned in a recent study using juxtaposed C termini of ERα and ERβ mutants to address the same issue (Damdimopoulos *et al.*, 2008). However, in the latter study ERβ wild type did not respond to ICI 182,780 so further investigations using methods such as FRET or immuno-precipitation are required.

It has also been suggested that a result of ICI 182,780 binding is impairment of nucleocytoplasmic shuttling (Dauvois *et al.*, 1993b). This is in agreement with the results observed in the current study where no change in ERβ2-YFP distribution is seen following a 1 hour treatment with E2 compared with the weak fluorescent distribution observed in the cell nuclei following ICI 182, 780 treatment (data not shown), suggesting impaired nucleocytoplasmic shuttling.

Table 3.2 Comparison of intranuclear mobility responses to ligand treatment in MDA, Ishikawa and hTERT lines

Treatment	Construct	Cell Line		
		MDA	**Ishikawa**	**hTERT**
DMSO	ERα	*M*	*M*	*M*
	ERβ	*M*	*M*	*M*
	ERβ2	*M*	*M*	*M*
E2	ERα	*D*	*D*	*D*
	ERβ	*D*	*D*	*D*
	ERβ2	*M*	*M*	*D*
ICI (+/-E2)	ERα	-	*I*	-
	ERβ	-	*D*	-
	ERβ2	-	*M*	-
PPT™	ERα	*D*	*D*	*D*
	ERβ	*M*	*M*	*M*
	ERβ2	*M*	*M*	*M*
DPN™	ERα	*D*	*M*	*M*
	ERβ	*D*	*D*	*D*
	ERβ2	*M*	*M*	*M*

The changes in the mobility of each protein were scored as:

Mobile (M, rapid recovery into ROI within ~25 seconds)

Dynamic (D, with reduced percentage recovery compared with control cells)

Immobile (I, percentage recovery does not increase post-bleach)

3.4.4 Impact of co-infecting two ER subtypes on intra-nuclear dynamics

The formation of heterodimers between different ER subtypes can alter the nature of the gene expression pathways that can be targeted within different cell types. FRET

studies conducted within the lab have revealed high percentage FRET efficiency after ligand treatment following co-infection of differentially labelled ERs (i.e. with YFP and CFP tags respectively) (unpublished data). Further to these observations suggesting close proximity (i.e. within 10 Angstroms) between the combinations of ERα and ERβ, ERα and ERβ2, and ERβ and ERβ2, FRAP experiments were conducted to elucidate the heterodimeric response to the same panel of agonists (E2, PPT™ and DPN™) used for testing of individual ERs (putative homodimers). These experiments were conducted in the MDA cell line so as to study the heterodimeric responses independently of background endogenous receptor levels. Cells were infected with equal ratios of one unlabelled receptor construct and one YFP-labelled receptor construct whose mobility was tracked and heterodimerisation was assumed based on the results of the concurrent FRET investigations (Karen Tuzi, unpublished).

FRAP experiments using MDA cells that were co-infected with unlabelled ERα and ERβ-YFP and treated with E2 demonstrated a significant decrease in mobility of the tagged receptor that matched the level of significance acquired following infection with either ERα or ERβ alone. It is possible that this result reflects the action of an ERβ-YFP homodimer response but co-infection of the similar ERα and ERβ-YFP constructs followed by E2 stimulation gave rise to relatively high FRET efficiency values (Karen Tuzi, unpublished data) consistent with formation of heterodimers. Treatment with PPT™ did not have a significant impact on the final Y_{MAX} level reached compared to the DMSO vehicle control. This insignificant impact mirrors the result acquired following infection of ERβ alone and may only reflect the ERβ homodimeric response. This result could also be interpreted as a heterodimeric response whereby the ERβ partner of the dimer infers a dominant negative role on the ERα. The response of co-infected MDA cells (ERβ-YFP and ERα) to DPN™ was a significant decrease in mobility albeit not to the extent acquired with either of the homodimers for ERα or ERβ. The result indicates that DPN™ has a stronger effect on a homodimeric partnership over a heterodimeric state.

MDA cells co-infected with unlabelled ERα and ERβ2-YFP in equal ratio and incubated with ligand were also examined. In this set of experiments the YFP of the adenoviral ERβ2 construct was monitored and heterodimerisation between ERα and ERβ2 was assumed. Notably, the response of the co-infected cells to E2 treatment favours this supposition as a significant decrease in the mobility of ERβ2-YFP was observed following 1 hour incubations with E2. This result was markedly different from the response of MDA cells infected with ERβ2-YFP alone and mirrored the findings (albeit to slightly less extent) of the ERα homodimer. This result suggests a role for ERβ2 in a heterodimeric partnership whereby it does not drastically impair the functional output of ERα and as such substantiates the fact that only one pair of a dimer is required to be ligand-bound to elicit a significant effect (Leung *et al.*, 2006). No impact of PPT™ or DPN™ treatments on cells co-infected with ERα and ERβ2-YFP was observed. This result may reflect a role for ERβ2 as a dominant negative inhibitor of ERα with DPN™ treatment. It may also however be indicative of a ERβ2-YFP homodimeric response although our FRET studies suggest association of ERα and ERβ2 in response to PPT™ (Karen Tuzi, unpublished).

Treatment of MDA cells co-infected with ERβ and ERβ2-YFP with E2 resulted in an insignificant impact on the mobility of ERβ2-YFP. FRET efficiency curves have demonstrated close proximity values of these two ERs following E2 stimulation. The results of the FRAP study suggest a dominant inhibitory role for ERβ2 whereby the ERβ response to E2 is completely abrogated or it may depict the results of ERβ2 homodimeric responses only. FRAP analyses of cells co-infected with ERβ-YFP and ERβ2 demonstrated an insignificant response of ERβ-YFP to PPT™. This observation echoed the responses of both ERβ and ERβ2 responses to the compound when infected individually and is consistent with PPT™ acting as a selective agonist for ERα. In contrast, there was a significant DPN™-mediated impact on mobility determined in cells co-infected with ERβ-YFP and ERβ2, and although not to the extent of that determined upon infection with ERβ alone, it was greater that that following infection with ERβ2 alone. This result implies an attenuated ERβ response to DPN™ in the presence of the splice variant ERβ2 in this cellular context.

3.4.5 The ability of natural and synthetic ligands to transactivate ER subtypes alone and in combination at an Oestrogen Response Element

As an extension of the FRAP study on the intranuclear dynamics of ER subtypes, the same panel of natural and synthetic agonists were used to assess the transcriptional activity of the ligand-activated receptors using a 3xERE promoter sequence fused to the luciferase gene. The aim of this study was to establish if any correlation exists between the mobility patterns and the functional integrity of the ER subtypes under investigation and it was conducted using MDA cells.

There was no significant difference between the luciferase output in response to E2 and PPT™ in MDA cells infected with ERα-YFP. Both compounds induced a significant ~15X increase in the luciferase activity in comparison to a DMSO control vehicle. There was no significant activity induced at the ERE by ERα following DPN™ incubation. To validate the FRAP experiments using YFP labelled ER subtypes, concomitant luciferase assays were conducted using unlabelled ERs. There were no discrepancies found between assay outputs using untagged versus YFP tagged receptors. A significant impact on the mobility of ERα-YFP was established in response to each of the three agonists in the FRAP studies of MDA cells. This effect on mobility is mirrored by the transcriptional activity of ERα in response to E2 and PPT™ but not with DPN™ treatment.

While E2 and DPN™ treatments yielded a similar effect by increasing the luciferase activity driven from the ERE in ERβ-YFP infected MDA cells, there was no effect observed following PPT™ treatment, confirming that PPT™ functions as a potent agonist for ERα but not for ERβ. The increase in E2-mediated ERβ activity was noted as being lower than that of the E2-mediated ERα response and this attenuated transcriptional activity of ERβ has been previously described (Tremblay *et al.*, 1997, Pettersson *et al.*, 1997). Cells infected with ERβ2-YFP alone and subjected to E2, PPT™ and DPN™ treatments did not generate any activity at the ERE. The results of the luciferase activity response assays to homodimers confirms the selective

nature of PPT™ and DPN™ and their ability to potentiate transcription at an ERE after binding to ERα and ERβ respectively. While the tracking of ER mobility within the nucleoplasm tends to be indicative of a final transcriptional output, the two measures are not inherently linked and contradictory results have been found (e.g. ERα + DPN™).

The formation of heterodimers between different ER subtypes could putatively expand the regulatory potential of the receptors. The activity of heterodimers was explored with a series of experiments involving co-infection of two receptors in equal ratio in the MDA cell line. FRET studies conducted within the lab have highlighted close proximal formations between each of the combinations tested in response to E2, PPT™ and DPN™ treatments (Karen Tuzi, unpublished data). Previous studies have identified that the heterodimer is the preferential state of ERβ when in the presence of ERα (Cowley *et al.*, 1997). The ~12X increase in luciferase activity in response to E2 following co-infection with ERα and ERβ reflects an altered response to that of either receptor infected individually. The combination of ERα and ERβ gives rise to a slight increase over the response observed with the ERβ homodimer while at the same time the impact of ERβ in a conformation with ERα serves to weaken the transcriptional activity of ERα in comparison to its homodimeric state. Equal decreases on the intranuclear dynamics of each of the three combinations was derived from the FRAP study. This highlights a caveat in FRAP interpretation whereby the results cannot be presented in isolation as they do not necessarily represent a complete picture on the nature of activity of the protein being studied.

PPT™ had no impact on the transcriptional output of the luciferase assay system in cells co-expressing ERα and ERβ. The lack of activity observed following PPT™ treatment in the presence of ERβ homodimers was not rescued in the partnership with ERα suggesting that ERβ imposed a dominant negative influence on ERα in this context. In FRAP experiments, an impact on mobility was only observed in ERα

infected cells in response to PPT™. Taken together, these results highlight the selective nature of PPT™ for ERα.

DPN™ was primarily ERβ selective according to the results of the luciferase assays in accordance with expectations based on previously published papers (Meyers *et al.*, 2001, Sierens *et al.*, 2004). The increase in luciferase activity was slightly greater in the heterodimeric formation between ERβ and ERα than with ERβ alone and this may underlie the apparent favoured state of ERβ to be in a heterodimeric association over a homodimeric pairing. There is a negligible effect on transcriptional output in response to DPN™ in ERα infected cells. The 12X increase in luciferase activity in the heterodimeric conformation substantiates the perception that only one partner of a dimer is required to be bound to ligand to facilitate active transcription (Tremblay G.B. *et al.*, 1999).

The formation of ERα–ERβ2 heterodimers is assumed based on the differential responses to luciferase activity generated in comparison to the independent homodimer formations. For example, E2 elicited a ~15X increase in activity of the luciferase gene in MDA cells co-infected with ERα and ERβ2 in equal measure. This response conveys an attenuated ERα impact in comparison to the ERα homodimer that may be an influence caused by ERβ2. These results mirror the effect observed with the FRAP analyses whereby the level of significance on the decrease in mobility was lower in the heterodimer in comparison to the ERα homodimer. There were no changes brought about in intranuclear dynamics or transcriptional activity following incubation of any of the agonists tested on ERβ2. Furthermore, the response of ERα to PPT™ was maintained in the presence of ERβ2 in the luciferase assay. While a significant decrease on the mobility of ERα was found in response to PPT™ in the FRAP study, co-expression of unlabelled ERα with ERβ2-YFP and incubation with PPT™ had no impact on mobility of the latter. Cumulatively, the results of the co-infection studies may signify that heterodimerisation does not occur between ERα and ERβ2 in response to PPT™. The weak luciferase emission acquired following DPN™ incubation in ERα infected MDA cells was not replicated following co-

infection with ERβ2. These results are in line with those of the FRAP experiments whereby DPN™ treatment yielded a significant effect in slowing down the mobility of ERα-YFP infected cells. A decrease, albeit to a lesser degree of significance was found following co-infection of ERα with ERβ2-YFP. Taken together, these results demonstrate active heterodimeric association between ERα and ERβ2 in response to DPN™ because of 1) the difference on the impact on mobility observed when tracking ERβ2 alone (no effect on mobility) and when co-infected with unlabelled ERα and 2) the differential transcriptional output response noted between ERα in isolation and when co-infected with ERβ2. As ERβ2 is not thought to bind DPN™ this suggests the ligand has induced a change in the conformation of ERα favouring binding to ERβ2.

Incubation of E2 with ERβ-ERβ2 resulted in transcriptional activity that was less than that of the ERβ alone. This finding indicates that heterodimeric associations between ERβ and ERβ2 many occur although no significant effect was observed in relation to intranuclear dynamics. In concurrence with the FRAP study PPT™ had no effect on the transcriptional activity of ERβ or ERβ2 alone or in combination at the ERE but an attenuating effect of ERβ2 on the mobility and transcriptional response of ERβ was observed in response to DPN™. These results are suggestive of a function for ERβ2 in antagonising the response to ligand-bound ERβ.

3.5 Conclusions

The results of this study have identified differential responses of ER subtypes to natural and synthetic compounds that behave as agonists and antagonists of the ER. Characteristic ER subtype responses have also been found to be dependent on cellular context. These assessments are based upon investigation of the mobility patterns observed within the nucleus and the functional capacity as defined by activation of a cognate response element. It was found that the dynamic patterns largely translated with the final transcriptional output and that these separate functions may be linked. The impact of ligands on receptor heterodimers was also examined and revealed further complexity and variation in responses.

Evidence presented in this chapter indicated a putative role for the truncated splice variant ERβ2 as a partner in an active heterodimer. A number of clinical studies (Peng *et al.,* 2003, Davies *et al.,* 2004, Shaaban *et al.,* 2008) have suggested the use of truncated ER isoforms as potential diagnostic markers. The next chapter of this thesis therefore focuses on the intranuclear response of the particular splice variant ERβ5 to ligand. Unlike ERβ2, ERβ5 is completely devoid of the LBD and the following study investigates the role of the ERβ5 isoform in the endometrium in mediating a cellular response.

Chapter 4

Role of ERβ5 in the human endometrium

4 Role of ERβ5 in the human endometrium

4.1 Introduction

ERα has long been employed as the gold standard prognostic tool when assigning breast cancer cases for endocrine therapy (Pertschuk and Axiotis, 1999). Despite this, it has been shown that up to 40% of ERα-positive breast neoplasms are non-responsive to anti-oestrogen therapy (Locker, 1998). Investigations into expression of ERs in various reproductive pathologies have revealed the co-expression of ERα and ERβ mRNA and protein (reviewed in Saunders and Critchley, 2002). Specific examination of the expression patterns of the truncated human ERβ splice variants has detected their expression in several cell lines including the MDA-MB435 breast cancer line (Moore *et al.*, 1998), COS-1 cells (Inoue *et al.*, 2000) and Ishikawa cells (Scobie *et al.*, 2002).

The two human receptor isoforms, ERβ2 and ERβ5, diverge from ERβ at amino acid 469 (Moore *et al.*, 1998). ERβ2 has a distinct C-terminal domain in place of the amino acids encoded by exon 8 in the wild type, full-length human ERβ protein comprising of a unique 26 amino acid sequence encoded by a different exon (Zhao *et al.*, 2008). ERβ5 completely lacks a ligand-binding domain and the C-terminus is defined by the intron code found between exons seven and eight in full length human ERβ (Peng *et al.*, 2003; Poola *et al.*, 2005a).

Several clinical studies examining the role of human ERβ splice variants as putative diagnostic candidates have alluded to the importance of investigating expression of the different isoforms (Peng *et al.*, 2003). A study of neoplastic breast tissue demonstrated higher expression of ERβ2 and ERβ5 mRNAs compared with ERβ1 mRNA levels and with normal breast tissue levels (Leygue *et al.*, 1999b). Davies *et al.* reported significant association of ERβ2 and ERβ5 expression with relapse free survival in a study of post-menopausal breast cancer patients undergoing adjuvant therapy, with a particular correlation between ERβ2 and overall survival (OS) (Davies *et al.*, 2004). Another study reported that expression of nuclear ERβ2 was

associated with better OS and disease free survival but conversely cytoplasmic ERβ2 was related to poor prognosis. This study also demonstrated that nuclear ERβ5 expression was associated with improved survival (Shaaban *et al.*, 2008).

Cowley *et al.* reported that co-expression of ERα and ERβ in a 1:1 or 1:2 ratio resulted in preferential heterodimerisation between the two subtypes (Cowley *et al.*, 1997). Heterodimerisation between ERα and each of the splice variant isoforms has also been demonstrated as well as heterodimer formation between the ERβ isoforms themselves (Leung *et al.*, 2006). Preferential binding of ERβ2 with ERα rather than ERβ has been reported (Ogawa *et al.*, 1998c) and Hall and McDonnell described an AF-1 mediated repressor function of ERβ at subsaturating hormone levels that can compete at the ERE to block ERα function in cells where the receptors are co-expressed (Hall and McDonnell, 1999).

As ERβ2 and ERβ5 are reported to have an attenuated DNA-binding capacity and an inability to recruit coactivators, they may not initiate transcription in a ligand-dependent manner (Ogawa *et al.*, 1998b, Moore *et al.*, 1998, Peng *et al.*, 2003). Irrespective of this, studies have demonstrated the ability of ERα variants; ERαΔE3 and ERαΔE5 (Bollig and Miksicek, 2000) and the ERβ splice variants; ERβ2 and ERβ5 (Peng *et al.*, 2003) to repress ERE-mediated transcription of ERα. Conversely, a role for ERα in the regulation of ERβ was demonstrated through the inhibition of E2-independent transactivation of ERβ5 *in vitro* (Poola *et al.*, 2005a). Cumulatively, the studies to date suggest that co-expression of ERβ splice variants with ERα can alter ERα-dependent gene expression. These observations may indicate differential modulation of E2-dependent and independent action based on ER expression status and may be of pharmacological relevance in designing novel treatments based on different ratios of receptors.

4.1.1 Aims of the chapter

In the previous chapter, the intranuclear dynamics of full length ERs and the truncated splice variant ERβ2 in response to ligand stimulation were examined.

ERβ2 demonstrated a putative role as a partner in an active heterodimeric state with ERα. A role for ERβ splice variants as diagnostic tools has been postulated and therefore, the intranuclear response and functionality of ERβ5 upon ligand stimulation is examined in this chapter.

The overall aim of this chapter was to determine whether the ERβ splice variant ERβ5 might have an impact on oestrogen responsiveness in the normal human endometrium. Expression of ERβ5 was examined using immunohistochemistry. The regulation of ERβ5 through the examination of the intranuclear dynamics of ERβ5 in response to known ER effector compounds both as a single entity (homodimers) and in combination with ERα or ERβ (heterodimers) was studied. The impact of ERβ5 on ERE-promoter element was examined in the presence and absence of the full length ERα subtype.

4.2 Materials and Methods

4.2.1 Taqman® qRT-PCR

RNA was extracted from lysed cells using a Qiashredder™ spin column for cell homogenisation (section 2.5.1) and quantified using the Nanodrop® ND 1000 (Labtech International, East Crawley, UK). Complementary DNA was prepared using random hexamers (section 2.5.4.1) and was used for the Taqman reaction protocol outlined in section 2.5.4.3. Taqman analysis of mRNA using the Roche Universal Probe Library™ was conducted in triplicate for ERα, ERβ and ERβ5. Data output from the detection system was quantified in accordance with the $2^{-\Delta\Delta Ct}$ algorithm (section 2.5.4.4). Results are expressed as means and standard errors and statistical analysis was conducted using a Student's t-test.

4.2.2 Collection of endometrial tissue

As detailed in Chapter 2, section 2.2.1, human endometrial tissue was acquired from different phases of the menstrual cycle following hysterectomy, hysteroscopy or laparoscopic sterilisation performed at the Royal Infirmary, Edinburgh, UK. All patients gave written informed consent following discussion with research nurses.

Histological staging was performed by an expert histologist as previously reported (Critchley *et al.*, 2001, Critchley *et al.*, 2002).

4.2.3 Immunohistochemistry

Immunohistochemistry was performed using thin sections of paraffin embedded endometrial tissue to identify the expression patterns of the proteins of interest as outlined in section 2.4.1

4.2.3.1 Non Fluorescent Immunohistochemistry

In brief, tissue was processed and sections mounted on glass slides as described in section 2.4.1.1. The sections were then dewaxed, rehydrated (2.4.1.2) and subjected to antigen retrieval by means of pressure cooking in citrate buffer (2.4.2). Three blocking steps were employed to prevent endogenous peroxidase activity, non-specific binding of the secondary antibody and the formation of avidin-peroxidase complexes binding directly to the tissue where endogenous biotin is expressed as outlined in 2.4.3.1, 2.4.3.2 and 2.4.3.3 respectively. A mouse ERβ5 monoclonal antibody (Wong *et al.*, 2005, Collins *et al.*, 2009) was incubated with the tissue overnight at 4°C (Table 2.1). Bound antibody was detected with a goat anti-mouse biotinylated secondary antibody (Table 2.2) used and the signal was localised using the chromogenic substance DAB (K3468; DAKO) diluted in its substrate. The corresponding negative control sections were incubated with blocking serum only to enable confirmation of antibody specificity.

4.2.3.2 Immunofluorescence

Dual fluorescent immunohistochemistry was employed in order to co-localise two ERs simultaneously (2.4.7). The primary and secondary antibodies used are listed in Table 4.1.

Table 4.1 Summary of primary and secondary antibodies and the fluorescent labels used for immunofluorescence

Antigen 1	**Dilution**	**2° Antibody**	**Fluorescent Label**	**Antigen 2**	**Dilution**	**2° Antibody**	**Fluorescent Label**
ERβ5	1:40	GAM (Fab)-b	Alexa 488	**ERα**	1:20	GAM-p	Tyr cy 3
ERβ5	1:40	GAM (Fab)-b	Alexa 488	**ERβ**	1:20	GAM-p	Tyr cy 3
ERβ5	1:40	GAM (Fab)-b	Alexa 488	**ERβ2**	1:200	GAM-p	Tyr cy 3

Key:

GAM (Fab)-b: Goat anti-mouse Fab fragment biotinylated

Alexa 488: Alexafluor 488 (green)

GAM-p: Goat anti-mouse peroxidase

Tyr cy 3: Tyramide Cy3 (red)

4.2.4 Western Immunoblotting

Western blotting was performed on nuclear protein extracts (section 2.6.2) from Ishikawa cells that had been infected with adenoviral constructs expressing untagged ERβ5. The infected cells were lysed and separated into cytoplasmic and nuclear fractions and quantified in accordance with the Biorad DC Protein Assay (section 2.6.3). The nuclear protein extracts were separated on acrylamide gels (section 2.7.2), electro-transferred to PVDF membrane (section 2.7.3) and scanned for detection using the LI-COR™ infrared detection system (2.7.5). Membranes were incubated with the anti-ERβ5 monoclonal antibody for verification of protein size.

Table 4.2 Primary antibodies used for Western blotting

Antigen	Host Species	Dilution	Source
ERβ5	Mouse	1:100	In-house[1]
β-tubulin	Rabbit	1:600	Santa Cruz[2]

[1] In collaboration with Prof. N. Groome, Oxford Brookes University, Oxford, UK

[2]Santa Cruz Biotechnology, CA, USA

4.2.5 Cell treatments

To establish the impact of ligands on functional activity of ERβ5, cells were incubated with either E2 or one of the selective agonists PPT™ and DPN™ at a final concentration of 10^{-8}M. The impact of antagonist treatment was investigated by incubating cells with ICI 182,780 at a final concentration of 10^{-8}M. Control treatments using the DMSO vehicle at 10^{-8}M were conducted and used to analyse the overriding effects of agonist and antagonist treatment. Ligand treatment was conducted 1 hour prior to live-cell FRAP analyses and 24 hours in advance of cell harvesting for luciferase assays.

4.2.6 FRAP

FRAP was conducted on a LSM 510 confocal inverted light scanning microscope (section 2.8.6). In brief, live cells were maintained in PBS buffered with 10mM HEPES in an enclosed chamber heated to 37°C (section 2.8.2). Cells expressing YFP were selected for bleaching on the basis of uniform distribution of levels of fluorescence. Three ROIs were of equal dimension were chosen (section 2.8.5). Two prebleach images were captured at 3 second intervals followed by photobleaching owing to a series of focused pulsed iterations using the Argon 12 laser (488 and 514nm) laser at maximal power. Eight subsequent images were taken to establish recovery patterns using an attenuated laser (514nm set between 1-5% power) (section 2.8.6). Data collation and quantitation was conducted and subject to correction, normalisation and statistical evaluation as outlined (section 2.8.7).

4.2.7 Luciferase Gene Reporter Assay

Luciferase reporter assay were carried out as previously described (section 2.9.1). Luciferase output was measured as relative light units using the FLUOstar OPTIMA luminometer (BMG Labtech) and normalised against total protein content from samples of the same experiment and conditions using the Biorad DC Protein Assay (section 2.6.3).

4.3 Results

4.3.1 ERβ5 expression pattern in the endometrium

4.3.1.1 ER mRNA expression across the menstrual cycle

Analysis of expression of mRNA encoding different ER subtypes during the proliferative and secretory phases of the menstrual cycle using quantitative RT-PCR revealed very high levels of ERα mRNA in the proliferative endometrium that tapered off with progression into the secretory stages of the cycle (Fig. 4.1 A). In agreement with previous publications (Critchley *et al.*, 2002), the endogenous mRNA concentrations of ERβ and its splice variants ERβ2 and ERβ5 were much lower than the levels of expression detected for ERα. However, there were changes in the levels of expression observed where the pattern of ERβ expression opposed that of ERα with increasing levels determined with progression of the menstrual cycle (Fig. 4.1 B). This pattern of expression was mimicked by ERβ5 (Fig. 4.1 D). Although ERβ2 mRNA was greatest during the early secretory stage of the cycle, this observation may be sample dependent and is representative only of an N=3 (Fig. 4.1.C).

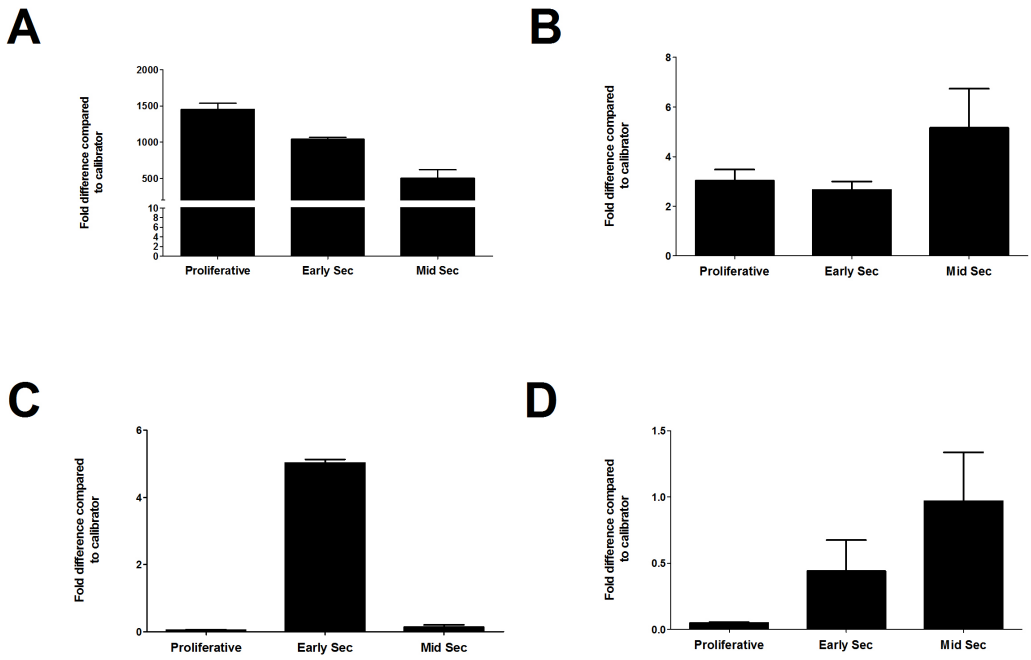

Figure 4.1 Expression of mRNAs encoding ER subtypes ERα and ERβ and the splice variants ERβ2 and ERβ5 in normal endometrium during the proliferative and secretory (luteal) phases of the menstrual cycle.

Decreasing levels of ERα mRNA were detected with progression of the cycle (A) and sustained low basal levels of ERβ (B), ERβ2 (C) and ERβ5 (D) were found. The fold differences expressed are relative to the levels of expression determined from a human RNA control (Applied Biosystems); N=3.

4.3.1.2 Immunolocalisation of Endometrial ERβ5 in endometrium across the cycle

On endometrial tissue sections, the specificity of the antibodies used against ERβ, ERβ2 and ERβ5 was validated (Fig. 4.2 upper panels). Nuclear staining with the monoclonal antibodies against ERβ, ERβ2 and ERβ5 was abolished by preabsorbing with the concomitant recombinant antigen protein (Fig. 4.2 lower panels).

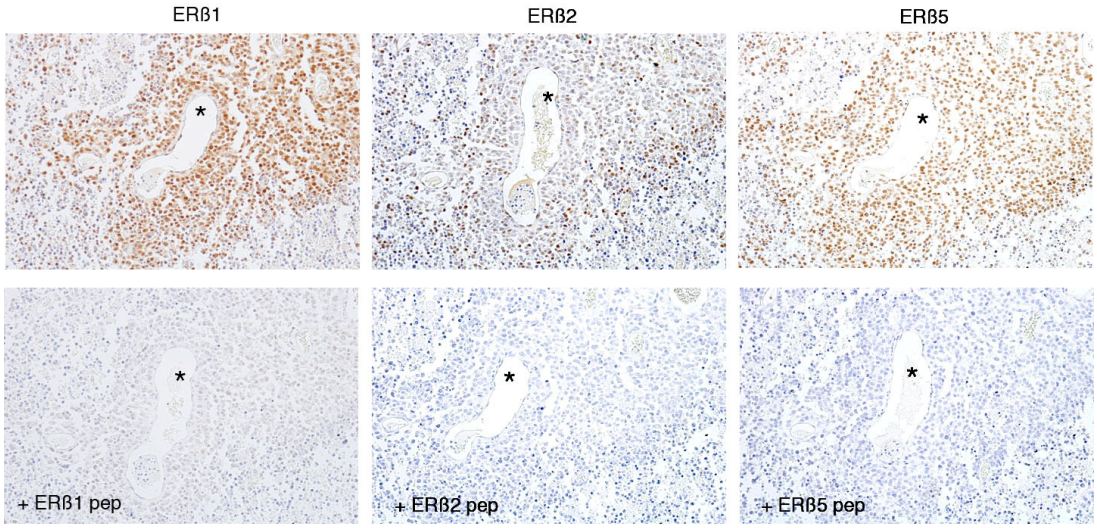

Figure 4.2 Validation of anti-ERβ antibodies used for histological evaluation of human endometrial tissue.

Immunodetection of ERβ, ERβ2 and ERβ5 in the endometrium (upper panel) were compared with images acquired of controls preabsorbed in the associated antigen peptide (lower panel), using the same tissue sample.

Using the specific monoclonal antibody ERβ5 was immunolocalised to cell nuclei throughout the endometrium at all phases of the menstrual cycle investigated (proliferative, early-, mid- and late-secretory) (Fig. 4.3). Intense ERβ5 immunoexpression was detected in the cell nuclei of stromal cells and epithelial cells lining the glands (Fig. 4.4) as well as endothelial cells lining the vasculature at all stages of the cycle (Fig. 4.3 and 4.4 arrows).

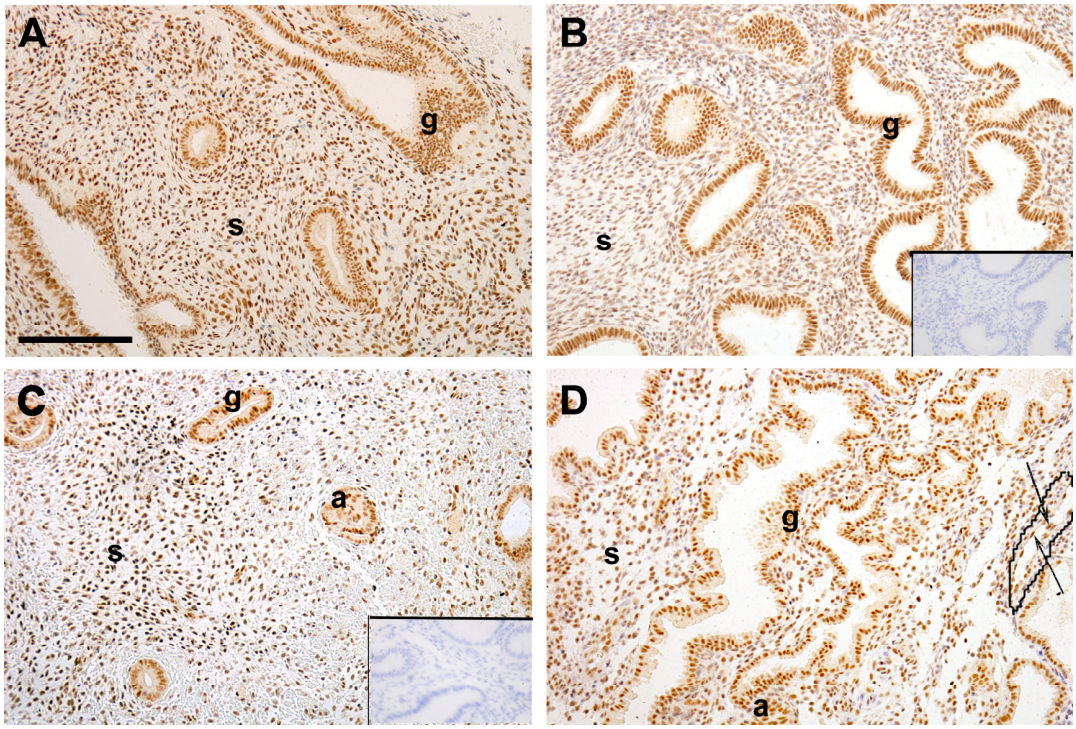

Figure 4.3 ERβ5 immunoexpression in the endometrium.

Immunodetection of ERβ5 in the functionalis of human endometrium during the proliferative (A), early secretory (B), mid-secretory (C) and late secretory (D) phases of the menstrual cycle. ERβ5 was detected in nuclei of the glandular epithelial (g) and stromal (s) cells at all phases of the cycle. ERβ5 staining was detected in the vascular muscle of the spiral arteries (a) and the vascular endothelium (arrows) in the mid- and late secretory phases. Insets are negative controls. Magnification X20; scale bar, 100μm.

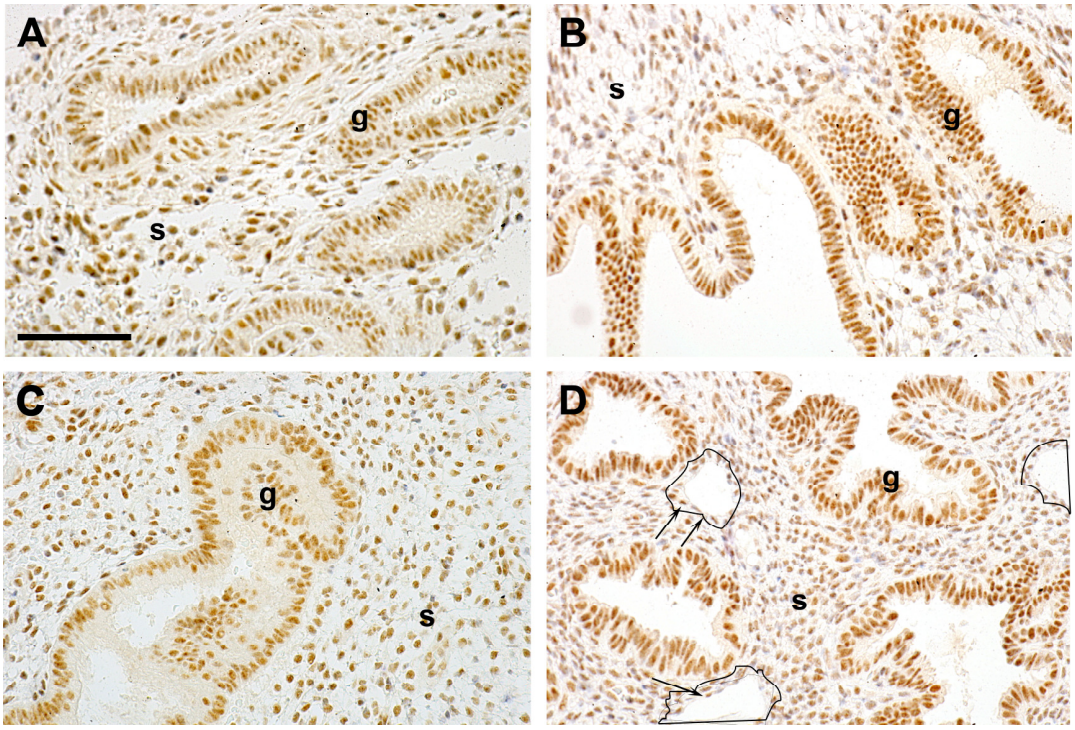

Figure 4.4 High power view of ERβ5 expression in human endometrium.

Immunolocalisation of ERβ5 in the nuclei of glandular epithelial (g), stromal (s) and vascular epithelial (arrows) during the proliferative (A), early secretory (B), mid-secretory (C) and late secretory (D) phases of the menstrual cycle. In panel D the vascular compartment is outlined and arrows are pointing to immunopositive endothelial cells. Magnification X40; scale bar, 100μm.

4.3.1.3 Co-localisation of ERβ5 and ERα in endometrial tissue

Using double fluorescent immunohistochemistry ERβ5 immunopositive nuclei (green) were found to co-localise with ERα positive nuclei (red) in the proliferative and early-mid secretory phases of the cycle in the endometrium (Fig. 4.5 merged panel; yellow nuclei). The weak immunopositive staining detected by the anti-ERα antibody at the later stages of the secretory stage was overwhelmed by intense ERβ5 staining in cell nuclei of the stromal and epithelial compartments so that most nuclei appeared green (Fig. 4.5).

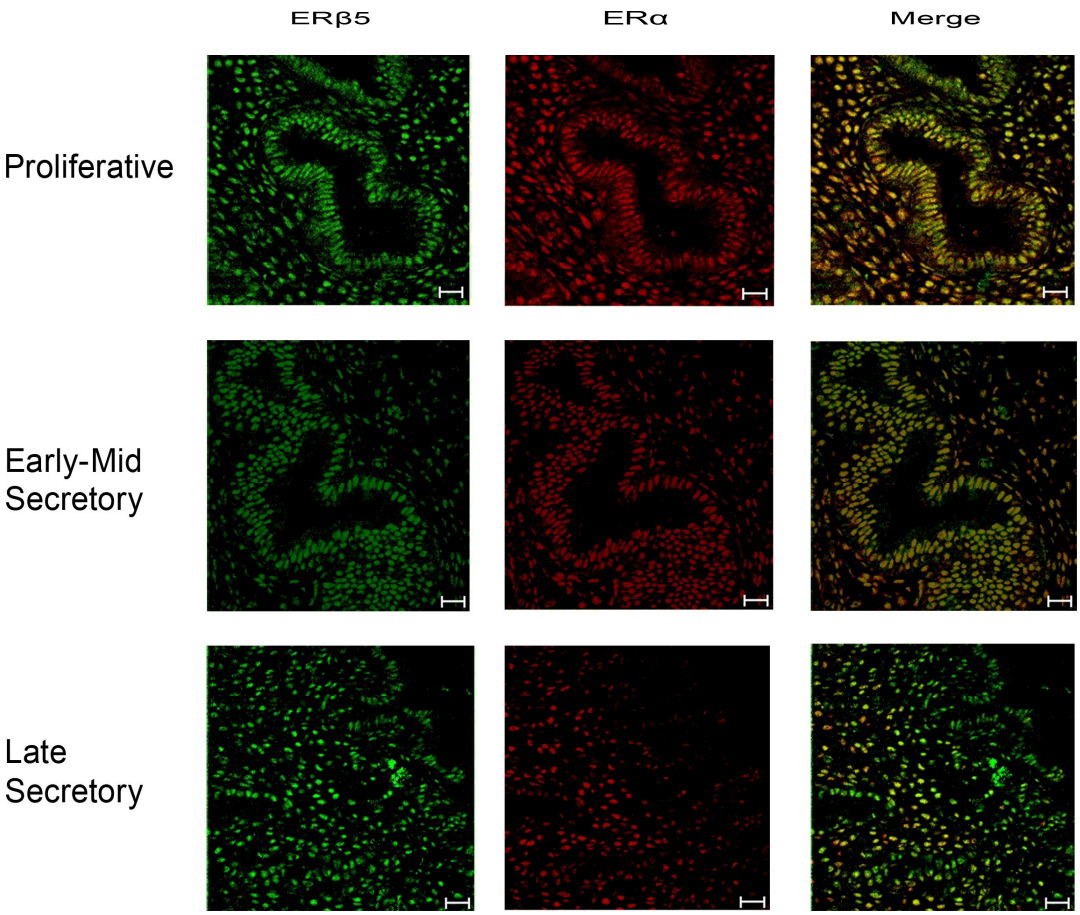

Figure 4.5 Co-expression of ERβ5 (green) and ERα (red) in normal endometrial tissue from stages across the menstrual cycle.

The merged image depicts co-localisation of the two ERs (yellow) in both the stromal (s) and epithelial cells of the glandular (g) compartments in the proliferative and early secretory phases. ERβ5 expression predominates in the merged image of the late secretory phase endometrium. Scale bar, 20μm.

4.3.1.4 Co-localisation of ERβ5 and ERβ

Dual immunofluorescent staining for ERβ5 (green) and ERβ (red) revealed co-expression of the proteins in nuclei of stromal and epithelial cell types throughout the menstrual cycle. Weaker ERβ protein immunoexpression at the late secretory phase resulted in dominant intense ERβ5 staining in the endothelial cells lining the blood vessels (arrows) and the epithelial nuclei of the glandular regions (Fig. 4.6).

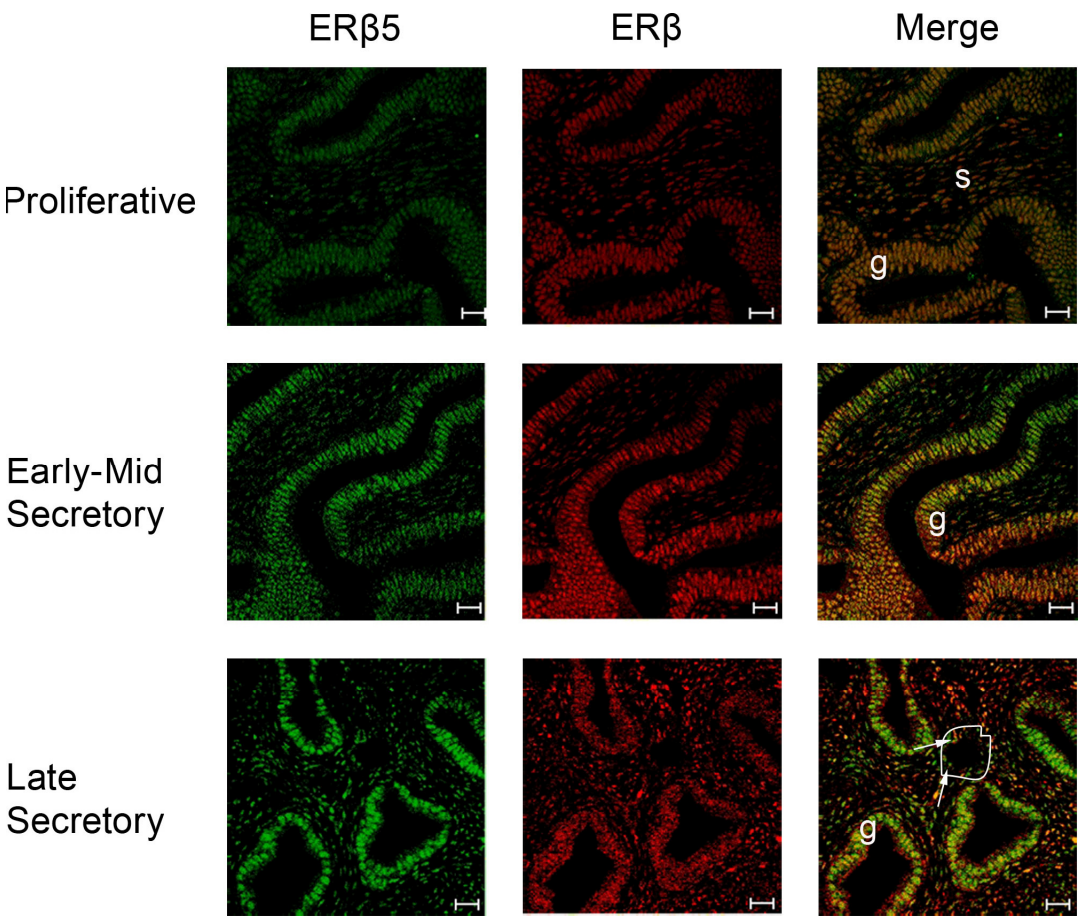

Figure 4.6 Co-expression of ERβ1 (red) and ERβ5 (green) in normal endometrial tissue from stages across the menstrual cycle.

The merged image depicts co-localisation of the two ERs (yellow) in both the stromal (s) and epithelial cells of the glandular (g) compartments in the proliferative and early secretory phases. ERβ5 expression is dominant in both the epithelial cells of the glands (g) and the endothelial cells surrounding the blood vessels (arrows) in the merged image of the late secretory phase endometrium. Scale bar, 20μm.

4.3.1.5 Co-localisation of ERβ5 and ERβ2

Immunofluorescent co-staining for ERβ5 (green) and ERβ2 (red) was detected across all phases of the menstrual cycle examined in the stromal and gland regions (Fig. 4.7).

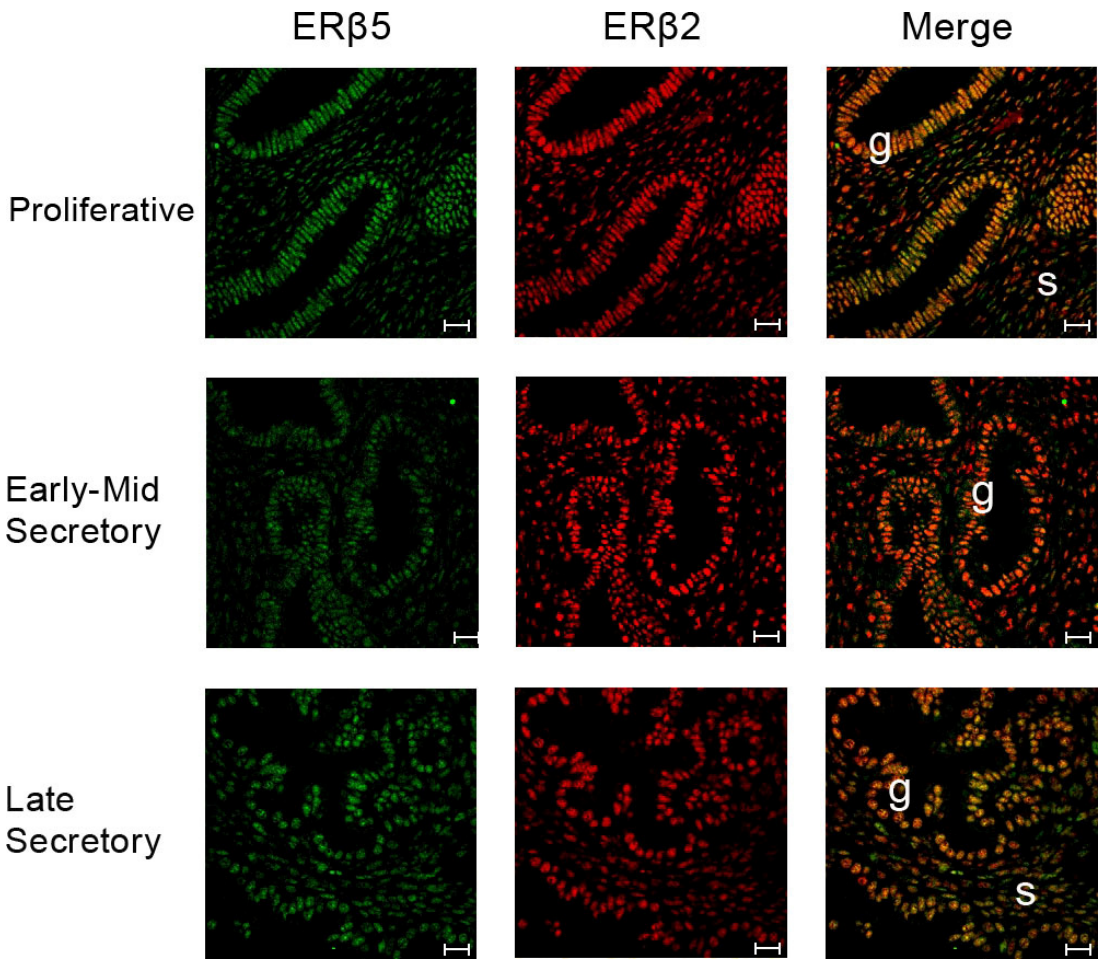

Figure 4.7 Co-expression of ERβ2 (red) and ERβ5 (green) in normal endometrial tissue from stages across the menstrual cycle.

The merged image depicts co-localisation of the two ERs (yellow) in both the stromal (s) and epithelial cells of the glandular (g) compartments across the proliferative and secretory phases of the menstrual cycle. Scale bar, 20μm.

4.3.2 Western analysis of ERβ5 in Ishikawa cells

The expression of endogenous ERβ5 in Ishikawa cells was examined using nuclear protein extracts from untreated Ishikawa cells and compared with nuclear protein from Ishikawa cells that had been infected with untagged ERβ5 (MOI 50) using Western immunoblotting. ERβ5 protein of the expected molecular weight of 53kDa was detected in all Ishikawa cells (Fig. 4.8).

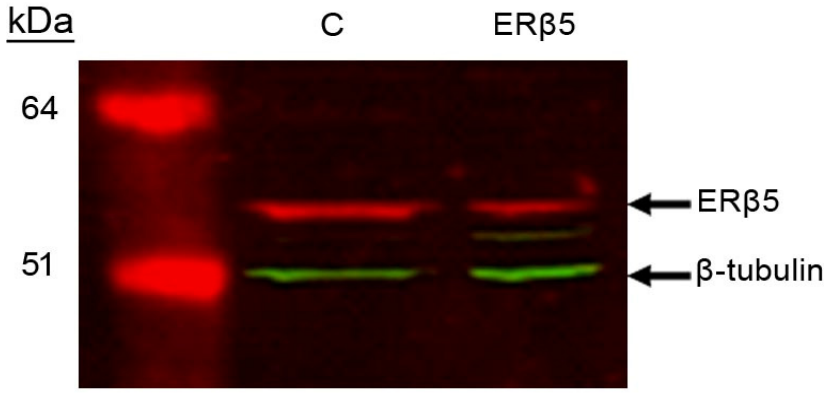

Figure 4.8 Determination of ERβ5 protein levels in the Ishikawa cell line.

This is a representative Western blot following nuclear protein extraction and probing for ERβ5 endogenous protein expression in the Ishikawa cells (Lane 1, Control, C) and in Ishikawa cells infected with an ERβ5 adenoviral construct (Lane 2, ERβ5).

4.3.3 Intranuclear dynamics of ERβ5 protein

4.3.3.1 ERβ5 response to incubation with agonists in Ishikawa cells

Infection of Ishikawa cells with ERβ5-YFP resulted in uniform nuclear distribution of fluorescence. The application of a DMSO vehicle control for 1 hour did not affect this state. There were no changes in morphological appearance of the nuclei in response to any treatments (E2, PPT™, DPN™; Fig 4.9).

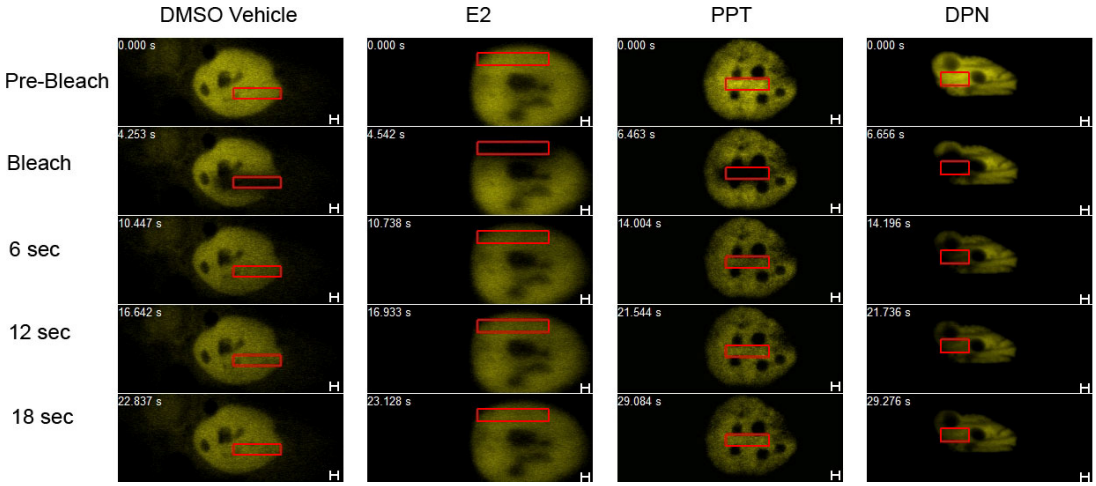

Figure 4.9 Qualitative FRAP assessment of ERβ5 infected Ishikawa cells.

Cells were treated with a DMSO vehicle control, E2 10^{-8}M, PPT 10^{-8}M or DPN 10^{-8}M for 60 minutes.

In agreement with the observational analysis of ERβ5-YFP infected Ishikawa cells, there were no significant ligand-mediated influences by any treatment (E2, PPT™ and DPN™) revealed by analysis of the percentage recovery values (Fig. 4.10). For PPT™ and DPN™ treatments, the recovery patterns mimicked that of the DMSO vehicle control response. E2 incubation induced a trend towards reduced percentage recovery compared with the DMSO-treated control cells (Fig. 4.10A).

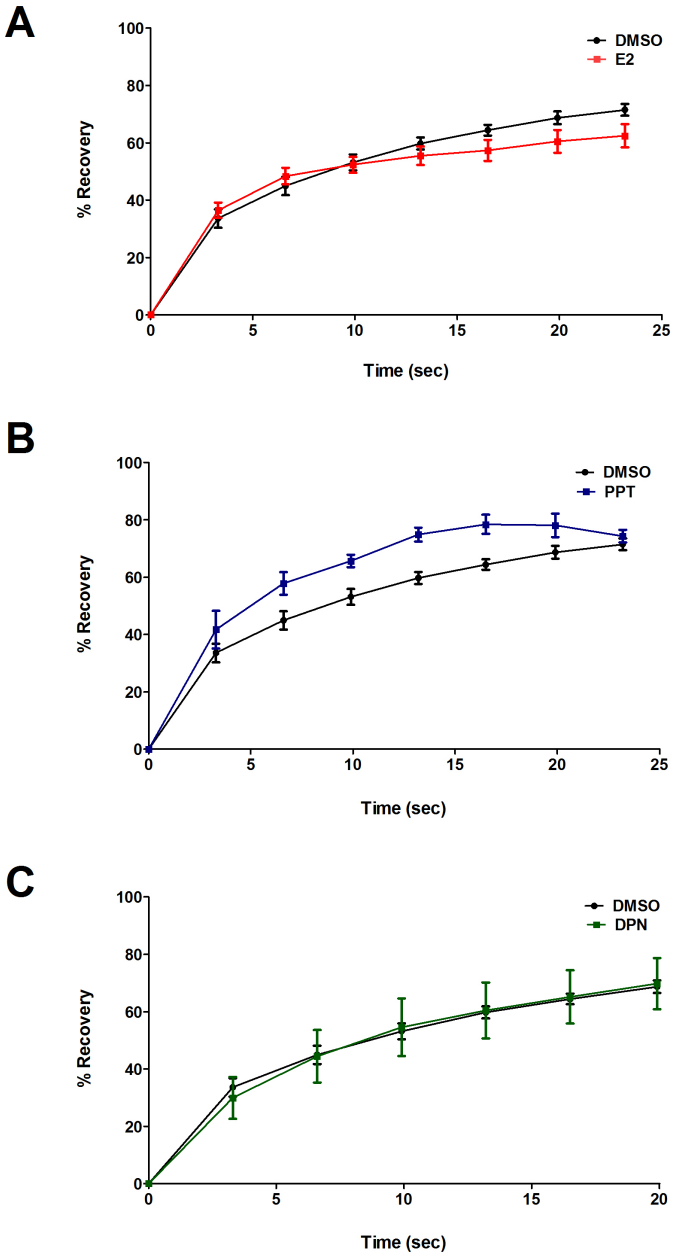

Figure 4.10 Quantitative analysis of intra-nuclear kinetics of ERβ5-infected Ishikawa cells.

Graphical depiction of impact of ligand treatment on the recovery rates of ERβ5-YFP fluorophores over time back into the bleached zone. This recovery is denoted by the point at which the Y_{MAX} is achieved and a plateau is reached on the graph. Recovery rates of ERβ5-YFP infected Ishikawa cells are presented in response to E2 (A), PPT (B) and DPN (C) stimulation at a concentration of 10^{-8}M. Significance of results was examined using the Student's t-test (N≥8).

4.3.3.2 ERβ5 Response to agonists in hTERT cells

The results acquired from the intranuclear dynamics investigation of ERβ5-YFP in the hTERT cell line mirrored those of the Ishikawa analysis (section 4.3.5.1). The homogenous distribution of ERβ5-YFP dispersed throughout the nucleus remained unchanged following incubation with either the DMSO vehicle control or any of the treatments E2, PPT™ and DPN™ for 1 hour (Fig. 4.11). Longer treatment times with E2 (up to 3 hours) were also tested with no effect on the YFP distribution pattern (data not presented). The rapid recovery of the bleached zone (red box) is observed within 6 seconds of photobleaching following each of the treatments.

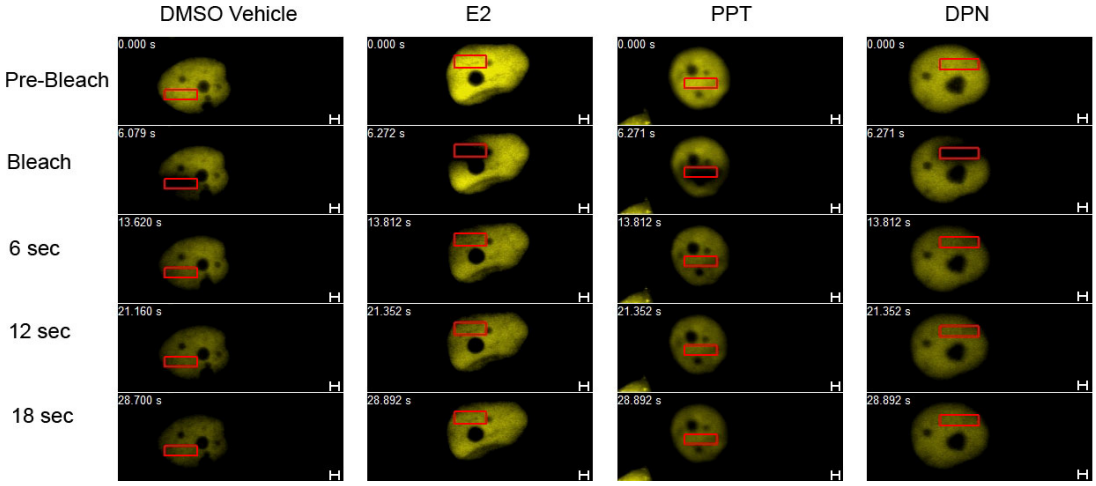

Figure 4.11 Qualitative FRAP assessment of ERβ5 infected hTERT cells.

Cells were treated with a DMSO vehicle control, E2 10-8M, PPT 10-8M or DPN 10-8M for 60 minutes.

Analysis of the statistical parameters of FRAP compound the observational data where no change in recovery response (Y_{MAX}) following incubation with PPT™ or DPN™ is discernable in comparison to the values obtained from the DMSO vehicle control treatment (Fig. 4.12B and C). However, a slight trend towards a decrease in mobility of ERβ5-YFP infected cells treated with E2 was observed (Fig. 4.12A).

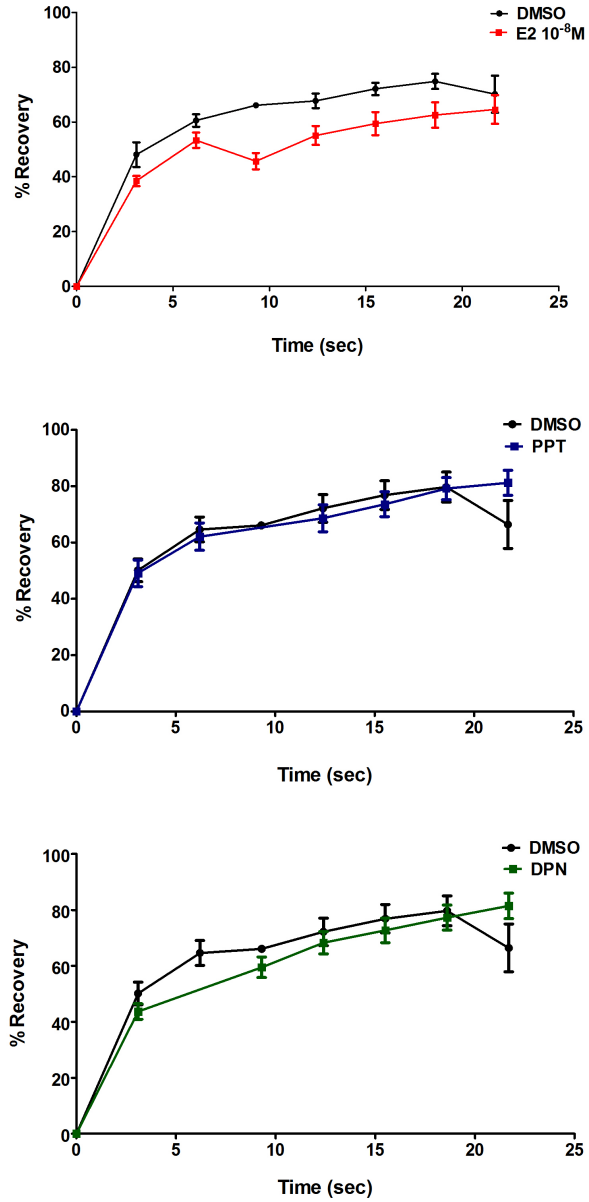

Figure 4.12 Quantitative analysis of intra-nuclear kinetics of ERβ5-infected hTERT cells.

Graphical depiction of impact of ligand treatment on the recovery rates of ERβ5 fluorophores over time back into the bleached zone. This recovery is denoted by the point at which the Y_{MAX} is achieved and a plateau is reached on the graph. Recovery rates of ERβ5-infected hTERT cells are presented in response to E2 (A), PPT (B) and DPN (C) stimulation at a concentration of 10^{-8}M. Recovery rates of ERα-infected Ishikawa cells are presented in response to E2 (A), PPT (B) and DPN (C) stimulation at a concentration of 10^{-8}M. Significance of results was examined using the Student's t-test (N≥8).

4.3.3.3 ERβ5 Response to antagonist in Ishikawa cells

Treatment of Ishikawa cells expressing ERβ5-YFP with ICI 182,780 resulted in redistributed fluorescence in the nucleus and a punctate appearance similar to that brought about (ICI 182,780 induced) in ERα-YFP infected Ishikawa cells (section 3.3.2.2.1). After photobleaching, levels of fluorescence in the bleached zone did not recover rapidly and were therefore examined over extended time periods (data not presented).

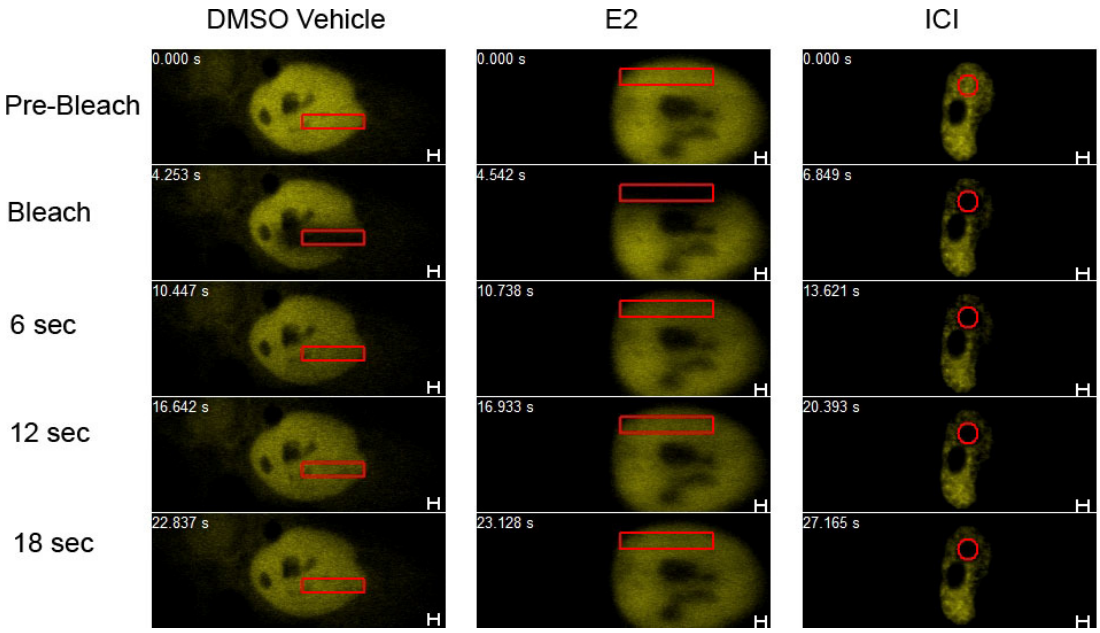

Figure 4.13 Qualitative FRAP assessment of ERβ5 infected Ishikawa cells.
Cells were treated with a DMSO vehicle control, E2 10^{-8}M or ICI 182,780 10^{-8}M.

ICI 182,780 treatment yielded a significant decrease in the mobility of ERβ5-YFP in Ishikawa cells that decreased Y_{MAX} from ~65% to ~25% (Fig. 4.14).

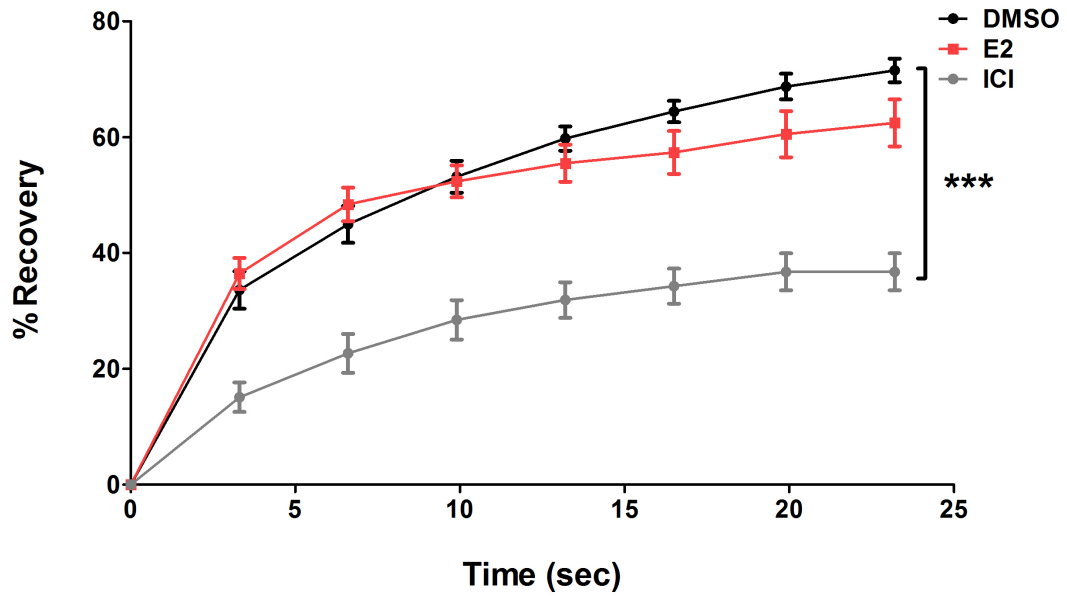

Figure 4.14 Quantitative analysis of intra-nuclear kinetics of ERβ5-infected Ishikawa cells.

Graphical depiction of impact of ligand treatment on the recovery rates of ERβ5 fluorophores over time back into the bleached zone. This recovery is denoted by the point at which the Y_{MAX} is achieved and a plateau is reached on the graph. Recovery rates of ERβ5-infected Ishikawa cells are presented in response to E2 (red) and ICI 182,780 (grey) stimulation at a concentration of 10^{-8}M. Significance of results was examined using the Student's t-test (N≥8).

4.3.3.4 ERβ5 Response to antagonist in hTERT cells

The spatiotemporal effect of ICI 182,780 incubation on nuclear mobility of ERβ5-YFP infected into hTERT cells paralleled the results acquired following the same experimental setup in Ishikawa adenocarcinoma cells (section 4.3.3.3). A clear change in the nuclear patterning distribution of ERβ5 was seen alongside very poor recovery rates post-bleaching of the ROI I and this effect was sustained at up to 72 seconds post-bleach (red box) (Fig.4.15). The interaction of ICI 182,780 with ERβ5-YFP molecules in hTERT nuclei resulted in a striking and significant impact on the Y_{MAX} of the ERβ5 subtype (Fig. 4.16).

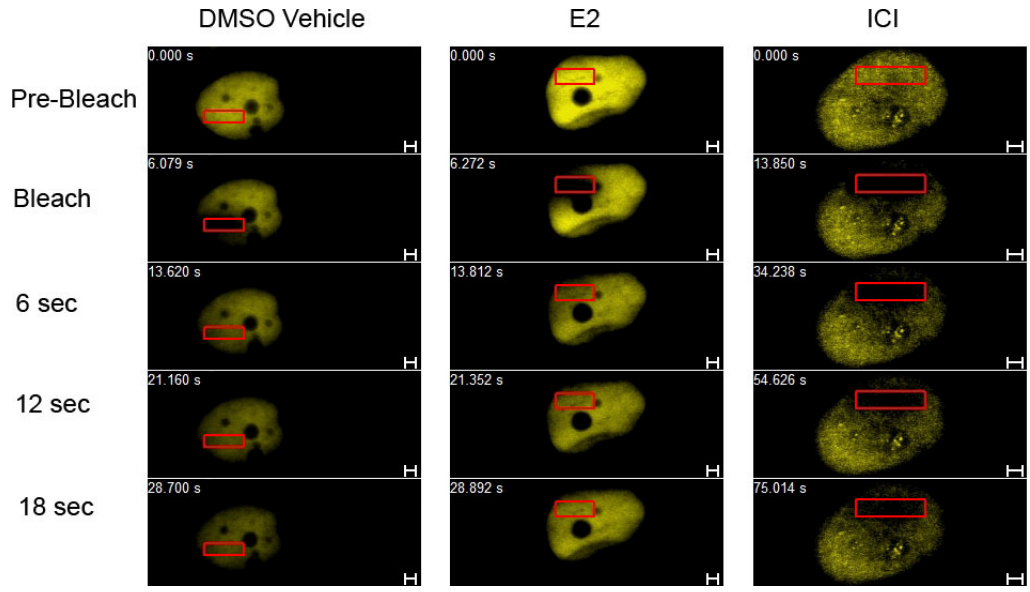

Figure 4.15 Qualitative FRAP assessment of ERβ5 infected hTERT cells.

Cells were treated with a DMSO vehicle control, E2 10-8M and ICI 182,780 10-8M. Note the ICI response was sustained at longer time periods examined i.e. 72 seconds post-bleach.

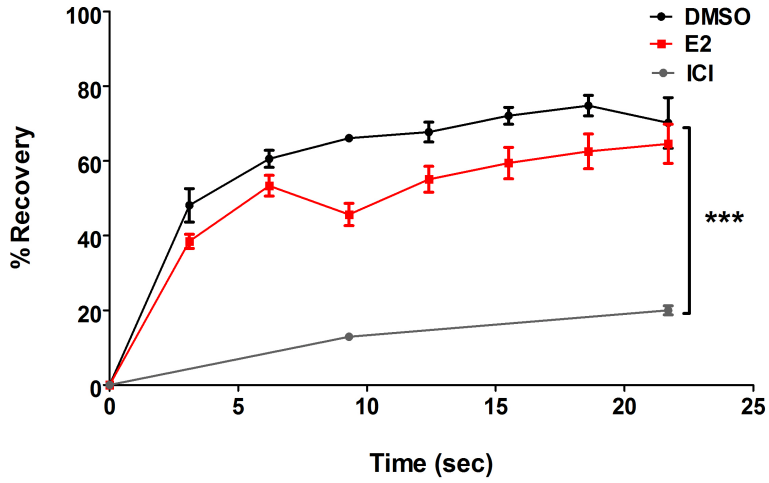

Figure 4.16 Quantitative analysis of intra-nuclear kinetics of ERβ5-infected hTERT cells.

Graphical depiction of impact of ligand treatment on the recovery rates of ERβ5 fluorophores over time back into the bleached zone. This recovery is denoted by the point at which the Y_{MAX} is achieved and a plateau is reached on the graph. Recovery rates of ERβ5-infected hTERT cells are presented in response to E2 (red) and ICI 182,780 (grey) stimulation at a concentration of 10^{-8}M. Significance of results was examined using the Student's t-test (N≥8).

4.3.4 Intranuclear dynamics of ERβ5 in combination with ERα

4.3.4.1 E2-mediated response on ERβ5-YFP and ERα in Ishikawa cells

Ishikawa cells express endogenous ERα (Fig. 4.10) but results obtained following infection of cells with ERβ5-YFP did not reveal a significant impact on receptor mobility although there was a trend towards reduced mobility with E2. Therefore ERα expression in the cells was increased by infection of untagged receptor and the impact of E2 treatment on ERβ5-YFP was re-examined. Although no obvious impact of the E2 treatment on redistribution of the receptor was discernable from the phenotypic analysis of the cell nuclei following bleaching (Fig. 4.17).

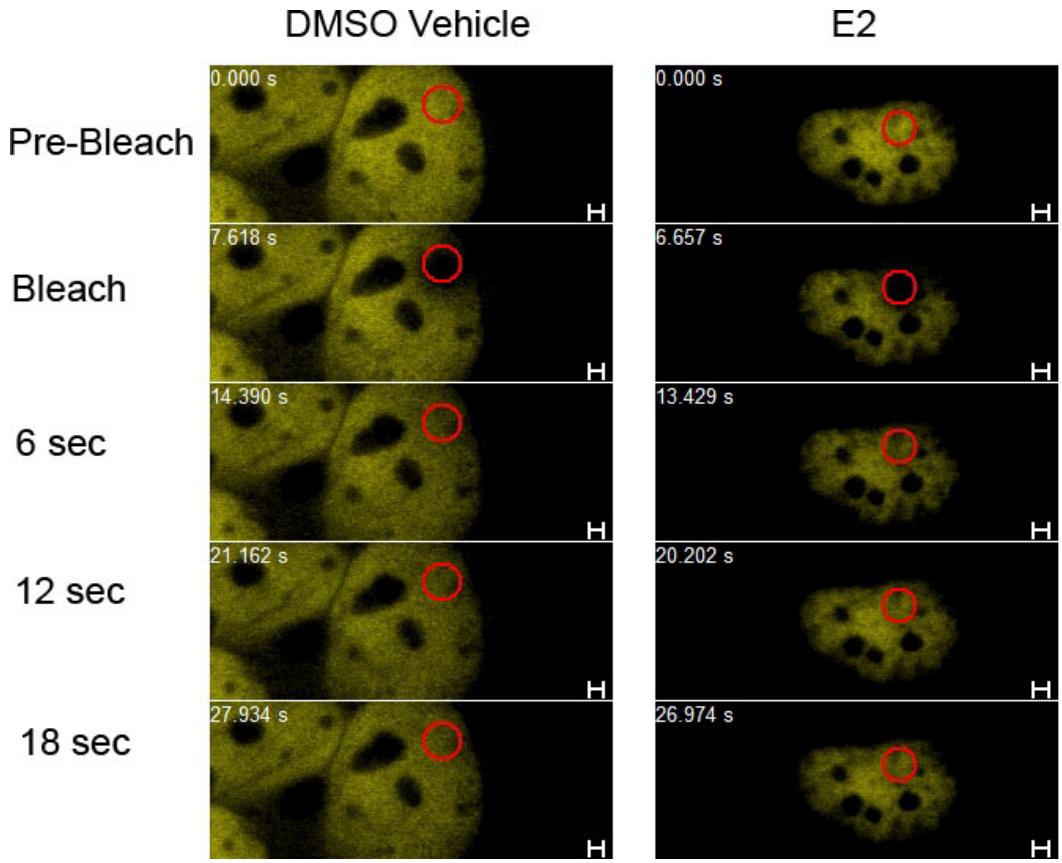

Figure 4.17 Qualitative FRAP assessment of ERβ5-YFP and ERα infected Ishikawa cells.

Cells infected with ERβ5-YFP and untagged ERα were treated with a DMSO vehicle control and E2 10^{-8}M for 60 minutes.

Statistical analysis of E2 treated Ishikawa cells co-infected with ERβ5-YFP and ERα revealed a significant impact of the treatment on the percentage recovery of the ERβ5-YFP molecule back into the bleached region upon photobleaching with reduced Y_{MAX} (Fig. 4.18).

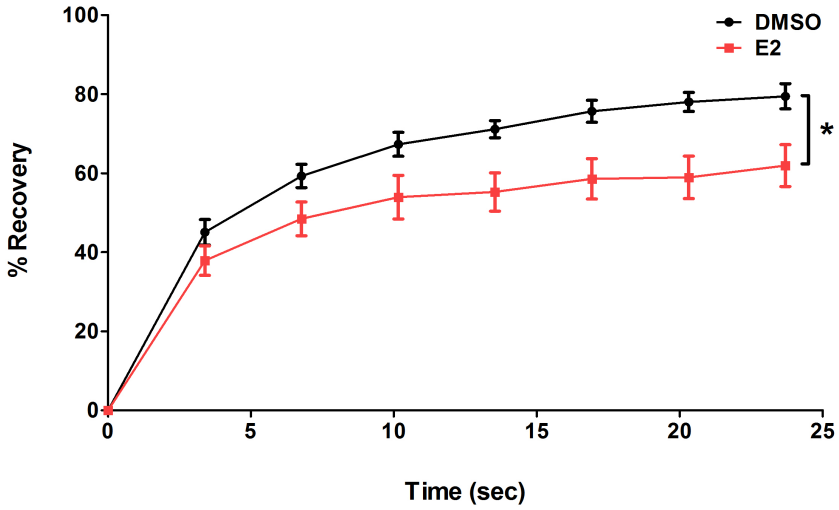

Figure 4.18 Quantitative analysis of intra-nuclear kinetics of ERβ5-YFP and untagged ERα infected Ishikawa cells.

Graphical depiction of impact of ligand treatment on the recovery rates of ERβ5 fluorophores over time back into the bleached zone. This recovery is denoted by the point at which the Y_{MAX} is achieved and a plateau is reached on the graph. Recovery rates of ERβ5-YFP are presented in response to E2 stimulation at a concentration of 10^{-8}M. Significance of results was determined using the Student's t-test (N≥8).

4.3.4.2 E2-mediated response of ERβ5-YFP and ERα in hTERT cells

An identical experiment to that described in section 4.3.4.1 was carried out in hTERT cells. As in Ishikawa cells, there was no obvious impact of E2 incubation on ERβ5-YFP on the confocal microscope (Fig. 4.19). However, statistical analysis of E2-stimulated co-infected hTERT cells revealed a significant impact on the mobility of the ERβ5-YFP with a dramatic reduction in Y_{MAX} (Fig. 4.20).

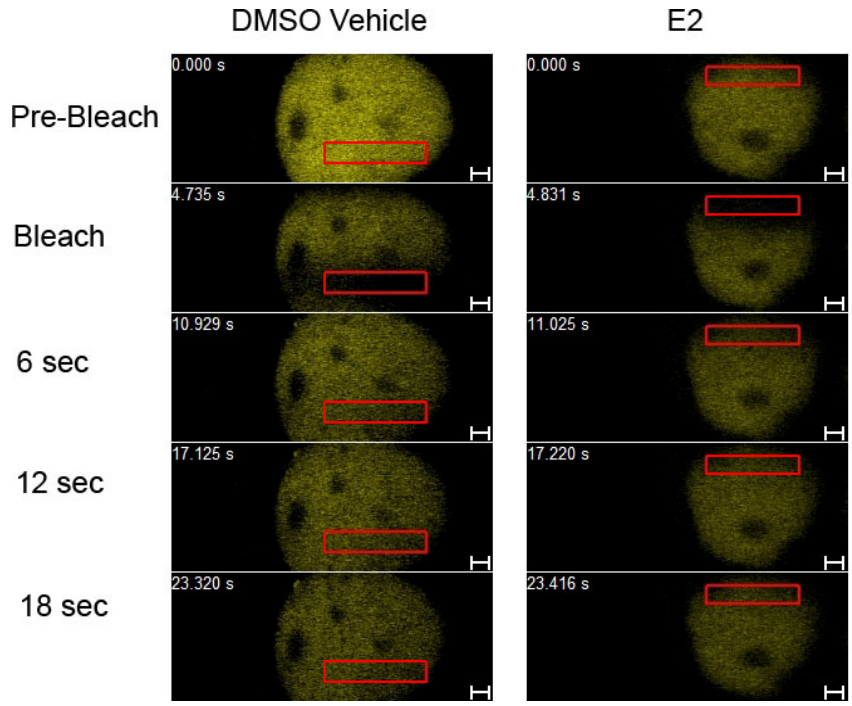

Figure 4.19 Qualitative FRAP assessment of ERβ5-YFP and ERα infected hTERT cells.

Cells were treated with a DMSO vehicle control, E2 10^{-8}M and ICI 182,780 10^{-8}M.

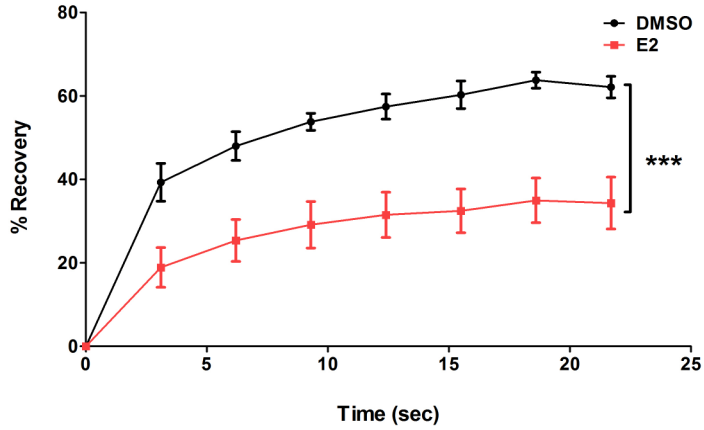

Figure 4.20 Quantitative analysis of intra-nuclear kinetics of ERβ5-YFP and untagged ERα infected hTERT cells.

Graphical depiction of impact of ligand treatment on the recovery rates of ERβ5 fluorophores over time back into the bleached zone. This recovery is denoted by the point at which the Y_{MAX} is achieved and a plateau is reached on the graph. Recovery rates of ERβ5-YFP are presented in response to E2 (red) stimulation at a concentration of 10^{-8}M. Significance of results was examined using the Student's t-test (N≥8).

4.3.5 Analysis of reporter gene activation in response to ER activity

4.3.5.1 Comparison of YFP labelled versus unlabelled ERβ5 constructs

In order to validate the use of YFP-labelled ERβ5 in the FRAP studies, experiments were set up in MDA cells that lack endogenous ER expression to compare the functional activity of YFP-tagged versus untagged ER constructs in response to the primary natural oestrogen, E2. No significant difference in luciferase reporter output between tagged and untagged constructs was detected consistent with the studies using tagged and untagged ERα and ERβ (Chapter 3) (Fig. 4.21).

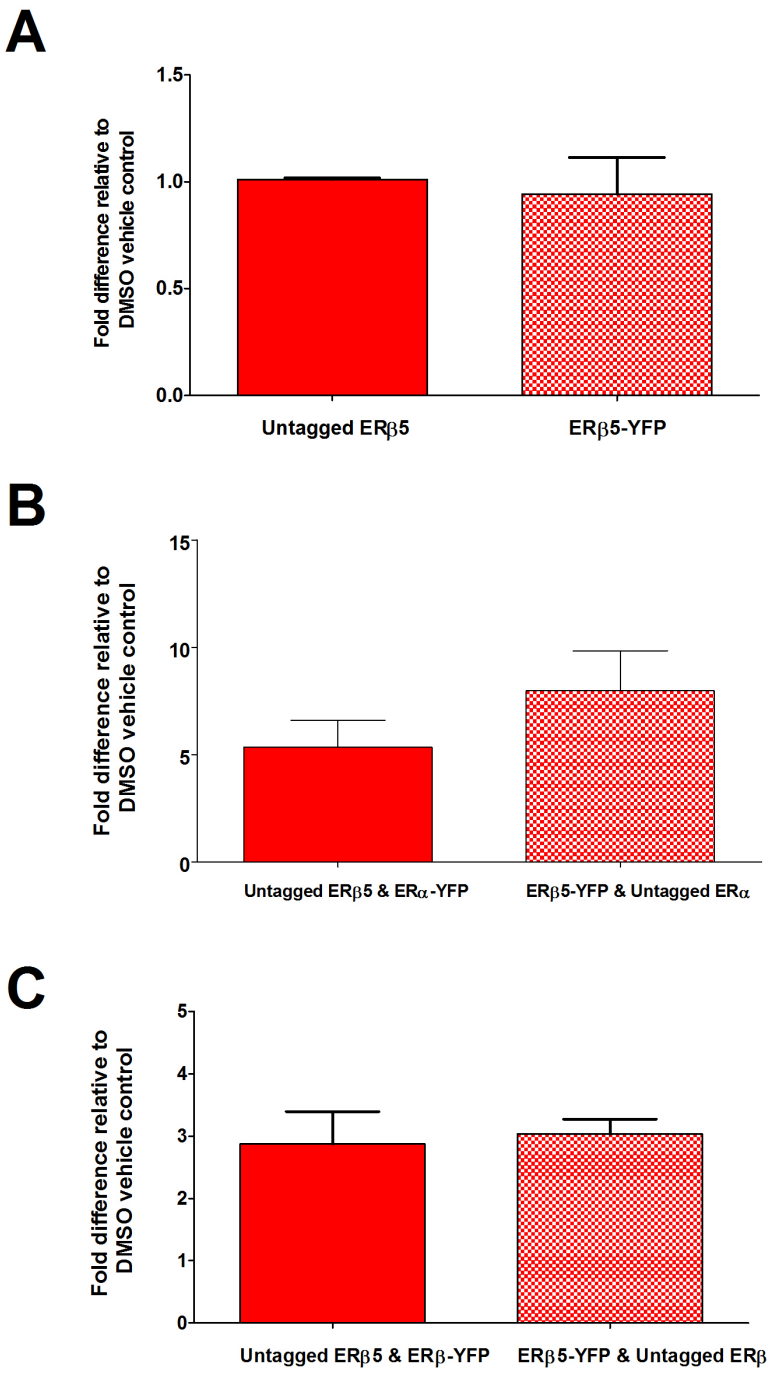

Figure 4.21 Comparison of tagged versus untagged constructs in MDA cells.

Luciferase reporter assays were conducted comparing untagged ERβ5 and ERβ5-YFP (A), untagged ERβ5 with ERα-YFP and ERβ5-YFP with untagged ERα (B) and untagged ERβ5 with ERβ-YFP and ERβ5-YFP with untagged ERβ (C) following E2 treatment. No difference was observed (N=2).

4.3.5.2 Role of agonists and antagonists on the functional capacity of ERs in Ishikawa cells

Further to the FRAP analyses, the functional activity of ERβ5 was compared with that of ERα, ERβ and ERβ2 using Ishikawa cells; the treatments tested were the same as those used for FRAP but luciferase activity was measured after 24 hours. Treatment of control, uninfected cells with E2 induced a 6X increase in luciferase activity compared with a DMSO control (Fig. 4.22A *black column*) consistent with endogenous expression of ERs in these cells (see Chapter 3). Overexpression of ERα, ERβ2 or ERβ5 did not increase luciferase activity. However, consistent with previous reports using T-47D cells (Lin *et al.*, 2007), overexpression of ERβ attenuated the E2-mediated response. Incubation of cells with ICI 182,780 blocked all transcriptional activity of the ERE reporter construct in the Ishikawa cells (Fig. 4.22B). In the same study, incubation with PPT™ induced a 3X increase in luciferase activity in comparison to DMSO treated cells in the Ishikawa cell line and overexpression of ERα in these cells suggested a trend towards a further increase in luciferase activity (albeit not significantly greater than the response observed in the uninfected Ishikawa cells) (Fig.4.22C). The DPN™-mediated effect on endogenous receptors of the Ishikawa cell line mirrored the response of the E2-treated cells with a 6X increase in luciferase activity in comparison to DMSO control cells. Overexpression of ERα, ERβ, ERβ2 and ERβ5 did not alter this response (Fig. 4.22D).

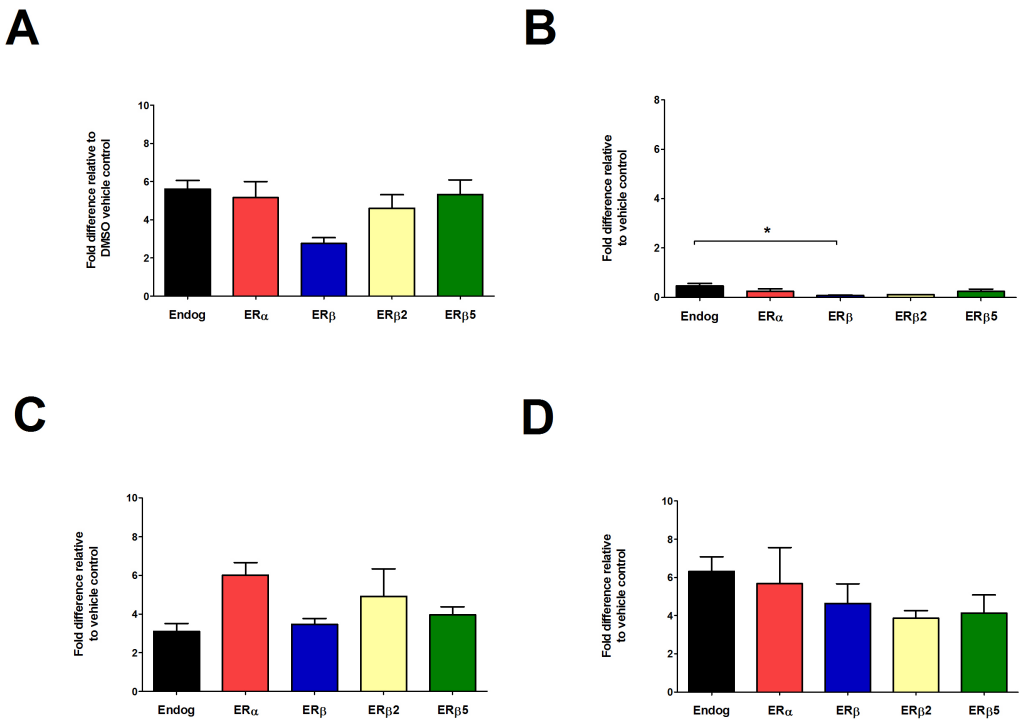

Figure 4.22 Impact of natural and synthetic agonists with ERs on luciferase reporter activity in Ishikawa cells.

Cells were infected with ERα (red), ERβ (blue), ERβ2 (yellow) or ERβ5 (green) and each with the 3x-ERE-Luc reporter. Treatment was with E2 10^{-8}M (A), ICI 182,780 (B), PPT™ 10^{-8}M (C) or DPN (D) 10^{-8}M for 24 hours prior to luciferase production reading. Fold difference is expressed relative to the vehicle-treated cell, each bar represents N=3±SEM and has been normalised to protein levels and compared to luciferase output following treatment in each case with a DMSO vehicle control.

4.3.5.3 E2-mediated transcriptional response of ERα and ERβ5 after single or co-expression of receptors

The impact of E2 treatment on ERE-mediated reporter gene activation was compared between cells infected with ERα or ERβ5 alone with those co-infected with both ERβ5 and ERα. This investigation was conducted in both Ishikawa and hTERT cells to elucidate the relevance of cell context on transcriptional activity. In Ishikawa cells overexpression of either ERα or ERβ5 resulted in an identical induction of luciferase activity to that in uninfected cells (Fig. 4.23). However, co-infection of cells with ERα and ERβ5 resulted in a significant increase in reporter gene expression

suggesting a cumulative effect of ERα and ERβ5 working together (Fig. 4.23A). However in hTERT cell line (Fig. 4.23B) co-expression had no significant impact when compared with that seen in uninfected cells although there was a trend for overexpression of ERβ5 alone to increase luciferase activity.

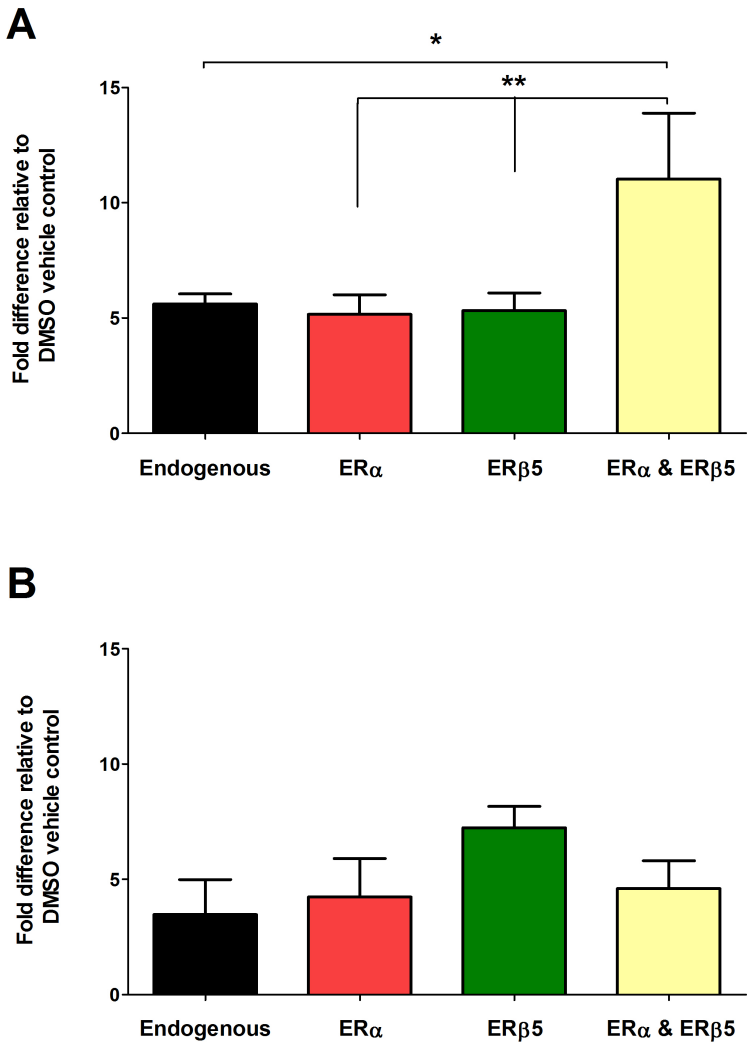

Figure 4.23 Comparison of impact of E2 on luciferase activity in Ishikawa (A) and hTERT (B) cell contexts.

Cells were infected with either ERα (red) or ERβ5 (green) or the combination of ERα and ERβ5 together in equal ratio (yellow). The cells were treated for 24 hours with E2 10^{-8}M. Fold difference is expressed relative to the vehicle-treated cell, each bar represents N=3±SEM.

4.4 Discussion

4.4.1 Protein expression of ERβ5 in the human endometrium

Differential patterns of individual ER subtype mRNAs were demonstrated using extracts from the functional layer of normal pre-menopausal endometrial tissue obtained at different phases of the menstrual cycle. Consistent with previous studies, ERα mRNA levels decline with advancement of the cycle owing to the progesterone-mediated down-regulation of the gene (Henderson *et al.*, 2003). In line with results reported by Brandenberger and colleagues, overall expression of ERβ mRNA was detected at lower levels than that of ERα (Brandenberger *et al.*, 1997). In spite of this, an inverse expression pattern of mRNAs encoding ERβ and its splice variant isoforms (ERβ2 and ERβ5) was detected with a trend toward increased expression during the secretory phase. While the mRNA expression of ERβ and ERβ2 has previously been described (Critchley *et al.*, 2002), we believe that this is the first study that has examined the expression of ERβ5 mRNA in the normal endometrium.

ERβ5 protein was immunolocalised to the nuclei of the glandular epithelial and stromal cells as well as the endothelial cell population at all phases of the cycle. Co-localisation of ERβ5 with ERα revealed that the reduced expression of the *ESR1* gene during the secretory phase of the cycle resulted in weak ERα immunostaining in sections of mid-late secretory phase endometrium while ERβ5 immunoexpression was ubiquitous and sustained at all stages. A previous study reported expression of ERβ in the endothelial cells (Critchley *et al.*, 2001) and in the current study the detection of ERβ5 in these same cells supports the hypothesis that ERβ isoforms regulate E2-dependent action(s) within the endothelial cell population of the endometrium.

Taken together, the sustained expression of ERβ and its isoforms ERβ2 and ERβ5 when ERα declines (mid-late secretory phases of the cycle) and the widespread expression of ERβ and ERβ5 in all cell types of the functional layer of the endometrium suggests ERβ-dependent regulation of gene expression in response to

E2 levels may be important in the normal pre-menopausal endometrium during the secretory phase.

In other studies, investigations of ERβ variant expression have revealed increased ERβ2 and ERβ5 mRNAs (Leygue *et al.*, 1999b) and ERβ2 protein (Omoto *et al.*, 2002) in comparison with full length ERβ in breast cancer cell lines and pre-menopausal breast tumour tissue. Park *et al.* demonstrated increased expression of ERβ5 mRNA in breast cancer of post-menopausal patient tissue (Park *et al.*, 2006) irrespective of ERα being reported as the dominant subtype at the post-menopausal stage (Jarvinen *et al.*, 2000). Further to this, numerous recent studies have reported on increased immunoexpression of ERβ5 as a feature of cancer cells in primary colorectal carcinomas (Wong *et al.*, 2005), breast cancer (Shaaban *et al.*, 2008) and endometrial carcinoma tissue (Collins *et al.*, 2009).

There are conflicting reports regarding the importance of ERβ as a therapeutic marker in breast cancer states. Fuqua *et al.* reported no correlation between ERβ expression and tumourigenesis (Fuqua *et al.*, 2003). However, an epidemiological study by the same group implied that the high expression levels of ERβ and ERβ5 mRNAs in ERα negative breast cancer tissues of African-Americans compared with the Caucasian population underlies the poor survival statistics for the African-American patients (Poola *et al.*, 2005b). Other studies have suggested that loss of ERβ protein may define a tumour phenotype with high metastatic capability (Jarvinen *et al.*, 2000). In line with this view, there is accumulating evidence that the expression of ERβ in breast cancer tissue is associated with a favourable prognosis (Omoto *et al.*, 2001) and disease free survival attributable to an inverse affiliation with the coactivator SRC-1 (Myers *et al.*, 2004). A role for ERβ as a tumour suppressor agent has also been described (Treeck *et al.*, 2009).

4.4.2 ERβ5 intranuclear mobility is not influenced by oestrogenic ligand but is responsive to anti-oestrogenic treatment

A previous study has questioned the ability of the truncated splice variant of ERβ to form homodimers (Leung *et al.*, 2006) originally claimed in the study by Moore *et al.* (Moore *et al.*, 1998). However Leung *et al.* ascribed a functional role for the splice variants ERβ2, ERβ4 and ERβ5 in heterodimeric partnership with their cognate full length ERβ (Leung *et al.*, 2006).

In the present study FRAP analysis has revealed that ERβ5 is a highly mobile protein within the nucleus and shown that incubation with E2, PPT™ or DPN™ did not alter the rapid recovery times of ERβ5 upon photobleaching. These results are the first to examine ERβ5 intranuclear dynamics and are consistent with studies claiming that this truncated splice variant does not contain all the sequences that are required for a fully functional ligand binding pocket like that found in the full length wild type ERβ receptor. Interestingly, the anti-oestrogen ICI 182,780 had a significant impact on subnuclear mobility of ERβ5 in both the Ishikawa and hTERT cells. Furthermore incubation with ICI 182, 780 resulted in a distinct change in the nuclear distribution of ERβ5-YFP. These changes were ICI-dependent and there were no differences in cells that were exposed to E2 before or after ICI 182,780 treatment (data not presented).

Stenoien *et al.*, suggested ICI-mediated immobilisation of ERα was Helix 12-dependent (Stenoien *et al.*, 2001b). However, the ERβ5 splice variant lacks Helix 12 so this would suggest a different mechanism. Unlike the receptor immobilisation that resulted from ICI 182,780 treatment of ERα and ERβ tagged constructs in the same cell contexts (Chapter 3, section 3.3.2.2), ICI 182,780 reduced the mobility of ERβ5 in both the Ishikawa and hTERT cells. Furthermore, a significant increase in the half-time (i.e. time taken to reach 50% of the final maximal recovery value Y_{MAX}) from 7.27 seconds in control cells to 29.17 seconds in the hTERT cells was noted.

A recent study in MCF-7 and HeLa cells reported differences in the ERβ response to ICI 182,780 compared to ERα. For example, ERβ unlike ERα, retained mobility (albeit reduced) following exposure to ICI 182,780 and mutation studies also argue against a role for Helix 12 (Damdimopoulos *et al.*, 2008). It has previously been suggested that the ICI-mediated degradation of ERα arises from disruption to dimerisation and nucleocytoplasmic shuttling caused by steric hindrance of the bulky side-chain of the compound itself (Dauvois *et al.*, 1993b) and interruption of ERα cycling at the promoter site that results in direct targeting of the ERα to the ubiquitin proteasome pathway (UPP) (Reid *et al.*, 2003). Hence, a plausible explanation for the discrepancy in the intranuclear response of ERβ5 compared with ERα and ERβ (Chapter 3, section 3.3.2.2) in response to ICI 182,780 is that the impact of the anti-oestrogen on ERβ5 is independent of proteasomal regulation.

4.4.3 Oestrogen exposure alters the intranuclear dynamics of endometrial cells co-infected with ERβ5-YFP and ERα *in vitro*

Early studies using COS-1 cells demonstrated ligand-independent heterodimeric formations between ERα and ERβ based on the relative expression patterns of the two subtypes (Cowley *et al.*, 1997, Pace *et al.*, 1997). In these studies, mutation assays revealed that the DNA binding domain of ERα was sufficient to enable heterodimers to occur (Pace *et al.*, 1997) and that the amino acids involved in homodimerisation of ERα were not identical to those required for heterodimerisation with ERβ (Cowley *et al.*, 1997).

In the current study, the co-expression of ERβ5-YFP with ERα resulted in a change in the intranuclear dynamics of ERβ5-YFP in response to E2. While the decrease in the mobility of ERβ5 in co-infected Ishikawa and hTERT cells was significant, a trend towards a decrease in mobility was observed from the results of E2 exposure on cells infected with ERβ5-YFP alone. While the capacity of ERβ splice variants to form homodimers has been questioned (Leung *et al.*, 2006), gel shift mobility assays have suggested that ERβ isoforms are capable of forming partnerships with ERα (Moore *et al.*, 1998) and between the ERβ isoforms themselves (Leung *et al.*, 2006).

The results of the current study suggest that overexpression of ERα may result in stabilisation of ERα-ERβ5 heterodimers in response to E2-binding of ERα. This implies that the change in ERβ5-YFP intranuclear dynamics is occurring only in a milieu of high expression levels of ERα, suggesting a distinct expression profile context (mixed dimer) in which E2 can elicit an effect on ERβ5 by virtue of its binding to ERα.

4.4.4 Oestrogen exposure effects the transcriptional capacity of endometrial cells co-infected with ERβ5 and ERα *in vitro*

Many studies using HeLa and HEK293 cells have suggested a dominant negative role for ERβ in heterodimeric complexes with ERα in response to E2 (Ogawa *et al.*, 1998a, Pettersson *et al.*, 2000, Hall *et al.*, 2001, Li *et al.*, 2004). In these studies, the interaction of the transactivation domains AF-1 and AF-2 within ERα has been suggested as the target for the repressive activity of ERβ repression (Pettersson *et al.*, 2000). Moreover, deletion studies have revealed that the AF-1 of ERβ is itself required to impart this inhibitory function (Gougelet *et al.*, 2007). In the current study, E2 treatment reduced transcriptional activity in cells overexpressing ERβ while there was no discernable change in ERE-luciferase reporter gene activity in the Ishikawa cells infected with either ERα, ERβ2 or ERβ5 alone in response to treatment with E2, ICI 182,780, PPT™ and DPN™. This is presumably due to the masking of responses stemming from the high levels of endogenous receptor activity.

Interestingly ERE-reporter activation in response to E2 treatment was higher in Ishikawa cells co-infected with ERα and ERβ5 than that in cells infected with ERα alone. A previous study reported that only one partner within a receptor heterodimer is required to be bound by E2 in order to induce transcriptional activity (Tremblay G.B. *et al.*, 1999). As there was no receptor gene activation in MDA cells lacking endogenous receptor when they were infected with ERβ5 and treated with E2, one can conclude ERβ5 binding of E2 is not responsible for the enhanced transcriptional activity. Rather, the cumulative result observed in the Ishikawa cell line implies a

response to an ERβ5-ERα heterodimer where ERβ5 is imparting a positive influence on transcriptional activity after ERα binding to E2.

4.5 Conclusion

Investigation of the expression pattern of ERβ5 in the human endometrium revealed ubiquitous expression of this splice variant in the stromal and epithelial compartments of the tissue at significant levels throughout the course of the menstrual cycle. Despite the inability of ERβ5 to actively bind agonist, there remains a putative role for this splice variant in a) responding to pure antagonist (ICI 182,780), b) functioning in a heterodimeric partnership, and c) imparting an effect on the functional capacity of the dimeric partner (e.g. ERα). In this study, the influence of cell treatments (agonist and antagonist) on the intranuclear dynamics of the ERβ5 splice variant was examined. Although natural and synthetic agonists had no impact on ERβ5 mobility, a role for anti-oestrogenic regulation by ICI 182,780 was revealed. Stimulation with ICI 182,780 resulted in a significant decrease in the mobility of ERβ5-YFP molecules and this effect was not rescued by post-treatment with E2 at physiological concentration. This suggests a universal dominant inhibitory effect of ICI 182,780 on ER subtypes that is irrespective of a truncated C-terminal domain and impaired canonical ligand-binding capacity.

Co-infection of ERβ5 with ERα had an impact on the E2-mediated transactivational activity in two endometrial cell lines (of adenocarcinoma and healthy patient origin) and ERE luciferase gene activity was upregulated when both ER isoforms were present in the Ishikawa cell line. While this effect was cell-dependent and not replicated in the hTERT cell line, the Ishikawa study revealed a cumulative effect when ERα and ERβ5 were infected together in comparison to the effect of either subtype infected independently. These results may have implications for the response of cancer tissues to oestrogenic ligands as previous data have implied overexpression of ERβ5 by cells in malignant tissue.

This chapter has explored the intranuclear dynamic response of ERβ5 in accordance with the canonical ligand-dependent mode of activation using a panel of ligands composed of natural and synthetic agonists. In the following chapter, the implication of an alternative ligand-independent mode of activation using GFs on ER dynamics and transcriptional activity is investigated. GFs have been implicated in the multifaceted maze of ER activation and as such pose as potential targets for controlling ER-dependent regulation of proliferation in human tissue. In particular, the influence of GFs on truncated ER variants lacking innate ligand-binding capacity is examined in the proceeding chapter.

Chapter 5

Alternative modes of activation

5 Alternative modes of activation

5.1 Introduction

EGF, the derivative of the transmembrane precursor (prepro-EGF) transduces its effects through binding to its cognate receptor EGFR. Studies using a variation of the conventional FRAP technique; total internal reflection/FRAP have previously revealed a strong affinity of EGF for the EGFR in A431 cells *in vitro* (Hellen, 1991). The EGFR is a member of a receptor tyrosine kinase family of receptors that encompasses the HER proteins (HER1-4) (reviewed in Citri and Yarden, 2006). These proteins are reported to be differentially expressed in the endometrium over the course of the menstrual cycle (Srinivasan *et al.*, 1999, Chobotova et al, 2005, Ejskjaer *et al.*, 2005).

A previous study demonstrated that treatment of ovariectomised mice with EGF had an impact on uterine function that mimicked the response to oestrogen treatment (Nelson *et al.*, 1991). The results of this study prompted the investigation into ligand-independent mechanisms of activation of ERs as well as the potential for cross-talk between E2 and EGF signalling pathways (reviewed in Smith, 1998, Levin, 2003).

There is now an accumulating body of evidence establishing EGF-mediated tyrosine signalling as the key pathway inducing phosphorylation of residues on both ERα (Kato *et al.*, 1995b, Joel *et al.*, 1998b, Shah and Rowan, 2005, Chen *et al.*, 1999, Cui *et al.*, 2004, Rogatsky *et al.*, 1999, Thomas *et al.*, 2008, Weis *et al.*, 1996) and ERβ (Tremblay A. *et al.*, 1999, Tremblay and Giguere, 2001, Sanchez *et al.*, 2007) that can transactivate the receptors independently of steroid ligands (Chapter 1, section 1.4.2). In addition to direct phosphorylation of ERs in response to GF signalling, GFs have also been shown to induce expression of oestrogen-regulated target genes including PR (Stoica *et al.*, 2000), pS2 (Martin *et al.*, 2000b), and COX2 (Su *et al.*, 2009).

The complex interplay of ligand-dependent and ligand-independent impacts on ER activity is also of importance from a clinical perspective. For example, bidirectional

cross-talk between MAPK and E2 signalling pathways augments ER activity in MCF-7 breast cancer cells and has been shown to result in accelerated tumour growth but without impacting on the sensitivity of anti-oestrogen treatment in severe combined immune-deficient (SCID) mice (Atanaskova *et al.*, 2002). Conflicting studies have suggested that HER2-dependent signalling impacts on ERα activation as a result of MAP kinase activity and confers resistance to 4HT, disruption of corepressor activity (Kurokawa *et al.*, 2000) or p38 signalling (Gutierrez *et al.*, 2005). Supporting studies have highlighted the MAPK-dependent phosphorylation of coregulators (e.g. amplified in breast cancer-1 (AIB1)/steroid receptor coactivator-3 (SRC-3)) as a complementary process to ER-dependent protein phosphorylation/gene activation. Increased AIB1 coactivator expression in breast cancer cells has been positively correlated with overexpression of HER2 (Osborne *et al.*, 2003) and HER3 (Kirkegaard *et al.*, 2007) and shown to be associated with 4HT resistance.

The discrepancies in the results of the studies relating to 4HT resistance may stem from differences in the complex network of signalling cascades that target specific sites on the ER protein for phosphorylation. Disruption of GF-mediated tyrosine kinase signalling via ERα has been explored using various GF inhibitors in preclinical tumour mouse models (Knowlden *et al.*, 2003, Nicholson *et al.*, 2004) but without a sustained effect on actual tumour growth (Massarweh *et al.*, 2006, Arpino *et al.*, 2007). Notably, the anti-HER2 monoclonal antibody trastuzumab (Herceptin®) is widely employed in the clinical setting for treatment of HER2 positive breast cancers (Vogel *et al.*, 2001) but has been linked with disease relapse (reviewed in Nahta and Esteva, 2006). Alternative compounds are being developed that target the multiple signalling pathways that converge at ERα and ERβ (Xia *et al.*, 2002, Rusnak *et al.*, 2001). For example Lapatimib serves as a dual inhibitor of both HER1 and HER2 transmembrane tyrosine kinase receptors (Spector *et al.*, 2005). The available evidence therefore suggests that GF-dependent and E2-dependent activation of gene expression are not mutually exclusive but their cumulative effects result in a more potent ER response in target tissues (reviewed in Arpino *et al.*, 2008). Combined

treatment modalities targeting both systems independently may be the future of clinical therapy to combat ER activity in cancers.

Irrespective of the mode of activation of ERα or ERβ, there is a growing body of evidence implicating the UPP as a primary regulator of ER subtype steady-state levels. Both ERα and ERβ are believed to undergo continual transient cycling on the DNA at specific promoter regions in both the unbound and ligand-bound state at approximate frequencies of 20 and 45 minutes respectively (Reid *et al.*, 2003). The UPP acts on receptors at these responsive promoter sites to degrade DNA-bound receptor and ensure continuation of this cycle.

Ubiquitylation is a well defined ordered process that involves three sequential enzymatic processes. In an energy-dependent reaction the 76 amino acid (8.6kDa) ubiquitin protein is activated by the ubiquitin-activator (Uba) enzyme 1 (E1). This results in the formation of a thioester bond between a specific cysteine residue of the E1 Uba and the carboxyl terminus of the ubiquitin protein itself. In this active state, ubiquitin is subsequently transferred to the cysteine residue of an ubiquitin-conjugating (Ubc) enzyme (E2). The ligase enzymes (E3) serve as adaptor proteins in the final stage of the process and localise the ubiquitin to the □-amino group of the target substrate (e.g. ER subtype) (Jentsch, 1992, Ciechanover, 1994).

Subsequent rounds of ubiquitylation ligate adjoining ubiquitin moieties at their lysine residues and signal the target protein for degradation by the 26S proteasome. Itself a multiplex protein, the 26S proteasome comprises a 19S regulatory cap in which the substrate becomes unfolded and directed into the 20S catalytic core barrel for degradation (Lipford and Deshaies, 2003). Studies using the proteasomal inhibitors MG132 and lactocystin have shown that disruption of the UPP results in abrogation of transcription and have implied that ubiquitinated ER is also necessary to mediate maximal transcriptional activation while the polyubiquitinated state is required to signal degradation of the receptors (Lonard *et al.*, 2000). FRAP studies have demonstrated that the same proteasomal inhibitors render ERs dysfunctional and they

remain localised to inactive sites of the nuclear matrix (Stenoien *et al.*, 2001b). Specific domains of ERα are targeted by ubiquitin and these regions have been shown to coincide with coactivator binding sites while coregulators (e.g. SRC-1, TIFII, RAC3, CBP) are also subject to proteasomal-mediated degradation (Reid *et al.*, 2002). A number of the ubiquitin enzymes have themselves been shown to interact with nuclear receptors including SUG1/TRIP1 (Masuyama and Hiramatsu, 2004), E2 Ubc9 (Poukka *et al.*, 1999) and the E3s; Rsp5/RPF-1 (Imhof and McDonnell, 1996), E6 associated protein (E6-AP) (Nawaz *et al.*, 1999). Taken together, these studies imply a central role for the UPP in ER turnover and maintenance of steady-state levels.

5.1.1 Aims of the chapter

Chapters 3 and 4 of this thesis have investigated ligand-dependent mediated effects on the intranuclear dynamics and functional capacity of ERα, ERβ and its cognate splice variants, ERβ2 and ERβ5. Conversely, the experiments described in this chapter sought to examine alternative modes of activation of the ER that were independent of oestrogenic ligands. In particular, this study investigated the functional activity of the ERβ splice variant, ERβ5, as a complement to studies on its expression in normal endometrium (Chapter 4). The impact of EGF on intranuclear mobility and transcriptional activity on ERs was investigated using FRAP and luciferase reporter assays and the impact of the UPP on ER kinetics and functional capacity was also explored.

5.2 Materials and Methods

5.2.1 Taqman® qRT-PCR

RNA was extracted from lysed cells using a Qiashredder™ spin column for cell homogenisation (section 2.5.1) and quantified using the Nanodrop® ND 1000 (Labtech International, East Crawley, UK). Complementary DNA was prepared using random hexamers (section 2.5.4.1) and was used for the Taqman reaction protocol outlined in section 2.5.4.3. Taqman analysis of EGFR was conducted in triplicate using probes from the Roche Universal Probe Library™ and run on the ABI Prism 7900. Data output from the detection system was quantified in accordance with the $2^{-\Delta\Delta Ct}$ algorithm (section 2.5.4.4). Results are expressed as means and standard errors and statistical analysis was conducted using a Student's t-test.

5.2.2 Collection of endometrial tissue

As detailed in Chapter 2, section 2.2.1, human endometrial tissue was obtained from different phases of the menstrual cycle following hysterectomy, hysteroscopy or laparoscopic sterilisation performed at the Royal Infirmary, Edinburgh, UK. The histological staging analysis was performed by an expert histologist as previously reported (Critchley *et al.*, 2001, Critchley *et al.*, 2002). All patients gave written informed consent prior to tissue recovery.

5.2.3 Immunohistochemistry

Immunohistochemistry was performed on paraffin embedded endometrial tissue to identify the location of the proteins of interest as outlined in section 2.4.1

5.2.3.1 Non Fluorescent Immunohistochemistry (DAB)

In brief, tissue was processed and sections mounted on glass slides as described in section 2.4.1.1. The sections were then dewaxed, rehydrated (2.4.1.2) and subjected to antigen retrieval by means of pressure cooking in citrate buffer (2.4.2). Three blocking steps were employed to prevent endogenous peroxidase activity, non-specific binding of the secondary antibody and the formation of avidin-peroxidase complexes binding directly to the tissue where endogenous biotin is expressed as outlined in 2.4.3.1, 2.4.3.2 and 2.4.3.3 respectively. The sheep anti-EGFR primary antibody was incubated with the tissue overnight at 4°C (Table 2.1). A rabbit anti-sheep biotinylated secondary antibody (Table 2.2) used and the signal was localised

using the chromogenic substance 3, 3'-diaminobenzidine (DAB, K3468; DAKO, Cambridge, UK) diluted in its substrate. The corresponding negative control sections were incubated with blocking serum alone to enable confirmation of antibody specificity. The primary and secondary antibodies used are listed in Table 5.1.

Table 5.1 Summary of primary and secondary antibodies used for DAB immunodetection

Target	Raised in	Dilution	Retrieval	Source
EGFR/ErbB1 (HER1)	Sheep	1:100	Citrate	Upstate[1]
ErbB2 (HER2)	Mouse	1:75	Citrate	Abcam[2]
ErbB3 (HER3)	Mouse	1:75	Citrate	Abcam[2]
ErbB4 (HER4)	Mouse	1:40	Citrate	Abcam[2]

[1]Upstate Biotechnology Inc., New York, USA

[2]Abcam plc, Cambridge, UK

5.2.4 Western Immunoblotting

Western analysis was performed using nuclear protein extracts (section 2.6.1) from Ishikawa and hTERT cells. The infected cells were lysed with 1X RIPA buffer (Chapter 2; section 2.6.2) and separated into cytoplasmic and nuclear fractions and quantified in accordance with the Biorad DC Protein Assay (section 2.6.3). Proteins were separated on polyacrylamide gels (section 2.7.2), electro-transferred to PVDF membrane (section 2.7.3), incubated with primary antibodies (section 2.7.4; Table 5.2) and scanned for detection using the LI-COR™ infrared detection system (section 2.7.5). These membranes were immunoprobed using an anti-EGFR for verification of endogenous EGFR protein expression and with anti-MAPK and anti-ERα and the phosphorylated states of each of these proteins respectively.

Table 5.2 Primary antibodies used for Western blotting

Antigen	Host Species	Dilution	Source
EGFR/ErbB1 (HER1)	Rabbit	1:200	Santa Cruz[1]
β-tubulin	Mouse	1:600	Sigma[2]
ERα	Mouse	1:200	Vector[3]
Phosphor-Ser118 ERα	Rabbit	1:1000	Cell Signaling[4]
p42/44 MAPK	Rabbit	1:1000	Cell Signaling[4]
Phospho p42/44 MAPK	Mouse	1:2000	Cell Signaling[4]

[1]Santa Cruz Biotechnology, CA, USA

[2]Sigma-Aldrich, St. Louis, MO, USA

[3]Vector Laboratories Ltd., Peterborough, UK

[4]Cell Signaling Technology®, MA, USA.

5.2.5 Cell treatments

To establish the impact of EGF on ER phosphorylation status, receptor mobility and activity, serum-starved cells were incubated with EGF at a final concentration of 10^{-7}M. Some cells were incubated with the MAP kinase inhibitor PD98059 at a final concentration of 10^{-8}M. Control treatments using a distilled H_2O alone (vehicle control) were conducted and used to compare the effects of agonist and antagonist incubation. Treatments were included 1 hour prior to live-cell FRAP analyses and 24 hours in advance of cell harvesting for luciferase assays.

5.2.6 FRAP

FRAP was conducted on a LSM 510 confocal inverted light scanning microscope (section 2.8.6). In brief, live cells were maintained in PBS buffered with 10mM HEPES in an enclosed chamber heated to 37°C (section 2.8.2). Cells expressing YFP-labelled ER subtypes were selected for bleaching on the basis of uniform distribution of levels of fluorescence. Three ROIs were of equal dimension were

chosen (section 2.8.5). Two pre-bleach images were captured at 3 second intervals followed by photobleaching owing to a series of focused pulsed iterations using the Argon 12 laser (488 and 514nm) laser at maximal power. Eight subsequent images were taken to establish recovery patterns using an attenuated laser (514nm set between 1-5% power) (section 2.8.6). Data collation and quantitation was conducted and subject to correction, normalisation and statistical evaluation as outlined (section 2.8.7).

5.2.7 Luciferase Gene Reporter Assay

Luciferase reporter assays were carried out as described (section 2.9.1). Luciferase output was expressed as relative light units using the FLUOstar OPTIMA luminometer (BMG Labtech) were normalised against total protein content from samples of the same experiment and conditions using the Biorad DC Protein Assay (section 2.6.3).

5.3 Results

5.3.1 The EGFR family of proteins are expressed in the human endometrium

To investigate the correlation of growth factor-mediated signalling on ER function, the expression of the complete repertoire of HER family of proteins (HER1–HER4) was investigated in the endometrium. Using tissue sections recovered from the proliferative phase of the menstrual cycle, the expression patterns of HER1, HER2, HER3 and HER4 were investigated using specific antibodies. HER1 expression was extensive and localised to the stromal and epithelial compartments of the tissue (Fig.5.1A). HER2 protein localised to the cytoplasm of the glandular epithelial lining and there was very weak detection of HER4 in this same region (Fig 5.1B and D). The detection of HER3 was strongest in the glandular epithelial cells but was also present in the stromal compartment of the tissue (Fig. 5.1C).

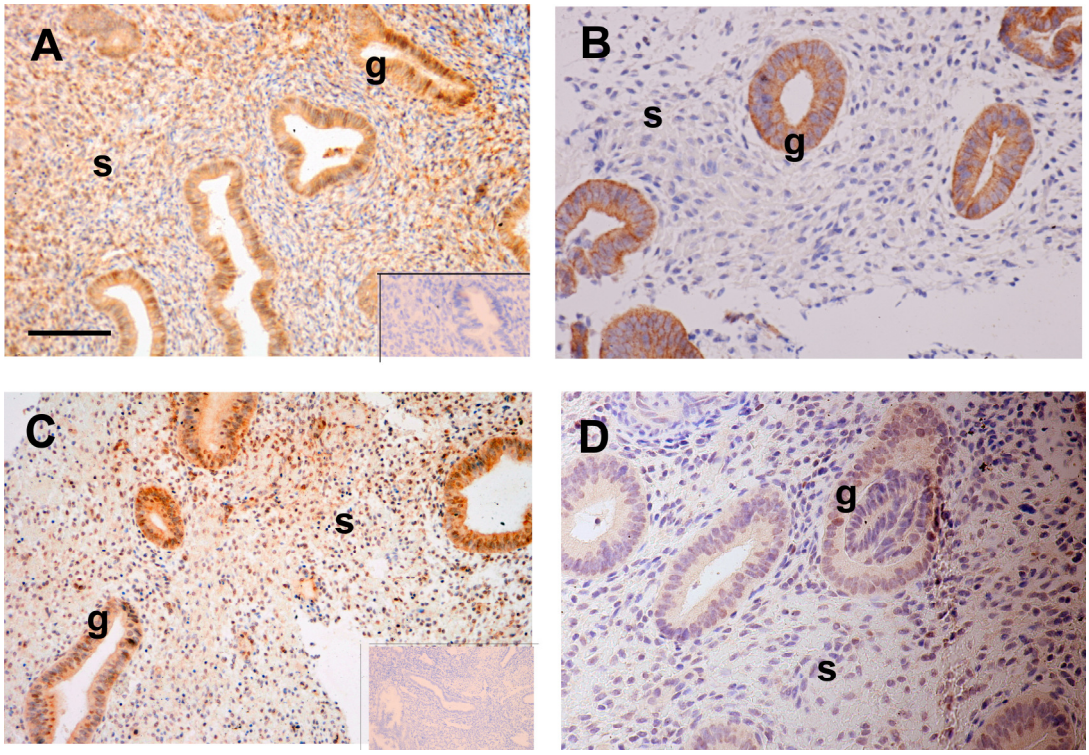

Figure 5.1 EGF receptor (EGFR) family immunoexpression in the human endometrium.

Immunodetection in the functional layer of the human endometrium from the proliferative phase. EGFR/ErbB1 (A), ErbB2 (B), ErbB3 (C) and ErbB4 (D). EGFR was detected in the glandular epithelial (g) and stromal (s) cells, ErbB2, ErbB3 and ErbB4 staining was localised to the epithelial cells. Insets are negative controls. Magnification X20 (A, C) and X40 (B, D); scale bar, 100μm.

5.3.2 RNA and protein expression of EGFR in cell lines

Quantitative real-time mRNA analysis revealed expression of the primary receptor of the HER family, HER1 in the MDA, Ishikawa and hTERT cell lines (Fig. 5.2). This data was important as it provided the platform to conduct further investigations on the impact of EGF on ER status and function. Total protein was also extracted from the MDA and Ishikawa cell lines and used to probe for expression of EGFR. Endogenous EGFR protein was detected at the correct molecular weight of ~170kDa in each of the three cell lines (Fig. 5.3).

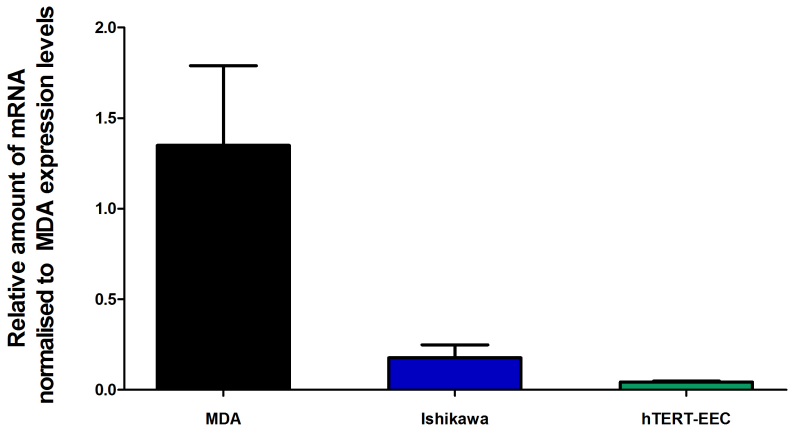

Figure 5.2 Comparison of mRNA expression of endogenous EGFR in Ishikawa and hTERT cell lines relative to the MDA cell line.

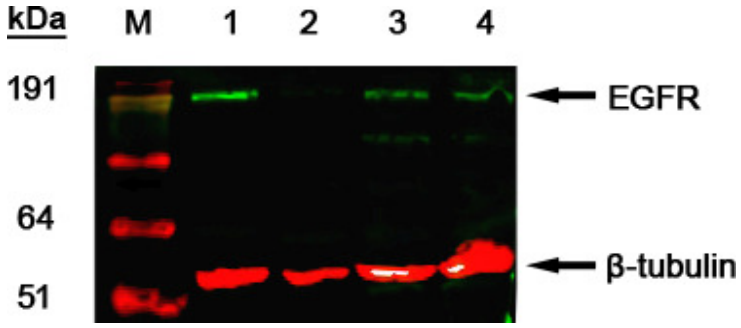

Figure 5.3 Determination of EGFR protein levels in the cell lines.

This is a representative Western blot following total protein extraction and probing for EGFR endogenous protein expression in the MDA cells (Lane 1) and Ishikawa cell protein extracts (Lane 3 and 4). Membrane was probed for EGFR (green) and β-tubulin loading control (red).

5.3.3 EGF functions through activation of the MAPK pathway in endometrial cells

The phosphorylation status of the members of the MAPK signalling cascade has been shown to be modified in response to EGF activation through the cognate transmembrane receptor EGFR (Miyamoto *et al.*, 1996). To establish whether this was also the case in endometrial cells, Ishikawa cells maintained in a serum-free environment were incubated with EGF treatment for 10, 20 and 30 minutes.

Thereafter the cells were lysed and total protein was extracted and used on Western blots that were probed with antibodies directed against phosphorylated and unphosphorylated forms of the p42/p44 (extracellular signal-regulated kinases) ERK 2 and ERK 1 proteins. Incubation with EGF induced phosphorylation of the MAPK proteins at each of the time-points and quantification of the band sizes revealed this was blocked when cells were pre-incubated with the MEK inhibitor PD98059 (Alessi *et al.*, 1995) for 1 hour (Fig. 5.4, *upper panel*; Fig. 5.5).

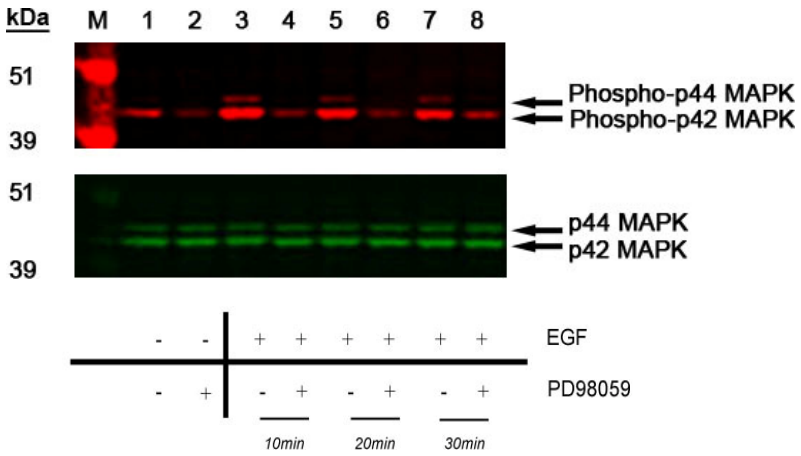

Figure 5.4 Western analysis of MAPK and phospho-MAPK proteins in Ishikawa cells.

Protein was extracted from Ishikawa cells following incubation with EGF and/or a MAPK inhibitor. Lane 1, dH_2O; Lane 2, ERK1/2 inhibitor PD98059 treatment for 1 hour; Lane 3, EGF 10^{-7}M incubation for 10 minutes; Lane 4, PD98059 1 hour treatment followed EGF 10^{-7}M for 10 minutes; Lane 5, EGF 10^{-7}M incubation for 20 minutes; Lane 6, PD98059 1 hour treatment followed EGF 10^{-7}M for 20 minutes; Lane 7, EGF 10^{-7}M incubation for 30 minutes; Lane 8, PD98059 1 hour treatment followed EGF 10^{-7}M for 30 minutes. Membrane was incubated with an anti-p42/p44 MAPK (green) and anti-phopho-p42/p44 MAPK (red).

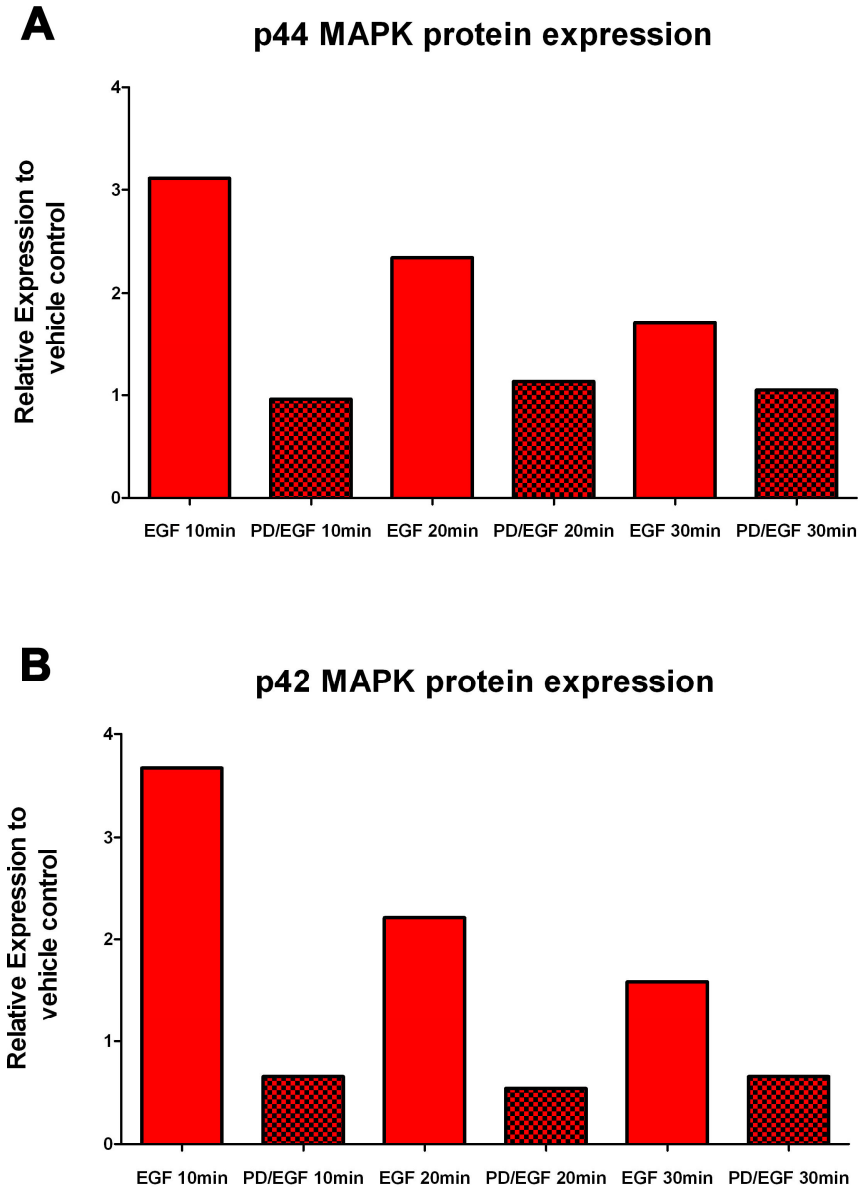

Figure 5.5 Quantification of Western blots p44 (ERK1) (A) and p42 (ERK2) (B) after EGF stimulation for 10, 20 and 30 minute intervals (N=1).

5.3.4 ERα is phosphorylated at the Ser118 residue in response to EGF-mediated signalling.

To determine if Ser118 was phosphorylated by EGF-mediated MAPK signalling *in vitro*, Ishikawa cells overexpressing ERα-YFP were maintained in serum-free media and then treated with EGF for 10, 20 or 30 minutes with or without the addition of the MEK inhibitor PD98059 for 1 hour. Total protein extracts were run on a Western

blot and probed with an antibody against total ERα (green bands) and an antibody directed against the phosphor-Ser118 residue of ERα (red bands) (Fig. 5.6). ERα-YFP with a phosphorylated residue at Ser118 was detected in all nuclear extracts prepared from cells incubated with EGF treatment. Surprisingly the ERK1/2 inhibitor did not reduce the total amount of Ser118 ERα (Fig. 5.7).

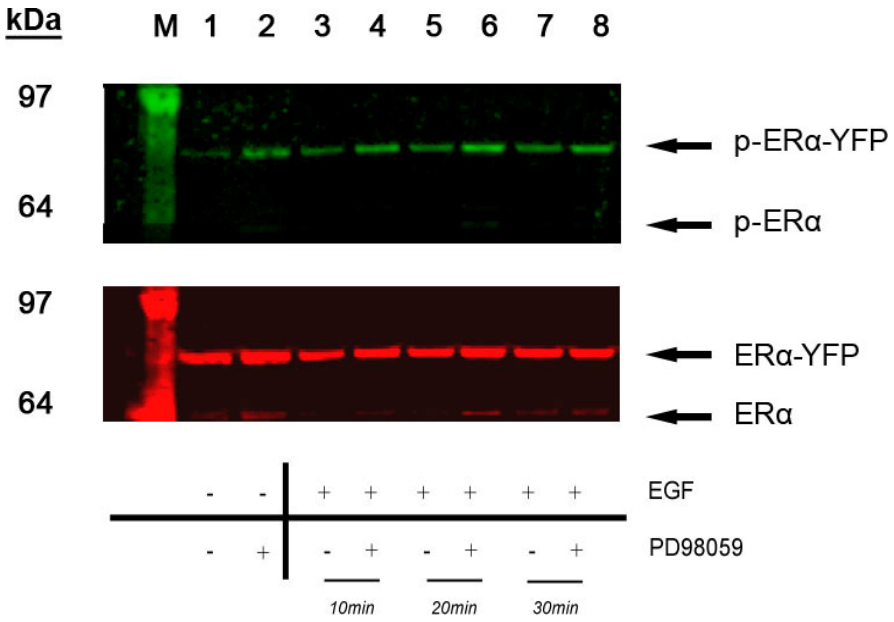

Figure 5.6 Western analysis of ERα and phosphorylated ERα at the Serine residue 118 protein in Ishikawa cells.

Protein was extracted from Ishikawa cells following EGF treatment: Lane 1, H_2O; Lane 2, ERK1/2 inhibitor PD98059 for 1 hour; Lane 3, EGF 10^{-7}M for 10 minutes; Lane 4, PD98059 for 1 hour followed EGF 10^{-7}M for 10 minutes; Lane 5, EGF 10^{-7}M incubation for 20 minutes; Lane 6, PD98059 for 1 hour followed EGF 10^{-7}M for 20 minutes; Lane 7, EGF 10^{-7}M incubation for 30 minutes; Lane 8, PD98059 for 1 hour followed EGF 10^{-7}M for 30 minutes. Membrane was probed with an anti-ERα (red) and anti-phopho-Ser118 ERα (green).

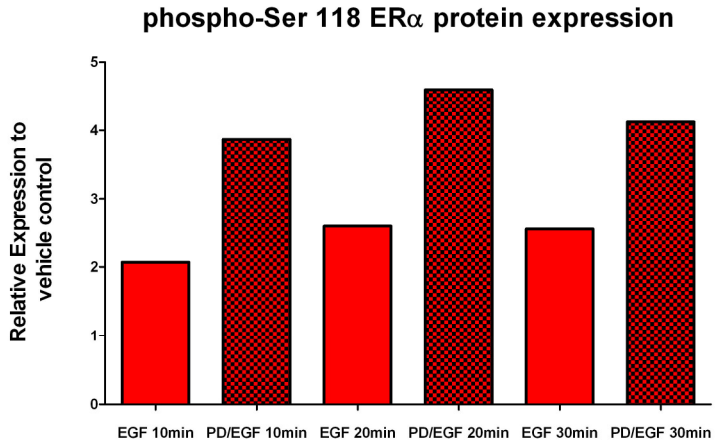

Figure 5.7 Quantification of Western blot for the Ser118 phosphorylation of ERα-YFP in Ishikawa cells (N=1).

5.3.5 Intranuclear dynamics of ERs in response to incubation with EGF

To investigate whether growth factor induced receptor phosphorylation could have an impact on intranuclear mobility of ERs in endometrial cells, Ishikawa cells were infected with fluorescently-labelled ER constructs, maintained in serum-free media, incubated with EGF over a range of time-points and assessed using FRAP analysis (Fig. 5.8). There was a significant effect on the recovery response of ERα-YFP molecules in response to EGF exposure for 10 minutes with a reduction in Y_{MAX}. However, this effect was not sustained following longer incubation periods with the growth factor (Fig. 5.9).

Incubation with EGF also had a detectable impact on the mobility of ERβ-YFP molecules in Ishikawa cells (Fig. 5.10). Significant effects were determined on the recovery response rates in response to EGF stimulation at 10, 20 and 30 minute time intervals with a reduction in Y_{MAX}. No change in recovery capacity was detectable after 60 minutes of EGF treatment (Fig. 5.11). The impact of EGF-dependent signalling on the ERβ5 splice variant that lacks the ability to bind oestrogens was also investigated using Ishikawa cells infected with ERβ5-YFP. Notably, EGF treatment over a range of time-points from 10 to 90 minutes had a significant impact

on overall percentage recovery suggestive of a ligand-independent impact on ERβ5-YFP mobility (Fig. 5.12).

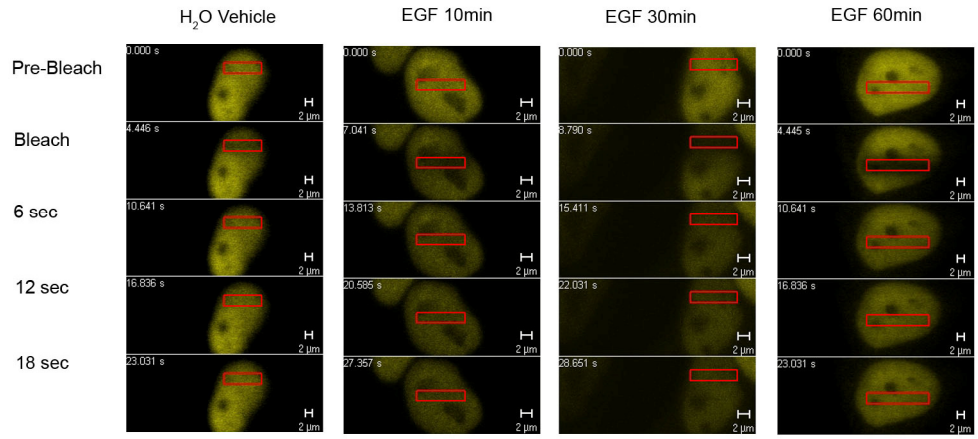

Figure 5.8 Qualitative FRAP assessment of ERα-YFP infected Ishikawa cells.

Cells were treated with a dH2O vehicle control and EGF 10-7M over a range of time-points (10, 20, 30, 60 and 90 minutes).

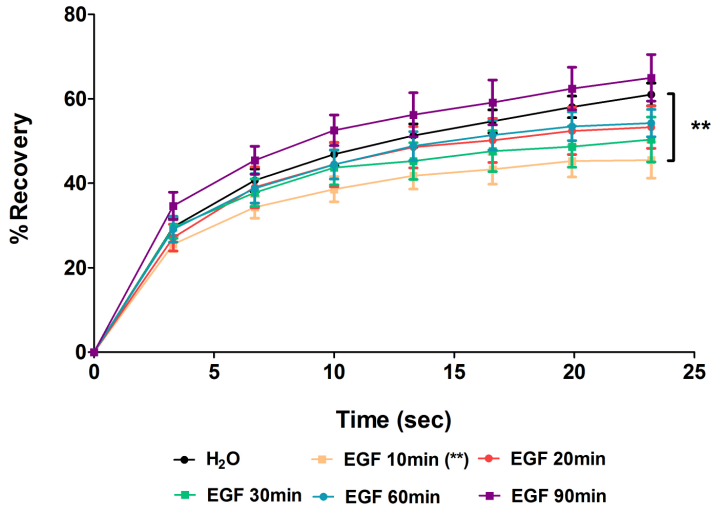

Figure 5.9 Quantitative analysis of intra-nuclear kinetics of ERα-YFP infected Ishikawa cells.

*Graphical depiction of impact of EGF treatment on the recovery rates of ERα-YFP over time into the bleached zone. This recovery is indicated by the point at which the Y_{MAX} is achieved. Recovery rates of ERα-infected cells are presented in response to EGF stimulation over a range of different time intervals (10, 20, 30, 60 and 90 minutes) at a concentration of 10^{-7}M. ** (P<0.01) denotes significance in variation of ligand treatments compared with the dH_2O vehicle control as derived from the Student's t-test (N≥8).*

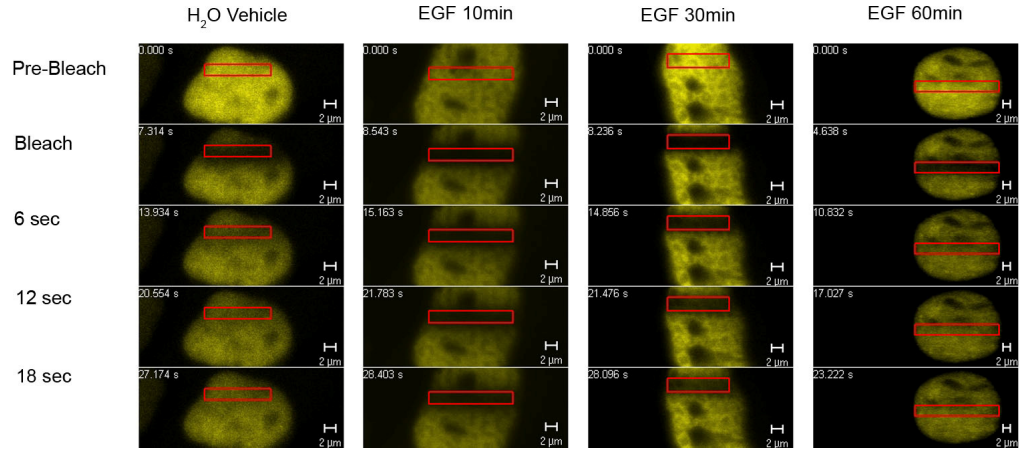

Figure 5.10 Qualitative FRAP assessment of ERβ-YFP infected Ishikawa cells.

Cells were treated with a dH2O vehicle control and EGF 10-7M over a range of time-points (10, 20, 30 and 60 minutes).

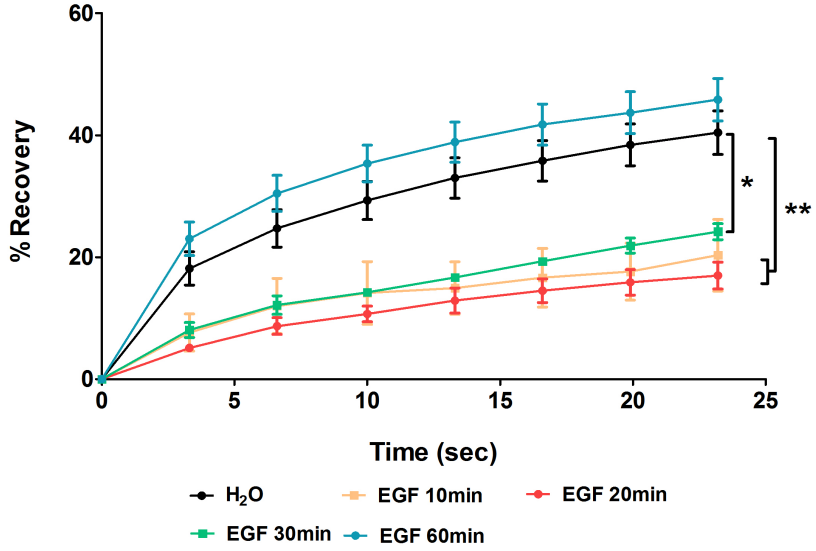

Figure 5.11 Quantitative analysis of intra-nuclear kinetics of ERβ-YFP infected Ishikawa cells.

*Impact of EGF treatment on the recovery rates of ERβ-YFP over time back into the bleached zone are denoted by the point at which the Y_{MAX} is achieved and a plateau is reached on the graph. Recovery rates of ERβ-infected Ishikawa cells are presented in response to EGF over a range of different time intervals (10, 20, 30 and 60 minutes) at a concentration of 10^{-7}M. Additional statistical parameters are presented in B. ** (P<0.01) and *(P<0.05) denotes significance in variation of ligand treatments compared with the dH_2O vehicle control as derived from the Student's t-test (N≥8).*

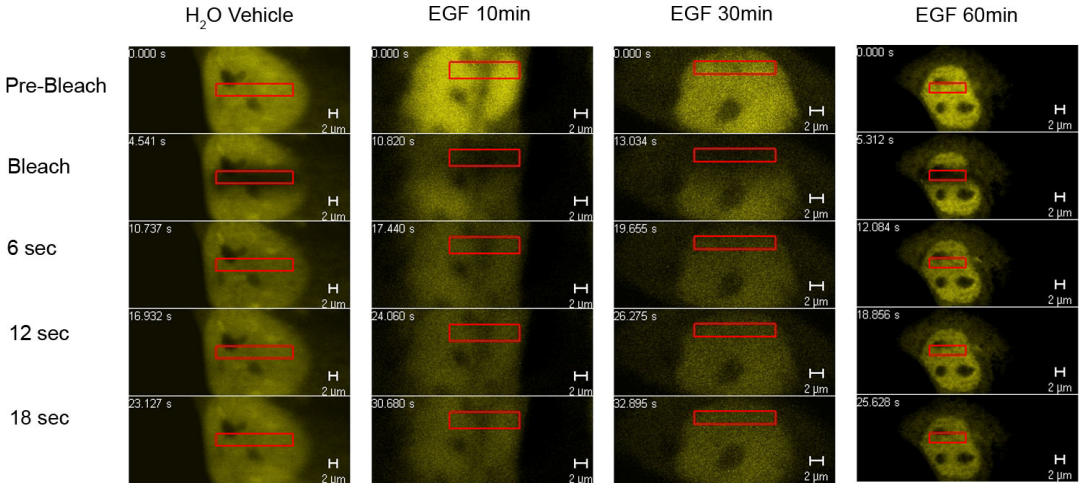

Figure 5.12 Qualitative FRAP assessment of ERβ5-YFP infected Ishikawa cells.

Cells were treated with a dH_2O vehicle control and EGF $10^{-7}M$ over a range of time-points (10, 20, 30, 60 and 90 minute intervals).

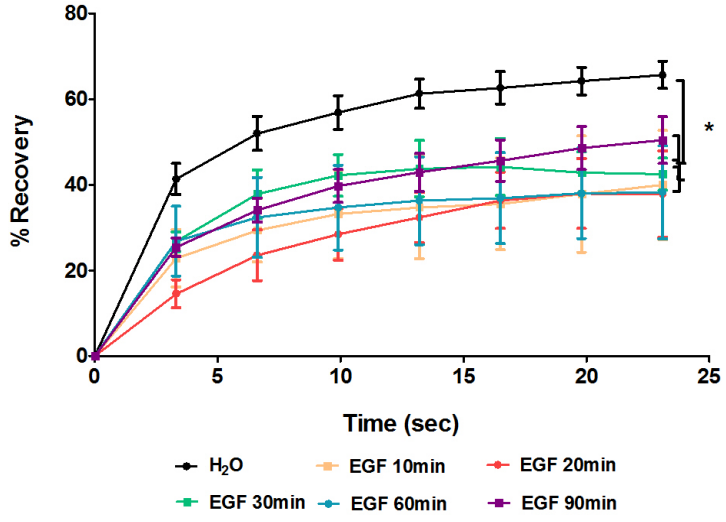

Figure 5.13 Quantitative analysis of intra-nuclear kinetics of ERβ5-YFP infected Ishikawa cells.

*Graphical depiction of impact of EGF on the recovery rates of ERβ5 fluorophores over time back into the bleached zone. This recovery is denoted by the point at which the Y_{MAX} is achieved and a plateau is reached on the graph. Recovery rates of ERβ5-YFP are presented over a range of different time intervals (10, 20, 30, 60 and 90 minutes) in response to EGF at a concentration of $10^{-7}M$. * ($P<0.05$) denotes significance in variation of ligand treatments compared with the dH_2O vehicle control as derived from the Student's t-test ($N\geq8$).*

The studies using ERβ5-YFP revealed that the impact of EGF on percentage recovery (Y_{MAX}) was sustained throughout the treatment period (10-90 minutes) (Fig. 5.13), a result that was in marked contrast to that observed with ERα-YFP (Fig. 5.9) or full length ERβ-YFP (Fig. 5.11). As an extension of the ERβ5-YFP study, the impact of EGF-mediated signalling on the behaviour of putative ER heterodimers was examined using Ishikawa cells co-infected with ERβ5-YFP and ERα treated with EGF for 90 minutes.

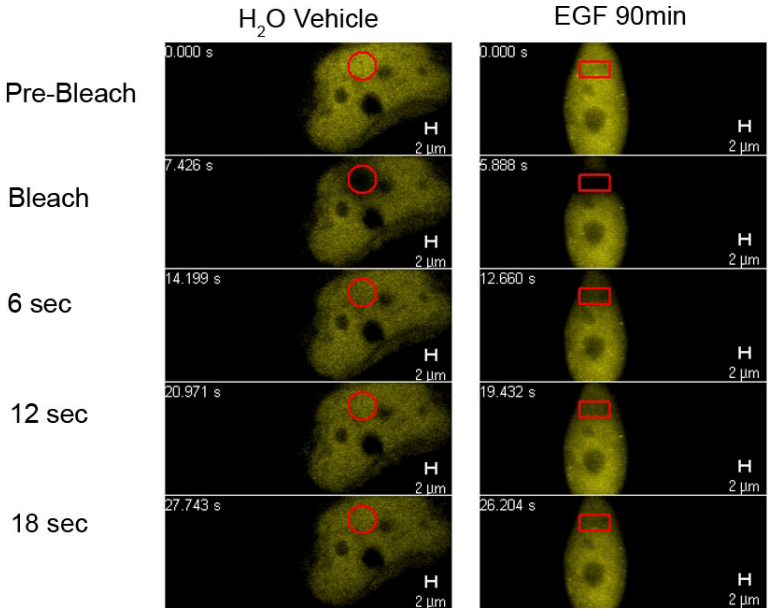

Figure 5.14 Qualitative FRAP assessment of ERβ5-YFP and ERα infected Ishikawa cells.

Cells infected with ERβ5-YFP and untagged ERα were treated with a dH_2O vehicle control and EGF $10^{-7}M$ for 90 minutes.

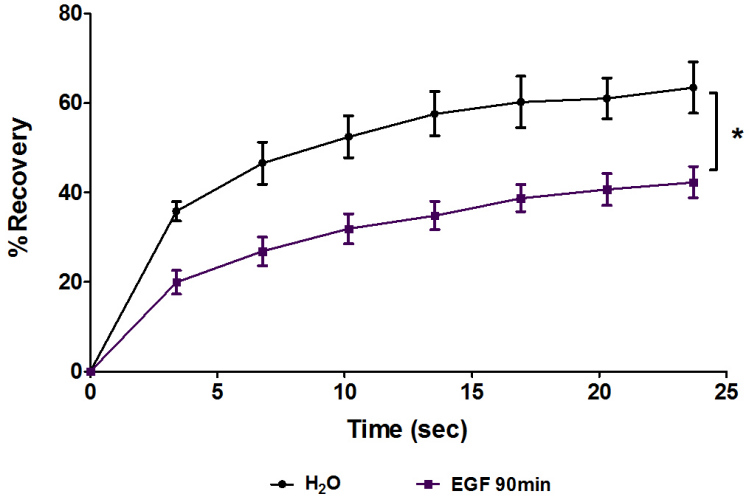

Figure 5.15 Quantitative analysis of intra-nuclear kinetics of ERβ5-YFP and untagged ERα in Ishikawa cells.

*Graphical depiction of impact of EGF treatment on the recovery rates of ERβ5 fluorophores over time back into the bleached zone. This recovery is denoted by the point at which the Y_{MAX} is achieved and a plateau is reached on the graph. Recovery rates of ERβ5-YFP are presented in response to EGF stimulation for 90 minutes at a concentration of 10^{-7}M. *(P<0.05) denotes significance in variation of ligand treatments compared with the vehicle control as derived from the Student's t-test (N≥8).*

5.3.6 EGF induces ligand-independent transactivation of ERs at the ERE.

Having established that incubation of cells with EGF and putative activation of MAPK-dependent phosphorylation had a significant impact on the intranuclear dynamics of ERs, the effect of EGF treatment on ER transcriptional activity was examined. The effect of EGF incubation on uninfected, control Ishikawa cells and those infected with constructs expressing ERα, ERβ and ERβ5 was assessed following infection of all cells with the 3X-ERE-tk-luc adenoviral vector. Twenty-four hours after infection with the adenoviral constructs and incubation in serum-free media, the cells were treated with either EGF 10^{-7}M alone for a further 24 hours. All cells were then lysed and assayed for luciferase activity. Incubation with EGF stimulated reporter gene activity in control Ishikawa cells and this activity was not

significantly changed by overexpression of ERα, ERβ or ERβ5 (Fig.5.16) although there was a trend for activity to increase with ERα. Surprisingly the ERK1/2 inhibitor PD98059 did not abrogate the effect of EGF in this cell context and this may suggest the involvement of alternative ERK-independent signalling pathways in mediating the effect of EGF on ERE-dependent transcriptional activity (data not presented).

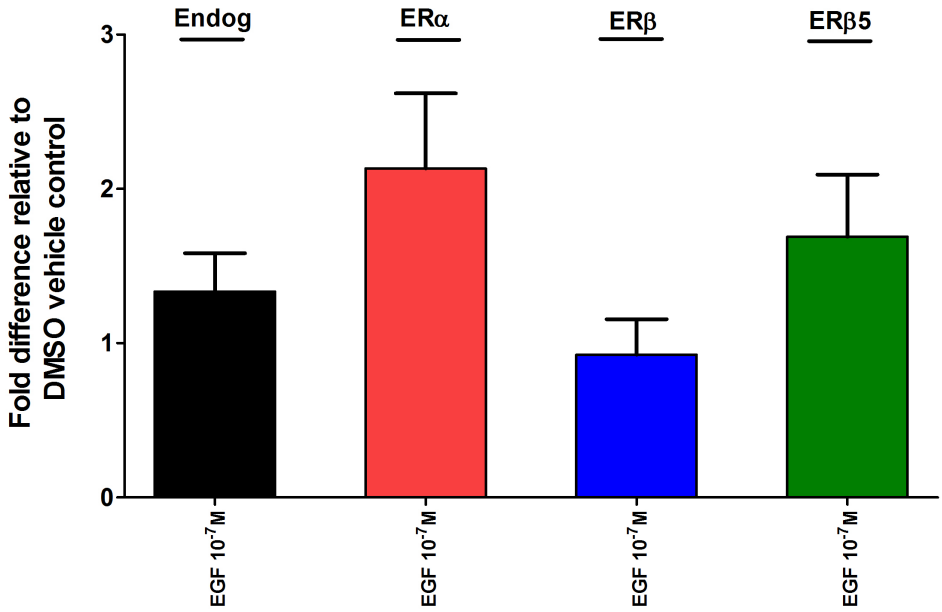

Figure 5.16 Impact of growth factor (EGF) with ERs on luciferase reporter activity in Ishikawa cells.

Cells were infected with ERα (red), ERβ (blue), ERβ2 (yellow) or ERβ5 (green) and each with the 3X-ERE-Luc reporter. Treatment was with EGF 10^{-7}M for 24hours before luciferase production reading. Fold difference is expressed relative to the vehicle-treated cell, each bar represents N=3±SEM and has been normalised to protein levels and compared to luciferase output following treatment in each case with a H_2O vehicle control.

The impact of EGF stimulation on ER transcriptional activity was also examined in control, uninfected hTERT cells as well as cells that had been infected with ERα, ERβ and ERβ5. All cells were infected with the 3X-ERE-tk-luc construct, incubated in a serum-free environment for 24 hours and then exposed to either EGF 10^{-7}M alone for a further 24 hours. The cells were lysed and assayed for luciferase activity. Reporter activity in the control cells was greater that that observed in the Ishikawa

cell line and overexpression of individual ER subtypes had no significant impact on the endogenous response although there was a trend for overexpression of ERβ to reduced reporter gene activity (Fig. 5.17).

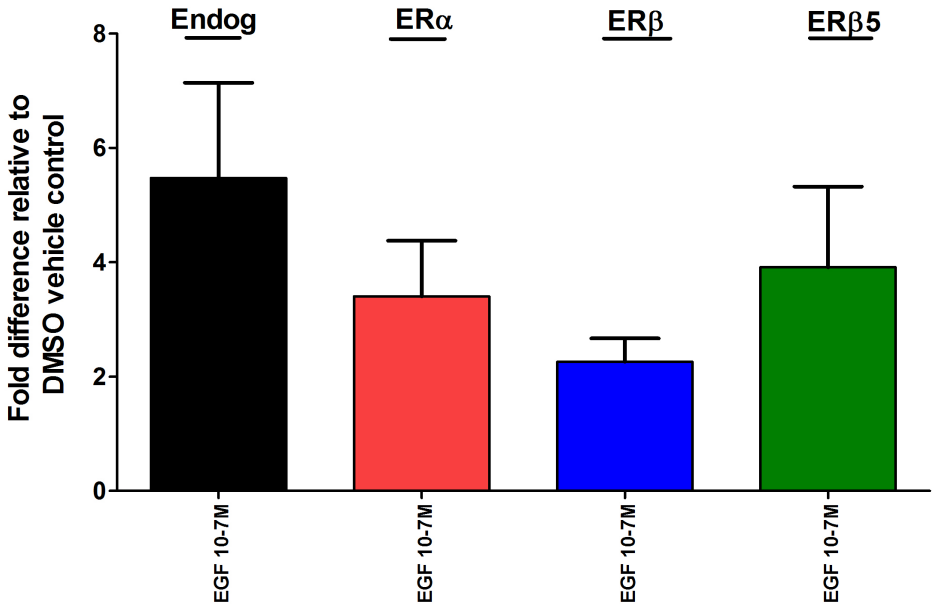

Figure 5.17 Impact of growth factor (EGF) with ERs on luciferase reporter activity in hTERT cells.

Cells were controls (black) or infected with ERα (red), ERβ (blue), ERβ2 (yellow) or ERβ5 (green) and each with the 3X-ERE-Luc reporter. Treatment was with EGF 10^{-7}M for 24hours before luciferase production reading. Fold difference is expressed relative to the vehicle-treated cell, each bar represents N=3±SEM and has been normalised to protein levels and compared to luciferase output following treatment in each case with a dH_2O vehicle control.

5.3.7 Impact of proteasome-dependent degradation on ER intranuclear dynamics

Studies examining intranuclear mobility and receptor turnover have identified an important role for the ubiquitin proteasome pathway in ER transcriptional activity (Stenoien *et al.*, 2001b). These studies have almost exclusively focused on the impact of receptor degradation on ERα (Reid *et al.*, 2003) although a recent study has demonstrated that the proteasome also plays a key role in activity of ERβ (Picard *et al.*, 2008). To date no studies have considered the impact of receptor turnover in the activity of human ERβ variants. A preliminary study was therefore undertaken to investigate the impact of a proteasome inhibitor on E2-induced intranuclear dynamics of YFP-labelled ERs infected in hTERT cells.

Incubation of cells with the 26S proteasome inhibitor MG132 prior to addition of E2 altered the mobility patterns of ERα-YFP (Fig. 5.18) and ERβ-YFP (Fig. 5.20) proteins in hTERT cells. In line with previous results (Chapter 3) both receptors were highly mobile in cells treated with DMSO but incubation with the proteasome inhibitor for 2 hours followed by a further 1 hour with E2 resulted in a significant and sustained decrease in the mobility kinetics of both receptors; ERα-YFP (Fig. 5.19) and ERβ-YFP (Fig. 5.21) that closely mirrored that seen with E2 alone.

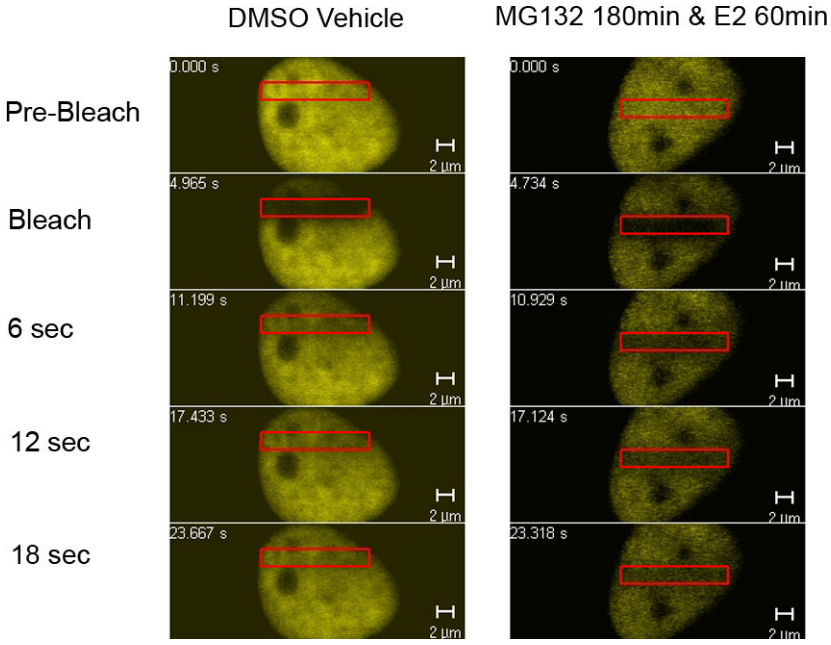

Figure 5.18 Qualitative FRAP assessment of ERα-YFP infected hTERT cells.

Cells were treated with either a DMSO vehicle control (left hand panel) or a combination of MG132 10^{-6}M for 180 minutes with E2 10^{-8}M for 60 minutes (right hand panel).

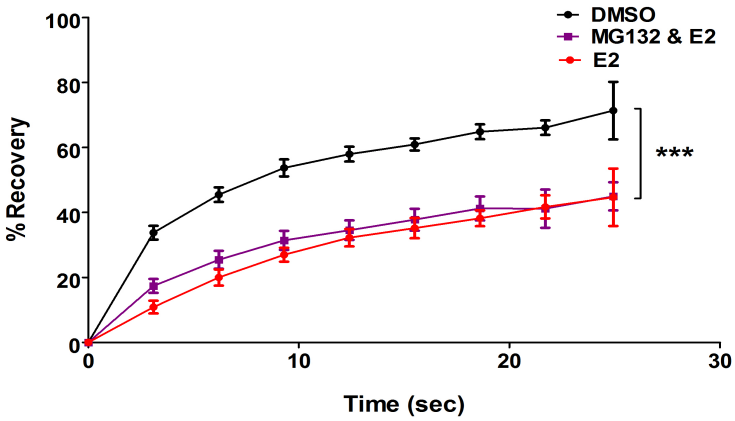

Figure 5.19 Quantitative analysis of intra-nuclear kinetics of ERα-YFP infected hTERT cells.

*Graphical depiction of the recovery rates of ERα-YFP over time into the bleached zone. This recovery is denoted by the point at which the Y_{MAX} is achieved. Recovery rates of ERα-infected cells are presented in response to MG132 10^{-6}M for 180 minutes and E2 for 60 minutes at 10^{-8}M. *** ($P<0.001$) denotes significance in variation of ligand treatments compared with the DMSO vehicle control using the Student's t-test ($N\geq8$).*

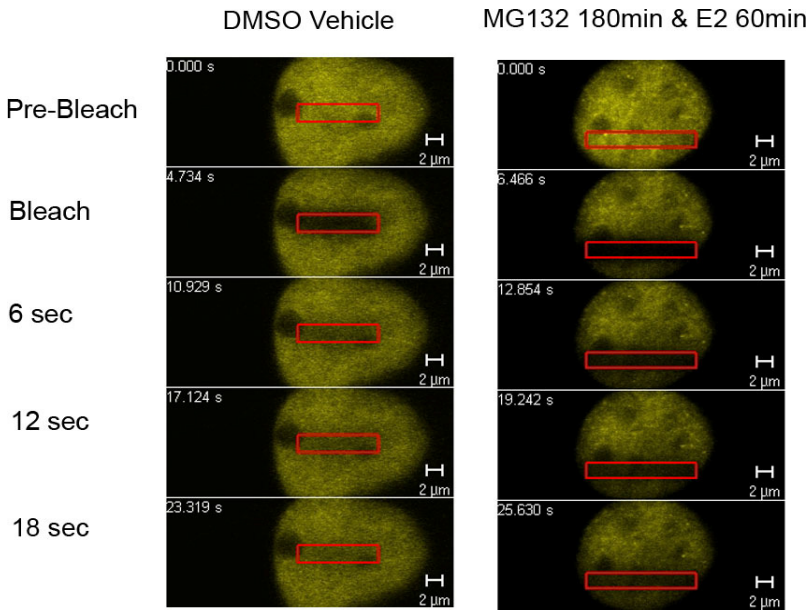

Figure 5.20 Qualitative FRAP assessment of ERβ-YFP infected hTERT cells.

Cells were treated with either a DMSO vehicle control (left hand panel) or a combination of MG132 10^{-6}M for 180 minutes with E2 10^{-8}M for 60 minutes (right hand panel).

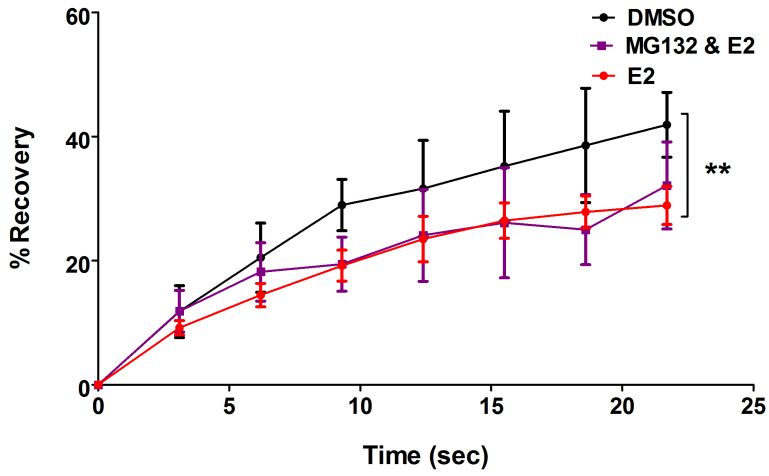

Figure 5.21 Quantitative analysis of intra-nuclear kinetics of ERβ-YFP infected hTERT cells.

*Graphical depiction of the recovery rates of ERβ-YFP over time into the bleached zone. This recovery is denoted by the point at which the Y_{MAX} is achieved. Recovery rates of ERβ-infected cells were in response to MG132 10^{-6}M for 180 minutes and E2 for 60 minutes at 10^{-8}M. ** ($P<0.01$) denotes significance in variation of treatments compared with the DMSO vehicle using the Student's t-test ($N\geq8$).*

It has been previously suggested that the AF-1 domain of ERβ plays an essential role in marking the receptor for ubiquitination and subsequent degradation in the 26S proteasome (Picard *et al.*, 2008). To test the importance of the AF-1 domain in regulating proteasomal degradation, two ERβ splice variants, ERβ2 and ERβ5 that contain an intact AF-1 domain but are truncated at their C terminus compared with the full length ERβ receptor were assessed using MG132 and E2 as above. Using this treatment regime there was no significant change in the intranuclear dynamics of either ERβ2-YFP (data not presented) or ERβ5-YFP (Fig. 5.22, Fig 5.23) in comparison to the same receptors incubated with DMSO (vehicle control). The response of putative ERα-ERβ5 heterodimers to proteasomal regulation was examined using hTERT cells treated with a combination of MG132 and E2 for 180 minutes and 60 minutes respectively. Incubation of cells with MG132 and E2 reduced the mobility of the ERβ5-YFP in comparison to DMSO-treated control cells (Fig. 5.24 and 5.25), a result that was in contrast to that obtained with ERβ5-YFP alone suggesting ERα played a role in facilitating proteasomal regulation of the heterodimer.

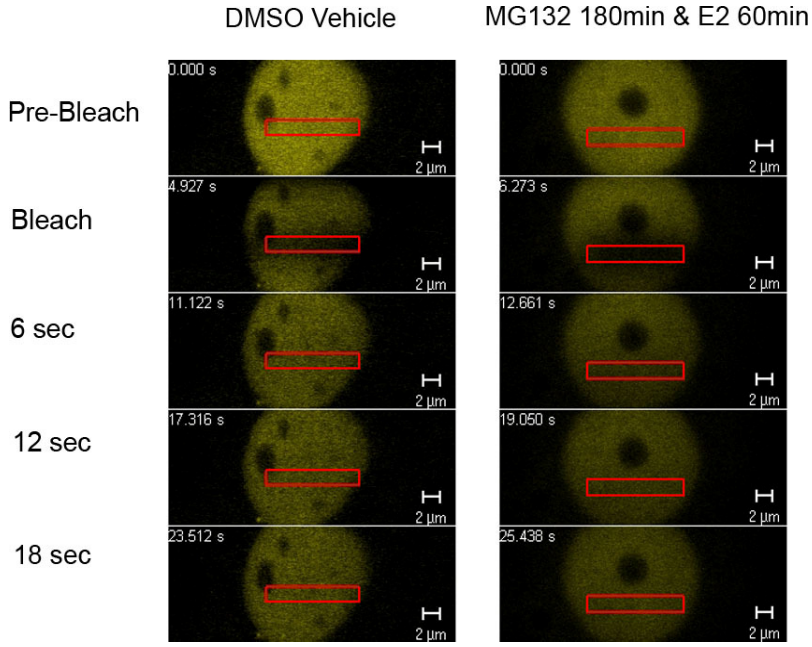

Figure 5.22 Qualitative FRAP assessment of ERβ5-YFP infected hTERT cells.

Cells were treated with either a DMSO vehicle control (left hand panel) or a combination of MG132 10^{-6}M for 180 minutes with E2 10^{-8}M for 60 minutes (right hand panel).

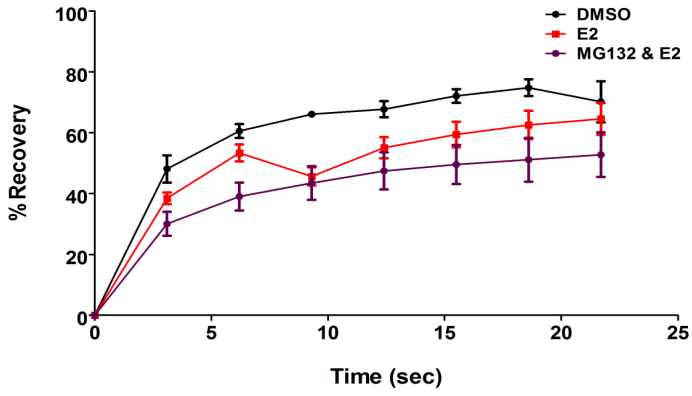

Figure 5.23 Quantitative analysis of intra-nuclear kinetics of ERβ5-YFP infected hTERT cells.

Graphical depiction of the recovery rates of ERβ5-YFP over time into the bleached zone. This recovery is denoted by the point at which the Y_{MAX} is achieved. Recovery rates of ERβ5-infected cells are presented in response to MG132 10^{-6}M for 180 minutes and E2 for 60 minutes 10^{-8}M. Significance in variation of ligand treatments was compared with the DMSO vehicle control using the Student's t-test (N≥8).

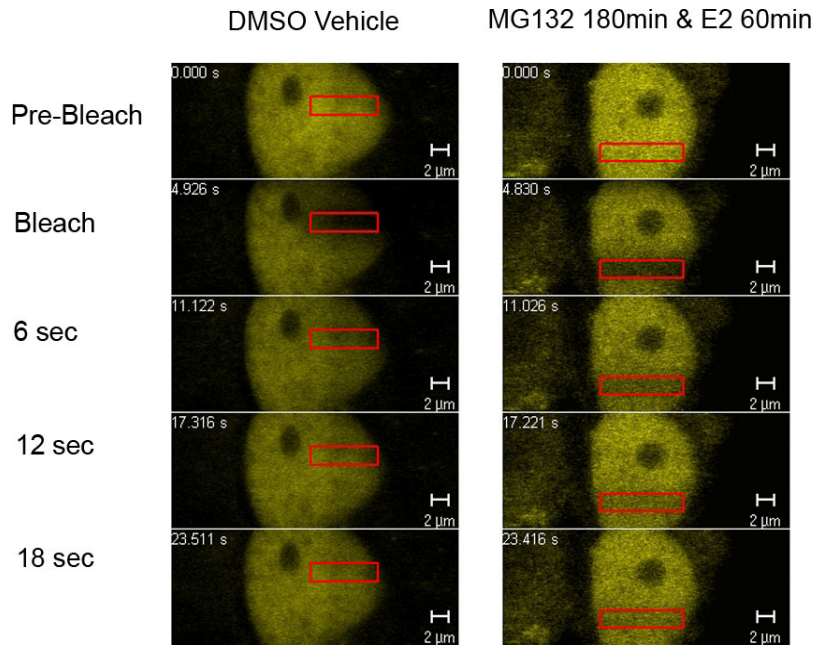

Figure 5.24 Qualitative FRAP assessment of ERβ5-YFP and ERα infected hTERT cells.

Cells were treated with either a DMSO vehicle control (left hand panel) or a combination of MG132 10^{-6}M for 180 minutes with E2 10^{-8}M for 60 minutes (right hand panel).

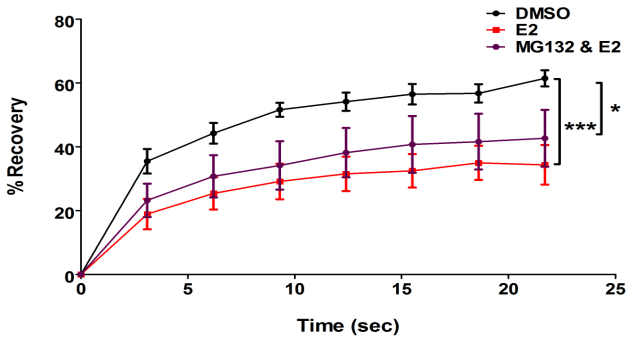

Figure 5.25 Quantitative analysis of intra-nuclear kinetics of ERβ5-YFP and untagged ERα infected hTERT cells.

*Graphical depiction of impact of ligand treatment on the recovery rates of ERβ5-YFP over time back into the bleached zone. This recovery is denoted by the point at which the Y_{MAX} is achieved and a plateau is reached on the graph. Recovery rates of ERβ5-YFP and ERα-infected hTERT cells are presented in response to MG132 10^{-6}M for 180 minutes and E2 for 60 minutes at a concentration of 10^{-8}M. * ($P<0.05$) and *** ($P<0.001$) denotes significance in variation of ligand treatments compared with the DMSO vehicle control as derived from the Student's t-test ($N\geq8$).*

5.3.8 ER activity is regulated by proteasomal function

To further investigate the relationship between the turnover of ERα and ERβ5 and E2-mediated transcriptional activity, luciferase assays were conducted that examined the effects of the MG132 proteasome inhibitor on cells infected with ERα and ERβ5 alone or in combination. Cells infected separately with ERα and ERβ5 adenoviral constructs and a 3X-ERE-tk-luc reporter construct were treated with a DMSO vehicle control, MG132 alone, E2 alone or a combination of MG132 for 1 hour followed by addition of E2. Luciferase activity was measured after 24 hours and normalised to total protein levels (Section 2.9).

In Ishikawa cells, treatment with E2 alone induced reporter gene activity in line with expectations based on previous studies (Chapter 4) and when cells were treated with MG132 alone, there was no significant change in ERE-dependent luciferase gene expression compared to the vehicle control suggesting that the inhibitor did not have any direct impact on the reporter construct (Deroo and Archer, 2002). Addition of MG132 had no significant impact on E2-mediated reporter gene activation in the control Ishikawa cells. However following increased expression of ERα or ERβ5 alone or in combination E2-driven reporter gene activity was significantly attenuated by addition of MG132 (Fig. 5.26). This result suggests a role for the 26S proteasome in maximising ligand-dependent activation of ERs in this cell context.

The impact of inhibiting proteasomal degradation of the ER on reporter gene activation was also investigated in the hTERT cell line. As in the Ishikawa cells treatment of the cells with MG132 alone matched the DMSO vehicle response. Surprisingly incubation of cells with MG132 did not abrogate the E2-drived transcriptional response in cells infected with ERα or ERβ5 alone or in combination (Fig. 5.27). These results are in contrast to those acquired in the Ishikawa cell line and may reflect a cell context dependant reliance on proteasomal function in the Ishikawa cells. This result also suggests that the 26S proteasome does not exclusively determine the optimal transcriptional response of ERs in all cell types.

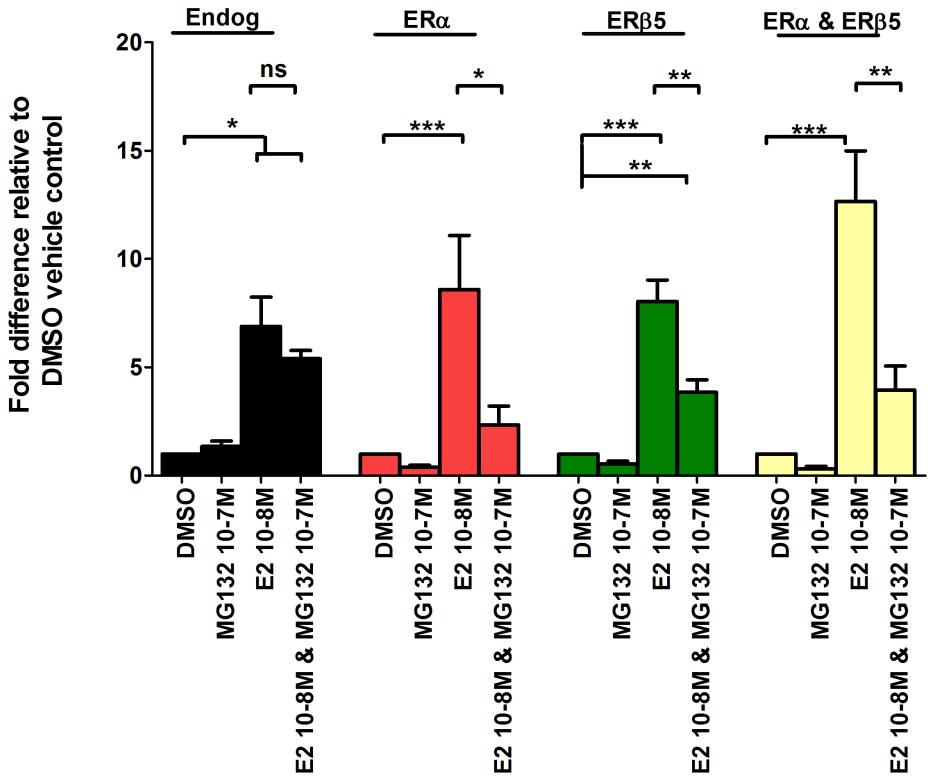

Figure 5.26 Impact of transcriptional inhibitor (MG132) with ERs on luciferase reporter activity in Ishikawa cells.

*Cells were infected with ERα (red), ERβ5 (green), or both ERα and ERβ5 (yellow); all cells were infected with the 3x-ERE-Luc reporter. Treatment was with MG132 10^{-6}M, E2 10^{-8}M or a combination of MG132 for 1 hour followed by E2 10^{-8}M for 24 hours before luciferase activity was measured. Fold difference is expressed relative to the DMSO vehicle-treated cell, each bar represents N=3±SEM and has been normalised to protein levels. *** (P<0.001), ** (P<0.01) and *(P<0.05) denotes significance in variation of ligand treatments compared with the vehicle control as derived from one-way ANOVA and Tukey's post-test comparing all pairs of data sets (N≥8).*

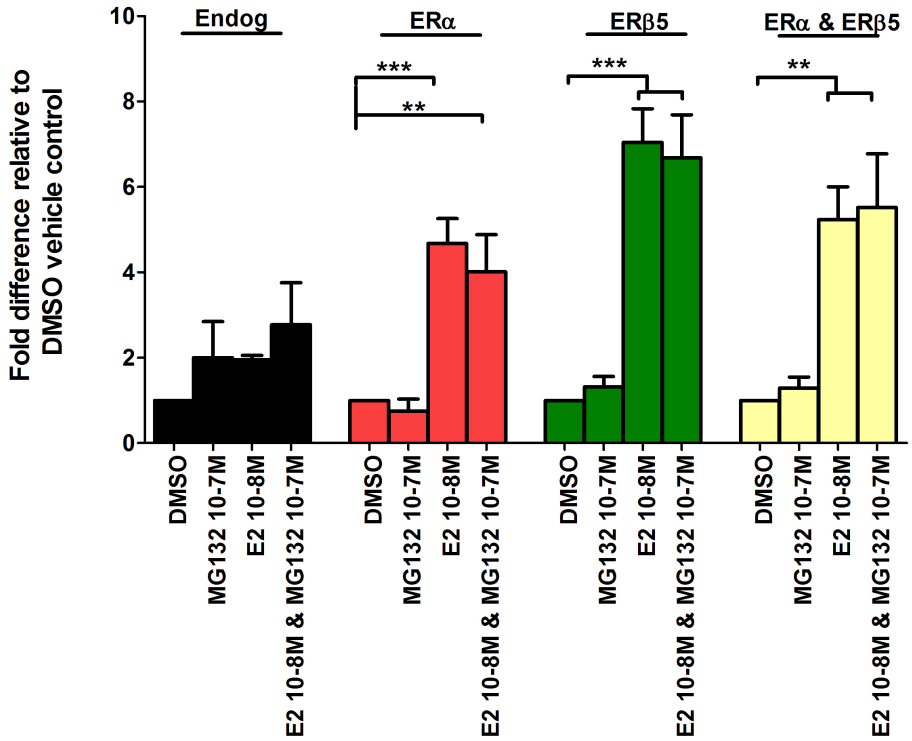

Figure 5.27 Impact of transcriptional inhibitor (MG132) with ERs on luciferase reporter activity in hTERT cells.

*Cells were infected with ERα (red), ERβ5 (green), or both ERα and ERβ5 (yellow) and all cells were infected with the 3x-ERE-Luc reporter construct. Treatment was with MG132 10^{-6}M, E2 10^{-8}M and a combination of MG132 for 1 hour prior to E2 for 24 hours before luciferase activity was measured. Fold difference is expressed relative to the DMSO vehicle-treated cell, each bar represents N=3±SEM and has been normalised to protein levels. *** (P<0.001), ** (P<0.01) and *(P<0.05) denotes significance in variation of ligand treatments compared with the vehicle control as derived from one-way ANOVA and Tukey's post-test comparing all pairs of data sets (N≥8).*

5.4 Discussion

In order to gain an understanding of the functional role of the truncated splice variant ERβ5 in endometrial cells, experiments in the current chapter have investigated alternative ligand-independent modes of activation of receptors. Two endometrial cell lines were employed in order to determine the impact of EGF-mediated MAPK signalling on activation of ERα and ERβ5. The impact of receptor turnover on receptor activity was also examined with regard to ERα and ERβ5 through disruption of the UPP.

5.4.1 The EGF family of receptors are expressed in the human endometrium

Immunohistochemistry documented the expression of the different members of the human epidermal growth factor family of receptors (HER family) in human endometrium recovered during the proliferative phase of the cycle. The HER family of transmembrane receptor tyrosine kinases (HER 1-4) is believed to have evolved from a single primordial tyrosine kinase into four different cell surface receptors through sequential gene fusion and duplication events (Citri and Yarden, 2006). Human HER1 and HER4 both bind a myriad of peptide growth factors including heparin-binding EGF (HB-EGF), betacullin (BCL) and epiregulin (EPI) among others (Harris *et al.*, 2003). The accumulation of mutations over time has rendered HER2 and HER3 non-autonomous and these receptors are only functional in a heterodimeric partnership (Klapper *et al.*, 1999, Guy *et al.*, 1994).

Immunohistochemical analysis revealed widespread immunoreactivity for HER 1 in both the stromal and glandular compartment of the healthy proliferative premenopausal endometrial tissue. HER2 positive staining was solely localised to the epithelial cells. HER3 positive cells were detected in both stromal and epithelial cells while HER4 staining was very weak and localised to the glandular epithelium. Previous studies have reported cycle-dependent regulation of HERs (Ejskjaer *et al.*, 2005) where HER4 expression has been determined to be greatest at the early and late secretory phases and may account for the weak staining observed at the

proliferative phase in this study (Srinivasan *et al.*, 1999, Chobotova *et al.*, 2005). A recent clinical study has described the prognostic value of HER4 due to its upregulation in endometrial cancer tissue (Ejskjær *et al.*, 2007) compared to expression in the normal premenopausal endometrium where it is speculated that HER4 may be behaving as an inhibitor of proliferation (Ejskjaer *et al.*, 2005). In this study, protein expression of HER1 was detected in the Ishikawa adenocarcinoma endometrial cell line and this cell line was therefore used for further experimental investigation.

Amongst the numerous downstream response signalling pathways induced by the receptor kinase activity of the HER family is the activation of MAPK pathways (Wells, 1999). Early mouse studies implied a role for growth factor signalling in the activation of ERs that was independent of oestrogenic ligands (Nelson *et al.*, 1991, Ignar-Trowbridge *et al.*, 1992). EGF-mediated activation of MAPK signalling has been shown to result in the rapid phosphorylation of ERα in human cell lines *in vitro* (Kato *et al.*, 1995b, Bunone *et al.*, 1996). This study has localised the members of the HER family of receptors to site-specific cells of the endometrium and indicates a putative alternative mechanistic model for ligand-independent activation of the ERs.

Phosphorylation of the p42/p44 (ERK2/ERK1) MAPKs in an Ishikawa cell line in a time-dependent manner in response to EGF exposure was demonstrated. The greatest accumulation of phosphorylated MAPK protein was observed ten minutes after EGF stimulation. This effect was specifically abrogated by treatment with the ERK inhibitor PD98059. ERα protein containing phospho-Ser118 residues was detected after EGF treatment in the same cell line (YFP-tagged and endogenous receptor). As ERα, ERβ and ERβ splice variants and HERs are all expressed in endometrial cells, further studies were conducted to examine the impact of EGF on receptor function.

5.4.2 EGF treatment has an impact on the intranuclear dynamics of ER subtypes in endometrial cells *in vitro*

E2-induced nuclear redistribution of the full length ER subtypes (ERα and ERβ) was previously described (Chapter 3). Complementary studies described in this chapter have shown that EGF can also induce receptor redistribution. Notably, an EGF-dependent redistribution of the truncated ERβ5 splice variant was also demonstrated in the endometrial adenocarcinoma Ishikawa cell line. This impact of EGF was time-dependent with distinct time-courses of redistribution revealed for individual ER subtypes. These data are the first time that a growth factor-dependent change in ERβ5 activity has been demonstrated.

Several studies have reported that the ER proteins have phosphorylation target sites clustered within the AF-1 region of their N-terminal domains. These kinase directed consensus sites have been defined in human ERα at serine residues 104, 106, 118 and 167 (Thomas *et al.*, 2008, Bunone *et al.*, 1996, Ignar-Trowbridge *et al.*, 1996, Kato *et al.*, 1995a, Joel *et al.*, 1998a) and mouse ERβ at serine residues 16, 106 and 124 (Cheng and Hart, 2001, Tremblay A. *et al.*, 1999). In addition, phosphorylation within the AF-1 domain of mouse ERβ is reported to facilitate recruitment of the coactivators SRC-1 and CREB binding protein (CBP) and activation of the receptor (Tremblay and Giguere, 2001). Binding of these regulatory proteins has also recently been implicated in enabling hypoxia inducible factor HIF-1α to activate ERβ under hypoxic conditions in HEK293 cells (Lim *et al.*, 2009).

It has been reported that EGF-induced phosphorylation of ERα at Ser118 residue occurs by 15 minutes post-EGF treatment in COS-1 cells (Kato *et al.*, 1995d). In agreement with this, it was observed that EGF treatment stimulated nuclear redistribution of ERα-GFP in MCF-7 cells within 10 minutes, with maximal redistribution at 60 minutes after treatment (Takahashi *et al.*, 2005). In the current studies, rapid nuclear redistribution was observed after EGF incubation with each of the ER subtypes (ERα, ERβ and ERβ5) when this was quantified in the Ishikawa cell line. Cells were maintained in serum-free media to prevent stimulation by growth

factors or steroids in the serum and to ensure the results observed were EGF-dependent. Subnuclear distribution into a punctate state mirrored the changes observed following treatment of cells infected with ERα-YFP or ERβ-YFP after they were exposed to E2 (Chapter 3).

In this study, ERβ5-YFP in cells maintained without serum was highly mobile and reached maximal recovery into the bleached zone (Y_{MAX}) in ~2.6 seconds which was slightly faster than ERα-YFP and ERβ-YFP (4.2, 5.8 seconds respectively). Using FRAP analyses, it was shown that incubation of cells with EGF leads to reorganisation of each of the tagged ERs within 10 minutes of the start of treatment. In Ishikawa cells this effect was sustained at 20 and 30 minutes post-EGF treatment in ERβ-YFP infected cells and additionally at 60 and 90 minute timepoints in the ERβ5-YFP infected cells. In addition to a decrease in the recovery rate of ERβ5 molecules back into the bleached region (ROI I), a significant change in the half-time (i.e. the time taken to reach 50% of the maximal recovery (Y_{MAX}) was noted from 2.6 seconds of the unliganded ERβ5-YFP to 5.3 seconds at 20 minutes post-EGF incubation. These novel results reveal that EGF can have an impact on the intranuclear kinetics of ERβ5, a receptor subtype that does not bind E2.

5.4.3 EGF treatment has an effect on the transcriptional activity of ERs *in vitro*

In Chapter 3, a correlation between the E2-dependent nuclear redistribution pattern and transcriptional activity was confirmed. This observation would be in agreement with the expectation that the 'punctate' appearance reflects DNA-bound associations that underlie activation of the transcriptional machinery. Other studies have suggested that nuclear redistribution and transcriptional activity are not linked as the punctate foci preclude polymerase II associations (Stenoien *et al.*, 2001a).

Earlier studies have demonstrated increased activity at a consensus ERE in ERα-transfected HeLa cells (Bunone *et al.*, 1996b, Hafner *et al.*, 1996) and ER positive BG-1 human ovarian adenocarcinoma cells (Ignar-Trowbridge *et al.*, 1996) in

response to EGF treatment. Analysis of the transcriptional activity of ERs using an ERE-luciferase reporter gene construct in this study revealed an increase in the relative luciferase activity in comparison to the vehicle control by the endogenous receptors in both Ishikawa and hTERT cell lines (~1.5 and ~5.4 fold induction respectively). While there was no significant increase in transcriptional output derived from overexpression of ERα, ERβ or ERβ5 in the Ishikawa cell, a trend towards increased luciferase activity was observed in the ERα and ERβ5-infected cells. It has been suggested however that the EGF-mediated activity in Ishikawa cells is promoter-dependent (Gehm *et al.*, 2000) and may involve a mechanism involving EGF-driven ER activity at alternative promoter regions such as AP-1 sites.

5.4.4 Inhibition of the 26S proteome relayed effects on the intranuclear dynamics of ERs *in vitro* in endometrial cells

Earlier studies have implicated proteasomal-mediated degradation through the UPP as an important regulator of ERα transcriptional activity in rats (Nirmala and Thampan, 1995) and mammalian cell cultures (Nawaz and O'Malley, 2004, Priesler-Mashek, 2002). For example, it has been demonstrated that the inhibition of UPP-directed turnover of ERα using the proteasomal inhibitor MG132 completely abolishes the intranuclear mobility of ERα in a number of human cell lines. These studies reported ERα immobilisation at the nuclear matrix in response to MG132 both in the absence (Stenoien *et al.*, 2001b, Reid *et al.*, 2003) and presence of oestrogenic ligands (Reid *et al.*, 2003). Consistent with a recent publication (Damdimopoulos *et al.*, 2008), there were no differences between the ERα and ERβ responses to MG132 treatment in hTERT cells. In the current study, MG132 combined with E2 treatment had a significant impact in reducing the mobility of ERα and ERβ in hTERT cells and an increased half-time of ~5.4 seconds was determined for the MG132/E2 treated ERα-infected cells in comparison with the vehicle control cells (T1/2 = 3.6 seconds). However, complete immobilisation of the receptors was not observed and there appeared to be no difference between receptor dynamics in cells treated with E2 and those treated with a combination of MG132 and E2. This discrepancy from results demonstrated in other reports may stem from the MG132

incubation time of 3 hours which falls short of the longer exposure times used in other studies (ranging from 3 to 10 hours) (reviewed in Hager *et al.*, 2004). The results obtained in the presence of ligand were identical to those in hTERT cells treated with MG132 alone (data not shown) implicating a role of the for the 26S proteasome irrespective of the ligand bound/unbound status of the receptor. MG132 treatment had no impact on ERβ2 (data not shown) or ERβ5-infected hTERT cells, indicating that these truncated variants are not completely regulated by proteasomal-mediated clearance. However, co-infection of ERβ-YFP and ERα resulted in the reduced mobility of the ERβ5-YFP molecule and is suggestive of a susceptibility of ERβ5 to degradation when in a heterodimeric partnership. These intriguing observations merit further study.

5.4.5 MG132-induced disruption of the ubiquitin protease pathway had an effect on activation of the ERE reporter gene

MG132 treatment retarded the mobility of ERα and ERβ in both the presence and absence of ligand in hTERT cells (section 5.4.4). The accumulated population of ER in response to disruption of the UPP has been hypothesised as a dysfunctional pool of receptors (Stenoien *et al.*, 2001b) that bind to the nuclear matrix and differs from the canonical ligand-bound receptor that are active at chromatin sites (Picard *et al.*, 2008). Further work has elucidated differences in the underlying mechanisms of UPP-mediated degradation based upon the ligand bound/unbound status of ERα at the pS2 promoter region (Reid *et al.*, 2003) and the activity of ERβ (Tateishi *et al.*, 2006, Picard *et al.*, 2008).

Inhibition of UPP-mediated degradation by MG132 treatment for 24 hours in Ishikawa cells attenuated the E2-dependent transcriptional output by ERα and ERβ at the ERE. In other studies MG132 treatment has been shown to impair ERα-mediated transcription and the AF-1 domain has been implicated as a key component in regulating UPP-directed proteolysis of E2-bound ERα in transfected HeLa (Lonard *et al.*, 2000) and HEK293 cells (Valley *et al.*, 2005) and of ERβ also in HEK293 cells (Picard *et al.*, 2008). This N terminal domain is intact in ERβ5 and is identical to that

of its homologue ERβ. In contrast to the insignificant effect of MG132 exposure (3 hour timecourse) on the dynamics of ERβ5, the results of the luciferase reporter assay demonstrated a significant abrogation of transcriptional activity in ERα-positive Ishikawa cells following infection with ERβ5 alone or in combination with ERα. These results are suggestive of a role for proteasomal degradation in maintaining steady-state ER levels (including ERβ5) and facilitating ongoing ER-mediated transcription. However, this result was cell context dependent and was not replicated in the hTERT cell line where the E2-driven response was sustained even in the presence of MG132. This discrepancy may stem from a promoter-based effect as it has been previously published that MG132 can impart a deleterious effect on the luciferase enzyme itself in some cellular contexts (Deroo and Archer, 2002). Furthermore, Fan *et al.*. (Fan *et al.*, 2004) demonstrated increased transactivation in response to E2 and MG132 combined treatment in MCF-7 cells and have dismissed a central role for the UPP in regulating ERα function. Taken together, these preliminary results examining the intranuclear dynamics and the transcriptional response to MG132 imply a salient role for the UPP in governing optimal activity of the ERs in a cell context dependent manner and merit further investigation.

5.4.6 Conclusions

The results presented in this chapter have examined a ligand-independent mode of receptor activation and the impact of proteasomal-degradation on regulation of ERs. It has been demonstrated that treatment of cells with EGF has an impact on receptor dynamics and transcriptional activity that conforms to distinct timeframes that are subtype dependent. For the first time it has been revealed that ERβ5 is also a putative candidate for EGF-induced post-translational modifications that impact on intranuclear dynamics and transcriptional activity. Ubiquitination of the ER via the UPP appears to be of importance to the regulation of ERα, ERβ and ERβ5 transcriptional activity in a cell context-dependent manner. The results established a link between the proteasome and changes on the intranuclear dynamics of the full length ERα and ERβ subtypes. Further studies will be required to discern the reason for discrepancies in the impact of MG132 in different endometrial cell lines.

Chapter 6

General Discussion

6 Final Discussion

The oestrogen receptors are members of a ligand-regulated superfamily of transcription factors that mediate pleiotrophic biological effects (Hewitt and Korach, 2002). Receptor dependent changes in gene expression are influenced by conformational changes in the 3D structure of the receptors, formation of homo- or hetero-dimers and the resulting association with coregulators and/or basal transcriptional factors at specific sequences within the promoter sequences of target genes (Tsai and O'Malley, 1994a, Brzozowski *et al.*, 1997, Steinmetz *et al.*, 2001) (reviewed in Nilsson *et al.*, 2001). The advent of quantitative confocal microscopy methods such as FRAP and FRET in parallel with the development of fluorescently labelled receptor proteins have enabled investigators to study of behaviour of receptors including ERs in the nuclei of living cells (Stenoien *et al.*, 2001a, Stenoien *et al.*, 2001b, Tamrazi *et al.*, 2003, Damdimopoulos *et al.*, 2008, van Royen *et al.*, 2009). Much of the published research on the intranuclear dynamics of ERα (Stenoien *et al.*, 2000, Stenoien *et al.*, 2001b, Reid *et al.*, 2003) and more recently, ERβ (Damdimopoulos *et al.*, 2008) has utilised constructs in transiently transfected cell lines. Stenoien *et al.* specifically reported significant variation in the levels of fluorescent protein expressed between transiently transfected cells and made a point of only using low fluorescing cells that were just sufficiently bright for use in FRAP analyses (Stenoien *et al.*, 2000, Stenoien *et al.*, 2001b). In contrast, the studies described in this thesis utilised cell lines into which the receptor constructs were introduced using adenoviral constructs. This approach allowed us to carefully titrate the amount of fluorescent protein in each call so that the cell was not ‘overloaded’ with an excess of receptor protein allowing us to have confidence that the behaviour of the fluorescently-tagged receptors would recapitulate that of endogenous receptors.

The primary objective of the work described in this thesis was to acquire a better understanding of what impact steroid ligands and growth factors have on the intranuclear dynamics and functional activity of human oestrogen receptors and to identify whether differences in responses occur between the full-length ‘wild type’ oestrogen receptors (ERα and ERβ) both of which have an intact oestrogen-binding pocket and AF-2 domain at their C-terminus. Parallel investigations were also carried out on two splice variant isoforms of human ERβ, ERβ2 and ERβ5 both of which

contain an intact DNA binding domain but lack an intact ligand binding pocket (Leung *et al.*, 2006). One of the key techniques used in these studies was FRAP, a method that measures intracellular mobility (van Royen *et al.*, 2007). An association between reduced mobility, interactions with euchromatin and changes in gene expression has been claimed for the PR (Arnett-Mansfield *et al.*, 2004) and glucocorticoid receptor (reviewed in DeFranco and Guerrero, 2000) making this an attractive system with which to visualise the impact of steroid ligand-dependent and steroid-ligand independent activation on the ER subtypes.

The specific aims of the studies described were: 1) to establish and optimise methods for measuring the intranuclear mobility of both full length ERα and ERβ and splice variant isoforms of human ERβ (ERβ2 and ERβ5); 2) to determine whether ERβ5 may play a role in oestrogen responsiveness in the normal human endometrium; 3) to examine alternative ligand-independent modes of activation of ER with particular reference to the truncated ERβ5 splice variant.

6.1 Relationship between nuclear dynamics of ER and transcriptional output

Studies on the impact of ligand binding to either ERα and/or ERβ on the intranuclear dynamics of both homo- and hetero-dimeric conformations of the receptors were carried out in the three cell lines; MDA, Ishikawa and hTERT. Infection with ERα-YFP adenoviral constructs resulted in homogeneous distribution of the fluorescent receptor within the nucleus of all three cell types. This was in contrast to their appearance following infection with ERβ-YFP that localised into discrete subnuclear foci in the cells. The predisposition of ERβ-YFP to adopt this arrangement is suggestive of a higher affinity of this protein for specific regions within the nucleus even in the absence of ligand.

Addition of E2 to ERα-YFP infected cells induced a rapid redistribution into a ‘punctate’ arrangement of distinct focal points in all the cell lines examined. This is in agreement with previous studies that demonstrated a significant decrease in mobility and redistribution of full length ERα in human cell lines in response to E2 stimulation and suggests this is one aspect of the cascade of events associated with ligand-

dependent activation of the receptor (Htun *et al.*, 1999, Stenoien *et al.*, 2001b, Maruvada *et al.*, 2003).

To date, there has been limited published data on the subnuclear dynamics of ERβ (Damdimopoulos *et al.*, 2008) and while ERβ shares significant homology with ERα, the two receptors differ in tissue distribution and functionality. Like ERα-YFP, treatment of ERβ-YFP infected cells with E2 resulted in a further nuclear re-organisation of the ERβ-YFP and a decrease in the mobility of the receptor within these foci. The decrease in mobility observed with both ERα-YFP and ERβ-YFP in response to E2 stimulation is suggestive of increased residence of the ERs DNA sites involved in transcriptional activation where they can associate with the enzymes and transcription factors required for formation of the pre-initiation complex.

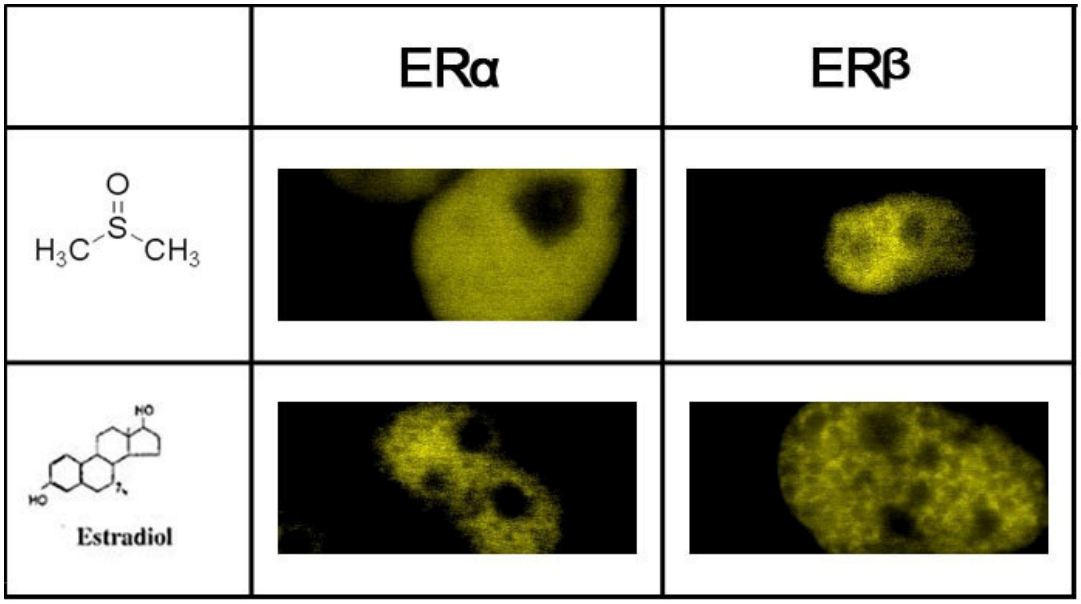

Figure 6.1 Morphological comparison of fluorescently-labelled ERα and ERβ in MDA cells between vehicle control versus E2-stimulated conditions.

The uniform distribution of ERα-YFP contrasts with the predisposed fluorescent foci of ERβ-YFP infected MDA cells. Treatment with E2 yields a punctate effect that is mirrored by both ER subtypes (ERα and ERβ).

The pure anti-oestrogen ICI 182,780 has been widely used to abrogate E2-induced activity. Association with this compound induces a distinct inhibitory conformation that prohibits AF-1 and AF-2 activity and coactivator association and promotes ERα turnover (Wakeling *et al.*, 1991, Dauvois *et al.*, 1993b). The studies in this thesis

revealed differences in the intranuclear mobility of ERα-YFP and ERβ-YFP in cells incubated with ICI 182,780; ERα-YFP became completely immobilised whereas a significant decrease in the mobility of ERβ-YFP was observed without complete immobilisation.

Binding of ERα within the nuclear matrix has been shown to result in extensive chromatin unfolding, an effect that can occur independently of ligand binding (Nye *et al.*, 2002). The decrease in mobility of both ERα-YFP and ERβ-YFP in this study in response to agonist is suggestive of ER-chromatin associations that may determine chromatin remodelling. The prediction is that should this occur at the site of an ERE it would provide a receptive context for coactivator recruitment and transcriptional initiation. A key observation from the current study was that while ICI 182,780 treatment resulted in the immobilisation of ERα-YFP to the DNA template and caused a significant reduction in the ERβ-YFP mobility suggestive of DNA binding, this was not associated with activation of luciferase reporter gene suggesting that the ER-ICI 182,780 conformation does not yield activity at the chromatin.

Co-expression of ERα and ERβ in many cell contexts has been shown to result the formation of heterodimers (Pace *et al.*, 1997, Tremblay G.B. *et al.*, 1999); this conformation is reported as being favoured over that of ERβ homodimers (Cowley *et al.*, 1997). FRET studies conducted in our lab have demonstrated close proximity of ERα-YFP and ERβ-CFP in response to E2, PPT™ and DPN™ treatments (Karen Tuzi, unpublished data) consistent with formation of heterodimers following binding of a range of ligands. In agreement with these results, FRAP analyses revealed changes in mobility of ER-YFP constructs when they were co-expressed with another untagged full length receptor (ERα or ERβ). Surprisingly, in cells co-expressing ERα and ERβ-YFP, there was no change in the subnuclear dynamics of the tagged receptor in response to stimulation with PPT™. Based on the FRET analyses that suggested heterodimerisation between these two subtypes, this result could suggest a dominant inhibitory role for ERβ-YFP in the ERα response to PPT™. This is consistent with other reported studies in mouse (Lindberg *et al.*, 2003) and human cell lines (Strom *et al.*, 2004, Chang *et al.*, 2006, Papoutsi *et al.*, 2009). Further experimental data including ChIP analyses are necessary to verify that this response reflects that of the ERβ/α heterodimer and not ERβ homodimers.

Subtype-specific agonists are designed by exploiting the different conformations that can arise at helix 12 of the ERs (Shang, 2006). This study examined the influence of the signature agonist-induced conformations of ERα-selective PPT™ and ERβ-selective DPN™ on ERα-YFP and ERβ-YFP in MDA, Ishikawa and hTERT cell lines. The observations and results from the FRAP analyses using PPT™ and DPN™ were largely consistent across each of the cell lines investigated. PPT™ specifically caused a significant decrease in mobility of ERα-YFP that was not observed with ERβ-YFP infected cells. DPN™ appeared to exhibit specificity for ERβ-YFP infected cells with MDA cells.

In order to establish whether changes in receptor distribution and mobility were paralleled by changes in the transcriptional activity of the receptors the same combinations of receptor homo- and hetero-dimers and ligands were tested using an assay system in which a luciferase reporter gene was under the control of three copies of a consensus ERE using a number of different cell lines including those that lacked endogenous receptors. Previous investigators have suggested that changes in the subnuclear distribution of ERs reflect transcriptional activity because they are a consequence of active recruitment of coactivators such as SRC-1 (Stenoien *et al.*, 2000). Although we detected a clear parallel between reduced mobility following binding of E2 to either ERα or ERβ and increased expression of the ERE-dependent reporter gene, the results using the ERα and ERβ selective agonists PPT™ and DPN™ were more variable. PPT™ selectively activated transcription at the ERE in ERα-YFP infected MDA cells to the same extent as E2 but this was not recapitulated in ERβ-YFP infected MDA cells. This result correlated with the decrease in mobility of the ERα-YFP infected cells being associated with transcription initiation. In contrast, although DPN™ is reported to have a 70X higher binding affinity for ERβ over ERα (Meyers *et al.*, 2001), incubation of cells with this agonist induced changes in the intranuclear mobility of both ERα-YFP and ERβ-YFP homodimers and ERα-ERβ heterodimers. However, the reduction in ERα-YFP mobility did not result in a demonstrable change in transcriptional activity at the luciferase-tagged ERE. Treatment with DPN™ induced luciferase reporter activity in ERβ-YFP infected cells but not in those expressing ERα-YFP. These results suggest that subnuclear dynamics and transcriptional output are not inherently linked. There are a number of lines of

evidence that are in agreement with these observations; Carroll and Brown presented the results of ChIP on chip arrays that demonstrated an excess of binding sites in comparison to the estimated numbers of ER-regulated genes, suggesting that many of these sites may be redundant and not involved in a productive transcription complex (Carroll and Brown, 2006). A previous study demonstrated that the location of bound-ERα excluded RNA polymerase II interaction, a transcriptional factor that is indispensable at the transcriptional start site (Stenoien *et al.*, 2001b). While the FRAP data indicate efficient ERα-YFP-DPN™ binding that results in dissociation from the repressive hsp90 complex and marked by a decrease in ERα-YFP mobility, this observation alone does not signal optimal activity at the ERE-luciferase construct. A third potential/possible explanation is that DPN™ binding to ERα is sufficient to activate non-genomic activity through MAPK signalling (Lahm *et al.*, 2008) and this is not addressed by the luciferase reporter system. Further investigation of this result could include examination of the phosphorylation status of the ERα in response to DPN™ to determine if changes in subnuclear mobility could be attributable to non-genomic signalling by the ER.

The results that have been presented indicate that receptor tethering at the DNA inferred by the observed decrease in nuclear mobility does not always mean that the receptor is actively engaged in transcription and underlines the necessity of forming a complete gene transcriptional apparatus including ERs as part of the pre-ininitiation complex in association with the transcriptional start site (Fig. 6.1). This study has expanded our knowledge of ER subnuclear responses to ligand, demonstrating that ligand binding facilitates conformational changes that drive selective ER regulation. While changes in mobility are indicative of association with the DNA, binding of the ER alone is not always sufficient to orchestrate functional output at an ERE (Fig. 6.1). Additional studies with ERα and ERβ-specific antagonists in the presence or absence of their respective agonists PPT™ and DPN™ and examination of coregulator assembly at the DNA may enable further characterisation of the role of the complete protein complex that is required for activity at the preinitiation complex.

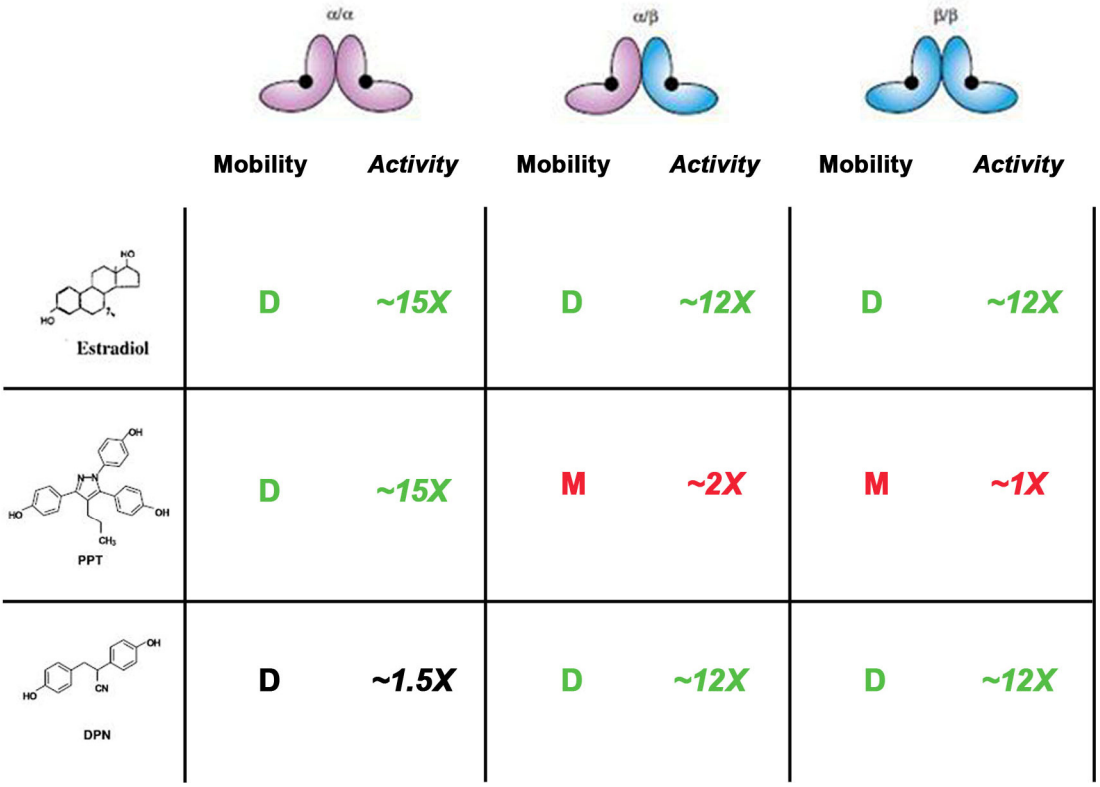

Figure 6.2 Summary of relationship between mobility and luciferase reporter activity in the current study.

M (Mobile, rapid recovery into ROI within ~25 seconds)
D (Dynamic, with reduced percentage recovery compared with control cells).

6.2 A role for truncated ERβ splice variants

Alternative splicing of exons within both the human ERα and ERβ genes results in the generation of multiple variant isoforms of both proteins (Moore *et al.*, 1998, Palmieri *et al.*, 2002, Speirs *et al.*, 2004). In particular, the splice variants of human ERβ known as ERβ2 (or ERβcx; Ogawa *et al.*, 1998c) and ERβ5 are derived from distinct coding sequences in place of 'wild type' exon 8 that results in translation of truncated variants lacking an intact LBD (Poola *et al.*, 2002, Leung *et al.*, 2006). This lab has previously documented the patterns of expression of ERα, ERβ1 and ERβ2 in normal human endometrium (Saunders and Critchley, 2002, Critchley *et al.*, 2002). In the current study these results were complemented and extended by including analysis of the pattern of expression of ERβ5 that documented for the first time that this isoform is expressed in this tissue. A number of studies have reported that ERβ2 and ERβ5 mRNAs have increased distribution in cancer pathologies (Fujimura *et al.*, 2001, Skrzypczak *et al.*, 2004, Esslimani-Sahla *et al.*, 2005). This lab has documented expression in cancers of the endometrium (Collins *et al.*, 2009) and in collaboration

with other groups has reported expression in the breast (Shaaban *et al.*, 2008) and colon (Wong *et al.*, 2005). This and other observations suggests that more accurate therapeutic targeting could be achieved through identification of the specific subtypes of ER isoforms that can mediate oestrogen receptor dependent changes in gene expression in endometrial and other reproductive tissue carcinomas (Taylor *et al.*, 2010).

To date, there have been no published reports documenting the subnuclear mobility of either ERβ2 or ERβ5 splice variants in human cell lines. By comparing the intranuclear dynamics and transcriptional activity of these isoforms the current study reemphasised the importance of having an intact LBD in order to facilitate agonist-driven changes in nuclear distribution. The ability of ERβ2 and ERβ5 to exist in homodimers has been challenged with a report suggesting that their sole activity is as a supporting role in a heterodimer with a full-length ERβ receptor (Leung *et al.*, 2006). The results in this thesis found that there was no change in receptor dynamics or luciferase reporter activity using MDA cells (lack endogenous receptor) infected with either ERβ2 or ERβ5 alone when incubated with E2. This finding is in agreement with molecular models that show the absence of a functional ligand binding pocket in these variants (Leung *et al.*, 2006).

FRAP analysis conducted using MDA cells co-expressing ERβ2-YFP and ERα revealed a change in the mobility of ERβ2-YFP that was both E2 and ERα dependent consistent with the formation of a hetero-dimer where ligand binding to one partner was sufficient to change the activity of the complex (Li *et al.*, 2004). This result concurs with a previous report that revealed a dominant inhibitory influence of ERβ2 on ERα transactivation at ERE and AP-1 sites in breast cancer cells (Zhao *et al.*, 2007). Co-expression of ERβ5-YFP with ERα resulted in an ERβ5-YFP decrease in mobility that was not observed in cells infected with ERβ5-YFP alone. This response implies a functional role for ERβ5 when in partnership with the full length ERα subtype. Furthermore, in a response that was cell context-dependent (Ishikawa endometrial adenocarcinoma cell line), co-expression of ERβ5 with ERα resulted in a luciferase transcriptional response that exceeded the luciferase reporter output of either subtype infected independently.

The novelty of these results lies in the finding that truncated variants that lack a competent ligand-binding domain can either a) form an inhibitory complex that blunts the ERα response to E2 (by ERβ2) or b) exploit the ligand binding capacity of ERα to yield a greater transcriptional effort in response to E2 (ERβ5). These studies are consistent with a putative role for the truncated splice variants in the regulation of their 'parent' counterparts and further expansion of this area should include ChIP array analyses to ascertain the binding sites for these functional heterodimers.

6.3 Influence of growth factor signalling on ER functionality

ERs have been shown to integrate signals from extracellular stimuli such as GFs (Hamelers and Steenbergh, 2003, Chen *et al.*, 2009). The effects of EGF are mediated via MAPK signalling that can induce phosphorylation of ERα at serine 118 within the N-terminal AF-1-containing domain (Kato *et al.*, 1995c). Treatment of cells with EGF has been shown to determine changes in nuclear redistribution of ERα in MCF-7 cells with a time-frame that is distinct from E2 (Takahashi *et al.*, 2005). Nuclear re-patterning was recapitulated in the current study using endometrial adenocarcinoma cells infected with ERα-YFP, ERβ-YFP and ERβ5-YFP. The preliminary results provided evidence for a temporal effect of EGF in reducing the mobility of these ERs in cells starved of endogenous ligand as early as ten minutes after addition of EGF. This is the first evidence of an activation mechanism for the truncated ERβ5 isoform. Studies have provided evidence for phosphorylation target sites at the N-terminus of full length mouse ERβ (Cheng and Hart, 2001, Tremblay G.B. *et al.*, 1999). The AF-1 domain of ERβ5 is intact and therefore provides a putative target site for ligand-independent activation of the variant. The novel observation of a decrease in mobility of ERβ5 when cells were treated with EGF may be evidence for a putative activation mechanism of this receptor. It has been shown that EGF treatment of HeLa cells resulted in large scale chromatin modifications by ERα at a defined transcriptional start locus (prolactin enhancer/promoter reporter construct) (Berno *et al.*, 2008). This report demonstrated chromatin decondensation after treatment with EGF that was similar to the response induced by treatment with E2 although over a longer time-scale (ten minutes versus thirty minutes for E2 and EGF respectively) (Berno *et al.*, 2008).

The changes in nuclear redistribution did not cause a significant increase in transcriptional activity although a trend towards this effect was demonstrated. However, this result concurs with the previous data where it was demonstrated that chromatin association alone is insufficient to drive high rates of transcriptional efficiency. This study is in its infancy and has potential to be expanded by further examination of the distinct temporal effects of EGF treatment and investigation of the effect of IGF-dependent signalling.

6.4 General Conclusions

Oestrogen receptors can play a pivotal role in changing the behaviour of different cell types because they can regulate gene expression through a variety of mechanisms including both direct and indirect interactions with DNA, some of which involve different transcription factors (Nilsson *et al.*, 2001). Changes in receptor activity may be induced either by direct binding of steroid ligands or as result of phosphorylation downstream of growth factor signalling cascades. Accordingly, the present study sought to examine the spatio-temporal effect of ligand-induced activity at the nuclear level. This involved examination of how ligand influenced ER behaviour and mobility in the nucleus and the influences that discriminate between signature ER subtype responses. In summary, the results described in this thesis elucidated differential ER subnuclear redistribution and mobility as a characteristic that distinguishes the different pharmacological compounds tested. This is a corollary of the signature conformational changes each compound induces at Helix 12 of the ER-LBD as revealed using site-specific fluorescence microscopy (Tamrazi *et al.*, 2003). It also demonstrated how direct (E2) and indirect (EGF) modes of activation compare in terms of nuclear behaviour, association with the nuclear architecture and transcriptional output. Using quantitative confocal imaging and analysis, this study revealed a dynamic portrait of selective changes in ER subtype distribution and mobility that were dependent on the nature of the ligand and the co-existence of other ER isoforms, and largely coincident with transcriptional efficacy although the precise physiological relevance of changes to nuclear re-patterning remain elusive. Furthermore, this study indicated an active role for truncated ERβ splicing variants in partnership with full length receptors and provided evidence for a previously unshown mechanism of indirect (EGF) influence on ERβ5 dynamics.

Chapter 7

Bibliography

References

ALBRIGHT, F., SMITH P. H., RICHARDSON, A. M. (1941) Postmenopausal osteoporosis. *JAMA,* 116**,** 2465-2474.

ALESSI, D. R., CUENDA, A., COHEN, P., DUDLEY, D. T. & SALTIEL, A. R. (1995) PD 098059 Is a Specific Inhibitor of the Activation of Mitogen-activated Protein Kinase Kinase in Vitro and in Vivo. *J Biol Chem,* 270(46), 27489-94.

ALI, S., METZGER, D., BORNERT, J. M. & CHAMBON, P. (1993) Modulation of transcriptional activation by ligand-dependent phosphorylation of the human oestrogen receptor A/B region. *Embo J,* 12**,** 1153-60.

AN, J., TZAGARAKIS-FOSTER, C., SCHARSCHMIDT, T. C., LOMRI, N. & LEITMAN, D. C. (2001) Estrogen receptor beta-selective transcriptional activity and recruitment of coregulators by phytoestrogens. *J Biol Chem,* 276**,** 17808-14.

ANSTEAD, G. M., CARLSON, K. E. & KATZENELLENBOGEN, J. A. (1997) The estradiol pharmacophore: ligand structure-estrogen receptor binding affinity relationships and a model for the receptor binding site. *Steroids,* 62**,** 268-303.

ARNETT-MANSFIELD, R. L., DEFAZIO, A., MOTE, P. A. & CLARKE, C. L. (2004) Subnuclear distribution of progesterone receptors A and B in normal and malignant endometrium. *J Clin Endocrinol Metab,* 89**,** 1429-42.

ARNOLD, S. F., MELAMED, M., VOROJEIKINA, D. P., NOTIDES, A. C. & SASSON, S. (1997) Estradiol-Binding Mechanism and Binding Capacity of the Human Estrogen Receptor Is Regulated by Tyrosine Phosphorylation. *Mol Endocrinol,* 11 (1): 48-53

ARNOLD, S. F., OBOURN, J. D., JAFFE, H. & NOTIDES, A. C. (1994) Serine 167 is the major estradiol-induced phosphorylation site on the human estrogen receptor. *Mol Endocrinol,* 8(9), 1208-14.

ARPINO, G., GUTIERREZ, C., WEISS, H., RIMAWI, M., MASSARWEH, S., BHARWANI, L., DE PLACIDO, S., OSBORNE, C. K. & SCHIFF, R. (2007) Treatment of Human Epidermal Growth Factor Receptor 2-Overexpressing Breast Cancer Xenografts With Multiagent HER-Targeted Therapy. *J Natl Cancer Inst,* 99(9), 694-705.

ARPINO, G., WIECHMANN, L., OSBORNE, C. K. & SCHIFF, R. (2008) Crosstalk between the Estrogen Receptor and the HER Tyrosine Kinase Receptor Family: Molecular Mechanism and Clinical Implications for Endocrine Therapy Resistance. *Endocr Rev,* 29(2), 217-33.

ATANASKOVA, N., KESHAMOUNI, V. G., KRUEGER, J. S., SCHWARTZ, J. A., MILLER, F. & REDDY, K. B. (2002) MAP kinase/estrogen receptor cross-talk enhances estrogen-mediated signaling and tumor growth but does not confer tamoxifen resistance. *Oncogene,* 21**,** 4000-8.

AXELROD, D., KOPPEL, D. E., SCHLESSINGER, J., ELSON, E. & WEBB, W. W. (1976) Mobility measurement by analysis of fluorescence photobleaching recovery kinetics. *Biophys J,* 16**,** 1055-69.

BARKHEM, T., CARLSSON, B., NILSSON, Y., ENMARK, E., GUSTAFSSON, J. & NILSSON, S. (1998) Differential response of estrogen receptor alpha and estrogen receptor beta to partial estrogen agonists/antagonists. *Mol Pharmacol,* 54**,** 105-12.

BELANDIA, B., ORFORD, R. L., HURST, H. C. & PARKER, M. G. (2002) Targeting of SWI/SNF chromatin remodelling complexes to estrogen-responsive genes. *Embo J,* 21**,** 4094-103.

BERAL, V., BULL, D. & REEVES, G. (2005) Endometrial cancer and hormone-replacement therapy in the Million Women Study. *Lancet,* 365**,** 1543-51.

BERNO, V., AMAZIT, L., HINOJOS, C., ZHONG, J., MANCINI, M. G., SHARP, Z. D. & MANCINI, M. A. (2008) Activation of estrogen receptor-alpha by E2 or EGF induces temporally distinct patterns of large-scale chromatin modification and mRNA transcription. *PLoS ONE,* 3**,** e2286.

BERRY, M., NUNEZ, A. M. & CHAMBON, P. (1989) Estrogen-responsive element of the human pS2 gene is an imperfectly palindromic sequence. *Proc Natl Acad Sci U S A,* 86**,** 1218-22.

BEYER, C., CANCHOLA, E. & LARSSON, K. (1981) Facilitation of lordosis behavior in the ovariectomized estrogen primed rat by dibutyryl cAMP. *Physiol Behav,* 26**,** 249-51.

BOLLIG, A. & MIKSICEK, R. J. (2000) An estrogen receptor-a splicing variant mediates both positive and negative effects on gene transcription. *Molecular Endocrinology,* 14**,** 634-649.

BOOKOUT, A. L., JEONG, Y., DOWNES, M., YU, R. T., EVANS, R. M. & MANGELSDORF, D. J. (2006) Anatomical profiling of nuclear receptor expression reveals a hierarchical transcriptional network. *Cell,* 126**,** 789-99.

BOURGUET, W., RUFF, M., CHAMBON, P., GRONEMEYER, H. & MORAS, D. (1995) Crystal structure of the ligand binding domain of the human nuclear receptor RXR-alpha. *Nature,* 375**,** 377-382.

BRANDENBERGER, A. W., TEE, M. K., LEE, J. Y., CHAO, V. & JAFFE, R. B. (1997) Tissue disribution of estrogen receptors alpha (ER-α) and beta (ER-β) mRNA in the midgestation human fetus. *Journal of Clinical Endocrinology and Metabolism,* 82**,** 3509-3512.

BRZOZOWSKI, A. M., PIKE, A. C. W., DAUTER, Z., HUBBARD, R. E., BONN, T., ENGSTROM, O., OHMAN, L., GREENE, G. L., GUSTAFSSON, J.-A. & CARLQUIST, M. (1997) Molecular basis of agonism and antagonism in the estrogen receptor. *Nature,* 389**,** 753-758.

BUNONE, G., BRIAND, P. A., MIKSICEK, R. J. & PICARD, D. (1996) Activation of the unliganded estrogen receptor by EGF involves the MAP kinase pathway and direct phosphorylation. *Embo J,* 15**,** 2174-83.

BURGER, H. G. (2000) Selective oestrogen receptor modulators. *Horm Res,* 53 Suppl 3**,** 25-9.

CAILLEAU, R., YOUNG, R., OLIVE, M. & REEVES, W. J., JR. (1974) Breast tumor cell lines from pleural effusions. *J Natl Cancer Inst,* 53**,** 661-74.

CAMPBELL, R. A., BHAT-NAKSHATRI, P., PATEL, N. M., CONSTANTINIDOU, D., ALI, S. & NAKSHATRI, H. (2001) Phosphatidylinositol 3-kinase/AKT-mediated activation of estrogen receptor alpha: a new model for anti-estrogen resistance. *J Biol Chem,* 276(13), 9817-24.

CAMPOS, H., SACKS, F. M., WALSH, B. W., SCHIFF, I., O'HANESIAN, M. A. & KRAUSS, R. M. (1993) Differential effects of estrogen on low-density lipoprotein subclasses in healthy postmenopausal women. *Metabolism,* 42**,** 1153-8.

CAMPOS, H., WALSH, B. W., JUDGE, H. & SACKS, F. M. (1997) Effect of estrogen on very low density lipoprotein and low density lipoprotein subclass

metabolism in postmenopausal women. *J Clin Endocrinol Metab,* 82**,** 3955-63.

CARPENTER, G., KING, L., JR. & COHEN, S. (1978) Epidermal growth factor stimulates phosphorylation in membrane preparations in vitro. *Nature,* 276**,** 409-10.

CARROLL, J. S. & BROWN, M. (2006) Estrogen receptor target gene: an evolving concept. *Mol Endocrinol,* 20**,** 1707-14.

CARROLL, J. S., LIU, X. S., BRODSKY, A. S., LI, W., MEYER, C. A., SZARY, A. J., EECKHOUTE, J., SHAO, W., HESTERMANN, E. V., GEISTLINGER, T. R., FOX, E. A., SILVER, P. A. & BROWN, M. (2005) Chromosome-wide mapping of estrogen receptor binding reveals long-range regulation requiring the forkhead protein FoxA1. *Cell,* 122**,** 33-43.

CATTORETTI, G., PILERI, S., PARRAVICINI, C., BECKER, M. H., POGGI, S., BIFULCO, C., KEY, G., D'AMATO, L., SABATTINI, E., FEUDALE, E. & *ET AL.* (1993) Antigen unmasking on formalin-fixed, paraffin-embedded tissue sections. *J Pathol,* 171**,** 83-98.

CENNI, B. & PICARD, D. (1999) Ligand-independent Activation of Steroid Receptors: New Roles for Old Players. *Trends Endocrinol Metab,* 10**,** 41-46.

CHAKRAVARTY, D., SRINIVASAN, R., GHOSH, S., GOPALAN, S., RAJWANSHI, A. & MAJUMDAR, S. (2007) Estrogen receptor beta1 and the beta2/betacx isoforms in nonneoplastic endometrium and in endometrioid carcinoma. *Int J Gynecol Cancer,* 17**,** 905-13.

CHANG, E. C., FRASOR, J., KOMM, B. & KATZENELLENBOGEN, B. S. (2006) Impact of estrogen receptor beta on gene networks regulated by estrogen receptor alpha in breast cancer cells. *Endocrinology,* 147**,** 4831-42.

CHEN, D., PACE, P. E., COOMBES, R. C. & ALI, S. (1999) Phosphorylation of Human Estrogen Receptor alpha by Protein Kinase A Regulates Dimerization. *Mol Cell Biol,* 19(2), 1002-15.

CHEN, D., RIEDL, T., WASHBROOK, E., PACE, P. E., COOMBES, R. C., EGLY, J. M. & ALI, S. (2000) Activation of estrogen receptor alpha by S118 phosphorylation involves a ligand-dependent interaction with TFIIH and participation of CDK7. *Mol Cell,* 6**,** 127-37.

CHEN, J. D. & EVANS, R. M. (1995) A transcriptional co-repressor that interacts with nuclear hormone receptors. *Nature,* 377**,** 454-7.

CHEN, S., BANGARU, M. L. Y., SNEADE, L., DUNCKLEY, J. A., BEN-JONATHAN, N. & KANSRA, S. (2009) Epidermal growth factor receptor cross-talks with ligand-occupied estrogen receptor-alpha to modulate both lactotroph proliferation and prolactin gene expression. *Am J Physiol Endocrinol Metab,* 297(2), E331-9.

CHENG, X. & HART, G. W. (2001) AlternativeO-Glycosylation/O-Phosphorylation of Serine-16 in Murine Estrogen Receptor Beta. POST-TRANSLATIONAL REGULATION OF TURNOVER AND TRANSACTIVATION ACTIVITY. *J. Biol. Chem,* 276, 10570-10575.

CHOBOTOVA, K., KARPOVICH, N., CARVER, J., MANEK, S., GULLICK, W. J., BARLOW, D. H. & MARDON, H. J. (2005) Heparin-Binding Epidermal Growth Factor and Its Receptors Mediate Decidualization and Potentiate Survival of Human Endometrial Stromal Cells. *The J of Clin Endocrinol & Metabol,* 90(2), 913-919.

CIECHANOVER, A. (1994) The ubiquitin-proteasome proteolytic pathway. *Cell,* 79**,** 13-21.

CITRI, A. & YARDEN, Y. (2006) EGF-ERBB signalling: towards the systems level. *Nat Rev Mol Cell Biol,* 7**,** 505-16.

CLEMONS, M. & GOSS, P. (2001) Estrogen and the risk of breast cancer. *N Engl J Med,* 344**,** 276-85.

COLE, N. B., SMITH, C. L., SCIAKY, N., TERASAKI, M., EDIDIN, M. & LIPPINCOTT-SCHWARTZ, J. (1996) Diffusional mobility of Golgi proteins in membranes of living cells. *Science,* 273**,** 797-801.

COLLINS, F., MACPHERSON, S., BROWN, P., BOMBAIL, V., WILLIAMS, A. R., ANDERSON, R. A., JABBOUR, H. N. & SAUNDERS, P. T. (2009) Expression of oestrogen receptors, ERalpha, ERbeta, and ERbeta variants, in endometrial cancers and evidence that prostaglandin F may play a role in regulating expression of ERalpha. *BMC Cancer,* 9**,** 330.

COUSE, J. F., CURTIS, S. W., WASHBURN, T. F., LINDZEY, J., GOLDING, T. S., LUBAHN, D. B., SMITHIES, O. & KORACH, K. S. (1995) Analysis of transcription and estrogen insensitivity in the female mouse after targeted disruption of the estrogen receptor gene. *Mol Endocrinol,* 9**,** 1441-1454.

COUSE, J. F. & KORACH, K. S. (1999) Estrogen receptor null mice: what have we learned and where will they lead us? *Endocr Rev,* 20**,** 358-417.

COWLEY, S. M., HOARE, S., MOSSELMAN, S. & PARKER, M. G. (1997) Estrogen receptors alpha and beta form heterodimers on DNA. *J Biol Chem,* 272**,** 19858-62.

COWLEY, S. M. & PARKER, M. G. (1999) A comparison of transcriptional activation by ER alpha and ER beta. *J Steroid Biochem Mol Biol,* 69**,** 165-75.

CRITCHLEY, H. O., HENDERSON, T. A., KELLY, R. W., SCOBIE, G. S., EVANS, L. R., GROOME, N. P. & SAUNDERS, P. T. (2002) Wild-type estrogen receptor (ERbeta1) and the splice variant (ERbetacx/beta2) are both expressed within the human endometrium throughout the normal menstrual cycle. *J Clin Endocrinol Metab,* 87**,** 5265-73.

CRITCHLEY, H. O. D. (2000) Endometrial steroid receptor expression throughout the menstrual cycle. IN O'BRIEN, P. M. S., CAMERON, I. T. & MACLEAN, A. (Eds.) *Disorders of the Menstrual Cycle.* London, RCOG Press.

CRITCHLEY, H. O. D., BRENNER, R. M., HENDERSON, T. A., WILLIAMS, K., NAYAK, N. R., SLAYDEN, O. D., MILLAR, M. R. & SAUNDERS, P. T. K. (2001) Estrogen receptor beta, but not estrogen receptor alpha, is present in the vascular endothelium of the human and nonhuman primate endometrium. *J Clin Endocrinol Metab,* 86**,** 1370-8.

CUI, Y., ZHANG, M., PESTELL, R., CURRAN, E. M., WELSHONS, W. V. & FUQUA, S. A. W. (2004) Phosphorylation of Estrogen Receptor alpha Blocks Its Acetylation and Regulates Estrogen Sensitivity. *Cancer Res,* 64; 9199.

DAMDIMOPOULOS, A. E., SPYROU, G. & GUSTAFSSON, J. A. (2008) Ligands differentially modify the nuclear mobility of estrogen receptors alpha and beta. *Endocrinology,* 149**,** 339-45.

DAUVOIS, S., WHITE, R. & PARKER, M. (1993) The antiestorgen ICI 182780 disrupts estrogen receptor nucleocytoplasmic shuttling. *Journal of Cell Science,* 106**,** 1377-1388.

DAVIES, M. P., O'NEILL P, A., INNES, H., SIBSON, D. R., PRIME, W., HOLCOMBE, C. & FOSTER, C. S. (2004) Correlation of mRNA for oestrogen receptor beta splice variants ERbeta1, ERbeta2/ERbetacx and ERbeta5 with outcome in endocrine-treated breast cancer. *J Mol Endocrinol,* 33**,** 773-782.

DEFRANCO, D. B. & GUERRERO, J. (2000) Nuclear matrix targeting of steroid receptors: specific signal sequences and acceptor proteins. *Crit Rev Eukaryot Gene Expr,* 10**,** 39-44.

DENGER, S., REID, G., BRAND, H., KOS, M. & GANNON, F. (2001a) Tissue-specific expression of human ERalpha and ERbeta in the male. *Mol Cell Endocrinol,* 178**,** 155-60.

DENGER, S., REID, G., KOS, M., FLOURIOT, G., PARSCH, D., BRAND, H., KORACH, K. S., SONNTAG-BUCK, V. & GANNON, F. (2001b) ERalpha gene expression in human primary osteoblasts: evidence for the expression of two receptor proteins. *Mol Endocrinol,* 15**,** 2064-77.

DEROO, B. J. & ARCHER, T. K. (2002) Proteasome Inhibitors Reduce Luciferase and Beta-Galactosidase Activity in Tissue Culture Cells. *The Journal of Biological Chemistry, 277, 20120-20123.*

DEROO, B. J. & KORACH, K. S. (2006) Estrogen receptors and human disease. *J Clin Invest,* 116**,** 561-70.

DRISCOLL, M. D., SATHYA, G., MUYAN, M., KLINGE, C. M., HILF, R. & BAMBARA, R. A. (1998) Sequence requirements for estrogen receptor binding to estrogen response elements. *J Biol Chem,* 273**,** 29321-30.

DUPONT, S., KRUST, A., GANSMULLER, A., DIERICH, A., CHAMBON, P. & MARK, M. (2000) Effect of single and compound knockouts of estrogen receptors alpha (ERalpha) and beta (ERbeta) on mouse reproductive phenotypes. *Development,* 127**,** 4277-91.

EGAN, K. M., LAWSON, J. A., FRIES, S., KOLLER, B., RADER, D. J., SMYTH, E. M. & FITZGERALD, G. A. (2004) COX-2-derived prostacyclin confers atheroprotection on female mice. *Science,* 306**,** 1954-7.

EJSKJÆR, K., SØRENSEN, B. S., POULSEN, S. S., FORMAN, A., NEXØ, E. & MOGENSEN, O. (2007) Expression of the epidermal growth factor system in endometrioid endometrial cancer. *Gynecologic Oncology,* 104**,** 158-167.

EJSKJAER, K., SORENSEN, B. S., POULSEN, S. S., MOGENSEN, O., FORMAN, A. & NEXO, E. (2005) Expression of the epidermal growth factor system in human endometrium during the menstrual cycle. *Mol Hum Reprod,* 11(8), 543-51.

ENDOH, H., MARUYAMA, K., MASUHIRO, Y., KOBAYASHI, Y., GOTO, M., TAI, H., YANAGISAWA, J., METZGER, D., HASHIMOTO, S. & KATO, S. (1999) Purification and identification of p68 RNA helicase acting as a transcriptional coactivator specific for the activation function 1 of human estrogen receptor alpha. *Mol Cell Biol,* 19**,** 5363-72.

ENMARK, E., PELTO-HUIKKO, M., GRANDIEN, K., LAGERCRANTZ, S., LAGERCRANTZ, J., FRIED, G., NORDENSKJOLD, M. & GUSTAFSSON, J. A. (1997) Human estrogen receptor beta-gene structure, chromosomal localization, and expression pattern. *J Clin Endocrinol Metab,* 82**,** 4258-65.

ESCRIVA, H., DELAUNAY, F. & LAUDET, V. (2000) Ligand binding and nuclear receptor evolution. *Bioessays,* 22**,** 717-27.

ESSLIMANI-SAHLA, M., KRAMAR, A., SIMONY-LAFONTAINE, J., WARNER, M., GUSTAFSSON, J. A. & ROCHEFORT, H. (2005) Increased estrogen receptor betacx expression during mammary carcinogenesis. *Clin Cancer Res,* 11**,** 3170-4.

FAN, M., NAKSHATRI, H. & NEPHEW, K. P. (2004) Inhibiting Proteasomal Proteolysis Sustains Estrogen Receptor-alpha Activation. *Mol Endocrinol,* 18(11), 2603-15.

FERENCZY, A. (1993) Ultrastructure of the normal menstrual cycle: a review. *Microsc Res Tech,* 25**,** 91-105.

FISHER, B., COSTANTINO, J. P., REDMOND, C. K., FISHER, E. R., WICKERHAM, D. L. & CRONIN, W. M. (1994) Endometrial cancer in tamoxifen-treated breast cancer patients: findings from the National Surgical Adjuvant Breast and Bowel Project (NSABP) B-14. *J Natl Cancer Inst,* 86**,** 527-37.

FISHER, C. R., GRAVES, K. H., PARLOW, A. F. & SIMPSON, E. R. (1998) Characterization of mice deficient in aromatase (ArKO) because of targeted disruption of the cyp19 gene. *Proc Natl Acad Sci U S A,* 95**,** 6965-70.

FLOURIOT, G., BRAND, H., DENGER, S., METIVIER, R., KOS, M., REID, G., SONNTAG-BUCK, V. & GANNON, F. (2000) Identification of a new isoform of the human estrogen receptor-alpha (hER-alpha) that is encoded by distinct transcripts and that is able to repress hER-alpha activation function 1. *Embo J,* 19**,** 4688-700.

FONT DE MORA, J. & BROWN, M. (2000) AIB1 is a conduit for kinase-mediated growth factor signaling to the estrogen receptor. *Mol Cell Biol,* 20**,** 5041-7.

FORCE, T. & BONVENTRE, J. V. (1998) Growth Factors and Mitogen-Activated Protein Kinases. *Hypertension,* 31, 152-161.

FORMAN, B. M. & SAMUELS, H. H. (1990) Interactions among a subfamily of nuclear hormone receptors: the regulatory zipper model. *Molecular Endocrinology,* 4**,** 1293-1301.

FUJIMURA, T., TAKAHASHI, S., URANO, T., OGAWA, S., OUCHI, Y., KITAMURA, T., MURAMATSU, M. & INOUE, S. (2001) Differential expression of estrogen receptor beta (ERbeta) and its C-terminal truncated splice variant ERbetacx as prognostic predictors in human prostatic cancer. *Biochem Biophys Res Commun,* 289**,** 692-9.

FUQUA, S. A., SCHIFF, R., PARRA, I., MOORE, J. T., MOHSIN, S. K., OSBORNE, C. K., CLARK, G. M. & ALLRED, D. C. (2003) Estrogen receptor beta protein in human breast cancer: correlation with clinical tumor parameters. *Cancer Res,* 63**,** 2434-9.

GBURCIK, V., BOT, N., MAGGIOLINI, M. & PICARD, D. (2005) SPBP Is a Phosphoserine-Specific Repressor of Estrogen Receptor alpha. *Mol Cell Biol,* 25(9), 3421-30.

GEHM, B. D., MCANDREWS, J. M., JORDAN, V. C. & JAMESON, J. L. (2000) EGF activates highly selective estrogen-responsive reporter plasmids by an ER-independent pathway. *Mol Cell Endocrinol,* 159**,** 53-62.

GERMAIN, P., STAELS, B., DACQUET, C., SPEDDING, M. & LAUDET, V. (2006) Overview of nomenclature of nuclear receptors. *Pharmacol Rev,* 58**,** 685-704.

GIGUERE, V. (1999) Orphan nuclear receptors: from gene to function. *Endocr Rev,* 20**,** 689-725.

GILL, G. & PTASHNE, M. (1988) Negative effect of the transcriptional activator GAL4. *Nature,* 334**,** 721-4.

GOLDSTEIN, S. R., SCHEELE, W. H., RAJAGOPALAN, S. K., WILKIE, J. L., WALSH, B. W. & PARSONS, A. K. (2000) A 12-month comparative study of raloxifene, estrogen, and placebo on the postmenopausal endometrium. *Obstet Gynecol,* 95**,** 95-103.

GOUGELET, A., MUELLER, S. O., KORACH, K. S. & RENOIR, J. M. (2007) Oestrogen receptors pathways to oestrogen responsive elements: the

transactivation function-1 acts as the keystone of oestrogen receptor (ER)beta-mediated transcriptional repression of ERalpha. *J Steroid Biochem Mol Biol,* 104**,** 110-22.

GRANDIEN, K. (1996) Determination of transcription start sites in the human estrogen receptor gene and identification of a novel, tissue-specific, estrogen receptor-mRNA isoform. *Mol Cell Endocrinol,* 116**,** 207-12.

GREEN, S., WALTER, P., GREENE, G., KRUST, A., GOFFIN, C., JENSEN, E., SCRACE, G., WATERFIELD, M. & CHAMBON, P. (1986a) Cloning of the human oestrogen receptor cDNA. *J Steroid Biochem,* 24**,** 77-83.

GREEN, S., WALTER, P., KUMAR, V., KRUST, A., BORNERT, J. M., ARGOS, P. & CHAMBON, P. (1986b) Human oestrogen receptor cDNA: sequence, expression and homology to v-erb-A. *Nature,* 320**,** 134-9.

GREENE, G. L., GILNA, P., WATERFIELD, M., BAKER, A., HORT, Y. & SHINE, J. (1986) Sequence and expression of human estrogen receptor complementary DNA. *Science,* 231**,** 1150-4.

GRIEKSPOOR, A., ZWART, W., NEEFJES, J. & MICHALIDES, R. (2007) Visualizing the action of steroid hormone receptors in living cells. *Nucl Recept Signal,* 5**,** e003.

GU, Q., KORACH, K. S. & MOSS, R. L. (1999) Rapid action of 17beta-estradiol on kainate-induced currents in hippocampal neurons lacking intracellular estrogen receptors. *Endocrinology,* 140**,** 660-6.

GUETTA, V. & CANNON, R. O., 3RD (1996) Cardiovascular effects of estrogen and lipid-lowering therapies in postmenopausal women. *Circulation,* 93**,** 1928-37.

GUTIERREZ, M. C., DETRE, S., JOHNSTON, S., MOHSIN, S. K., SHOU, J., ALLRED, D. C., SCHIFF, R., OSBORNE, C. K. & DOWSETT, M. (2005) Molecular Changes in Tamoxifen-Resistant Breast Cancer: Relationship Between Estrogen Receptor, HER-2, and p38 Mitogen-Activated Protein Kinase. *J Clin Oncol,* 23(11), 2469-76

GUY, P. M., PLATKO, J. V., CANTLEY, L. C., CERIONE, R. A. & CARRAWAY, K. L. (1994) Insect cell-expressed p180erbB3 possesses an impaired tyrosine kinase activity. *Proc Natl Acad Sci U S A,* 91(17), 8132–8136.

HAFNER, F., HOLLER, E. & VON ANGERER, E. (1996) Effect of growth factors on estrogen receptor mediated gene expression. *J Steroid Biochem Mol Biol,* 58**,** 385-93.

HAGER, G. L., NAGAICH, A. K., JOHNSON, T. A., WALKER, D. A. & JOHN, S. (2004) Dynamics of nuclear receptor movement and transcription. *Biochim Biophys Acta,* 1677**,** 46-51.

HALE, G. E., HUGHES, C. L. & CLINE, J. M. (2002) Endometrial cancer: hormonal factors, the perimenopausal "window of risk," and isoflavones. *J Clin Endocrinol Metab,* 87**,** 3-15.

HALL, J. M., COUSE, J. F. & KORACH, K. S. (2001) The multifaceted mechanisms of estradiol and estrogen receptor signaling. *J Biol Chem,* 276**,** 36869-72.

HALL, J. M. & MCDONNELL, D. P. (2005) Coregulators in nuclear estrogen receptor action: from concept to therapeutic targeting. *Mol Interv,* 5**,** 343-57.

HALL, J. M. & MCDONNELL, D. P. (1999) The estrogen receptor beta-isoform (ERbeta) of the human estrogen receptor modulates ERalpha transcriptional activity and is a key regulator of the cellular response to estrogens and antiestrogens. *Endocrinology,* 140**,** 5566-78.

HALL, M. J. & KORACH, K. S. (2002) Analysis of the molecular mechanisms of human estrogen receptors a and β reveals differential specificity in target

promoter regulation by xenoestrogens. *Journal of Biological Chemistry,* 277**,** 44455-44461.

HAMELERS, I. H. & STEENBERGH, P. H. (2003) Interactions between estrogen and insulin-like growth factor signaling pathways in human breast tumor cells. *Endocr Relat Cancer,* 10**,** 331-45.

HARRIS, H. A., BAPAT, A. R., GONDER, D. S. & FRAIL, D. E. (2002) The ligand binding profiles of estrogen receptors alpha and beta are species dependent. *Steroids,* 67**,** 379-84.

HARRIS, R. C., CHUNG, E. & COFFEY, R. J. (2003) EGF receptor ligands. *Exp Cell Res,* 284**,** 2-13.

HEERY, D. M., HOARE, S., HUSSAIN, S., PARKER, M. G. & SHEPPARD, H. (2001) Core LXXLL motif sequences in CREB-binding protein, SRC-1, and RIP140 define affinity and selectivity for steroid and retinoid receptors. *J Biol Chem,* 276**,** 6695-702.

HEERY, D. M., KALKHOVEN, E., HOARE, S. & PARKER, M. G. (1997) A signature motif in transcriptional co-activators mediates binding to nuclear receptors. *Nature,* 387**,** 733-736.

HELDRING, N., PIKE, A., ANDERSSON, S., MATTHEWS, J., CHENG, G., HARTMAN, J., TUJAGUE, M., STROM, A., TREUTER, E., WARNER, M. & GUSTAFSSON, J. A. (2007) Estrogen receptors: how do they signal and what are their targets. *Physiol Rev,* 87**,** 905-31.

HELLEN, E. H. A. A. D. (1991) Kinetics of Epidermal Growth Factor/Receptor Binding on Cells Measured by Total Internal Reflection/Fluorescence Recovery After Photobleaching. *Journal of Fluorescence,* 1(2), 113-28.

HENDERSON, T. A., SAUNDERS, P. T., MOFFETT-KING, A., GROOME, N. P. & CRITCHLEY, H. O. (2003) Steroid receptor expression in uterine natural killer cells. *J Clin Endocrinol Metab,* 88**,** 440-9.

HENTTU, P. M., KALKHOVEN, E. & PARKER, M. G. (1997) AF-2 activity and recruitment of steroid receptor coactivator 1 to the estrogen receptor depend on a lysine residue conserved in nuclear receptors. *Mol Cell Biol,* 17**,** 1832-9.

HEWITT, S. C. & KORACH, K. S. (2002) Estrogen receptors: structure, mechanisms and function. *Rev Endocr Metab Disord,* 3**,** 193-200.

HEWITT, S. C. & KORACH, K. S. (2003) Oestrogen receptor knockout mice: roles for oestrogen receptors alpha and beta in reproductive tissues. *Reproduction,* 125**,** 143-9.

HILLISCH, A., PETERS, O., KOSEMUND, D., MULLER, G., WALTER, A., SCHNEIDER, B., REDDERSEN, G., ELGER, W. & FRITZEMEIER, K.-H. (2004) Dissecting physiological roles of estrogen receptor a and β with potent selective ligands from structure based design. *Mol Endocrinol,* 18**,** 1599-1609.

HODGIN, J. B., KREGE, J. H., REDDICK, R. L., KORACH, K. S., SMITHIES, O. & MAEDA, N. (2001) Estrogen receptor alpha is a major mediator of 17beta-estradiol's atheroprotective effects on lesion size in Apoe-/- mice. *J Clin Invest,* 107**,** 333-40.

HOLLI, K. (2002) Tamoxifen versus toremifene in the adjuvant treatment of breast cancer. *Eur J Cancer,* 38 Suppl 6**,** S37-8.

HOMBACH-KLONISCH, S., KEHLEN, A., FOWLER, P. A., HUPPERTZ, B., JUGERT, J. F., BISCHOFF, G., SCHLUTER, E., BUCHMANN, J. & KLONISCH, T. (2005) Regulation of functional steroid receptors and ligand-induced responses in telomerase-immortalized human endometrial epithelial cells. *J Mol Endocrinol,* 34**,** 517-34.

HORLEIN, A. J., NAAR, A. M., HEINZEL, T., TORCHIA, J., GLOSS, B., KUROKAWA, R., RYAN, A., KAMEI, Y., SODERSTROM, M., GLASS, C. K. & ROSENFELD M. G. (1995) Ligand-independent repression by the thyroid hormone receptor mediated by a nuclear receptor co-repressor. *Nature,* 377**,** 397-404.

HOUTSMULLER, A. B. & VERMEULEN, W. (2001) Macromolecular dynamics in living cell nuclei revealed by fluorescence redistribution after photobleaching. *Histochem Cell Biol,* 115**,** 13-21.

HOWELL, A., DEFRIEND, D., ROBERTSON, J., BLAMEY, R. & WALTON, P. (1995) Response to a specific antioestrogen (ICI 182780) in tamoxifen-resistant breast cancer. *Lancet,* 345**,** 29-30.

HOWELL, A., ROBERTSON, J. F., QUARESMA ALBANO, J., ASCHERMANNOVA, A., MAURIAC, L., KLEEBERG, U. R., VERGOTE, I., ERIKSTEIN, B., WEBSTER, A. & MORRIS, C. (2002) Fulvestrant, formerly ICI 182,780, is as effective as anastrozole in postmenopausal women with advanced breast cancer progressing after prior endocrine treatment. *J Clin Oncol,* 20**,** 3396-403.

HTUN, H., HOLTH, L. T., WALKER, D., DAVIE, J. R. & HAGER, G. L. (1999) Direct visualization of the human estrogen receptor alpha reveals a role for ligand in the nuclear distribution of the receptor. *Mol Biol Cell,* 10**,** 471-86.

HU, X. & LAZAR, M. A. (1999) The CoRNR motif controls the recruitment of corepressors by nuclear hormone receptors. *Nature,* 402**,** 93-6.

HU, X. & LAZAR, M. A. (2000) Transcriptional repression by nuclear hormone receptors. *Trends Endocrinol Metab,* 11**,** 6-10.

IGNAR-TROWBRIDGE, D. M., NELSON, K. G., BIDWELL, M. C., CURTIS, S. W., WASHBURN, T. F., MCLACHLAN, J. A. & KORACH, K. S. (1992) Coupling of dual signaling pathways: epidermal growth factor action involves the estrogen receptor. *Proc Natl Acad Sci U S A,* 89(10), 4658-4662.

IGNAR-TROWBRIDGE, D. M., PIMENTEL, M., PARKER, M. G., MCLACHLAN, J. A. & KORACH, K. S. (1996) Peptide growth factor cross-talk with the estrogen receptor requires the A/B domain and occurs independently of protein kinase C or estradiol. *Endocrinology,* 137**,** 1735-44.

IKEDA, K., OGAWA, S., TSUKUI, T., HORIE-INOUE, K., OUCHI, Y., KATO, S., MURAMATSU, M. & INOUE, S. (2004) Protein Phosphatase 5 Is a Negative Regulator of Estrogen Receptor-Mediated Transcription. *Mol Endocrinol,* 18(5), 1131-43.

IMHOF, M. O. & MCDONNELL, D. P. (1996) Yeast RSP5 and its human homolog hRPF1 potentiate hormone-dependent activation of transcription by human progesterone and glucocorticoid receptors. *Mol Cell Biol,* 16**,** 2594-605.

INOUE, S., OGAWA, S., HORIE, K., HOSHINO, S., GOTO, W., HOSOI, T., TSUTSUMI, O., MURAMATSU, M. & OUCHI, Y. (2000) An estrogen receptor beta isoform that lacks exon 5 has dominant negative activity on both ERalpha and ERbeta. *Biochem Biophys Res Commun,* 279**,** 814-9.

JABBOUR, H. N., KELLY, R. W., FRASER, H. M. & CRITCHLEY, H. O. (2006) Endocrine regulation of menstruation. *Endocr Rev,* 27**,** 17-46.

JACKSON, T. A., RICHER, J. K., BAIN, D. L., TAKIMOTO, G. S., TUNG, L. & HORWITZ, K. B. (1997) The partial agonist activity of antagonist-occupied steroid receptors is controlled by a novel hinge domain-binding coactivator L7/SPA and the corepressors N-CoR or SMRT. *Mol Endocrinol,* 11**,** 693-705.

JAKACKA, M., ITO, M., WEISS, J., CHIEN, P. Y., GEHM, B. D. & JAMESON, J. L. (2001) Estrogen receptor binding to DNA is not required for its activity through the nonclassical AP1 pathway. *J Biol Chem,* 276**,** 13615-21.

JARVINEN, T. A., PELTO-HUIKKO, M., HOLLI, K. & ISOLA, J. (2000) Estrogen receptor beta is coexpressed with ERalpha and PR and associated with nodal status, grade, and proliferation rate in breast cancer. *Am J Pathol,* 156**,** 29-35.

JELINEK, T., DENT, P., STURGILL, T. W. & WEBER, M. J. (1996) Ras-induced activation of Raf-1 is dependent on tyrosine phosphorylation. *Mol Cell Biol,* 16**,** 1027-34.

JENSEN E. V., JACOBSON H. I. (1962) Basic guides to the mechanism of estrogen action. *Recent Prog. Horm. Res,* 18**,** 387-414.

JENTSCH, S. (1992) The ubiquitin-conjugation system. *Annu Rev Genet,* 26**,** 179-207.

JOEL, P. B., SMITH, J., STURGILL, T. W., FISHER, T. L., BLENIS, J. & LANNIGAN, D. A. (1998a) pp90rsk1 regulates estrogen receptor-mediated transcription through phosphorylation of Ser-167. *Mol Cell Biol,* 18**,** 1978-84.

JOEL, P. B., TRAISH, A. M. & LANNIGAN, D. A. (1995) Estradiol and phorbol ester cause phosphorylation of serine 118 in the human estrogen receptor. *Mol Endocrinol,* 9**,** 1041-52.

JOEL, P. B., TRAISH, A. M. & LANNIGAN, D. A. (1998b) Estradiol-induced phosphorylation of serine 118 in the estrogen receptor is independent of p42/p44 mitogen-activated protein kinase. *J Biol Chem,* 273**,** 13317-23.

KALKHOVEN, E., VALENTINE, J. E., HEERY, D. M. & PARKER, M. G. (1998) Isoforms of steroid receptor co-activator 1 differ in their ability to potentiate transcription by the oestrogen receptor. *Embo J,* 17**,** 232-43.

KATO, S., ENDOH, H., MASUHIRO, Y., KITAMOTO, T., UCHIYAMA, S., SASAKI, H., MASUSHIGE, S., GOTOH, Y., NISHIDA, E., KAWASHIMA, H., METZGER, D. & CHAMBON, P. (1995) Activation of the estrogen receptor through phosphorylation by mitogen-activated protein kinase. *Science,* 270**,** 1491-4.

KATZENELLENBOGEN, B. S., CHOI, I., DELAGE-MOURROUX, R., EDIGER, T. R., MARTINI, P. G., MONTANO, M., SUN, J., WEIS, K. & KATZENELLENBOGEN, J. A. (2000) Molecular mechanisms of estrogen action: selective ligands and receptor pharmacology. *J Steroid Biochem Mol Biol,* 74**,** 279-85.

KATZENELLENBOGEN, B. S. & NORMAN, M. J. (1990) Multihormonal regulation of the progesterone receptor in MCF-7 human breast cancer cells: interrelationships among insulin/insulin-like growth factor-I, serum, and estrogen. *Endocrinology,* 126**,** 891-8.

KATZENELLENBOGEN, J. A. & KATZENELLENBOGEN, B. S. (1996) Nuclear hormone receptors: ligand-activated regulators of transcription and diverse cell responses. *Chem Biol,* 3**,** 529-36.

KATZENELLENBOGEN, J. A., MUTHYALA R. AND KATZENELLENBOGEN B.S. (2003) The nature of the ligand-binding pocket of estrogen receptor alpha and beta: The search for subtype-selective ligands and implications for the prediction of estrogenic activity. *Pure and Applied Chemistry,* 75**,** 7.

KEAVENEY, M., KLUG, J., DAWSON, M. T., NESTOR, P. V., NEILAN, J. G., FORDE, R. C. & GANNON, F. (1991) Evidence for a previously unidentified upstream exon in the human oestrogen receptor gene. *J Mol Endocrinol,* 6**,** 111-5.

KIM, J. H., LI, H. & STALLCUP, M. R. (2003) CoCoA, a nuclear receptor coactivator which acts through an N-terminal activation domain of p160 coactivators. *Mol Cell,* 12**,** 1537-49.

KIRKEGAARD, T., MCGLYNN, L. M., CAMPBELL, F. M., MÃ¼LLER, S., TOVEY, S. M., DUNNE, B., NIELSEN, K. V., COOKE, T. G. & BARTLETT, J. M. S. (2007) Amplified in breast cancer 1 in human epidermal growth factor receptor-positive tumors of tamoxifen-treated breast cancer patients. *Clinical Cancer Research,* 13; 1405.

KLAPPER, L. N., GLATHE, S., VAISMAN, N., HYNES, N. E., ANDREWS, G. C., SELA, M. & YARDEN, Y. (1999) The ErbB-2/HER2 oncoprotein of human carcinomas may function solely as a shared coreceptor for multiple stroma-derived growth factors. *Proc Natl Acad Sci U S A,* 96(9), 4995-5000.

KLEIN-HITPASS, L., RYFFEL, G. U., HEITLINGER, E. & CATO, A. C. (1988) A 13 bp palindrome is a functional estrogen responsive element and interacts specifically with estrogen receptor. *Nucleic Acids Res,* 16**,** 647-63.

KLINGE, C. M. (2000) Estrogen receptor interaction with co-activators and co-repressors. *Steroids,* 65**,** 227-251.

KLINGE, C. M. (2001) Estrogen receptor interaction with estrogen response elements. *Nucleic Acids Res,* 29**,** 2905-19.

KLOTZ, D. M., HEWITT, S. C., CIANA, P., RAVISCIONI, M., LINDZEY, J. K., FOLEY, J., MAGGI, A., DIAUGUSTINE, R. P. & KORACH, K. S. (2002) Requirement of estrogen receptor-alpha in insulin-like growth factor-1 (IGF-1)-induced uterine responses and in vivo evidence for IGF-1/estrogen receptor cross-talk. *J Biol Chem,* 277**,** 8531-7.

KNOWLDEN, J. M., HUTCHESON, I. R., JONES, H. E., MADDEN, T., GEE, J. M. W., HARPER, M. E., BARROW, D., WAKELING, A. E. & NICHOLSON, R. I. (2003) Elevated Levels of Epidermal Growth Factor Receptor/c-erbB2 Heterodimers Mediate an Autocrine Growth Regulatory Pathway in Tamoxifen-Resistant MCF-7 Cells. *Endocrinology* 144(3), 1032-1044.

KOUSTENI, S., BELLIDO, T., PLOTKIN, L. I., O'BRIEN, C. A., BODENNER, D. L., HAN, L., HAN, K., DIGREGORIO, G. B., KATZENELLENBOGEN, J. A., KATZENELLENBOGEN, B. S., ROBERSON, P. K., WEINSTEIN, R. S., JILKA, R. L. & MANOLAGAS, S. C. (2001) Nongenotropic, sex-nonspecific signaling through the estrogen or androgen receptors: dissociation from transcriptional activity. *Cell,* 104**,** 719-30.

KREGE, J. H., HODGIN, J. B., COUSE, J. F., ENMARK, E., WARNER, M., MAHLER, J. F., SAR, M., KORACH, K. S., GUSTAFSSON, J. A. & SMITHIES, O. (1998) Generation and reproductive phenotypes of mice lacking estrogen receptor beta. *Proc Natl Acad Sci U S A,* 95**,** 15677-82.

KRIKUN, G., SCHATZ, F., TAYLOR, R., CRITCHLEY, H. O., ROGERS, P. A., HUANG, J. & LOCKWOOD, C. J. (2005) Endometrial endothelial cell steroid receptor expression and steroid effects on gene expression. *J Clin Endocrinol Metab,* 90**,** 1812-8.

KRISHNAN, V., PORTER, W., SANTOSTEFANO, M., WANG, X. & SAFE, S. (1995) Molecular mechanism of inhibition of estrogen-induced cathepsin D gene expression by 2,3,7,8-tetrachlorodibenzo-p-dioxin (TCDD) in MCF-7 cells. *Mol Cell Biol,* 15**,** 6710-9.

KRISTENSEN, V. N. & BORRESEN-DALE, A. L. (2000) Molecular epidemiology of breast cancer: genetic variation in steroid hormone metabolism. *Mutat Res,* 462**,** 323-33.

KUIPER, G. G., ENMARK, E., PELTO-HUIKKO, M., NILSSON, S. & GUSTAFSSON, J. A. (1996) Cloning of a novel receptor expressed in rat prostate and ovary. *Proc Natl Acad Sci U S A,* 93**,** 5925-30.

KUROKAWA, H., LENFERINK, A. E., SIMPSON, J. F., PISACANE, P. I., SLIWKOWSKI, M. X., FORBES, J. T. & ARTEAGA, C. L. (2000) Inhibition of HER2/neu (erbB-2) and mitogen-activated protein kinases enhances tamoxifen action against HER2-overexpressing, tamoxifen-resistant breast cancer cells. *Cancer Res.* 60(20), 5887-94.

KURZER, M. S. & XU, X. (1997) Dietary phytoestrogens. *Annu Rev Nutr,* 17**,** 353-81.

KUSHNER, P. J., AGARD, D. A., GREENE, G. L., SCANLAN, T. S., SHIAU, A. K., UHT, R. M. & WEBB, P. (2000) Estrogen receptor pathways to AP-1. *Journal of Steroid Biochemistry and Molecular Biology,* 74**,** 311-317.

LAHM, T., CRISOSTOMO, P. R., MARKEL, T. A., WANG, M., WANG, Y., TAN, J. & MELDRUM, D. R. (2008) Selective estrogen receptor-alpha and estrogen receptor-beta agonists rapidly decrease pulmonary artery vasoconstriction by a nitric oxide-dependent mechanism. *Am J Physiol Regul Integr Comp Physiol,* 295**,** R1486-93.

LANNIGAN, D. A. (2003) Estrogen receptor phosphorylation. *Steroids* 68(1), 1-9.

LANZ, R. B., MCKENNA, N. J., ONATE, S. A., ALBRECHT, U., WONG, J., TSAI, S. Y., TSAI, M. J. & O'MALLEY, B. W. (1999) A steroid receptor coactivator, SRA, functions as an RNA and is present in an SRC-1 complex. *Cell,* 97**,** 17-27.

LAVINSKY, R. M., JEPSEN, K., HEINZEL, T., TORCHIA, J., MULLEN, T. M., SCHIFF, R., DEL-RIO, A. L., RICOTE, M., NGO, S., GEMSCH, J., HILSENBECK, S. G., OSBORNE, C. K., GLASS, C. K., ROSENFELD, M. G. & ROSE, D. W. (1998) Diverse signaling pathways modulate nuclear receptor recruitment of N-CoR and SMRT complexes. *Proc Natl Acad Sci U S A,* 95**,** 2920-5.

LE GOFF, P., MONTANO, M. M., SCHODIN, D. J. & KATZENELLENBOGEN, B. S. (1994) Phosphorylation of the human estrogen receptor. Identification of hormone-regulated sites and examination of their influence on transcriptional activity. *J Biol Chem,* 269**,** 4458-66.

LECCE, G., MEDURI, G., ANCELIN, M., BERGERON, C. & PERROT-APPLANAT, M. (2001) Presence of estrogen receptor beta in the human endometrium through the cycle: expression in glandular, stromal, and vascular cells. *Journal of Clinical Endocrinology and Metabolism,* 86**,** 1379-86.

LEE, H. & BAI, W. (2002) Regulation of Estrogen Receptor Nuclear Export by Ligand-Induced and p38-Mediated Receptor Phosphorylation. *Mol Cell Biol,* 22(16), 5835-45.

LEUNG, Y. K., MAK, P., HASSAN, S. & HO, S. M. (2006) Estrogen receptor (ER)-beta isoforms: a key to understanding ER-beta signaling. *Proc Natl Acad Sci U S A,* 103**,** 13162-7.

LEVIN, E. R. (2003) Bidirectional Signaling between the Estrogen Receptor and the Epidermal Growth Factor Receptor. *Mol Endocrinol,* 17**,** 309-17.

LEVIN, E. R. (2009) Plasma membrane estrogen receptors. *Trends Endocrinol Metab,* 20**,** 477-82.

LEYGUE, E., DOTZLAW, H., WATSON, P. H. & MURPHY, L. C. (1999a) Altered expression of estrogen receptor-alpha variant messenger RNAs between

adjacent normal breast and breast tumor tissues. *Breast Cancer Research,* 2**,** 64-72.

LEYGUE, E., DOTZLAW, H., WATSON, P. H. & MURPHY, L. C. (1999b) Expression of estrogen receptor beta1, beta2, and beta5 messenger RNAs in human breast tissue. *Cancer Res,* 59(6), 1175-9.

LI, L., HAYNES, M. P. & BENDER, J. R. (2003) Plasma membrane localization and function of the estrogen receptor alpha variant (ER46) in human endothelial cells. *Proc Natl Acad Sci U S A,* 100**,** 4807-12.

LI, X., HUANG, J., YI, P., BAMBARA, R. A., HILF, R. & MUYAN, M. (2004) Single-chain estrogen receptors (ERs) reveal that the ERalpha/beta heterodimer emulates functions of the ERalpha dimer in genomic estrogen signaling pathways. *Mol Cell Biol,* 24**,** 7681-94.

LIKHITE, V. S., STOSSI, F., KIM, K., KATZENELLENBOGEN, B. S. & KATZENELLENBOGEN, J. A. (2006) Kinase-specific phosphorylation of the estrogen receptor changes receptor interactions with ligand, deoxyribonucleic acid, and coregulators associated with alterations in estrogen and tamoxifen activity. *Mol Endocrinol,* 20**,** 3120-32.

LIM, W., CHO, J., KWON, H. Y., PARK, Y., RHYU, M. R. & LEE, Y. (2009) Hypoxia-inducible factor 1 alpha activates and is inhibited by unoccupied estrogen receptor beta. *FEBS Lett,* 583**,** 1314-8.

LIN, C. Y., STROM, A., LI KONG, S., KIETZ, S., THOMSEN, J. S., TEE, J. B., VEGA, V. B., MILLER, L. D., SMEDS, J., BERGH, J., GUSTAFSSON, J. A. & LIU, E. T. (2007) Inhibitory effects of estrogen receptor beta on specific hormone-responsive gene expression and association with disease outcome in primary breast cancer. *Breast Cancer Res,* 9**,** R25.

LINDBERG, M. K., MOVERARE, S., SKRTIC, S., GAO, H., DAHLMAN-WRIGHT, K., GUSTAFSSON, J. A. & OHLSSON, C. (2003) Estrogen Receptor (ER)-beta Reduces ERalpha-Regulated Gene Transcription, Supporting a "Ying Yang" Relationship between ERalpha and ERbeta in Mice. *Mol Endocrinol,* 17**,** 203-8.

LIPFORD, J. R. & DESHAIES, R. J. (2003) Diverse roles for ubiquitin-dependent proteolysis in transcriptional activation. *Nat Cell Biol,* 5**,** 845-850.

LIPPINCOTT-SCHWARTZ, J. & SMITH, C. L. (1997) Insights into secretory and endocytic membrane traffic using green fluorescent protein chimeras. *Curr Opin Neurobiol,* 7**,** 631-9.

LIU, Y., GAO, H., MARSTRAND, T. T., STROM, A., VALEN, E., SANDELIN, A., GUSTAFSSON, J. A. & DAHLMAN-WRIGHT, K. (2008) The genome landscape of ERalpha- and ERbeta-binding DNA regions. *Proc Natl Acad Sci U S A,* 105**,** 2604-9.

LIVAK, K. J. & SCHMITTGEN, T. D. (2001) Analysis of relative gene expression data using real-time quantitative PCR and the 2(-Delta Delta C(T)) Method. *Methods,* 25**,** 402-8.

LOCKER, G. Y. (1998) Hormonal therapy of breast cancer. *Cancer Treat Rev,* 24**,** 221-40.

LONARD, D. M., NAWAZ, Z., SMITH, C. L. & O'MALLEY, B. W. (2000) The 26S proteasome is required for estrogen receptor-alpha and coactivator turnover and for efficient estrogen receptor-alpha transactivation. *Mol Cell,* 5**,** 939-48.

LOPEZ, G. N., TURCK, C. W., SCHAUFELE, F., STALLCUP, M. R. & KUSHNER, P. J. (2001) Growth Factors Signal to Steroid Receptors through

Mitogen-activated Protein Kinase Regulation of p160 Coactivator Activity. *J Biol Chem,* 276(25), 22177-82.

LUBAHN, D. B., MOYER, J. S., GOLDING, T. S., COUSE, J. F., KORACH, K. S. & SMITHIES, O. (1993) Alteration of reproductive function but not prenatal sexual development after insertional disruption of the mouse estrogen receptor gene. *Proc Natl Acad Sci U S A,* 90**,** 11162-6.

LUISI, B., XU, W., OTWINWSKI, Z., FEEDMAN, L., YAMAMOTO, K. & SIGLER, P. (1991) Crystallographic analysis of the interaction of the glucocorticoid receptor with DNA. *Nature,* 352**,** 497-505.

MADAK-ERDOGAN, Z., KIESER, K. J., KIM, S. H., KOMM, B., KATZENELLENBOGEN, J. A. & KATZENELLENBOGEN, B. S. (2008) Nuclear and extranuclear pathway inputs in the regulation of global gene expression by estrogen receptors. *Mol Endocrinol,* 22**,** 2116-27.

MALAMAS, M. S., MANAS, E. S., MCDEVITT, R. E., GUNAWAN, I., XU, Z. B., COLLINI, M. D., MILLER, C. P., DINH, T., HENDERSON, R. A., KEITH, J. C., JR. & HARRIS, H. A. (2004) Design and synthesis of aryl diphenolic azoles as potent and selective estrogen receptor-beta ligands. *J Med Chem,* 47**,** 5021-40.

MANAS, E. S., UNWALLA, R. J., XU, Z. B., MALAMAS, M. S., MILLER, C. P., HARRIS, H. A., HSIAO, C., AKOPIAN, T., HUM, W. T., MALAKIAN, K., WOLFROM, S., BAPAT, A., BHAT, R. A., STAHL, M. L., SOMERS, W. S. & ALVAREZ, J. C. (2004) Structure-based design of estrogen receptor-beta selective ligands. *J Am Chem Soc,* 126**,** 15106-19.

MANGELSDORF, D. J., THUMMEL, C., BEATO, M., HERRLICH, P., SCHUTZ, G., UMESONO, K., BLUMBERG, B., KASTNER, P., MARK, M., CHAMBON, P. & EVANS, R. (1995) The nuclear receptor superfamily: the second decade. *Cell,* 83**,** 835-839.

MANOLAGAS, S. C. & KOUSTENI, S. (2001) Perspective: nonreproductive sites of action of reproductive hormones. *Endocrinology,* 142**,** 2200-4.

MARTIN, M. B., FRANKE, T. F., STOICA, G. E., CHAMBON, P., KATZENELLENBOGEN, B. S., STOICA, B. A., MCLEMORE, M. S., OLIVO, S. E. & STOICA, A. (2000) A role for Akt in mediating the estrogenic functions of epidermal growth factor and insulin-like growth factor I. *Endocrinology,* 141**,** 4503-11.

MARUVADA, P., BAUMANN, C. T., HAGER, G. L. & YEN, P. M. (2003) Dynamic shuttling and intranuclear mobility of nuclear hormone receptors. *J Biol Chem,* 278**,** 12425-32.

MASSARWEH, S., OSBORNE, C. K., JIANG, S., WAKELING, A. E., RIMAWI, M., MOHSIN, S. K., HILSENBECK, S. & SCHIFF, R. (2006) Mechanisms of Tumor Regression and Resistance to Estrogen Deprivation and Fulvestrant in a Model of Estrogen Receptor-Positive, HER-2/neu-Positive Breast Cancer. *Cancer Res,* 66(16), 8266-73.

MASUHIRO, Y., MEZAKI, Y., SAKARI, M., TAKEYAMA, K.-I., YOSHIDA, T., INOUE, K., YANAGISAWA, J., HANAZAWA, S., O'MALLEY, B. W. & KATO, S. (2005) Splicing potentiation by growth factor signals via estrogen receptor phosphorylation. *Proc Natl Acad Sci USA*, 102(23), 8126-31.

MASUYAMA, H. & HIRAMATSU, Y. (2004) Involvement of Suppressor for Gal 1 in the Ubiquitin/Proteasome-mediated Degradation of Estrogen Receptors. *J Biol Chem,* 279(13), 12020-6.

MCDONNELL, D. P. & NORRIS, J. D. (2002) Connections and regulation of the human estrogen receptor. *Science,* 296**,** 1642-4.

MCINERNEY, E. M. & KATZENELLENBOGEN, B. S. (1996) Different regions in activation function-1 of the human estrogen receptor required for antiestrogen- and estradiol-dependent transcription activation. *J Biol Chem,* 271**,** 24172-8.

MCINERNEY, E. M., WEIS, K. E., SUN, J., MOSSELMAN, S. & KATZENELLENBOGEN, B. S. (1998) Transcriptional activation by the human estrogen receptor subtype β (ERβ) studied with ERβ and ERa receptor chimeras. *Endocrinology,* 139**,** 4513-4522.

MCKENNA, N. J., LANZ, R. B. & O'MALLEY, B. W. (1999) Nuclear receptor co-regulators: cellular and molecular biology. *Endocrine Reviews,* 20**,** 321-344.

MEDUNJANIN, S., HERMANI, A., DE SERVI, B., GRISOUARD, J., RINCKE, G. & MAYER, D. (2005) Glycogen synthase kinase-3 interacts with and phosphorylates estrogen receptor alpha and is involved in the regulation of receptor activity. *J Biol Chem,* 280(38), 33006-14.

MENDELSOHN, M. E. (2000) Nongenomic, ER-mediated activation of endothelial nitric oxide synthase: how does it work? What does it mean? *Circ Res,* 87**,** 956-60.

MESSINA, M. J., PERSKY, V., SETCHELL, K. D. & BARNES, S. (1994) Soy intake and cancer risk: a review of the in vitro and in vivo data. *Nutr Cancer,* 21**,** 113-31.

METZGER, D., ALI, S., BORNERT, J. M. & CHAMBON, P. (1995) Characterization of the amino-terminal transcriptional activation function of the human estrogen receptor in animal and yeast cells. *J Biol Chem,* 270**,** 9535-42.

MEYER, M. E., GRONEMEYER, H., TURCOTTE, B., BOCQUEL, M. T., TASSET, D. & CHAMBON, P. (1989) Steroid hormone receptors compete for factors that mediate their enhancer function. *Cell,* 57**,** 433-42.

MEYERS, M. J., SUN, J., CARLSON, K. E., MARRINER, G. A., KATZENELLENBOGEN, B. S. & KATZENELLENBOGEN, J. A. (2001) Estrogen receptor-beta potency-selective ligands: structure-activity relationship studies of diarylpropionitriles and their acetylene and polar analogues. *J Med Chem,* 44**,** 4230-51.

MEYVIS, T. K., DE SMEDT, S. C., VAN OOSTVELDT, P. & DEMEESTER, J. (1999) Fluorescence recovery after photobleaching: a versatile tool for mobility and interaction measurements in pharmaceutical research. *Pharm Res,* 16**,** 1153-62.

MICHALIDES, R., GRIEKSPOOR, A., BALKENENDE, A., VERWOERD, D., JANSSEN, L., JALINK, K., FLOORE, A., VELDS, A., VAN'T VEER, L. & NEEFJES, J. (2004) Tamoxifen resistance by a conformational arrest of the estrogen receptor alpha after PKA activation in breast cancer. *Cancer Cell,* 5**,** 597-605.

MILLER, C. P., COLLINI, M. D. & HARRIS, H. A. (2003) Constrained phytoestrogens and analogues as ERbeta selective ligands. *Bioorg Med Chem Lett,* 13**,** 2399-403.

MISTELI, T. (2001) Protein dynamics: implications for nuclear architecture and gene expression. *Science,* 291**,** 843-7.

MITRUNEN, K. & HIRVONEN, A. (2003) Molecular epidemiology of sporadic breast cancer: The role of polymorphic genes involved in oestrogen

biosynthesis and metabolism. *Mutation Research/Reviews in Mutation Research,* 544**,** 9-41.

MIYAMOTO, S., TERAMOTO, H., GUTKIND, J. S. & YAMADA, K. M. (1996) Integrins can collaborate with growth factors for phosphorylation of receptor tyrosine kinases and MAP kinase activation: roles of integrin aggregation and occupancy of receptors. *J Cell Biol,* 135(6 Pt 1),1633-42.

MOORE, J. T., MCKEE, D. D., SLENTZ-KESLER, K., MOORE, L. B., JONES, S. A., HORNE, E. L., SU, J. L., KLIEWER, S. A., LEHMANN, J. M. & WILLSON, T. M. (1998) Cloning and characterization of human estrogen receptor beta isoforms. *Biochem Biophys Res Commun,* 247**,** 75-8.

MORGAN, J. M., NAVABI, H., SCHMID, K. W. & JASANI, B. (1994) Possible role of tissue-bound calcium ions in citrate-mediated high-temperature antigen retrieval. *J Pathol,* 174**,** 301-7.

MORTON, C. C., BYERS, M. G., NAKAI, H., BELL, G. I. & SHOWS, T. B. (1986) Human genes for insulin-like growth factors I and II and epidermal growth factor are located on 12q22----q24.1, 11p15, and 4q25----q27, respectively. *Cytogenet Cell Genet,* 41**,** 245-9.

MOSSELMAN, S., POLMAN, J. & DIJKEMA, R. (1996) ERbeta: identification and characterization of a novel human estrogen receptor. *FEBS letters,* 392**,** 49-53.

MURPHY, L., CHERLET, T., ADEYINKA, A., NIU, Y., SNELL, L. & WATSON, P. (2004) Phospho-serine-118 estrogen receptor-alpha detection in human breast tumors in vivo. *Clin Cancer Res,* 10(4), 1354-9.

MYERS, E., FLEMING, F. J., CROTTY, T. B., KELLY, G., MCDERMOTT, E. W., O'HIGGINS N, J., HILL, A. D. & YOUNG, L. S. (2004) Inverse relationship between ER-beta and SRC-1 predicts outcome in endocrine-resistant breast cancer. *Br J Cancer,* 91**,** 1687-93.

NAGEL, S. C., HAGELBARGER, J. L. & MCDONNELL, D. P. (2001) Development of an ER action indicator mouse for the study of estrogens, selective ER modulators (SERMs), and Xenobiotics. *Endocrinology,* 142**,** 4721-8.

NAHTA, R. & ESTEVA, F. J. (2006) Herceptin: mechanisms of action and resistance. *Cancer Letters,* 232**,** 123-138.

NAWAZ, Z., LONARD, D. M., DENNIS, A. P., SMITH, C. L. & O'MALLEY, B. W. (1999) Proteasome-dependent degradation of the human estrogen receptor. *Proc Natl Acad Sci U S A,* 96**,** 1858-62.

NAWAZ, Z. & O'MALLEY, B. W. (2004) Urban Renewal in the Nucleus: Is Protein Turnover by Proteasomes Absolutely Required for Nuclear Receptor-Regulated Transcription? *Mol Endocrinol* 18(3), 493-499

NELSON, K. G., TAKAHASHI, T., BOSSERT, N. L., WALMER, D. K. & MCLACHLAN, J. A. (1991) Epidermal growth factor replaces estrogen in the stimulation of female genital-tract growth and differentiation. *Proc Natl Acad Sci U S A,* 88**,** 21-5.

NEUMAN, E., LADHA, M. H., LIN, N., UPTON, T. M., MILLER, S. J., DIRENZO, J., PESTELL, R. G., HINDS, P. W., DOWDY, S. F., BROWN, M. & EWEN, M. E. (1997) Cyclin D1 stimulation of estrogen receptor transcriptional activity independent of cdk4. *Mol Cell Biol,* 17**,** 5338-47.

NICHOLSON, R. I., HUTCHESON, I. R., KNOWLDEN, J. M., JONES, H. E., HARPER, M. E., JORDAN, N., HISCOX, S. E., BARROW, D. & GEE, J. M. W. (2004) Nonendocrine Pathways and Endocrine Resistance: observations

with antiestrogens and signal transduction inhibitors in combination. *Clinical Cancer Research* 10, 346S-354S

NILSSON, S., MAKELA, S., TREUTER, E., TUJAGUE, M., THOMSEN, J., ANDERSSON, G., ENMARK, E., PETTERSSON, K., WARNER, M. & GUSTAFSSON, J. (2001) Mechanisms of estrogen action. *Physiol Rev,* 81**,** 1535-65.

NIRMALA, P. B. & THAMPAN, R. V. (1995) Ubiquitination of the rat uterine estrogen receptor: dependence on estradiol. *Biochem Biophys Res Commun,* 213**,** 24-31.

NISHIDA M, K. K., KANEKO M, IWASAKI H. (1985) Establishment of a new human endometrial adenocarcinoma cell line, Ishikawa cells, containing estrogen and progesterone receptors. *Acta Obstet Gynecol* 37**,** 1103-11.

NYE, A. C., RAJENDRAN, R. R., STENOIEN, D. L., MANCINI, M. A., KATZENELLENBOGEN, B. S. & BELMONT, A. S. (2002) Alteration of large-scale chromatin structure by estrogen receptor. *Mol Cell Biol,* 22**,** 3437-49.

O'MALLEY, B. W., QIN, J. & LANZ, R. B. (2008) Cracking the coregulator codes. *Curr Opin Cell Biol,* 20**,** 310-5.

OGAWA, S., CHAN, J., CHESTER, A. E., GUSTAFSSON, J. A., KORACH, K. S. & PFAFF, D. W. (1999) Survival of reproductive behaviors in estrogen receptor beta gene-deficient (betaERKO) male and female mice. *Proc Natl Acad Sci U S A,* 96**,** 12887-92.

OGAWA, S., INOUE, S., WATANABE, T., HIROI, H., ORIMO, A., HOSOI, T., OUCHI, Y. & MURAMATSU, M. (1998a) The complete primary structure of human estrogen receptor beta (hER beta) and its heterodimerization with ER alpha in vivo and in vitro. *Biochemical Biophysical Research Communications,* 243**,** 122-126.

OGAWA, S., INOUE, S., WATANABE, T., ORIMO, A., HOSOI, T., OUCHI, Y. & MURAMATSU, M. (1998b) Molecular cloning and characterization of human estrogen receptor betacx: a potential inhibitor ofestrogen action in human. *Nucleic Acids Res,* 26**,** 3505-12.

OLEFSKY, J. M. (2001) Nuclear receptor minireview series. *J Biol Chem,* 276**,** 36863-4.

OMOTO, Y., INOUE, S., OGAWA, S., TOYAMA, T., YAMASHITA, H., MURAMATSU, M., KOBAYASHI, S. & IWASE, H. (2001) Clinical value of the wild-type estrogen receptor beta expression in breast cancer. *Cancer Lett,* 163**,** 207-12.

OMOTO, Y., KOBAYASHI, S., INOUE, S., OGAWA, S., TOYAMA, T., YAMASHITA, H., MURAMATSU, M., GUSTAFSSON, J. A. & IWASE, H. (2002) Evaluation of oestrogen receptor beta wild-type and variant protein expression, and relationship with clinicopathological factors in breast cancers. *Eur J Cancer,* 38**,** 380-6.

OMURA, T. & MOROHASHI, K. (1995) Gene regulation of steroidogenesis. *J Steroid Biochem Mol Biol,* 53**,** 19-25.

ONATE, S. A., BOONYARATANAKORNKIT, V., SPENCER, T. E., TSAI, S. Y., TSAI, M. J., EDWARDS, D. P. & O'MALLEY, B. W. (1998) The steroid receptor coactivator-1 contains multiple receptor interacting and activation domains that cooperatively enhance the activation function 1 (AF-1) and AF-2 domains of steroid receptors. *J Biol Chem,* 273**,** 12101-8.

ONATE, S. A., TSAI, S. Y., TSAI, M. J. & O'MALLEY, B. W. (1995) Sequence and characterization of a coactivator for the steroid hormone receptor superfamily. *Science,* 270**,** 1354-7.

OSBORNE, C. K. (1998) Tamoxifen in the Treatment of Breast Cancer. *N Engl J Med* 339, 1609-1618

OSBORNE, C. K., BARDOU, V., HOPP, T. A., CHAMNESS, G. C., HILSENBECK, S. G., FUQUA, S. A. W., WONG, J., ALLRED, D. C., CLARK, G. M. & SCHIFF, R. (2003) Role of the Estrogen Receptor Coactivator AIB1 (SRC-3) and HER-2/neu in Tamoxifen Resistance in Breast Cancer. *J Nat Cancer Instit,* 95(5), 353-361(9).

OSBORNE, C. K., SHOU, J., MASSARWEH, S. & SCHIFF, R. (2005) Crosstalk between estrogen receptor and growth factor receptor pathways as a cause for endocrine therapy resistance in breast cancer. *Clin Cancer Res,* 11**,** 865s-70s.

OSBORNE, C. K., ZHAO, H. & FUQUA, S. A. (2000) Selective estrogen receptor modulators: structure, function, and clinical use. *J Clin Oncol,* 18**,** 3172-86.

PACE, P., TAYLOR, J., SUNTHARALINGAM, S., COOMBES, R. C. & ALI, S. (1997) Human estrogen receptor beta binds DNA in a manner similar to, and dimerizes with, estrogen receptor alpha. *Journal of Biological Chemistry,* 272**,** 25832-25838.

PAECH, K., WEBB, P., KUIPER, G. G., NILSSON, S., GUSTAFSSON, J., KUSHNER, P. J. & SCANLAN, T. S. (1997) Differential ligand activation of estrogen receptors ERalpha and ERbeta at AP1 sites. *Science,* 277**,** 1508-10.

PALMIERI, C., CHENG, G., SAJI, S., ZELADA-HEDMAN, M., Z, VAN NOORDEN, S., WAHLSTROM, T., COOMBES, R. C., WARNER, M. & GUSTAFSSON, J. A. (2002) Estrogen receptor beta in breast cancer. *Endocrine Related Cancer,* 9**,** 1-13.

PAPOUTSI, Z., ZHAO, C., PUTNIK, M., GUSTAFSSON, J. A. & DAHLMAN-WRIGHT, K. (2009) Binding of estrogen receptor alpha/beta heterodimers to chromatin in MCF-7 cells. *J Mol Endocrinol,* 43**,** 65-72.

PARK, B. W., KIM, K. S., HEO, M. K., YANG, W. I., KIM, S. I., KIM, J. H., KIM, G. E. & LEE, K. S. (2006) The changes of estrogen receptor-beta variants expression in breast carcinogenesis: Decrease of estrogen receptor-beta2 expression is the key event in breast cancer development. *J Surg Oncol,* 93**,** 504-10.

PARKER, M. G. (1993) Action of "pure" antiestrogens in inhibiting estrogen receptor action. *Breast Cancer Res Treat,* 26**,** 131-7.

PEARSON, G., ROBINSON, F., BEERS GIBSON, T., XU, B. E., KARANDIKAR, M., BERMAN, K. & COBB, M. H. (2001) Mitogen-activated protein (MAP) kinase pathways: regulation and physiological functions. *Endocr Rev,* 22**,** 153-83.

PELLETIER, G. & EL-ALFY, M. (2000) Immunocytochemical localization of estrogen receptor alpha and beta in human reproductive organs. *Journal of Clinical Endocrinology and Metabolism,* 85**,** 4835-4840.

PENG, B., LU, B., LEYGUE, E. & MURPHY, L. C. (2003) Putative functional characteristics of human estrogen receptor-beta isoforms. *J Mol Endocrinol,* 30**,** 13-29.

PERROT-APPLANAT, M., GROYER-PICARD, M. T., GARCIA, E., LORENZO, F. & MILGROM, E. (1988) Immunocytochemical demonstration of oestrogen and progesterone receptors in muscle cells of uterine arteries in rabbits and humans. *Endocrinology,* 123**,** 1511-1519.

PERTSCHUK, L. P. & AXIOTIS, C. A. (1999) Steroid Hormone Receptor Immunohistochemistry in Breast Cancer: Past, Present, and Future. *Breast J,* 5**,** 3-12.

PETTERSSON, K., DELAUNAY, F. & GUSTAFSSON, J. A. (2000) Estrogen receptor beta acts as a dominant regulator of estrogen signaling. *Oncogene,* 19**,** 4970-8.

PETTERSSON, K., GRANDIEN, K., KUIPER, G. G. & GUSTAFSSON, J. A. (1997) Mouse estrogen receptor beta forms estrogen response element-binding heterodimers with estrogen receptor alpha. *Mol Endocrinol,* 11**,** 1486-96.

PETTERSSON, K. & GUSTAFSSON, J.-A. (2001) Role of estrogen receptor beta in estrogen action. *Annual Review of Physiology,* 63**,** 165-192.

.

PHILIPS, A., CHALBOS, D. & ROCHEFORT, H. (1993) Estradiol increases and anti-estrogens antagonize the growth factor-induced activator protein-1 activity in MCF7 breast cancer cells without affecting c-fos and c-jun synthesis. *J Biol Chem,* 268**,** 14103-8.

PICARD, D., BUNONE, G., LIU, J. W. & DONZE, O. (1997) Steroid-independent activation of steroid receptors in mammalian and yeast cells and in breast cancer. *Biochem Soc Trans,* 25**,** 597-602.

PICARD, N., CHARBONNEAU, C., SANCHEZ, M., LICZNAR, A., BUSSON, M., LAZENNEC, G. & TREMBLAY, A. (2008) Phosphorylation of activation function-1 regulates proteasome-dependent nuclear mobility and E6-associated protein ubiquitin ligase recruitment to the estrogen receptor beta. *Mol Endocrinol,* 22**,** 317-30.

PIKE, A. C. (2006) Lessons learnt from structural studies of the oestrogen receptor. *Best Pract Res Clin Endocrinol Metab,* 20**,** 1-14.

PIKE, A. C., BRZOZOWSKI, A. M., HUBBARD, R. E., BONN, T., THORSELL, A. G., ENGSTROM, O., LJUNGGREN, J., GUSTAFSSON, J. A. & CARLQUIST, M. (1999) Structure of the ligand-binding domain of oestrogen receptor beta in the presence of a partial agonist and a full antagonist. *Embo J,* 18**,** 4608-18.

PIKE, A. C., BRZOZOWSKI, A. M., WALTON, J., HUBBARD, R. E., THORSELL, A. G., LI, Y. L., GUSTAFSSON, J. A. & CARLQUIST, M. (2001) Structural insights into the mode of action of a pure antiestrogen. *Structure,* 9**,** 145-53.

PLOWMAN, G. D., CULOUSCOU, J. M., WHITNEY, G. S., GREEN, J. M., CARLTON, G. W., FOY, L., NEUBAUER, M. G. & SHOYAB, M. (1993) Ligand-specific activation of HER4/p180erbB4, a fourth member of the epidermal growth factor receptor family. *Proc Natl Acad Sci U S A,* 90**,** 1746-50.

POLKINGHORNE, J. (1989) *Review of the Guidance on the Research Use of Fetuses and Fetal Material,* London, HMSO.

PONGLIKITMONGKOL, M., GREEN, S. & CHAMBON, P. (1988) Genomic organization of the human oestrogen receptor gene. *Embo J,* 7**,** 3385-8.

POO, M. & CONE, R. A. (1973) Lateral diffusion of rhodopsin in the visual receptor membrane. *J Supramol Struct,* 1**,** 354.

POOLA, I., ABRAHAM, J. & BALDWIN, K. (2002) Identification of ten exon deleted ERbeta mRNAs in human ovary, breast, uterus and bone tissues: alternate splicing pattern of estrogen receptor beta mRNA is distinct from that of estrogen receptor alpha. *FEBS Lett,* 516**,** 133-8.

POOLA, I., ABRAHAM, J., BALDWIN, K., SAUNDERS, A. & BHATNAGAR R. (2005a) Estrogen receptors beta4 and beta5 are full length functionally distinct ERbeta isoforms: cloning from human ovary and functional characterization. *Endocrine,* 27**,** 227-38.

POOLA, I., FUQUA, S. A. W., DE WITTY, R. L., ABRAHAM, J., MARSHALLACK, J. J. & LIU, A. (2005b) Estrogen Receptor alpha-negative Breast Cancer Tissues Express Significant Levels of Estrogen-Independent Transcription Factors, ERbeta1 and ERbeta5: Potential Molecular Targets for Chemoprevention. *Clin Cancer Res,* 11, 7579-85

POOLA, I., KODURI, S., CHATRA, S. & CLARKE, R. (2000) Identification of twenty alternatively spliced estrogen receptor alpha mRNAs in breast cancer cell lines and tumors using splice targeted primer approach. *J Steroid Biochem Mol Biol,* 72**,** 249-58.

PORTER, W., SAVILLE, B., HOIVIK, D. & SAFE, S. (1997) Functional synergy between the transcription factor Sp1 and the estrogen receptor. *Mol Endocrinol,* 11**,** 1569-80.

PORTER, W., WANG, F., WANG, W., DUAN, R. & SAFE, S. (1996) Role of estrogen receptor/Sp1 complexes in estrogen-induced heat shock protein 27 gene expression. *Mol Endocrinol,* 10**,** 1371-8.

POUKKA, H., AARNISALO, P., KARVONEN, U., PALVIMO, J. J. & JANNE, O. A. (1999) Ubc9 interacts with the androgen receptor and activates receptor-dependent transcription. *J Biol Chem,* 274**,** 19441-6.

PRESS, M. F., XU, S. H., WANG, J. D. & GREENE, G. L. (1989) Subcellular distribution of estrogen receptor and progesterone receptor with and without specific ligand. *Am J Pathol,* 135**,** 857-64.

PRIESLER-MASHEK, N. S. B. L. S. M. K. T. E. T. A. M. T. (2002) Ligand-specific regulation of proteasome-mediated proteolysis of estrogen receptor-α. *American journal of physiology. Endocrinology and metabolism* E891-E898.

PRIGENT, S. A. & LEMOINE, N. R. (1992) The type 1 (EGFR-related) family of growth factor receptors and their ligands. *Prog Growth Factor Res,* 4**,** 1-24.

PROSSNITZ, E. R., ARTERBURN, J. B., SMITH, H. O., OPREA, T. I., SKLAR, L. A. & HATHAWAY, H. J. (2008) Estrogen signaling through the transmembrane G protein-coupled receptor GPR30. *Annu Rev Physiol,* 70**,** 165-90.

RAYALA, S. K., TALUKDER, A. H., BALASENTHIL, S., THARAKAN, R., BARNES, C. J., WANG, R.-A., ALDAZ, M., KHAN, S. & KUMAR, R. (2006) P21-activated kinase 1 regulation of estrogen receptor-alpha activation involves serine 305 activation linked with serine 118 phosphorylation. *Cancer Res* 66(3), 1694-701

RAZANDI, M., PEDRAM, A. & LEVIN, E. R. (2000) Plasma membrane estrogen receptors signal to antiapoptosis in breast cancer. *Mol Endocrinol,* 14**,** 1434-47.

REID, G., DENGER, S., KOS, M. & GANNON, F. (2002) Human estrogen receptor-alpha: regulation by synthesis, modification and degradation. *Cell Mol Life Sci,* 59**,** 821-31.

REID, G., HUBNER, M. R., METIVIER, R., BRAND, H., DENGER, S., MANU, D., BEAUDOUIN, J., ELLENBERG, J. & GANNON, F. (2003) Cyclic, proteasome-mediated turnover of unliganded and liganded ERalpha on responsive promoters is an integral feature of estrogen signaling. *Mol Cell,* 11**,** 695-707.

RENSHAW, M. W., REN, X.-D. & SCHWARTZ, M. A. (1997) Growth factor activation of MAP kinase requires cell adhesion. *EMBO J,* 16**,** 5592-5599.

REVANKAR, C. M., CIMINO, D. F., SKLAR, L. A., ARTERBURN, J. B. & PROSSNITZ, E. R. (2005) A transmembrane intracellular estrogen receptor mediates rapid cell signaling. *Science,* 307**,** 1625-30.

RIGGS, B. L., KHOSLA, S. & MELTON, L. J., 3RD (1998) A unitary model for involutional osteoporosis: estrogen deficiency causes both type I and type II osteoporosis in postmenopausal women and contributes to bone loss in aging men. *J Bone Miner Res,* 13**,** 763-73.

RIGGS, B. L. & MELTON, L. J., 3RD (1995) The worldwide problem of osteoporosis: insights afforded by epidemiology. *Bone,* 17**,** 505S-511S.

RISHI, A. K., SHAO, Z. M., BAUMANN, R. G., LI, X. S., SHEIKH, M. S., KIMURA, S., BASHIRELAHI, N. & FONTANA, J. A. (1995) Estradiol regulation of the human retinoic acid receptor alpha gene in human breast carcinoma cells is mediated via an imperfect half-palindromic estrogen response element and Sp1 motifs. *Cancer Res,* 55**,** 4999-5006.

ROBINSON-RECHAVI, M., ESCRIVA GARCIA, H. & LAUDET, V. (2003) The nuclear receptor superfamily. *J Cell Sci,* 116**,** 585-6.

ROBYR, D., WOLFFE, A. P. & WAHLI, W. (2000) Nuclear hormone receptor coregulators in action: diversity for shared tasks. *Mol Endocrinol,* 14**,** 329-47.

ROGATSKY, I., TROWBRIDGE, J. M. & GARABEDIAN, M. J. (1999) Potentiation of human estrogen receptor alpha transcriptional activation through phosphorylation of serines 104 and 106 by the cyclin A-CDK2 complex. *Journal of Biol Chem,* 274, 22296

ROUTLEDGE, E. J., WHITE, R., PARKER, M. G. & SUMPTER, J. P. (2000) Differential effects of xenoestrogens on coactivator recruitment by estrogen receptor (ER) alpha and ERbeta. *J Biol Chem,* 275**,** 35986-93.

RUSNAK, D. W., LACKEY, K., AFFLECK, K., WOOD, E. R., ALLIGOOD, K. J., RHODES, N., KEITH, B. R., MURRAY, D. M., KNIGHT, W. B., MULLIN, R. J. & GILMER, T. M. (2001) The effects of the novel, reversible epidermal growth factor receptor/ErbB-2 tyrosine kinase inhibitor, GW2016, on the growth of human normal and tumor-derived cell lines in vitro and in vivo. *Mol Cancer Ther,* 1(2), 85-94.

RUSSELL, K. S., HAYNES, M. P., SINHA, D., CLERISME, E. & BENDER, J. R. (2000) Human vascular endothelial cells contain membrane binding sites for estradiol, which mediate rapid intracellular signaling. *Proc Natl Acad Sci U S A,* 97**,** 5930-5.

SANCHEZ, M. L., SAUVÉ, K., PICARD, N. & TREMBLAY, A. (2007) The hormonal response of estrogen receptor beta is decreased by the phosphatidylinositol 3-kinase/Akt pathway via a phosphorylation-dependent release of CREB-binding protein. *J Biol Chem,* 282(7), 4830-40.

SAUNDERS, P. T. (1998) Oestrogen receptor beta (ER beta). *Rev Reprod,* 3**,** 164-71.

SAUNDERS, P. T., MAGUIRE, S. M., GAUGHAN, J. & MILLAR, M. R. (1997) Expression of oestrogen receptor beta (ER beta) in multiple rat tissues visualised by immunohistochemistry. *J Endocrinol,* 154**,** R13-6.

SAUNDERS, P. T., MILLAR, M. R., WILLIAMS, K., MACPHERSON, S., BAYNE, C., O'SULLIVAN, C., ANDERSON, T. J., GROOME, N. P. & MILLER, W. R. (2002) Expression of oestrogen receptor beta (ERbeta1) protein in human breast cancer biopsies. *Br J Cancer,* 86**,** 250-6.

SAUNDERS, P. T., SHARPE, R. M., WILLIAMS, K., MACPHERSON, S., URQUART, H., IRVINE, D. S. & MILLAR, M. R. (2001) Differential expression of oestrogen receptor alpha and beta proteins in the testes and male reproductive system of human and non-human primates. *Mol Hum Reprod,* 7**,** 227-36.

SAUNDERS, P. T. K. & CRITCHLEY, H. O. D. (2002) Estrogen receptor subtypes in the female reproductive tract. *Reprod Med Rev,* 10**,** 149-164.

SAUNDERS, P. T. K., MILLAR, M. R., WILLIAMS, K., MACPHERSON, S., HARKISS, D., ANDERSON, R. A., ORR, B., GROOME, N. P., SCOBIE, G. & FRASER, H. M. (2000) Differential expression of estrogen receptor-alpha and -beta and androgen receptor in the ovaries of marmosets and humans. *Biol Reprod,* 63**,** 1098-105.

SAUNDERS, P. T. K., SIERENS, J E., GROOME, N P. AND MILLAR, M R (2003) Oestrogen receptors in the human and primate testis and reproductive tract. *Andrologie,* 13**,** 43-50.

SCHIFF, R. (2002) The importance of estrogen receptor in breast cancer. *Breast Cancer: Prognosis, Treatment and Prevention.* New York: Marcel Dekker Inc.

SCHIFF, R., MASSARWEH, S., SHOU, J. & OSBORNE, C. K. (2003) Breast cancer endocrine resistance: how growth factor signaling and estrogen receptor coregulators modulate response. *Clin Cancer Res,* 9(1 Pt 2), 447S-54S.

SCHOMBERG, D., COUSE, J., MUKHERJEE, A., LUBAHN, D., SAR, M., MAYO, K. & KORACH, K. (1999) Targeted disruption of the estrogen receptor-a gene in female mice: characterization of ovarian responses and phenotype in the adult. *Endocrinology,* 140**,** 2733-2744.

SCHWABE, J. W., CHAPMAN, L., FINCH, J. T. & RHODES, D. (1993) The crystal structure of the estrogen receptor DNA-binding domain bound to DNA: how receptors discriminate between their response elements. *Cell,* 75**,** 567-78.

SCOBIE, G. A., MACPHERSON, S., MILLAR, M. R., GROOME, N. P., ROMANA, P. G. & SAUNDERS, P. T. (2002) Human oestrogen receptors: differential expression of ER alpha and beta and the identification of ER beta variants. *Steroids,* 67**,** 985-92.

SHAABAN, A. M., GREEN, A. R., KARTHIK, S., ALIZADEH, Y., HUGHES, T. A., HARKINS, L., ELLIS, I. O., ROBERTSON, J. F., PAISH, E. C., SAUNDERS, P. T., GROOME, N. P. & SPEIRS, V. (2008) Nuclear and cytoplasmic expression of ERbeta1, ERbeta2, and ERbeta5 identifies distinct prognostic outcome for breast cancer patients. *Clin Cancer Res,* 14**,** 5228-35.

SHAH, Y. M. & ROWAN, B. G. (2005) The Src Kinase Pathway Promotes Tamoxifen Agonist Action in Ishikawa Endometrial Cells through Phosphorylation-Dependent Stabilization of Estrogen Receptor alpha Promoter Interaction and Elevated Steroid Receptor Coactivator 1 Activity. *Mol Endocrinol* 19(3), 732-748

SHANG, Y. (2006) Molecular mechanisms of oestrogen and SERMs in endometrial carcinogenesis. *Nat Rev Cancer,* 6**,** 360-8.

SHAPIRO, S., KELLY, J. P., ROSENBERG, L., KAUFMAN, D. W., HELMRICH, S. P., ROSENSHEIN, N. B., LEWIS, J. L., JR., KNAPP, R. C., STOLLEY, P. D. & SCHOTTENFELD, D. (1985) Risk of localized and widespread endometrial cancer in relation to recent and discontinued use of conjugated estrogens. *N Engl J Med,* 313**,** 969-72.

SHARP, Z. D., MANCINI, M. G., HINOJOS, C. A., DAI, F., BERNO, V., SZAFRAN, A. T., SMITH, K. P., LELE, T. T., INGBER, D. E. & MANCINI,

M. A. (2006) Estrogen-receptor-alpha exchange and chromatin dynamics are ligand- and domain-dependent. *J Cell Science* 119, 4101-4116

SIERENS, J. E., SCOBIE, G. A., WILSON, J. & SAUNDERS, P. T. (2004) Cloning of oestrogen receptor beta from Old and New World primates: identification of splice variants and functional analysis. *J Mol Endocrinol,* 32**,** 703-18.

SIMMEN, F. A. & SIMMEN, R. C. (2006) Orchestrating the menstrual cycle: discerning the music from the noise. *Endocrinology,* 147**,** 1094-6.

SIMONCINI, T., HAFEZI-MOGHADAM, A., BRAZIL, D. P., LEY, K., CHIN, W. W. & LIAO, J. K. (2000) Interaction of oestrogen receptor with the regulatory subunit of phosphatidylinositol-3-OH kinase. *Nature,* 407**,** 538-41.

SIMPSON, E., RUBIN, G., CLYNE, C., ROBERTSON, K., O'DONNELL, L., DAVIS, S. & JONES, M. (1999) Local estrogen biosynthesis in males and females. *Endocr Relat Cancer,* 6**,** 131-7.

SIMPSON, E. R. & DAVIS, S. R. (2001) Minireview: aromatase and the regulation of estrogen biosynthesis--some new perspectives. *Endocrinology,* 142**,** 4589-94.

SKRZYPCZAK, M., BIECHE, I., SZYMCZAK, S., TOZLU, S., LEWANDOWSKI, S., GIRAULT, I., RADWANSKA, K., SZCZYLIK, C., JAKOWICKI, J. A., LIDEREAU, R. & KACZMAREK, L. (2004) Evaluation of mRNA expression of estrogen receptor beta and its isoforms in human normal and neoplastic endometrium. *Int J Cancer,* 110**,** 783-7.

SMITH, C. L. (1998) Cross-talk between peptide growth factor and estrogen receptor signaling pathways. *Biol Reprod,* 58**,** 627-32.

SNIJDERS, M. P., DE GEOIJ, A. F. P. M., DEBETS-TE BAERTS, M. J. C., ROUSCH, M. J. M., KOUDSTAAL, J. & BOSMAN, F. T. (1992) Immunocytochemical analysis of oestrogen receptors and progesterone receptors in the human uterus throughout the menstrual cycle and after the menopause. *Journal of Reproduction and Fertility,* 94**,** 363-371.

SPECTOR, N. L., XIA, W., BURRIS, H., III, HURWITZ, H., DEES, E. C., DOWLATI, A., O'NEIL, B., OVERMOYER, B., MARCOM, P. K., BLACKWELL, K. L., SMITH, D. A., KOCH, K. M., STEAD, A., MANGUM, S., ELLIS, M. J., LIU, L., MAN, A. K., BREMER, T. M., HARRIS, J. & BACUS, S. (2005) Study of the Biologic Effects of Lapatinib, a Reversible Inhibitor of ErbB1 and ErbB2 Tyrosine Kinases, on Tumor Growth and Survival Pathways in Patients With Advanced Malignancies. *J Clin Oncol,* 23(11), 2502-12.

SPEIRS, V., CARDER, P. J., LANE, S., DODWELL, D., LANSDOWN, M. R. & HANBY, A. M. (2004) Oestrogen receptor beta: what it means for patients with breast cancer. *Lancet Oncol,* 5**,** 174-81.

SRINIVASAN, R., BENTON, E., MCCORMICK, F., THOMAS, H. & GULLICK, W. J. (1999) Expression of the c-erbB-3/HER-3 and c-erbB-4/HER-4 growth factor receptors and their ligands, neuregulin-1 alpha, neuregulin-1 beta, and betacellulin, in normal endometrium and endometrial cancer. *Clin Cancer Res,* 5**,** 2877-83.

STALLCUP, M. R., CHEN, D., KOH, S. S., MA, H., LEE, Y. H., LI, H., SCHURTER, B. T. & ASWAD, D. W. (2000) Co-operation between protein-acetylating and protein-methylating co-activators in transcriptional activation. *Biochem Soc Trans,* 28**,** 415-8.

STAUFFER, S. R., COLETTA, C. J., TEDESCO, R., NISHIGUCHI, G., CARLSON, K., SUN, J., KATZENELLENBOGEN, B. S. & KATZENELLENBOGEN, J.

A. (2000) Pyrazole ligands: structure-affinity/activity relationships and estrogen receptor-alpha-selective agonists. *J Med Chem,* 43**,** 4934-47.

STEINMETZ, A. C., RENAUD, J. P. & MORAS, D. (2001) Binding of ligands and activation of transcription by nuclear receptors. *Annu Rev Biophys Biomol Struct,* 30**,** 329-59.

STENOIEN, D. L., MANCINI, M. G., PATEL, K., ALLEGRETTO, E. A., SMITH, C. L. & MANCINI, M. A. (2000) Subnuclear trafficking of estrogen receptor-alpha and steroid receptor coactivator-1. *Mol Endocrinol,* 14**,** 518-34.

STENOIEN, D. L., NYE, A. C., MANCINI, M. G., PATEL, K., DUTERTRE, M., O'MALLEY, B. W., SMITH, C. L., BELMONT, A. S. & MANCINI, M. A. (2001a) Ligand-mediated assembly and real-time cellular dynamics of estrogen receptor alpha-coactivator complexes in living cells. *Mol Cell Biol,* 21**,** 4404-12.

STENOIEN, D. L., PATEL, K., MANCINI, M. G., DUTERTRE, M., SMITH, C. L., O'MALLEY, B. W. & MANCINI, M. A. (2001b) FRAP reveals that mobility of oestrogen receptor-alpha is ligand- and proteasome-dependent. *Nat Cell Biol,* 3**,** 15-23.

STOICA, A., SACEDA, M., DORAISWAMY, V. L., COLEMAN, C. & MARTIN, M. B. (2000) Regulation of estrogen receptor-alpha gene expression by epidermal growth factor. *J Endocrinol* 165(2), 371-8.

STROM, A., HARTMAN, J., FOSTER, J. S., KIETZ, S., WIMALASENA, J. & GUSTAFSSON, J. A. (2004) Estrogen receptor beta inhibits 17beta-estradiol-stimulated proliferation of the breast cancer cell line T47D. *Proc Natl Acad Sci U S A,* 101**,** 1566-71.

SU, E. J., LIN, Z. H., ZEINE, R., YIN, P., REIERSTAD, S., INNES, J. E. & BULUN, S. E. (2009) Estrogen receptor-beta mediates cyclooxygenase-2 expression and vascular prostanoid levels in human placental villous endothelial cells. *Am J Obstet Gynecol,* 200**,** 427 e1-8.

SUBRAMANIAN, K., JIA, D., KAPOOR-VAZIRANI, P., POWELL, D. R., COLLINS, R. E., SHARMA, D., PENG, J., CHENG, X. & VERTINO, P. M. (2008) Regulation of estrogen receptor alpha by the SET7 lysine methyltransferase. *Mol Cell,* 30**,** 336-47.

SUN, J., BAUDRY, J., KATZENELLENBOGEN, J. A. & KATZENELLENBOGEN, B. S. (2003) Molecular Basis for the Subtype Discrimination of the Estrogen Receptor-beta-Selective Ligand, Diarylpropionitrile. *Mol Endocrinol,* 17**,** 247-58.

SUN, J., MEYERS, M. J., FINK, B. E., RAJENDRAN, R., KATZENELLENBOGEN, J. A. & KATZENELLENBOGEN, B. S. (1999) Novel ligands that function as selective estrogens or antiestrogens for estrogen receptor-a or estrogen receptor-β. *Endocrinology,* 140**,** 800-804.

TAKAHASHI, T., OHMICHI, M., KAWAGOE, J., OHSHIMA, C., DOSHIDA, M., OHTA, T., SAITOH, M., MORI-ABE, A., DU, B., IGARASHI, H., TAKAHASHI, K. & KURACHI, H. (2005) Growth factors change nuclear distribution of estrogen receptor-alpha via mitogen-activated protein kinase or phosphatidylinositol 3-kinase cascade in a human breast cancer cell line. *Endocrinology,* 146**,** 4082-9.

TAMRAZI, A., CARLSON, K. E. & KATZENELLENBOGEN, J. A. (2003) Molecular sensors of estrogen receptor conformations and dynamics. *Mol Endocrinol,* 17**,** 2593-602.

TANENBAUM, D. M., WANG, Y., WILLIAMS, S. P. & SIGLER, P. B. (1998) Crystallographic comparison of the estrogen and progesterone receptor's ligand binding domains. *Proceedings of the National Academy of Sciences USA,* 95**,** 5998-6003.

TATEISHI, Y., SONOO, R., SEKIYA, Y.-I., SUNAHARA, N., KAWANO, M., WAYAMA, M., HIROTA, R., KAWABE, Y.-I., MURAYAMA, A., KATO, S., KIMURA, K. & YANAGISAWA, J. (2006) Turning Off Estrogen Receptor {beta}-Mediated Transcription Requires Estrogen-Dependent Receptor Proteolysis. *Mol and Cell Biol,* , 26(21), 7966-7976

TAYLOR, A. H. & AL-AZZAWI, F. (2000) Immunolocalisation of oestrogen receptor beta in human tissues. *J Mol Endocrinol,* 24**,** 145-55.

TAYLOR, R. N., LEBOVIC, D. I., HORNUNG, D. & MUELLER, M. D. (2001) Endocrine and paracrine regulation of endometrial angiogenesis. *Ann N Y Acad Sci,* 943**,** 109-21.

TAYLOR, S. E., MARTIN-HIRSCH, P. L. & MARTIN, F. L. (2010) Oestrogen receptor splice variants in the pathogenesis of disease. *Cancer Lett,* 288**,** 133-48.

THARAKAN, R., LEPONT, P., SINGLETON, D., KUMAR, R. & KHAN, S. (2008) Phosphorylation of estrogen receptor alpha, serine residue 305 enhances activity. *Molecular and Cellular Endocrinology,* 295**,** 70-78.

THOMAS, R. S., SARWAR, N., PHOENIX, F., COOMBES, R. C. & ALI, S. (2008) Phosphorylation at serines 104 and 106 by Erk1/2 MAPK is important for estrogen receptor-alpha activity. *J Mol Endocrinol* 40(4), 173-84.

THORNTON, J. W. (2001) Evolution of vertebrate steroid receptors from an ancestral estrogen receptor by ligand exploitation and serial genome expansions. *Proc Natl Acad Sci U S A,* 98**,** 5671-6.

TREECK, O., LATTRICH, C., SPRINGWALD, A. & ORTMANN, O. (2009) Estrogen receptor beta exerts growth-inhibitory effects on human mammary epithelial cells. *Breast Cancer Res Treat*. 120(3), 557-65.

TREMBLAY, A. & GIGUERE, V. (2001) Contribution of steroid receptor coactivator-1 and CREB binding protein in ligand-independent activity of estrogen receptor beta. *J Steroid Biochem Mol Biol,* 77**,** 19-27.

TREMBLAY, A., TREMBLAY, G., LABRIE, F. & GIGUERE, V. (1999) Ligand-independent recruitment of SRC-1 to estrogen receptor beta through phosphorylation of activation function of AF-1. *Molecular Cell,* 3**,** 513-519.

TREMBLAY, G. B., TREMBLAY, A., COPELAND, N. G., GILBERT, D. J., JENKINS, N. A., LABRIE, F. & GIGUERE, V. (1997) Cloning, chromosomal localization, and functional analysis of the murine estrogen receptor beta. *Molecular Endocrinology,* 11**,** 353-365.

TREMBLAY, G. B., TREMBLAY, A., LABRIE, F. & GIGUERE, V. (1999) Dominant activity of activation function (AF-1) and differential stoichiometric requirements for AF-1 and -2 in the estrogen receptor alpha-beta heterodimeric complex. *Molecular Cell Biology,* 19**,** 1919-1927.

TROWBRIDGE, J. M., ROGATSKY, I. & GARABEDIAN, M. J. (1997) Regulation of estrogen receptor transcriptional enhancement by the cyclin A/Cdk2 complex. *PNAS,* 94(19), 10132-10137.

TSAI, M.-J. & O'MALLEY, B. (1994) Molecular mechanisms of action of steroid/thyroid receptor superfamily members. *Annual Review of Biochemistry,* 63**,** 451-486.

UMAYAHARA, Y., KAWAMORI, R., WATADA, H., IMANO, E., IWAMA, N., MORISHIMA, T., YAMASAKI, Y., KAJIMOTO, Y. & KAMADA, T. (1994) Estrogen regulation of the insulin-like growth factor I gene transcription involves an AP-1 enhancer. *J Biol Chem,* 269**,** 16433-42.

UMESONO, K. & EVANS, R. M. (1989) Determinants of target gene specificity for steroid/thyroid hormone receptors. *Cell,* 57**,** 1139-46.

VALLEY, C. C., METIVIER, R., SOLODIN, N. M., FOWLER, A. M., MASHEK, M. T., HILL, L. & ALARID, E. T. (2005) Differential Regulation of Estrogen-Inducible Proteolysis and Transcription by the Estrogen Receptor alpha N Terminus. *Mol Cell Biol,* 25(13), 5417-28.

VAN ROYEN, M. E., CUNHA, S. M., BRINK, M. C., MATTERN, K. A., NIGG, A. L., DUBBINK, H. J., VERSCHURE, P. J., TRAPMAN, J. & HOUTSMULLER, A. B. (2007) Compartmentalization of androgen receptor protein-protein interactions in living cells. *J Cell Biol,* 177**,** 63-72.

VAN ROYEN, M. E., FARLA, P., MATTERN, K. A., GEVERTS, B., TRAPMAN, J. & HOUTSMULLER, A. B. (2009) Fluorescence Recovery After Photobleaching (FRAP) to Study Nuclear Protein Dynamics in Living Cells. *Methods Mol Biol,* 464**,** 363-85.

VOGEL, C., COBLEIGH, M. A., TRIPATHY, D., GUTHEIL, J. C., HARRIS, L. N., FEHRENBACHER, L., SLAMON, D. J., MURPHY, M., NOVOTNY, W. F., BURCHMORE, M., SHAK, S. & STEWART, S. J. (2001) First-line, single-agent Herceptin® (trastuzumab) in metastatic breast cancer: a preliminary report. *European Journal of Cancer,* 37**,** 25-29.

WAKELING, A., DUKES, M. & BOWLER, J. (1991) A potent specific pure antiestrogen with clinical potential. *Cancer Research,* 51**,** 3867-3873.

WALKER, V. R. & KORACH, K. S. (2004) Estrogen receptor knockout mice as a model for endocrine research. *Ilar J,* 45**,** 455-61.

WALTER, P., GREEN, S., GREENE, G., KRUST, A., BORNERT, J. M., JELTSCH, J. M., STAUB, A., JENSEN, E., SCRACE, G., WATERFIELD, M. & *ET AL.* (1985) Cloning of the human estrogen receptor cDNA. *Proc Natl Acad Sci U S A,* 82**,** 7889-93.

WANG, R.-A., MAZUMDAR, A., VADLAMUDI, R. K. & KUMAR, R. (2002) P21-activated kinase-1 phosphorylates and transactivates estrogen receptor-[alpha] and promotes hyperplasia in mammary epithelium. *EMBO J,* 21**,** 5437-5447.

WANG, Z., ZHANG, X., SHEN, P., LOGGIE, B. W., CHANG, Y. & DEUEL, T. F. (2005) Identification, cloning, and expression of human estrogen receptor-alpha36, a novel variant of human estrogen receptor-alpha66. *Biochem Biophys Res Commun,* 336**,** 1023-7.

WARNMARK, A., ALMLOF, T., LEERS, J., GUSTAFSSON, J.-A. & TREUTER, E. (2001) Differential recruitment of the mammalian mediator subunit TRAP220 by estrogen receptors ERa and ERβ. *Journal of Biological Chemistry,* 276**,** 23397-23404.

WATSON, C. S. & GAMETCHU, B. (1999) Membrane-initiated steroid actions and the proteins that mediate them. *Proc Soc Exp Biol Med,* 220**,** 9-19.

WEBB, P., LOPEZ, G. N., UHT, R. M. & KUSHNER, P. J. (1995) Tamoxifen activation of the estrogen receptor/AP-1 pathway: potential origin for the cell-specific estrogen-like effects of antiestrogens. *Mol Endocrinol,* 9**,** 443-56.

WEBB, P., NGUYEN, P., SHINSAKO, J., ANDERSON, C., FENG, W., NGUYEN, M. P., CHEN, D., HUANG, S. M., SUBRAMANIAN, S., MCKINERNEY, E., KATZENELLENBOGEN, B. S., STALLCUP, M. R. & KUSHNER, P. J.

(1998) Estrogen receptor activation function 1 works by binding p160 coactivator proteins. *Mol Endocrinol,* 12**,** 1605-18.

WEBB, P., NGUYEN, P., VALENTINE, C., LOPEZ, G. N., KWOK, G. R., MCINERNEY, E., KATZENELLENBOGEN, B. S., ENMARK, E., GUSTAFSSON, J. A., NILSSON, S. & KUSHNER, P. J. (1999) The estrogen receptor enhances AP-1 activity by two distinct mechanisms with different requirements for receptor transactivation functions. *Mol Endocrinol,* 13**,** 1672-85.

WEIS, K. E., EKENA, K., THOMAS, J. A., LAZENNEC, G. & KATZENELLENBOGEN, B. S. (1996) Constitutively active human estrogen receptors containing amino acid substitutions for tyrosine 537 in the receptor protein. *Mol Endocrinol,* 10**,** 1388-98.

WELLS, A. (1999) EGF receptor. *The International Journal of Biochemistry & Cell Biology,* 31**,** 637-643.

WONG, N. A., MALCOMSON, R. D., JODRELL, D. I., GROOME, N. P., HARRISON, D. J. & SAUNDERS, P. T. (2005) ERbeta isoform expression in colorectal carcinoma: an in vivo and in vitro study of clinicopathological and molecular correlates. *J Pathol,* 207**,** 53-60.

WURTZ, J.-M., BOURGUET, W., RENAUD, J.-P., VIVAT, V., CHAMBON, P., MORAS, D. & GRONEMEYER, H. (1996) A canonical structure for the ligand-binding domain of nuclear receptors. *Nature Structural Biology,* 3**,** 87-94.

XIA, W., MULLIN, R. J., KEITH, B. R., LIU, L. H., MA, H., RUSNAK, D. W., OWENS, G., ALLIGOOD, K. J. & SPECTOR, N. L. (2002) Anti-tumor activity of GW572016: a dual tyrosine kinase inhibitor blocks EGF activation of EGFR/erbB2 and downstream Erk1/2 and AKT pathways. *Oncogene,* 21**,** 6255-63.

XIAO, B., SMERDON, S. J., JONES, D. H., DODSON, G. G., SONEJI, Y., AITKEN, A. & GAMBLIN, S. J. (1995) Structure of a 14-3-3 protein and implications for coordination of multiple signalling pathways. *Nature,* 376**,** 188-91.

YAGER, J. D. (2000) Endogenous estrogens act as carcinogens through metabolic activation. *Journal of the National Cancer Institute Monographs,* 27**,** 67-73.

YLIKOMI, T., BOCQUEL, M. T., BERRY, M., GRONEMEYER, H. & CHAMBON, P. (1992) Cooperation of proto-signals for nuclear accumulation of estrogen and progesterone receptors. *Embo J,* 11**,** 3681-94.

ZAWEL, L. & REINBERG, D. (1995) Common themes in assembly and function of eukaryotic transcription complexes. *Annu Rev Biochem,* 64**,** 533-61.

ZHAO, C., DAHLMAN-WRIGHT, K. & GUSTAFSSON, J. A. (2008) Estrogen receptor beta: an overview and update. *Nucl Recept Signal,* 6**,** e003.

ZHAO, C., MATTHEWS, J., TUJAGUE, M., WAN, J., STROM, A., TORESSON, G., LAM, E. W., CHENG, G., GUSTAFSSON, J. A. & DAHLMAN-WRIGHT, K. (2007) Estrogen receptor beta2 negatively regulates the transactivation of estrogen receptor alpha in human breast cancer cells. *Cancer Res,* 67**,** 3955-62.

ZWIJSEN, R. M., BUCKLE, R. S., HIJMANS, E. M., LOOMANS, C. J. & BERNARDS, R. (1998) Ligand-independent recruitment of steroid receptor coactivators to estrogen receptor by cyclin D1. *Genes Dev,* 12**,** 3488-98.